The monograph systematized a large amount of scientific works and researches on the impact of coal sulfur on the possibility of coal application in the energy and coke industries. The reader is invited to get acquainted with the methods and technologies aimed at reducing environmental pollution by sulfur oxides during coal combustion; the impact of coal sulfur on the quality of blast furnace coke.

Serhiy Pyshyev Department of Chemical Technology of Oil and Gas Processing, Lviv Polytechnic National University, Lviv, Ukraine
Denis Miroshnichenko Department of Technology of Oil, Gas and Solid Fuel Processing, National Technical University Kharkiv Polytechnic Institute, Kharkiv, Ukraine

978-620-2-68201-5

Pyshyev, Miroshnichenko

Serhiy Pyshyev
Denis Miroshnichenko

Sulfur, coal and coke: theory and practice

LAP LAMBERT Academic Publishing

Serhiy Pyshyev
Denis Miroshnichenko

Sulfur, coal and coke: theory and practice

Serhiy Pyshyev
Denis Miroshnichenko

Sulfur, coal and coke: theory and practice

LAP LAMBERT Academic Publishing

Imprint

Cover image: www.ingimage.com

Publisher:
LAP LAMBERT Academic Publishing
is a trademark of
International Book Market Service Ltd., member of OmniScriptum Publishing Group
17 Meldrum Street, Beau Bassin 71504, Mauritius
Printed at: see last page
ISBN: 978-620-2-68201-5

CONTENT

PREFACE

The monograph «Sulfur, coal and coke: theory and practice» is an attempt to systematize a large amount of scientific works and researches on the impact of coal sulfur on the possibility of its application in the energy and coke industries. The monograph also includes descriptions of research performed by the authors – Professor, D.Sc. Serhiy Pyshyev and Professor, D.Sc. Denis Miroshnichenko. The reader is invited to get acquainted with the methods and technologies aimed at reducing environmental pollution by sulfur oxides during coal combustion; the impact of coal sulfur on the quality of blast furnace coke.

The authors express special gratitude to the co-authors of their research and publications: Professor, D.Sc. Michael Bratychak, Associate Prof., PhD Yuriv Prysiazhnyi, Associate Prof., PhD Volodymyr Gunka, Senior Researcher Mark Ulanovsky, PhD Vasyl Hayvanovych, PhD Khrystyna Shevchuk and PhD Mariia Shved, D.Sc. Agnieszka Pattek-Janczyk, Professor, D.Sc. Lucjan Chmielarz and Professor, D.Sc. Piotr Kuśtrowski.

BASIC ABBREVIATIONS

BC	Basic charge
CFB	Circulating fluid bed
CIR	Coumarone-indene resin
COM	Coal organic matter
COMC	Coal organic matter conversion, degree of coal organic matter conversion
CRI	Coke reactivity index
CSD	Content of sulfur dioxide in the desulfurization gases
CSR	Coke strength after reaction with CO_2
EEA	European Environment Agency
EFCOMC, K_{ef}	Efficiency factor of coal organic matter conversion
EPA	Environmental Protection Agency
ESM	Experimental and statistical mathematical model
FGD	Flue gas desulphurization
DTA	Derivatographic analysis
DSTU, GOST	State standard
IEA	International Energy Agency
LCP	Large combustion plants
LRO	Linear rate of the oxidant
NSC	Nippon Steel Corporation
NVR	Non-volatile residues
OD	Oxidative desulfurization
OFR	Oxidant flow rate
PCI, PC	Pulverized coal injection technology, pulverized coal
PMB	Polymer-modified bitumen
RDS(T or P)	Removal degree of sulphur (total or pyritic)

SC(T or P)	Sulphur conversion (total or pyritic)
SEM	Scanning electronic microscope
TPS	Thermal power stations
XEA	X-ray emission analysis

INTRODUCTION

Today, oil, natural gas and coal are the main sources of energy in the world. Their shares in the structure of primary energy consumption in 2015 were 32.9; 23.8 and 29.2%, respectively (BP Statistical Review of World Energy, 2015). On the other hand, the world's coal reserves considerably exceed oil and gas reserves and the predicted period of coal use is at least twice as large. Table 1 presents data on proven reserves of coal at the end of 2015, its share in total energy resources and terms of proven reserves use.

Table 1 Proven reserves of coal in the end of 2015 (BP Statistical Review of World Energy)

Countries	Anthracite and bituminous, million tones	Sub-bituminous and lignite, million tones	Total, million tones	Share of total, million tones	Reserves-to-production (R/P) ratio
North America	112835	132253	245088	27.5	276
S. & Cent. America	7282	7359	14641	1.6	150
Europe & Eurasia	92557	217981	310538	34.8	273
Middle East & Africa	32722	214	32936	3.7	123
Asia Pacific	157803	130525	288328	32.3	53
Total World	403199	488332	891531	100.0	114
of which: European Union	4883	51199	56082	6.3	112

According to the latest data published in the BP Statistical Review of World Energy (2012-2017), the world’s proved reserves of coal do not

decrease with time but even demonstrate a slight increase (Fig. 1). At the same time the explored reserves of coal (Fig. 2) occupy a much larger share than other fossil fuels (BP Statistical Review of World Energy, 2017).

According to the statistics (BP Statistical Review of World Energy, 2017), taking into account the current level of consumption, world oil reserves remain for about 61 years, natural gas – 53 years, and solid fuels – 114 years. Therefore, in the nearest future coal can become the main source of human needs for energy resources and, possibly, chemical raw materials.

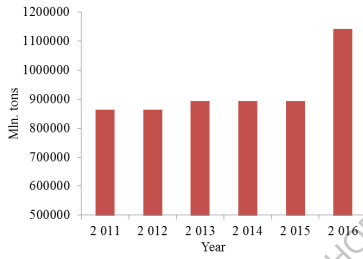

Fig. 1 The pattern of proved coal reserves

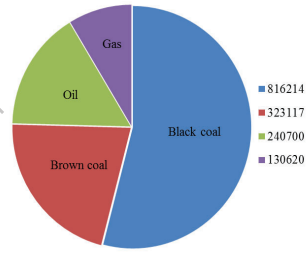

Fig. 2 The explored reserved of fossil fuels in the world, mln. tons

The direction of coal usage depends upon its metamorphism degree. In accordance with the scheme represented in Fig. 3 lignite and black coals with low and high metamorphism degree may be considered as power station coal used at thermal power stations (TPS).

Depending on the level of the industry development, the amount of produced coal used for heat and power generation varies from 60 to 90 % in different countries (coal is burned at thermal power stations or large combustion plants (LCP)). Generally, 40.4 % of world electricity is generated from coal (European Commission, 2016). Taking this fact into account, as well as the above-mentioned data and worldwide tendency to abandon nuclear energy (IEA, 2012), one can predict the sustainable usage

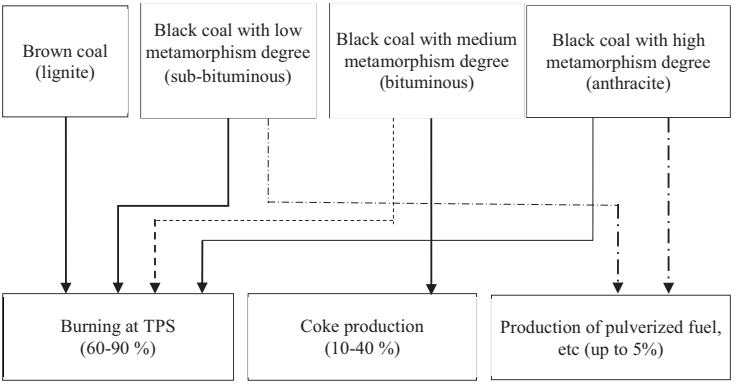

of coal for several decades (IEA (Technology roadmap), 2012).

Fig. 3 Main directions of coal application

During the combustion gas or coal, which are mainly used as fuel to produce electric and thermal energy, carbon monoxide, water vapor and a small amount of other oxides are formed. During the combustion, natural gas that contains a small amount of sulfur and nitrogen, CO_2 is mainly formed, whereas in the case of coal a large amount of harmful substances gets into the atmosphere, the main of which is sulfur dioxide (SO_2). The residence time of SO_2 in the atmosphere is short: 15-20 days in the relatively clean air. During this time SO_2 may be partially oxidized to SO_3 under the effect of oxygen, dissolved together with it in water and fall in the form of the so-called “acid rain”. Final products are distributed as follows: in the form of precipitates on the lithosphere surface - 43%, on the hydrosphere surface - 13%; they are absorbed by plants - 12%, by the hydrosphere - 13%. The precipitates have a harmful effect on human and animal health, the productivity of crops; they destroy materials and

protective coatings. For instance, SO_2 emission can cause diseases in the exposed humans which incur medical costs drawn from the governmental budgets. It has been calculated that depending on the level of economical development of a given country, such costs vary from 566 to 11,096 EUR per tone of SO_2.

To reduce the adverse environmental impact of combustion products a series of regulatory and technological arrangements is employed. During the last decade, a lot of attention was paid to the improvement of the environmental properties of motor fuels (diesel and gasoline). First of all the content of sulfuric compounds which form sulfur dioxide during combustion should be reduced. This led to the development of new regulations (The clean air act, 2004; Worldwide fuel charter, 2006), improvement of the industrial process (hydrocleaning) and the development of new technologies of sulfuric compounds removal from petroleum products. However, SO_2 emissions from vehicles is a small part of the total emissions of this harmful compound. Therefore, the above-mentioned measures allowed to reduce sulfur oxide emissions from motor-cars only by few tenths of a percent and from total vehicle – about two percents (see Table 2). Data from Table 2 confirm that heat and electric power production is the main environmental pollutant by SO_2 in the world. The dominant position is occupied by thermal power plants, which use mostly coal.

The reason for such a trend of SO_2 emissions in the atmosphere is extremely high (compared to other fuels) sulfur content in coal. If the sulfur content does not exceed 1.0-1.5 wt % in coal, it is regarded as a low-sulfur one (for comparison, the sulfur content in gasoline and diesel fuel, on average, is 0.00010-0.00005 wt %. There are many fields with a high sulfur content (up to 8-11 wt %). Some countries, including Ukraine, have

reserves of only sulfur and high sulfur coal.

Table 2 The structure of world emissions of sulfur (IV) oxide in the atmosphere, %

Sector	Year			
	2005 (EEA, 2010)	2009 (EEA, 2011)	2010 (EEA, 2012)	2011 (EEA, 2014)
Stationary source	95.0	97.3	96.9	97.3
Including energy production and distribution	62.0	70.2	57.4	58.1
Non-road transport	4.8	2.3	2.9	2.6
Road transport	0.9	0.2	0.1	0.1
Other	0.1	0.4	0.2	0.1

In view of the above, the energy sector has also developed and implemented a number of documents normalizing emissions of harmful flue gas from power stations, including sulfur dioxide, though works were started in this directions as early as in the 30s of the last century.

According to Directive EC (2001), the SO_2 content in the flue gas of new plants should be 200 mg/nm^3 (approx. 160 ppm or 0.007 vol.%), while for the modernized plants with a capacity above 500 MWth and those with a capacity up to 500 MWth, the respective limit values were set at 400 mg/nm^3 (approx. 320 ppm or 0.014 vol.%) and 400-2000 mg/nm^3 (approx. 320-1600 ppm or 0.014-0.07 vol.%). In order to achieve the SO_2 contents in flue gas of 200, 400 or 400-2000 mg/nm^3, the amount of sulfur in raw material should not exceed 0.1, 0.2 and 0.2-1.0 wt %, respectively.

Compliance with the above requirements of regulations regarding SO_2 emissions at thermal power stations is rather complicated from the

technological and economic points of view. The reduction of sulfur dioxide emissions with the flue gas produced during coal combustion can be achieved directly at TPS (by removing SO_2 from combustion products) or by the preventive removal of sulfur from coal.

Black coal with medium metamorphism degree is generally used for coke production but sometimes it may be used as a fuel at TSP (for example if its deposits are far away from the by-product coke plants, or have high ash or sulfur content). Pulverized fuel can be used as well as the obtained coke for cast iron production. In both cases, the sulfur present in coke or coal has a detrimental effect on the coking process, the quality of coke and pulverized coal. For example, when using coke or pulverized fuel with high sulfur content, it is necessary to increase the amount of additives to bind sulfur so that it does not get into the cast iron. Reducing the sulfur content by 0.1% reduces coke consumption by 0.8-3.5% and increases the productivity of the blast furnace by 2-8%. That is why the sulfur content in raw materials (coal) for the production of coke and pulverized fuel is limited to 1-1.5%.

High content of coal sulfur may also be one of the reasons that the production and consumption of coal may be reduced (Figs. 4, 5; BP Statistical Review of World Energy, 2012-2017).

So this monograph is dedicated to the characteristics of coal sulfur, the effect of sulfur on a number of properties of coke, and review of methods of emission reduction of sulfur dioxide produced during coal combustion, incl. coal desulfurization processes.

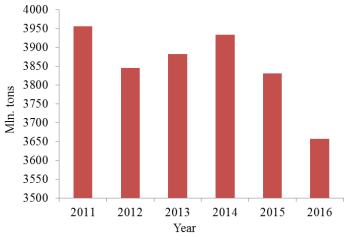

Fig. 4 The pattern of coal production in the

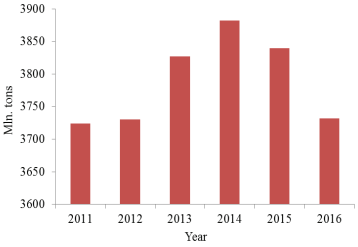

Fig. 5 The pattern of coal consumption

CHAPTER 1
SULFUR IN COAL AND COKE

Denis Miroshnichenko
Department of Technology of Oil, Gas and Solid Fuel Processing, Institute of Chemical Technology and Engineering, National Technical University Kharkiv Polytechnic Institute, Kharkiv, Ukraine

1.1 Methods of decline of sulfur in coke

Economic efficiency of modern domain process to a great extent is determined by quality of coke. For an estimation last most highly sought presently there are methods, characterizing his reactivity, the size of that, in turn, is conditioned by maintenance and by composition of mineral components of coke, in particular, his content of sulfur. So, from data of works [1, 2], increase of maintenance of general sulfur of S^d_t on 1 % results in the increase of reactivity of coke, determined for GOST 10089–89 and for «Nippon Steel» on 0,521cm^3/g·s and on a 17,5 %. Justice of this estimation confirms and circumstance that the increase of maintenance of sulfur in a coke on 1 % results in the increase of his expense on 10–14 % and to the decline of the productivity of high furnace on 8–12 % [3–5].

Taking into account so strong influence of sulfur on reactivity that is examined as integral description of quality of coke [6], it is expedient to analyze the modern state of problem of decline of his.

1.1.1. **Genesis and types of sulfur in coals.** In coals of deposits of Russia the amount of series varies from a few tenth percent in Western and

East Siberia to 8–12 % in Moscow Suburbs and Kizelovsky pools. The sulfur of coals of the Donetsk pool changes from 0,5 to 4,0 and more.

Composition of coal producers, petrographic and chemical composition of coals, composition of containing breeds, and also morphology of coal beds, have influence on the absolute value of total sulfur content. The content of sulfur is directly related to the phenomena of diagenesis, metamorphism, recovery and weathering of coals [7]. Some influence is rendered also by the terms of facies of formation of layers of coal and breeds of roof. So, they as follows stipulated AV maintenance of general sulfur in coals of Donbas [8]:

	S^d_t (middle), % wt
Coastal Continental	1.6
Same with weak sea effects	2.2
Coastal	3.4
- // - with long-term influence of the sea	3.9

Sulfur in coals is in four basic forms, and namely: organic, sulfate, pyrite (marcasite) and elemental. However, for technology goals is most important distinguish pyrite (S^d_p) and organic (S^d_o) forms of sulfur which are also most heavily represented in the total mass of sulfur compounds.

The average content of total, pyrite, organic sulfuric and sulfate sulfur in various coals areas of Donbass are presented in table 1.1 [9].

Their sulfur content in coals propensity for spontaneous combustion. Long the time was dominated by the pyrite theory of self-coal ignition. According to modern ideas the basis of this process is adsorption and chemisorption of oxygen. However complex studies of coal of various degrees of metamorphism in propensity to self-ignition revealed three highs for coal with a carbon content of 76, 85, 89 %, which are characterized, inter alia, and increased content of thioester and disulfide groups.

Table 1.1 The average content of total, pyrite, organic sulfuric and sulfate sulfur in various coals areas of Donbass

Area	Sulfur, %			
	total	pyrite	organic	sulfate
Red Army	2.66	1.50	1.09	0.07
Donetsk-Makeevsky	2.25	1.15	1.02	0.08
Central	3.33	2.23	1.00	0.10
Lysychansky	3.94	2.19	1.58	0.17
Diamond-Maryevsky	3.33	1.93	1.30	0.10
Seleznevsky	2.79	1.69	1.02	0.08
Lugansk	3.66	2.25	1.31	0.10
Belokalitvensky	3.79	2.84	0.85	0.10

With the problem of spontaneous combustion wounds also occur during storage rocks to dumps that are characterized high levels of total and pyrite sulfur. Pyrite sulfur in the process of self-heating of dump oxidizes with sulfating and clean Sulfur.

Between maintenance of general and pyrite sulfur there is cross-correlation dependence [10, 11]:

$$S^d_p=0,737\cdot S^d_t - 0,380; \quad (1.1)$$

$$S^d_p=0,737\cdot S^d_t - 0,377. \quad (1.2)$$

Similarity of equalizations (1.1) and (1.2), shown out at different times for coals of different pools, talks about universality intercommunications of maintenance of general and pyrite sulfur in coals.

In respect of «organic», then this term is designate the sulfur chemically related to the organic substances of coal. Sulfur in these connections is as a sulfide (1), disulfide (2), bistioether (3), thionic (4), thiophene (5), thiophane (6) groupments [12]:

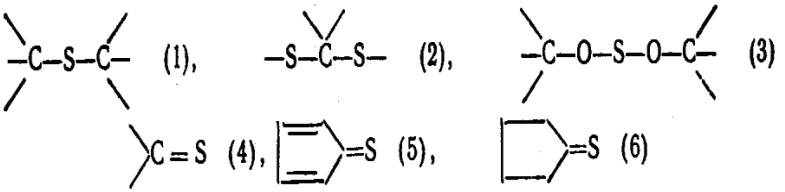

When studying the content of various forms of organic sulfur, the authors of [13] showed that as the degree of metamorphism, expressed by the calorific value, increases, the proportion of aliphatic sulfur decreases and its almost complete transition to an aromatic thiophen-like structure.

Approximately organic sulfur in coal can be calculated by the following equations:

$$S^d_o = 0{,}260 \cdot S^d_t + 0{,}2 \text{ [10]}; \quad (1.3)$$

$$S^d_o = 0{,}250 \cdot S^d_t + 0{,}367 \text{ [11]}; \quad (1.4)$$

$$S^d_o = (0{,}52 \cdot S^d_t + 0{,}15) \cdot (1 - A^d/100) \text{ [8]}. \quad (1.5)$$

It is noted that the proportion of organic sulfur in coal grows with a decrease in its total sulfur content.

Sulfate (sulfates of iron (III), sodium, magnesium and gypsum) and elemental sulfur in total rarely exceed 0.2 % and, therefore, do not have any significant impact on coal processing and quality the resulting coke.

It’s worth adding that high sulfate sulfur content characteristic of oxidized coals.

Coking sulfur behavior.

In the process of coking both mineral and organic sulfur compounds of coals undergo various transformations. According to [14], 45.0–74.9 % goes into coke sulfur, in coke oven gas – from 10 to 29 %, in coal tar – from 0.63 to 1.65 % and in tar water – from 0.4 to 1.5 %.

Conversion of sulfur to volatiles is mainly occurs in a plastic state (350–550 ºC), and during this period, which stood out in coal degradation process free hydrogen, intensely interacts with coal pyrite in reactions:

$$FeS_2+2H=FeS+H_2S \quad (1.6)$$

In the same temperature range occurs and dissociation of pyrite into elemental sulfur and FeS; reduction of sulfates to pyrrotite (possible conversion to organic sulfur) and calcium sulfide formation:

$$CaO+H_2S=CaS+H_2O; \quad (1.7)$$

$$FeS+CaO=CaS+FeO. \quad (1.8)$$

Organic sulfur decomposes and turns into gas evenly until the end of coking, however in the presence of a sufficient amount of pyrite, volatile organic sulfur substances actively interact with products destruction of pyrite sulfur.

Individual organosulfur compounds thermal stability next row [15]:

$$C_2H_5\text{-}SH < CH_3\text{-}S\text{-}CH_3 <$$

$$< C_4H_4S \text{ (thiophene)} < C_8H_6S \text{ (benzthiophene)}.$$

According to [16], the increased thermal stability organosulfur compounds that the sulfur atom can have two, four and six valence bonds. For a break these connections require accumulation much more energy than breaking one simple bonds in a hydrogen molecule or bonds carbon with hydrogen.

Estimates of the effect of sulfur on coke consumption in blast furnaces are very different (up opposite).

So according to [17] with a large content organic sulfur in coke decreases it consumption in a blast furnace (Fig. 1.1).

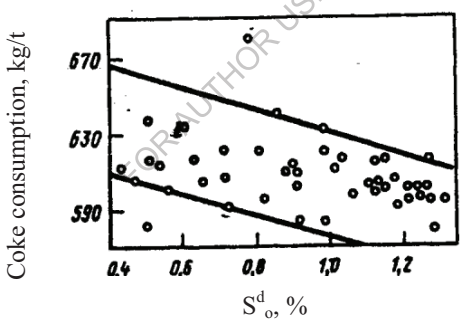

Fig. 1.1 Dependence of coke consumption per 1 ton of pig iron on organic sulfur compounds in coke [17]

According to [22], the change in the content of sulfur of coke in different ways reflect.

It is based on its consumption in a blast furnace (Table 1.2).

As can be seen, with equal sulfur content of coke 1.75 % coke consumption varies from 600 to 750 kg/t, and equal consumption of 600

kg/t achieved at sulfur content of coke 1.75 and 0.55 %, i.e. changing 3 times.

Table 1.2 Coke consumption of coke with different level of sulfur

Metallurgical factory	Coke consumption kg/t of cast iron	Sulfur in coke, %
Zaporizhstal	600	1.75
Cherepovetsky	570	0.52
Magnitogorsk	600	0.55
Petrovsky	750	1.75

The principal course of transformations of sulfur of coke compounds is shown in table 1.3 [18].

The data in Table 1.3 indicate that in coking process enrichment carbon material sulfide, and after 500 ºC and organic sulfur due to decomposition pyrite and sulfate sulfur. Besides, part of the sulfur is released in the form of hydrogen sulfide and volatile organic sulfur compounds. After 500 ºC there is some decrease the proportion of sulfide sulfur in the carbon residue coking coal. Iron sulfide decomposition continues and in a blast furnace, reducing the strength of lumps of coke.

The decomposition of iron sulfide continues in the blast furnace, reducing the strength of lumpy coke. According to the authors of [19], the released sulfur extrudes low-viscosity slag from the pores of coke, which leads to the liberation of the space occupied by sulfides and slag, resulting in a reducing agent gas (CO_2) receives unobstructed access to the internal structure of coke, most intensely destroying her. Possible methods are described below.

Table 1.3 The principal course of transformations of sulfur

Type of sulfur	The content of this type of sulfur (%) at different temperatures, °C				
	Source coal	300	400	500	1000
In solid residue:					
pyrite	1.75	1.75	1.42	0.31	0.00
sulfate	0.71	0.55	0.44	0.01	0.00
sulfide	0.00	0.13	0.44	0.93	0.84
organic	1.79	1.63	1.51	1.70	1.81
Total	4.25	4.06	3.81	2.95	2.65
Stand out in the gas in the form:					
H_2S	-	0.19	0.39	1.20	1.44
organic sulfur compounds	-	0.00	0.05	0.10	0.16

Reduction of coke sulfurization, as in the process coking coal, and with special processing finished coke.

Opportunities for Reducing Coke sulfur. Direct Recovery Intensification pyrite sulfur.

In the presence of hydrogen in coked coal pyrite, passing the stage of transition to sulfide (equation 1.6), is capable of reducing to metal iron [18]:

$$FeS+2H=Fe+H_2S. \quad (1.9)$$

Practical implementation of this method consists in adding to the coal charge organic substances that are intensely decompose in the temperature range

the plastic state of coal to form hydrogen. So, when added to coal 3 % anthracene oil sulfide coke managed to reduce by 0.3–0.5 %. Intensity sulfur release in this case is proportional the amount of pyrite sulfur in the mixture [18].

Contrary to theoretical justification, apparent simplicity and promise, it direction has not yet received practical application.

Addition of Ca-content additions

Essence of this method consists in fastening in accordance with the reactions (1.7, 1.8) of sulfur by Ca-containing additions ($CaCO_3$, CaO, $Ca(OH)_2$) in heat resistant connection – oldgamite (CaS) [18, 19, 21–24]. Although this method and has a row of defects (decline of thickness of plastic layer of charge, increase of temperature of transition of coal grains in the plastic state of and other) [23], however a resulting effect of leveling of negative influence of sulfur content in coke in a high furnace is rather significant and worthy of note.

Application in the domain production of the calcinated coke allows bringing down the expense of gumboils and basicity of slags. Being thermostable connection, oldgamite at passing of horizons of high furnace does not decompose, that assists maintenance of structure of coke. In addition, the direct transmission of sulfur of coke increases in a slag through an ash, passing a gas phase. It is needed to mark that the technic-economic indexes of domain process do not get worse here [21].

Influence of technological factors

To the technological parameters influencing on the degree of desulfurization of coal charge, belong: size of grade of charge, coking

period, eventual temperature, duration of self-control at this temperature, width of chamber, and also height of subroof space.

The authors of review investigated influence of degree of growing of charge shallow on maintenance of sulfur substances in a coke (table. 1.4).

Coking of charge was conducted in 3-kg and 5-kg of laboratory stove on the methodology described accordingly in-process [25] and [9]. Data from table 1.4 testify to that over thinning of grade of charge (Σ3–0 mm) brings to the decline of sulfur in coke (on the average on 0,35 % relative on every percent of increase Σ3–0 mm).

Morally, this effect is investigation of increase of general surface of gas evolution and including sulfur-containing volatile connections.

In-process [26] investigated influence of speed of heating of coals of different brands on a selection from them sulfur connections. It is experimentally set that at identical speed of heating on desulfurization considerably the degree of metamorphism of coals influences and, consequently, properties of their organic mass, thus more intensively the process of desulfurization flows at less metamorphosed coals high-yield volatiles, including sulfur-containing. With the increase of speed of heating of coals from 2,5 to 10,0 hail/of mines the degree of desulfurization of coal goes down, thus in a greater measure for less metamorphosed coals.

In a table 1.5 data are presented [27], reflecting influence of coking terms on the process of desulfurization.

With the increase of coking speed a from 13,6 to 14,6 mm/hour grows short time of stay of coals in the plastic state, destruction of sulfur connections intensifies with formation of secondary connections of sulfur, different enhanceable heat resistance. The sulfur of coke rises in the total [27].

Table 1.4 Influence of sieve content of coal blend

№	The sulfur content of the charge, $S^d_{t,}$, %	Coke sulfur, $S^d_{t,c}$, % from the charge of grinding (Σ3–0 mm),%		$S^d_{t,c}$ (80% (Σ3–0 mm)) $S^d_{t,c}$ (100% (Σ3–0 mm))
		80	100	
1	1.54	1.28	1.26	1,02
2	1.04	0.84	0.81	1,04
3	1.96	1.56	1.52	1,03
4	1.50	1.39	1.25	1,11
5	1.35	1.29	1.20	1,08
6	1.55	1.25	1.21	1,03
7	2.17	1.53	1.50	1,02
8	1.40	1.02	0.88	1,16
Mean		1.27	1.20	1.06

This effect is not observed at large maintenance in the charge of less metamorphosed coals. So, at the individual coking of coal of brand of G of «Mikhailovskaya» degree of desulfurization at the height of speed of coking did not change (fig. 1.2) practically [28].

Because the width of the stove chamber and coking period are directly constrained at a speed of coking, then data of researches about influence of coking speed on the process of desulfurization can be with the well-known stake of approaching carried and on these technological parameters.

The increase of temperature of subroof space also results in the height of dissociation of the sulfuretted hydrogen, that in turn, assists absorption the coke of becoming free sulfur [16].

Table 1.5 Influence of coking terms on the process of desulfurization

Indicators	Battery A	Battery B
Coking period, h	16.5	14.0
Chamber width, mm	450	410
Chamber height, m	5.0	5.5
Coking rate, mm/h	13.62	14.64
Sulfur content,%:		
Charge	2.2–2.3	2.01–2.2
Coke	1.73–1.81	1.81–1.83
Desulfurization coefficient	0.78	0.82

The table of contents of sulfur depends on the location of coke in a coke chamber. So, it is experimentally confirmed that maintenance of sulfur in a coke pie rises to direction from an axis to the walls of the stove chamber. It contingently the secondary reactions of sulfur-containing volatile connections with a burning hot coke in zones with more high temperature. For their braking there are authors [29] suggest to decrease a temperature gradient on length and height of coke pie.

Method of extinguishing of coke.

Influence of method of extinguishing of coke on distribution of sulfur on length of piece (from head to axial of his part) is studied in-process [30] (table 1.6).

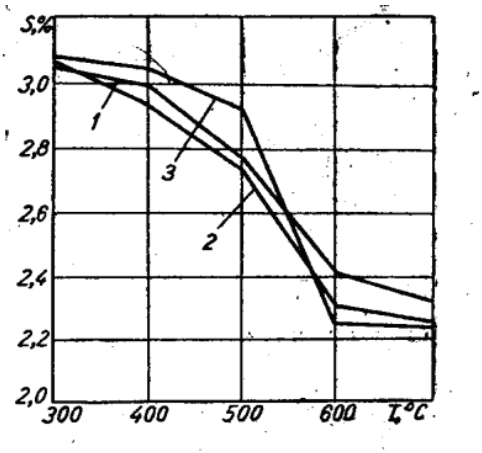

Fig.1.2 Dependence of maintenance of sulfur in a hard remain from an eventual temperature and speed of heating: 1 – 3 °C/min; 2 – 5 °C/min; 3 – 10 °C/min

As be obvious from a table 1.6, maintenance of general Sulfur in cokes grows in a row: dry extinguishing, extinguishing by technical water and extinguishing by phenic water. At extinguishing by technical water it is explained by the presence of high ash and high-sulfureous coke dust, and at extinguishing by phenic water-enhanceable maintenance in her salts of Na_2SO_4 and $Na_2S_2O_3$. Negative influence on quality of coke is related to the presence in phenic water of ions of both sulfur and sodium, that it is marked in [31] and accompanied by the increase of PC of coke.

These tables 1.6 testify that at the dry extinguishing organic sulfur is mainly concentrated in paraxial and middle, and sulfide – in head part of piece of coke.

Dependence of maintenance of types of sulfur on the largeness of coke is shown in a table 1.7 [16].

Table 1.6 Influence of method of extinguishing of coke on distribution of sulfur on length of piece

The mixture,%: G-50; Zh-15.1; K-17.0; OS-17.9												
quenching	dry				process water				phenolic water			
coke	source	head part	the middle	paraxial part	source	head part	the middle	paraxial part	source	head part	the middle	paraxial part
S^d_t, %	1.70	1.70	1.80	1.70	1.80	1.70	1.90*	1.80	2.01*)	2.10	2.00*)	2.10
S^d_s, %	0.23	0.36	0.12	0.23	0.26	0.30	0.33	0.15	0.24	0.24	0.33	0.14
S^d_o, %	1.49	1.32	1.66	1.45	1.47	1.37	1.44	1.62	1.59	1.58	1.48	1.70
S^d_{SO4},%	0.02	0.02	0.02	0.02	0.03	0.03	0.03	0.03	0.26	0.28	0.25	0.26
Remarks: [1]In the marked variants of $S^d_s + S^d_o + S^d_{SO4} \neq S^d_t$ (from data [29])												

Table 1.7 Dependence of maintenance of types of sulfur on the largeness of coke

Coke size, mm	Sulfur content, %			
	total	sulfide	elemental	organic
40–25	1.74	0.36	0.08	1.30
60–40	1.69	0.41	0.05	1.23
80–60	1.63	0.34	0.10	1.19

Enhanceable maintenance of general sulfur in more shallow class of largeness is conditioned, morally, by destruction of general structure of coke on the places of disseminations of mineral components, including sulfur-containing.

Physical and chemical treatment of coke.

In works [16, 32] investigated possibilities of treatment of coke different gases at enhanceable temperatures, and also heat treatments without application of reagents.

The system with new thermodynamics potential, the power level of that becomes higher (there is it because of aromatization of carbon structure – the AV amount of aromatic rings of carbon kernel increases from 7,2 to 1160), appears at the reheat of coke. If here energy of the thermal field becomes to commensurable with energy connection at the atom of sulfur, then terms at that the break of these connections and atoms of sulfur come freed are created [16, 32].

Experience is known of oil workers, reducing sulfur of petroleum coke at his calcining to the temperatures of 1500–1600 ^{o}C [33]. Authors [34] it is well-proven that under reaching the temperature of 2100–2200 ^{o}C of sulfur in a coke does not remain practically. Detailed study was undertaken a by the authors of work [16]. In a table 1.8 calcining over of coke (60–40 mm) given about influence of temperature is brought on distribution in him different types of sulfur (time of calcining is 60 mines).

Calcination of coke conduces to the decline of his sulfur thus, sulfide sulfur (37 % her retires already at calcining to 1100 ^{o}C) retires most full. In addition, it is set that calcining of coke of less largeness is most effective, because of his greater specific surface.

One of ways of decline of sulfur is treatment of coke gaseous reagents. So, at treatment of coke of different largeness by aquatic steam, hydrogen, chlorine and other gases at 1000 ^{o}C total sulfur of coke it maybe to bring down on 0,3–0,5 % abs. By the same gases, but at 1700 ^{o}C it is succeeded practically fully to delete sulfur from a coke [18].

Table 1.8 Sulfur content

Temperature calcination	Sulfur content by type, %			
	total	sulfide	organic	elemental
Before calcining	1.69/100	0.41/24.3	1.23/72.8	0.05/2.9
1100 °C	1.45/100	0.26/17.9	1.14/78.6	0.05/3.5
1300 °C	1.38/100	0.18/13.0	1.15/83.3	0.05/3.7
1500 °C	1.30/100	0.13/10.0	1.12/86.2	0.05/3.8
Remarks: [1]The absolute are presented in a numerator, and in a denominator relative values				

In-process [35] it is shown that practically feasibly moving away of sulfide sulfur at blowing out of bulk coke by water-wet air during 3–5 minutes at 900–1000 °C on a reaction:

$$FeS+H_2O=FeO+H_2S \quad (1.10).$$

Thus, adding to air of ammonia results in the increase of efficiency of sulfur release. It is explained by dissociation of ammonia with formation of atomic hydrogen that intensively co-operates with sulfur. Application of this method allows to bring down sulfur of coke on 0,1–0,2 % abs. [36, 37].

Described in [18, 35–37] the methods of decline of sulfur by treatment of coke aquatic steam and different gases are worked out 50–70 back, but practical application was not got.

Along with the technological receptions used for desulfurizing of coke, it is needed to mention also about a magnetic separation on more and less ash and sulfur factions. So, in-process [38] results over of magnetic separation of semicoke are brought from coals of pool of Moscow Suburbs. Authors succeeded to obtain the decline of sulfur on 3,68 % (abs.). It happened because of transformation of unmagnetic pyrite in connections,

possessing ferromagnetic properties and, first of all, in pyrrotite. Pyrrotite (in mixture with coal) got at heating has a grate with an imperfect structure and the formula of him looks as

$$Fe^{2+}_{1-3\delta}\, Fe^{3+}_{2\delta\,\delta}$$

where δ are vacancies.

Adding up the stated higher, it should be noted that possibility of practical realization of each of the indicated methods of decline of sulfur of coke (or their combinations) must be confirmed by the economic evaluation of the expected effect, with an account as additional expenses are in the production of coke, so declines of his expense in a domain process due to improvements of quality on the indexes of reactionary ability and thermomechanical durability of coke.

1.2 Sulfur in coal and its influence on the quality and consumption of coke in the blast furnace

The method of evaluating coke quality developed by Nippon Steel Corporation (NSC) has an indisputable benefit, as well as the deficiencies noted in [39–41]: it permits more profound study of the role of mineral components of the coal—in particular, sulfur compounds—in creating the physicomechanical and physicochemical properties of the coal.

Sulfur is a major component (a macrocomponent) of the mineral phase in coal, since it is present in a quantity greater than 1000 g/t of solid fuel; other macrocomponents are silicon, aluminum, iron, calcium, magnesium, sodium, potassium, and titanium. However, sulfur is not regarded as one of the basic ash-forming elements [42]. This view needs to be revised, for the following reasons.

1. From purely formal considerations, the sulfur content in the ash of many coals from different countries matches and often exceeds the content of Mg, K, or Na, which are regarded as basic ash-forming elements. Sometimes, the sulfur content exceeds the total content of these elements (Table 1.9).

Table 1.9 The total content of the main elements

Country	Mine or enrichment facility	Content in ash,[1] %			
		Mg	Na	K	S
1	2	3	4	5	6
Ukraine	Yuzhno-Donbasskaya No. 1 mine	0.54	0.67	0.70	0.62
	Stepnaya mine	0.50	0.92	0.93	0.93
	Yubileinaya mine	1.21	0.61	1.36	1.07
	Yasinovskaya-Glubokaya mine	0.50	1.97	0.61	0.78
	Kievskaya facility	0.50	1.29	086	1.04
	Samsonovskaya facility	0.50	0.70	0.83	0.95
	Komsomol'skaya facility	0.50	1.22	0.75	1.19
	Kalininskaya facility	0.60	0.58	0.74	1.00
	Proletarskaya facility	0.40	0.91	0.44	0.81
	Chumakovskaya facility	0.90	0.90	1.72	1.01
Russia	Zarechnaya mine	1.61	1.85	1.97	1.63
	Lakochitinskaya mine	0.70	0.79	0.60	2.45
	Esaul'skaya mine	0.76	1.43	1.80	1.36
	Bol'shevik mine	0.45	0.22	0.85	1.10
	November 7 mine	1.31	0.51	1.99	1.40
	Abashevskaya facility	0.76	1.10	1.82	1.43
	Raspadskaya facility	1.01	1.10	1.52	1.95
	Antonovskaya facility	1.41	1.03	1.31	2.32
	Vakhrushevskii mine	0.50	0.42	1.37	1.67
	Tomusinskii mine	1.00	1.67	0.59	2.58

1	2	3	4	5	6
	Mezhdurechenskii mine	1.06	1.53	0.64	2.24
	Kaa-Khemskii mine	3.02	0.77	0.51	3.72
USA	Mitsubishi Corporation	0.33	0.22	1.46	0.80
	Cucumber	0.62	0.40	0.99	1.85
	Enterprize	0.54	0.69	1.56	2.20
	Itochu	0.83	0.43	1.37	4.22
Australia	Norwich Park	0.45	0.55	0.80	0.55
	Carbonwall Inalta	0.40	0.70	2.42	0.46

Remarks:

[1] Calculated from the content of the *i* the oxide in the zone and from the mass content of Mg, Na, K, and S in the oxide (40, 73, 83, and 40 wt %, respectively).

2. The SO_3 content in the ash has a much stronger influence on the postreactive strength of the coke (CSR) determined by the NSC method than factors such as the packing density of the batch and the coking rate: 1% change in the SO_3 content in the ash changes CSR by – (20–24) % (abs.) [43].

3. As the coke passes from upper to lower levels of the blast furnace, the sulfur content in the coke ash practically quadruples (from 0.90 to 3.25 wt %), which is comparable with the change in content of alkali metals K + Na (from 2.36 to 10.69 wt %). By contrast, the silicon, iron, and aluminum content declines, while the change in the calcium and magnesium content is less than for sulfur [43].

The increase in the content of sulfur and alkali metals in the coke ash correlates with the practically nine fold increase in reactivity of the coke between the upper and lower levels of the blast furnace (from 0.14 to 1.22 ml/g·s) [43].

Together with the need to increase the temperature so as to permit more effective desulfurization of the hot metal, this increases the consumption of coke with a higher sulfur content in its ash.

Analysis of the reasons for the poor quality of Ukrainian coke in tests by the NSC method indicates a close relation between the total sulfur content in the batch S^d_t (by mass) and CRI of the coke

$$CRI = 12.37\ S^d_t + 25.92. \quad (1.11)$$

While it permits satisfactory prediction of CRI, with subsequent calculation of CSR by the generalized formula

$$CSR = 94.23 - 1.275CRI, \quad (1.12)$$

Eq. (1.11) does not reveal the physical significance of the relation between the coke quality and the total sulfur content in the batch, since the total sulfur content includes many forms of sulfur, including volatile compounds that do not enter the coke.

In addition, in coking, some types of sulfur are converted to other types, as shown in Table 1.10 (based on data from [45]).

The content of sulfate in the coal is small and remains basically constant on coking, whereas pyrite, which accounts for more than 70 % of the total sulfur in the given coal, breaks down to form thermostable sulfides and organic sulfur.

Table 1.10 Change in sulfur-compound content during heating

Form of sulfur	Change in sulfur-compound content[1], %			
	1		2	
	in coal	in coke	in coal	in coke
Total sulfur, S^d_t,	1.85	1.50	2.04	1.67
including:				
sulfate sulfur S^d_{SO4}	0.05	0.04	0.07	0.06
pyrite sulfur S^d_p	1.31	–	1.55	–
sulfide sulfur S^d_S	–	0.57	–	0.63
organic sulfur S^d_O	0.49	0.89	0.42	0.98
	total	1.50	total	1.67
volatile sulfur S^d_V	–	0.35	–	0.37
	Total	1.85	–	2.04

Remarks:

[1]Columns 1 and 2 correspond to the coking of Donetsk coal of ranks G + Zh and K, respectively.

In examining the relation between the total sulfur content in the coal and the coke quality (CRI and CSR), a large sample (n=156) characterizing S^d_t and the chemical composition of the ash in Donetsk and L'vov–Volynsk Basin coal and anthracite was subjected to statistical analysis in [41].

The analysis showed that we may speak with high probability (0.999) of a correlation between the total sulfur content (by mass) and the content of ferric oxide (Fe_2O_3) and calcium oxide (CaO) in the ash. These materials are catalysts of the gasification of carbon. On this basis, the relation between S^d_t for the coal and CRI and CSR for the coke may be

regarded as a reflection of the average influence of the iron and calcium compounds on the coke quality [41].

Thus, the mathematical models describing CRI (CSR) S^d_t of the coke may be differentiated in terms of for the batch [46]. This is consistent both with the predominant content of pyrite in Donetsk coal and of organic sulfur in Kuznetsk coal and with the different ash composition of the coal from these basins.

For batch where Donetsk coal predominates and correspondingly $S^d_t>1$, the model

$$CRI=14.18+12.39\cdot S^d_t+0.376\cdot V^{daf}, \quad (1.13)$$

is recommended; for batch where Kuznetsk coal predominates and correspondingly $S^d_t<1$, the model

$$CRI = 13.4 - 0.45\cdot(B_o)^2 + 9.35B_o. \quad (1.14)$$

is recommended. Here B_o is the basicity index of the ash, which is calculated from data on its chemical composition using the ratio of the total content of the basic oxides (Fe_2O_3, CaO, MgO, Na_2O_3, and K_2O) to the total content of acidic oxides (Al_2O_3 and SiO_2).

The largest oxide component Fe_2O_3 in the coal ash is formed from different iron compounds—primarily FeS_2.

The dependence of CRI and CSR on the Fe_2O_3 content in the ash of production batches at Ukrainian plants, in the ash of experimental batch with Russian coal from the Antonovskaya and Sibir enrichment facilities (according to the data of [47]), and in the ash of some US and Australian coal (according to quality-certificate data) is illustrated in Fig. 1.3.

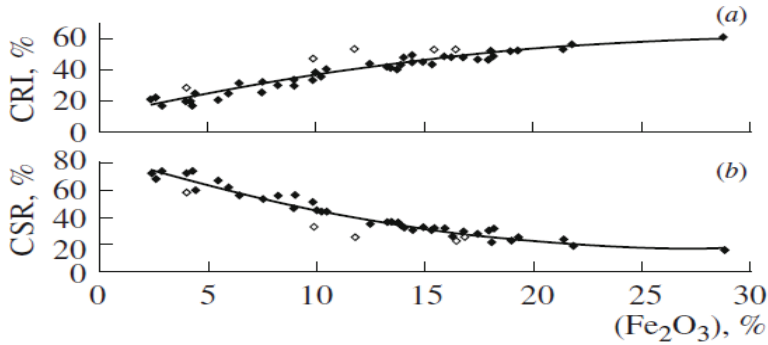

Fig. 1.3 Dependence of CRI (a) and CSR (b) of coke on the Fe_2O_3 content in the ash of the coal batch: ♦ – Ukraine coal; ◊ – other coal

The second-order regression equations

$$CRI = 10.11 - 0.0505(Fe_2O_3)^2 + 3.192(Fe_2O_3), \quad (1.15)$$

$$CRI = 86.25 + 0.0917(Fe_2O_3)^2 - 5.033(Fe_2O_3) \quad (1.16)$$

with multiple correlation coefficients 0.947 and 0.962, respectively, determine approximately 90% of the measured CRI values and 93% of the CSR values for the coke, with a mean square error of prediction σ=3.9%. The calculated and experimental values of CRI and CSR are compared in Fig. 1.4.

The mean square deviation σ of the calculated and experimental values is comparable with the permissible measurement errors for CRI and CSR according to the ISO 18894:2006 (E) standard: ≤3.0 (3.5) % for CRI and ≤3.0 (3.5) % for CSR (depending on the absolute values of CRI and CSR).

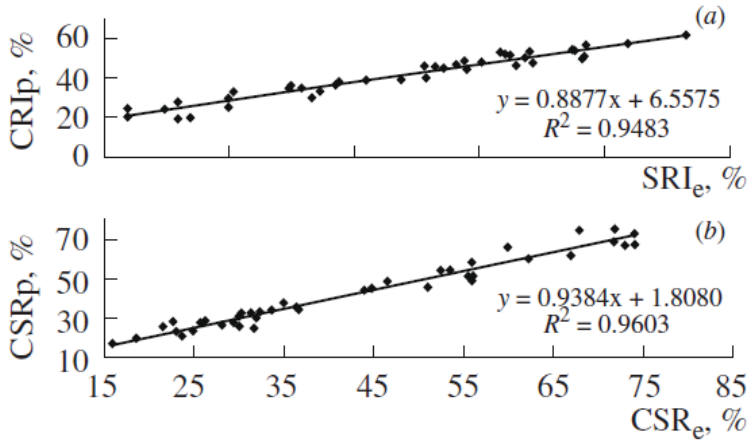

Fig. 1.4 Experimental and calculated values of CRI (a) and CSR (b) for the coke

The relation between CRI and CSR (Fig. 1.4) in the selected sample is described by the linear regression equation

$$CSR = 983 - 1.42CRI;\ r^2 = 0.9809;$$
$$r = 0.9904;\ \sigma = 3.1\%. \qquad (1.17)$$

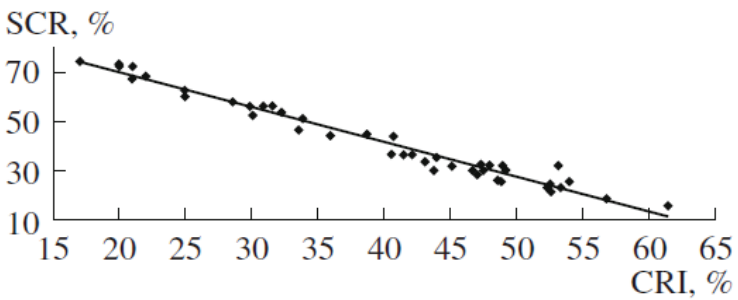

Fig. 1.5 Relation between the experimental CRI and CSR values for the coke

The unfavorable influence of pyrite on coke quality has been confirmed by a direct experiment, with the introduction of 0.7 and 1.4 wt % FeS_2 in the batch [48]. In comparison with coke from the basic batch, this is associated with decrease in mechanical properties of the coke (greater crumbling and wear) and deterioration in CRI (increase by 7.3 and 10.9 %) and CSR (decrease by 9.4 and 18.4 %).

A hypothetical mechanism by which pyrite influences the coke properties has been proposed [48]. According to this mechanism, FeS + Fe alloy is formed on coking the coal and melts on repeated heating of the coke (t_m = 985 °C), with an accompanying increase in stress, crack formation, and reactivity.

In comparison with the terms in Table 1.10, the fuel sulfur in coal S_C and ash sulfur in coal S_A are much less commonly used in coal and coke chemistry. These are defined, respectively, as the component of the total sulfur converted to gaseous oxides and the component remaining in the ash after complete coal combustion [49]. Fuel sulfur in the coal is released to the atmosphere in the form of SO_2 and SO_3, with the smokestack gases, and its minimization is a serious concern of energy specialists and ecologists [50]. The ash sulfur in coal has a great influence on the efficiency of fuel combustion and is taken into account in selecting slag- and ash-removal systems and designing furnaces.

In the blast furnace, ash sulfur is regarded as an undesirable component in coke, impairing its quality and increasing its consumption in hot-metal production. Therefore, estimating how much of the sulfur in the coal will be converted to sulfur trioxide is of great practical importance.

No method yet exists for direct determination of S_C, while the SO_3 content in the ash is determined from State Standard GOST 20538–87 [51]

and then converted to S_A by multiplication by the factor 0.4 (the mass content of sulfur in the SO_3). On the basis of S_A, in turn, the formula

$$S^*_{co} = A^d S_A/100, \quad (1.18)$$

where A^d is the ash content of the coal, provides an estimate of the coal's content of sulfur that is converted to SO_3 on combustion.

The quantity of fuel sulfur in the coal may be calculated from the balance equation for the total sulfur content in the coal

$$S^d_t = S_C + S^*_{co} \quad (1.19)$$

Statistical analysis of a sample containing coal from Ukraine, Russia, the USA, and Australia (Table 1.11) shows that the limiting A^d values of all the coal are relatively close, as are the limiting values of Russian, US, and Australian coal. For Ukrainian coal, S^d_t is much larger (four times larger at the lower limit, and 2.5 times larger at the upper limit).

The CaO content is much less for the ash of Ukrainian coal (by a factor of 3–6 at the upper limit), while its Fe_2O_3 content is larger. The SO_3 content in the ash of Ukrainian coal varies within a relatively narrow range (by a factor of 3.5, as against an order of magnitude for Russian, US, and Australian coal).

In the sample as a whole, only the relation between the content of calcium oxide and sulfur trioxide in the ash is statistically confirmed for the whole sample (Fig. 1.6a) with statistical estimates $R = 0.942$, $R^2 = 0.887$.

Table 1.11 Quality of coal and ash composition

Quality of coal and ash composition, %	Range		
	Ukraine	Russia	USA and Australia
A^d	7.7–10.5	6.5–11.0	6.3–10.0
S^d_t	1.04–2.17	0.28–0.90	0.30–0.86
CaO	1.16–4.21	1.05–23.83	0.20–11.95
Fe_2O_3	5.98–32.93	3.95–27.43	2.4–16.31
SO_3	1.05–3.68	0.12–9.29	0.10–7.75
n	26	17	11

$$(SO_3)_A = -0.0173(CaO)^2 + 0.8107(CaO) - 0.2183 \quad (1.20)$$

Converting the CaO content in the ash to the Ca content in the coal, and the SO_3 content in the ash to S^*_{co} in the coal, on the basis of Eq. (8), we may conclude that S^*_{co} is no more than 10 % of S^d_t in Ukrainian coal (Fig. 1.6b), as against 40% or more for many types of Russian coal and some types of US and Australian coal; sometimes, S^*_{co} and S^d_t are practically the same.

Thus, in Russian coal from the Kaa-Khemskii and Lakochitinskaya mines, S^*_{co} is more than 95 % (rel.) of $S^*_{co.}$

The differences in S^d_t and the SO_3 and CaO content for Ukrainian coal and the other coal considered (noted in Table 1.10 and in the text) are fundamentally due to the different distribution of the total sulfur content among the fuel component S_C and sulfur entering the ash S^*_{co}.

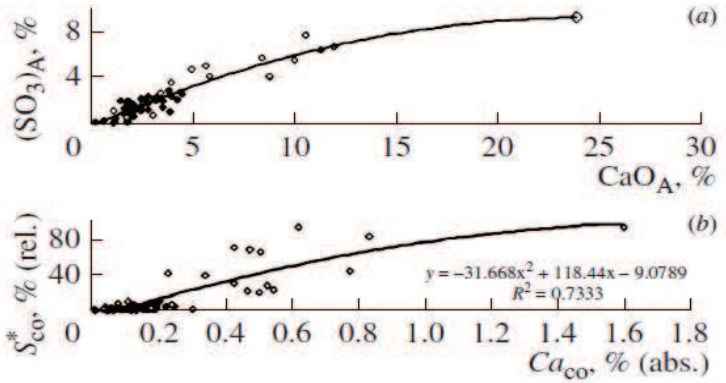

Fig. 1.6 Relation between the content (abs. %) of calcium oxide and sulfur trioxide in coal ash (a) and the content of calcium (abs. %) and S^*_{co} (% of S^d_t) in coal (b): ♦ – Ukraine coal; ◊ – other coal

It is evident from Figs. 1.6 and 1.7 that Ukrainian coal with a relatively low CaO content in the ash (<4.5 %) and Ca content in the coal (<0.30 %) is characterized by increase in the absolute content of S_C and S^*_{co} in the interval $1.0 \le S^d_t \le 2.2$ %; S_C is always more than 95 % (rel.) of S^d_t, whereas is no more than 5 % (rel.) of S^d_t. The graphs in Fig. 1.7 may be approximated by first order equations.

In Russian, US, and Australian coal with <8 % CaO in the ash (Fig. 6a), the S_C content increases in the range $0.28 \le S^d_t \le 0.90$ % and is always greater than in coal with 8–24 % CaO in the ash (Fig. 1.8b).

The curves in Fig.1.8 may be described by second-order equations with a large correlation coefficient ($R > 0.988$). Conversely, the absolute value S^*_{co} in these coals declines with increase in S^d_t and is always less in coals with a reduced CaO content in the ash (Fig. 1.9). When $S^d_t <$ 0.5 %, is 60–95 % (rel.), i.e., predominates in S^d_t, whereas the content of S_C declines from 40 to 5 % (rel.).

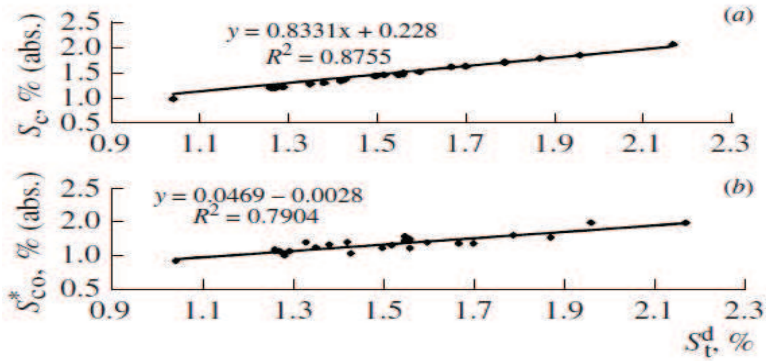

Fig. 1.7 Content of fuel sulfur (a) and sulfur passing to ash (b) as a function of the total sulfur content in Ukrainian coal

The share of S^d_t corresponding to S^*_{co} is greatest (98 %) for Russian coal from the Kaa-Khemskii mine, with the maximum CaO content in the ash of all the coal considered (23.83 %).

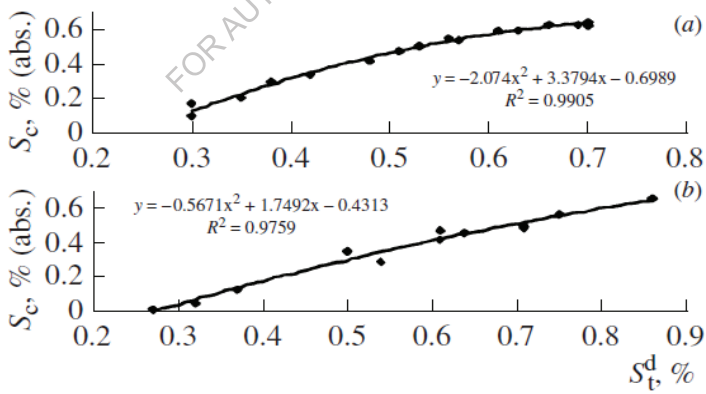

Fig. 1.8 Relation between the total sulfur content and fuel-sulfur content in coal imported to Ukraine: (a) with <8 wt % CaO in the ash; (b) with >8 wt % CaO in the ash

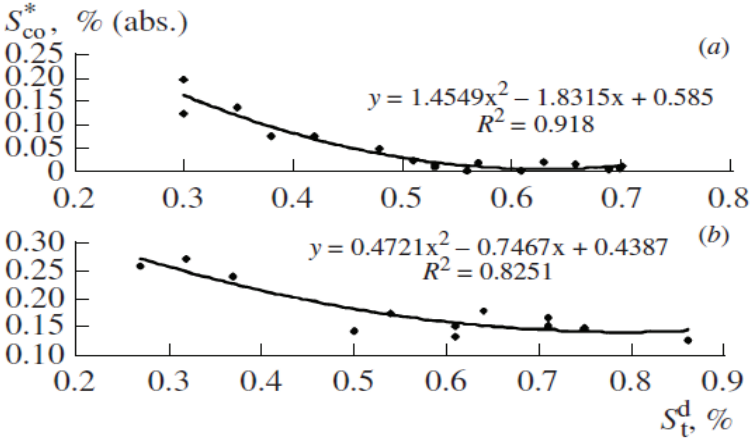

Fig. 1.9 Relation between the total sulfur content and the content of sulfur that enters the ash, in coal imported to Ukraine: (a) with <8 wt % CaO in the ash; (b) with >8 wt % CaO in the ash

This distribution of the total sulfur content among the S_C and S^*_{co} forms is probably due to the intense reaction of fuel sulfur with calcium, to form thermostable compounds $CaSO_4$, CaSO3, and CaS in the coal ash. However, this remains an open question, pending further research. Nevertheless, the presence of an increased content of sulfur compounds that pass to the ash in the low-sulfur coal presently or prospectively used for coking in Ukraine is of considerable interest.

Comparison shows that Ukrainian coal with up to 2.17 % S^d_t contains ≤0.10 % (abs.) of S^*_{co} (Fig. 1.7b), whereas coal from other countries with up to 0.90 % S^d_t contains ≥0.17% (abs.) S^*_{co} (Fig. 1.9b), i.e., increasing the content of imported coals in Ukraine coking batch, as well as decrease in S^d_t of the batch and hence in S^d_t of the coke, may be accompanied by increase in sulfur content in the ash for both the batch and the coke.

This agrees with the finding that the residual sulfur coefficient increases: in coking batch with S^d_t=2.2 and 0.40 %, the residual sulfur coefficient increases from 0.78–0.81 to 0.85–1.00, respectively, according to [52].

Greater content of thermostable sulfur compounds in the coal increases the thermostability of the sulfur compounds in the coke, the sulfur concentration in the gas phase within the tuyere zone of the blast furnace, and hence the sulfur content in the hot metal [53].

Thus, for the example of Rustav metallurgical plant, it has been established that increasing the proportion of Donetsk coal increases the sulfur content of coking batch $S^d_{t,b}$ from 1.20 to 1.85% and the sulfur content of the coke $S^d_{t,cok}$ from 0.90 to 1.50%, but the coke consumption in hot-metal production is reduced by ~12 kg/t of hot metal, rather than increasing [45]. This result, which seems to paradoxical at first glance, may be attributed not so much to improvement in the mechanical properties of the coke as to decrease in the sulfur content in coke ash on account of the high content of fuel sulfur in Donetsk coal, according to [45].

In our view, the increasing proportion of imported low-sulfur coal, especially coal with an elevated calcium content, in Ukrainian coking batch calls for research to refine the existing standard, according to which 0.1% decrease in sulfur content of the coke is equivalent to 0.3 % decrease in its consumption and a corresponding increase in blast-furnace productivity [54, 55].

Thus, the use of more imported coal in coking batch may unfavorably change the ratio of different forms of sulfur in the coal batch: in particular, it may increase the content of thermostable forms that enter the ash on coke combustion. This may considerably reduce the expected

effect of decreasing the total sulfur content in the coke, i.e., the expected decrease in coke consumption in hot-metal production.

1. Analysis of the quantitative ratios of elements in the ash of Ukrainian, Russian, US, and Australian coal indicates that sulfur is one of the basic ash-forming elements, along with magnesium, sodium, and potassium.

2. Ukrainian coal is characterized by increased iron content, primarily in the form of pyrite FeS_2, with a limited calcium content, on account of the predominance of fuel sulfur S_C in the total sulfur content of the coal.

3. Much of the low-sulfur coal imported to Ukraine for coking is characterized by increased calcium content. As a result, thermostable sulfur compounds that pass to the ash (S^*_{co}) will predominate in the coal's total sulfur content.

4. As a consequence of Ukraine's considerable and constantly rising imports of low-sulfur coal for coking, including coal with an elevated calcium content, together with the decrease in S^d_t in the batch and the coke, the proportion of sulfur passing to the ash may increase. This could slow the expected decrease in coke consumption during hot-metal production. There is evidently a need for research to refine the standards regarding the influence of sulfur in coke on its consumption in hot-metal production and on the blast-furnace productivity.

1.3 Relationship between sulfur compounds in coal with coke quality

In [56], the results of the analysis of the quantitative ratios of elements in the ash of the studied coals of Ukraine, the Russian Federation,

the USA, and Australia showed that sulfur can be attributed to the main ash-forming elements along with magnesium, sodium, and potassium.

It has been shown that Ukrainian coals are characterized by an increased iron content, mainly in the form of FeS_2, with a limited calcium content, which accounts for the predominant proportion of combustible sulfur (S_C) in the total sulfur of coal.

It has been established that many of the low-sulfur coals brought into Ukraine for coking are characterized by a high calcium content, which accounts for the predominant share of heat-resistant sulfur compounds that are part of the ash (S^*_y) in the total sulfur of coals.

An important assumption has been made that a large and increasing volume of low-sulfur coals imported into Ukraine for coking, including coals with a high calcium content, along with a decrease in the S^d_t of the charge and coke, may be accompanied by an increase in the proportion of sulfur that is converted to ash. In this case, a possible slowdown in the expected decrease in coke consumption in pig iron production, which stimulates work to clarify the standards for the influence of coke sulfur on its consumption and blast furnace productivity.

Given the fact that the work [56] was published in 2008, it is of interest to evaluate the previously obtained dependencies using the example of a modern raw material base PJSC Evraz-Dneprodzerzhinsky KHZ.

Table 1.12 shows the change in the share of Ukrainian and imported coal in the raw material base of plants in 2010–2014 [57].

From the above data it is seen that the share of Ukrainian coals in the raw material base of coking of coke-chemical enterprises of Ukraine (including PJSC Evraz-Dneprodzerzhinsky KHZ) over the past 5 years has decreased from 65.7 to 45.8 % or 19.9 %; the share of Russian coal increased from 24.3 to 33.0 % or by 8.7 %.

Table 1.12 Dynamics of changes in the share of Ukrainian and imported coal in the raw material base of Ukrainian plants in 2010–2014

Year	Ukraine	Russian Federation	Kazakhstan	USA + Australia + Canada	Other[1]
2010	65.7	25.2	3.0	5.8	0.3
2011	62.0	24.3	2.6	11.0	0.1
2012	52.3	30.3	3.3	13.2	0.9
2013	50.9	32.5	2.5	13.1	1.0
2014	45.8	33.0	3.9	16.4	0.9

Remarks:

[1]Other: Poland, Czech Republic, Colombia, Indonesia, Iran, Abkhazia

In general, the share of non-CIS coals (USA, Australia, Canada and others) for the period under review increased from 6.1 to 17.3 % or by 11.2 %.

Table 1.13 shows the quality indicators of the coals investigated in the CPL of PJSC Evraz-Dneprodzerzhinsky KHZ, which are part of the enterprise's raw material base. In particular, indicators of technical analysis (A^d ash and S^d_t total sulfur content), sulfur content (S_A) and calcium (Ca) in ash, coal content of that type of sulfur (S^*_y), which, when converted to ash, transforms to SO_3, are given the percentage of sulfur transferred from coal to ash (S^*_y/S^d_t), as well as reactivity (CRI) and post-reaction strength (CSR) of coke obtained by individual coking of the studied coals in the Karbotest furnace. In addition, table 1.13 shows the maximum (max), minimum (min) and average (mean) values of the quality indicators.

Table 1.13 Coal quality indicators

Provider	Grade	Proximate analysis of coal, %		The content of components in the ash, %		S_y^*, %	$S_y^* \cdot 100/S_t^d$, %	CRI, %	CSR, %
		A^d	S_t^d	S_A	Ca				
1	2	3	4	5	6	7	8	9	10
Ltd «Promugolservice», RF, pr. 1	G	9.1	0.55	0.38	2.76	0.03	6.29	44.5	31.3
Ltd «Promugolservice», RF, pr. 2	G	7.9	0.42	0.73	2.13	0.06	13.73	44.9	26.3
Ltd «Promugolservice», RF, pr. 3	G	7.9	0.46	0.73	2.13	0.06	12.54	48.2	30.0
EF(Enrichment Factory) «Dzerzhinskaya», RF	G	8.1	0.45	1.26	5.51	0.10	22.68	42.5	28.5
EF «Sholokhovskaya», RF, pr. 1	G	8.1	0.51	0.89	2.00	0.07	14.14	44.0	28.6
EF «Sholokhovskaya», RF, pr. 2	G	8.4	0.50	0.89	2.00	0.07	14.95	48.2	21.6
1	2	3	4	5	6	7	8	9	10
EF «Schedrukhinskaya», RF	G	8.9	0.43	1.53	5.08	0.14	31.67	44.1	38.6
CEF «Komsomolskaya», Ukraine, pr. 1	G	8.7	1.36	1.27	2.51	0.07	3.50	44.0	28.5
CEF «Komsomolskaya», Ukraine, pr. 2	G	8.8	1.90	2.04	4.13	0.14	8.01	59.8	19.2
CEF «Dobropolskaya», Ukraine	G	8.3	1.70	1.64	4.63	0.07	3.00	53.2	19.2

1	2	3	4	5	6	7	8	9	10
EF «Pechorskaya», RF	GFL	8.7	1.23	0.81	3.15	0.09	5.15	52.5	22.4
Goonyella, Australia	F	8.1	0.55	0.13	1.00	0.01	1.91	24.3	65.7
Wellmore, USA	F	7.7	0.45	0.43	2.25	0.03	7.36	44.1	34.8
Carter Roag, USA	F	9.7	0.60	0.44	2.00	0.04	7.11	44.5	32.8
CEF «Pervomaiskaya», Ukraine	F	7.4	1.33	0.36	1.75	0.03	2.00	28.3	48.9
Inter-Invest (m. Maria Glubokaya)	F	7.3	1.36	0.64	1.75	0.05	3.44	28.9	50.5
CEF «Samsonovskaya», Ukraine	F	8.0	2.12	0.71	2.13	0.06	3.77	37.1	40.6
CEF «Duvanskaya», Ukraine	F	9.0	1.63	0.58	1.88	0.06	2.68	38.0	35.1
CEF «Kiyevskaya», Ukraine, pr. 1	F	8.6	1.48	0.52	1.75	0.05	3.20	38.1	36.4
CEF «Kiyevskaya», Ukraine, pr. 2	F	7.9	1.57	0.41	1.13	0.04	3.02	39.3	34.2
CEF «Kalininskaya», Ukraine, pr. 1	F	7.0	2.12	1.06	2.38	0.02	1.08	43.6	30.7
CEF «Kalininskaya», Ukraine, pr. 2	F	6.7	2.07	0.58	1.75	0.09	4.11	46.5	35.4
CEF «Celidovskaya», Ukraine	F	7.8	1.65	1.09	3.51	0.04	1.88	47.3	26.2
CEF «Kalininskaya», Ukraine, pr. 1	C	9.0	0.91	0.74	0.78	0.07	7.32	29.0	56.7
CEF «Kalininskaya», Ukraine, pr. 2	C	7.9	1.71	0.66	1.75	0.05	3.05	35.2	47.0
CEF «Sviato-Varvarinskaya», Ukraine, pr. 1	C	7.5	0.80	0.42	0.75	0.03	3.94	27.6	57.08

1	2	3	4	5	6	7	8	9	10
CEF «Sviato-Varvarinskaya», Ukraine, pr. 2	C	9.0	0.45	0.47	0.75	0.04	9.40	30.6	52.7
Australian coal (hard)	C	7.2	0.47	1.07	3.13	0.08	16.39	31.5	63.4
JSC CC «Severniy Kuzbass», RF	C	8.9	0.57	1.77	2.86	0.16	27.64	38.7	57.7
JSC CC «Severniy Kuzbass», RF	C	9.3	0.54	1.63	3.38	0.15	28.07	41.8	48.0
CEF «Nerungrinskaya», RF	C	10.3	0.35	1.72	5.07	0.18	50.62	49.1	29.6
CEF «Kolosnikovskaya», Ukraine, pr. 1	C	9.7	1.58	0.60	1.50	0.05	3.05	35.7	43.6
CEF «Kolosnikovskaya», Ukraine, pr. 2	C	10.8	1.46	0.51	1.50	0.06	2.92	36.4	41.7
CEF «Tchumakovskaya», Ukraine	C	9.6	2.17	0.93	1.75	0.11	8.12	45.7	33.8
CEF «Uzlovskaya», Ukraine	C	8.9	2.04	0.67	2.00	0.06	3.68	36.0	46.7
CEF «Samsonovskaya», Ukraine	C	7.4	2.44	0.99	2.01	0.07	5.73	53.2	33.3
EF «Siberia», RF	CL/CS/LS	9.8	0.30	1.00	3.51	0.10	32.67	32.3	58.8
Batchatskiy coal mine, RF	CL	8.6	0.32	1.28	3.68	0.11	34.40	34.7	54.7
c.m. Krasniy Brod, RF	CS	6.9	0.39	0.88	2.76	0.06	15.57	34.9	51.7
Pocahontas, США	LS	9.5	0.75	0.43	1.38	0.04	5.45	33.2	50.4

1	2	3	4	5	6	7	8	9	10
Kepler Low Vol, США	LS	5.8	0.75	0.89	3.33	0.05	6.88	29.8	60.6
Bistrianskaya	No data	3.7	1.85	0.54	2.61	0.03	2.06	39.9	44.1
Mechel, США пр. 1	No data	6.9	0.98	0.16	1.25	0.01	1.13	36.2	43.3
Mechel, США пр. 2	No data	6.8	0.97	0.44	1.13	0.03	3.08	36.3	45.0
Max		10.8	2.44	2.04	5.51	0.18	50.62	59.8	65.7
Min		3.7	0.30	0.13	0.75	0.01	1.08	24.3	19.2
Mean		8.2	1.10	0.84	2.41	0.07	10.19	39.9	40.6

The analysis of the data shown in table 1.13 shows that the ash content of the investigated coals ranged from 3.7 to 10.8 %; total sulfur content from 0.30 to 2.44 %; the sulfur content in the ash from 0.13 to 2.04 %; the calcium content in the ash from 0.75 to 5.51 %, the sulfur content transferred to ash from coal from 1.08 to 50.62 %; CRI from 24.3 to 59.8 %; CSR from 19.2 to 65.7 %, i.e. in a very wide range.

Table 1.14 shows the values of the pair correlation coefficients between certain indicators of coal quality; moreover, the numerator shows values for coals characterized by an S^d_t content of less than 1.0%, and the denominator for coals with S^d_t more than 1.0 %.

This separation was based on previous studies on the effect of total sulfur content in coals on the prognosis of coke CRI and CSR [58]. The data in table 1.14 allow us to conclude that the total sulfur content in coals has a significant impact on the mechanism of its partial transition to ash and the CRI and CSR values obtained during their individual coking of coke.

Table 1.14 The correlation coefficients of the studied relationships[1]

	S^d_t	S_A	Ca	S_y^*	$S_y^* \cdot 100/S^d_t$	CRI	CSR
S^d_t	–	-0.48 0.22	-0.59 0.01	-0.49 0.14	-0.66 -0.19	-0.37 0.35	0.22 -0.07
S_A	-0.48 0.22	–	0.77 0.84	0.98 0.97	0.89 0.89	0.34 0.78	-0.04 -0.77
Ca	-0.59 0.01	0.77 0.84	–	0.75 0.77	0.79 0.76	0.43 0.71	-0.23 -0.75
S_y^*	-0.49 0.14	0.98 0.97	0.75 0.77	–	0.93 0.94	0.37 0.74	-0.08 -0.75
$S_y^* \cdot 100/S^d_t$	-0.66 -0.19	0.89 0.89	0.79 0.76	0.93 0.94	–	0.37 0.65	-0.11 0.75

Remarks:

[1] In the numerator, coal with an S^d_t content $\leq 1.0\%$; in the denominator – $S^d_t > 1$

Figure 1.20 shows, for example, a graphical representation of the dependence of the calcium content in the ash on the ratio $S_y^* \cdot 100/S^d_t$.

The graphical dependencies shown in Figure 1.20 show that the total sulfur content in coals has a significant effect on its behavior during combustion and transition to ash.

In the CPLPJSC Evraz-Dneprodzerzhinsky KHZ, a special study was conducted on the influence of the variability of the quality indicators and the chemical composition of the ash of one supplier on the reactivity (CRI) and post-reaction strength (CSR) of coke obtained from these coals.

Table 1.15 shows the quality indicators of 7 samples of coal "Czech Republic", their maximum, average and minimum values, and in table 1.16 pair correlation coefficients of the studied relationships.

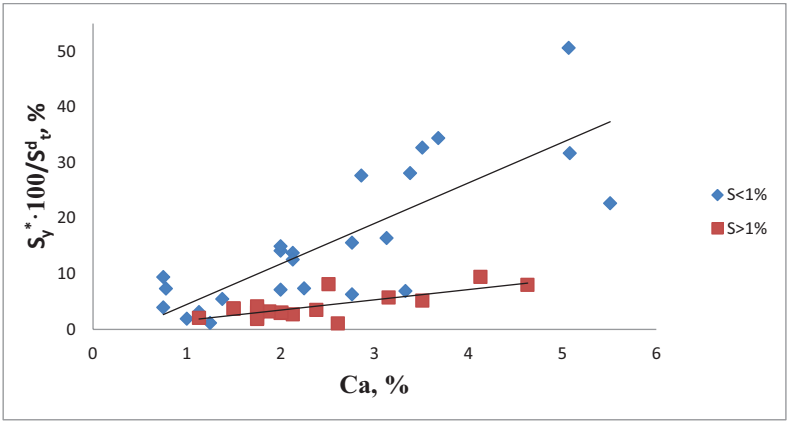

Fig. 1.20 The relationship between the calcium content in the ash and $S_y^* \cdot 100/S_t^d$

The analysis of the values of the pair correlation coefficients showed the presence of a fairly close relationship between certain indicators.

The graphical curves shown in Figure 1.21–1.24 show that the dependences of CRI and CSR on S_y* are linear, and on S_A and S_t^d they are quadratic.

Table 1.15 The fluctuation of coal quality indicators Czech Republic

№ sample	Proximate analysis of coal, %		The content of components in the ash, %		S_y^*, %	$S_y^* \cdot 100/S_t^d$, %	CRI, %	CSR, %
	A^d	S_t^d	S_A	Ca				
1	2	3	4	5	6	7	8	9
1	7.2	0.70	0.44	1.38	0.03	4.53	27.4	64.6
2	8.6	0.47	1.05	3.13	0.09	19.21	32.7	52.7
3	6.9	0.47	2.76	6.01	0.19	40.52	46.5	45.0
4	6.7	0.41	1.66	4.76	0.11	27.13	51.5	37.1

1	2	3	4	5	6	7	8	9
5	6.8	0.62	1.04	2.63	0.07	11.41	30.7	60.8
6	7.9	0.51	1.26	4.19	0.10	19.52	48.4	38.4
7	7.6	0.41	2.15	3.42	0.16	39.85	59.2	28.5
Max	8.6	0.7	2.76	6.01	0.19	40.52	59.2	64.6
Min	6.7	0.41	0.44	1.38	0.03	4.53	27.4	28.5
Mean	7.4	0.52	1.51	3.66	0.11	23.02	42.6	46.7

Table 1.16 Correlation coefficients of qualitative indicators of the studied coals Czech Republic

	S^d_t	S_A	Ca	S_y^*	S_y^*/S^d_t	CRI	CSR
S^d_t	-	-0.72	-0.72	-0.77	-0.84	-0.82	0.87
S_A	-0.72	-	0.85	0.99	0.96	0.74	-0.68
Ca	-0.72	0.85	-	0.83	0.78	0.64	-0.61
S_y^*	-0.77	0.99	0.83	-	0.98	0.76	-0.72
S_y^*/S^d_t	-0.84	0.96	0.78	0.98	-	0.83	-0.80

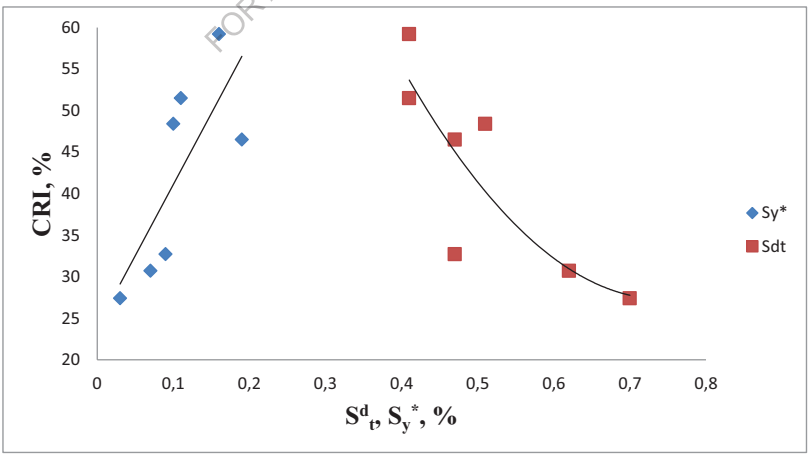

Fig. 1.21 The dependence of the reactivity of coke on the content of different types of sulfur in coal

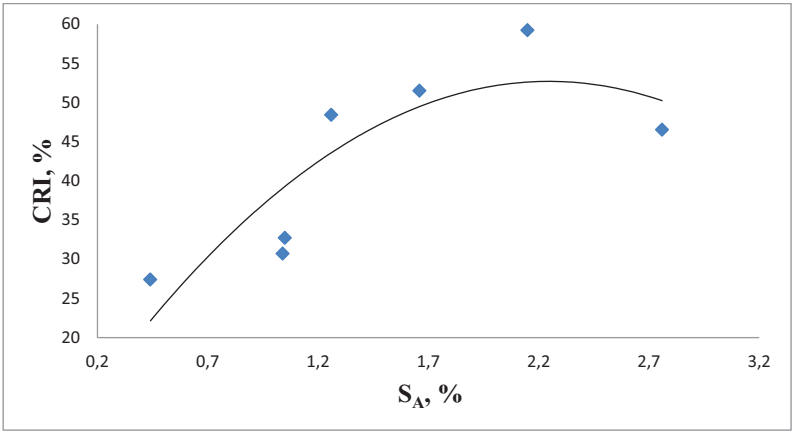

Fig. 1.22 The dependence of the reactivity of coke on the sulfur content in coal ash

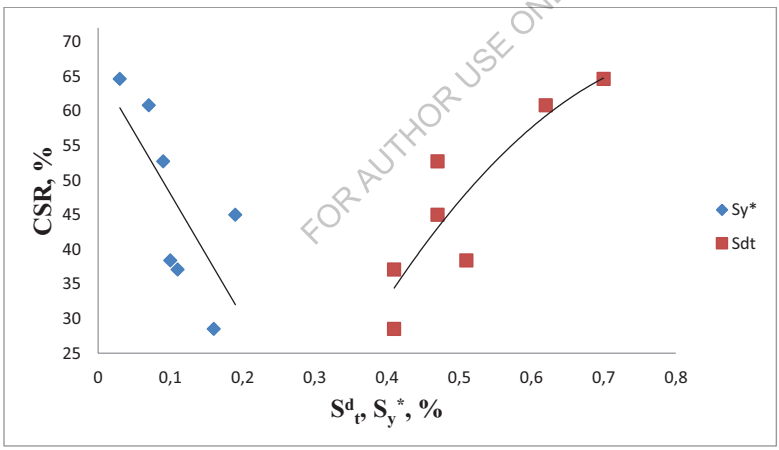

Fig. 1.23 Dependence of post-reaction strength of coke on the content of different types of sulfur in coal

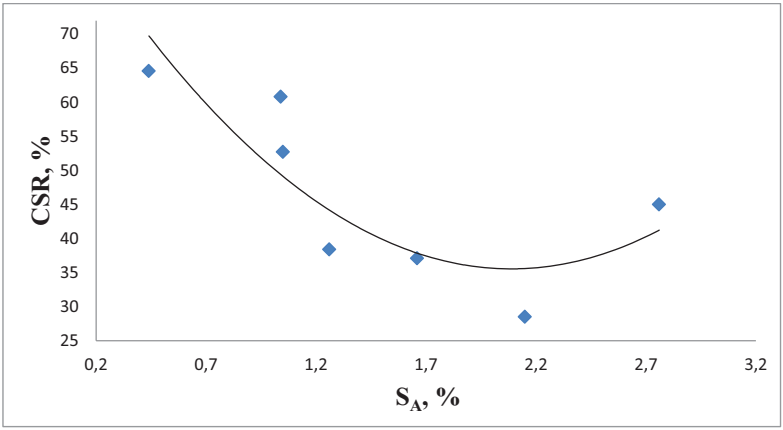

Fig. 1.24 Dependence of post-reaction strength of coke on sulfur content in coal ash

In general, the results of this part of the chapter include the following:

The share of sulfur passing to ash in Ukrainian high-sulfur coals does not exceed 10 %, and in low-sulfur coals of Russia, the USA, Australia it can reach 40 %.

Imported low-sulfur coals are mainly characterized by a high content of calcium, which leads to the predominant share of heat-resistant sulfur compounds passing into the ash composition.

An increase in the share of imported coal in the coking raw material base, along with a decrease in the total sulfur of the charge, may be accompanied by an increase in the sulfur content in its ash.

The selection of coal with a low sulfur content, passing into ash will allow to obtain coke with CRI <30 % and CSR> 60 %, which in turn will reduce its consumption in pig iron production.

References of chapter 1

1. Ulanovsky M.L., Miroshnichenko D.V., Kaftan Yu.S., Lichenko A.N. (2003). Sulfur and reactivity coke. Coal Chemistry Journal, 3–4, 45–48.

2. Ulanovsky M.L., Miroshnichenko D.V., Drozdnik I.D. and others. (2004). The relationship of reactivity and thermomechanical strength of coke. Coal Chemical Journal, 5–6, 46–51.

3. Vegman E.F, Zherebin B.N, Pokhvisnev A.N, Yusfin Yu.S. (1978). Iron metallurgy. Moscow, Metallurgy.

4. Ostroukhov M.Ya., Sparber L.Ya. Master's Referencethe dumper. (1977). Moscow, Metallurgy.

5. Dzhigota A.D., Boykov N.G. (2004). Technical and economic desulfurization of cast iron in blast furnace. Theory and cast iron production practice. Proceedings of the international scientific and technical conference dedicated to 70-the anniversary of the Kryvorizhstal State Mining and Metallurgical Company. Kryvyi Rih, 24–27 May, 356–358.

6. Tolstoy A.P., Sklyar M.G., Litvinov O.N. (1997). III International Coke Chemical Congress production. Coke and Chemistry, 4, 2–7.

7. Chernousov Ya.M. (1978) Processes and patterns coal formation. Kiev, Publishing Association “Vishka school”, Head Publishing House.

8. Dorofeev A.P. (1974). About sulfurization of medium carbon coals Donetsk basin. Solid Chemistry Fuel, 3, 54–59.

9. Handbook of coke chemist (1961). Ed. A.K. Shelkova.-M.: Metallurgy. v.1.

10. Yurovsky A.Z. (1960). Coal sulfur. M.: Publishing House Academy of Sciences of the USSR.

11. Miroshnichenko D.V., Bliznyuk T.I., Toryanik E.V. (2003). The effect of coal sulfurization on the reaction the ability of coke. Coal Chemical Journal, 5–6, 47–51.

12. Shpirt M.Ya., Claire V.R., Pertsikov I.Z. (1990). Inorganic components of solid fuels. M.: Chemistry.

13. Calkins W.H. (1987). Energy and Fuels, 1, 59–64.

14. Ruschev D.D. (1976). Chemistry of solid fuels. L., «Chemistry».

15. Yakovleva T.P., Dolzhanskaya Yu.B., Gapotchenko N.P. (1992). Organosulfur compounds of coal tar and pitch. Communication. 2. Coke and Chemistry, 12, 28–31.

16. Kazmina V.V. (1971). Reducing Coke Sulfur by heating it to high temperatures. Coke and chemistry, 6, 25–28.

17. Sheikhet A.M., Metreveli O.A., Pelikhova A.B. (1990). Differentiated Domain Sulfur Assessment fuel. Methods for assessing coke as a blast furnace.
Fuel. M.: Metallurgy.

18. Aronov S.G. (1968) Tasks for reducing coke sulfurization in the process of its production. Coke and Chemistry, 8, 7–13.

19. Katsman V.Kh., Simonov A.O. (1985). Behavior research sulfur coke in a blast furnace. Coke and Chemistry, 2, 16–18.

20. Kerkkonen O. (1997). Influence of Ash Reactions on Feed Coke Degradation in the Blast Furnace. Cokemaking International, 9, 34–41.

21. Mykolnikov I.A., Kudoyarov M.S., Efimov S.P. and etc. (1975). Obtaining calcined coke and conducting blast furnaces with his participation. Coke and Chemistry, 2, 19–22.

22. Volovik G.A. (1964). Sulfur in blast furnace coke and its conditions gasification. Coke and Chemistry, 9, 27–35.

23. Mykolnikov I.A., Iskhakov H.A. (1973). Influence limestone for sintering of the mixture and sulfurization fluxed coke. Solid fuel Chemistry, 5, 80–83.

24. Brook A.S., Kutovoi P.N., Goncharov V.F., Bezbach J.I. (1970). Features of the interaction of sulfur compounds fusion of coal with some minerals in destruction process. Solid fuel Chemistry, 1, 66–70.

25. Kaftan Yu.S., Shulga I.V., Minenko E.V. and etc. (2000). Properties of coke from coal blends with various additives. Coke and Chemistry, 6, 13–19.

26. Todavchich Z.I. (1973). On the effect of increasing temperature and coking rate for sulfur coke from Donetsk coal. Coke and Chemistry, 2, 15–18.

27. Vasyutin L.F., Galushkina S.A. (1979). Sulfur distribution charge in coking products. Coke and Chemistry, 8, 28–30.

28. Brook A.S., Bagel A.I., Leibovich R.E. and others. (1972). The influence of the heating rate on the process desulfurization of coal during coking. Metallurgy and Coke Chemistry, 32, 35–38.

29. Pakter M.K., Eidelman B.Ya., Pozhidaev A.T. (1971). Distribution of germanium and sulfur in coke. Coke and Chemistry, 4, 30–34.

30. Yelensky F.Z., Chernyshov Yu.A., Belichenko A.G. (1977). Study of the material composition, microstructure coke and its distribution of sulfur by species. Solid fuel Chemistry, 6, 57–62.

31. Vasiliev Yu.S., Ulanovsky M.L., Tsebriy L.S. and etc. (1990). About one of the sources of alkali metals in blast furnace coke. Coke and Chemistry, 10, 12–14.

32. Vlasov G.A., Chuishchev V.M., Barsky V.D., Rudnitsky A.G. (2004). Changes in the structure and properties of the solid phase in coking process. Coal Chemistry Journal, 1–2, 15–18.

33. Problems of processing sour oils. Materials of the 1st industry conference on processing sour oils. (1966).

34. Given. P.H., Jones J.R. (1966). Experiments of the Removal of Sulfur from Coal and Coke. Fuel, 45, 151–158.

35. Zimmerbach-Schneider. (1933). The basics of coke chemistry. ONTU.

36. Yurovsky A.Z., Livshits M.M., Cheremis A.A., Milfort N.V. (1939). Desulfurization of coke in the process extinguishing. Coke and Chemistry, 10–11. 16.

37. Bolotin Ya.S. (1941). Coke Desulfurization. Coke and Chemistry, 6, 17.

38. Obodova M.L., Taits E.M., Khanaeva O.K. and etc. (1979). Study of the mechanism of sulfide transformations iron compounds in coal near Moscow at their heat treatment. Solid fuel Chemistry, 4, 155–158.

39. Kargapol'tsev V.P. (2004). Nippon Steel Corporation Method. Coke and Chemistry, 10, 11–15.

40. Stepanov Yu.V., Koshkarov D.A. and Popova A.K. (2005) Methods of Determining and Estimating Coke Quality. Byul. Chernaya Metallurgiya, 1, 24–32.

41. Ulanovskii M.L. and Miroshnichenko D.V. (2005). Nippon Steel Corporation Method of Determining Coke Quality. Coke and Chemistry, 6, 18–21.

42. Shpirt M. Ya., Kler V.R., and Pertsikov I.Z. (1990) Inorganic Components of Solid Fuels, Moscow: Khimiya.

43. Hermann W. (1997) Influence of raw materials and coke oven operation on CSR and CRI values. General aspects. Cokemaking International, 9, 35–44.

44. Semisalov L.P. and Solodkaya L.T. (1971). Chemical Composition of Ash and Coke Reactivity. Theory and Practice of Coke Production, 24, 70–73.

45. Metreveli O.A. (1988). Rational Methods of Selecting Coal Batch for Coking and Predicting Coke Quality. Cand. Sci. Dissertation. Kharkiv.

46. Miroshnichenko D.V. (2006). Optimizing the Reactivity as an Integral Quality Characteristic of Coke. Cand. Sci. Dissertation, Kharkiv.

47. Kaftan Yu.S., Drozdnik I.D., Miroshnichenko D.V. et al. (2007). Relation of the Organic and Mineral Components of Coal Batch to the Cold and Hot Strength of Coke. Coal Chemistry Journal, 3–4, 3–13.

48. Ulanovskii M.L. and Miroshnichenko D.V. (2007). Influence of Mineral Components of the Coal on the Coke Quality (CRI and CSR). Coke and Chemistry, 4, 19–23.

49. GOST (State Standard) 17070-87: Coal: Terms and Definitions, 1987.

50. Turchanina, O.N., Butuzova, L.F., Safin, V.A., et al., Ecological Problems in Processing Sulfur-Bearing Coal // Vopr. Khim. Khim. Tekhnol., 2003, no. 2, pp. 139−142.

51. GOST (State Standard) 10538-87: Solid Fuel: Methods of Determining the Chemical Composition of the Ash, 1988.

52. Katsman, V.Kh. and Simonov, A.O., Estimating the Sulfur Distribution in Coking Batch with Additions of Low-Sulfur Coal //Coke and Chemistry. 1983. no. 11, pp. 24–25.

53. Katsman, V.Kh. and Simonov, A.O., Thermostability of Sulfur Compounds in Blast-Furnace Coke // Izv. Vyssh. Uchebn. Zaved., Chern. Metall., 1982, no. 33, p. 149.

54. Blast Furnaces: Standards for Coke Consumption: A Handbook, Moscow: MChM SSSR, 1987.

55. Hot-Metal Production: Technological Instructions, Appendix G: Technological Factors Influencing the Change in Blast-Furnace Productivity and Coke Consumption, Mariupol: MK Azovstal, 2004.

56. Ulanovsky M.L., Miroshnichenko D.V. Sulfur of coals and its influence on the quality and consumption of coke in a blast furnace // Coke and Chemistry. 2008. No. 8. P. 24–30.

57. Kovalev E.T., Drozdnik I.D., Kaftan Yu.S. Features of the formation of the coal resource base of coke-chemical enterprises of Ukraine in modern conditions // Coal Chemistry Journal. 2015. №1. P. 8–14.

58. Miroshnichenko D.V. Optimization of reactivity as an integral indicator of coke quality // Abstract of the dissertation of Cand. tech. Sciences: 05.17.07 – Kharkov, 2006. – 20 p.

CHAPTER 2
EMISSION REDUCTION OF SULFUR DIOXIDE PRODUCED DURING COAL COMBUSTION

Serhiy Pyshyev
Department of Chemical Technology of Oil and Gas Processing, Institute of Chemistry and Chemical Technology, Lviv Polytechnic National University, Lviv, Ukraine
Denis Miroshnichenko
Department of Technology of Oil, Gas and Solid Fuel Processing, Institute of Chemical Technology and Engineering, National Technical University Kharkiv Polytechnic Institute, Kharkiv, Ukraine

As already mentioned (see Introduction) coal sulfur has a detrimental effect on all major areas of its application.

In addition, it should be noted that the introduction of increasingly stringent environmental requirements led to the closure of a number of coke plants in Western Europe and the USA, as well as "beehive" furnaces in China. This could not but affect the change in the metallurgical market, namely, an increase in the share of sales blast furnace coke instead of coking coal. The consequence of this was a change in approach to the quality of coke – increased demands on him as a lump of blast furnace fuel. To date, many researchers believe that the main criterion for the quality of coke is its reactivity and thermomechanical strength, determined both by the Nippon Steel method and by the UKhIN method. A number of [1, 2] indicate the presence of the closest correlation between the sulfur content of coke and its high-temperature properties (according to the Nippon Steel method). This is especially evident in the conditions of high-sulfur raw

material coal base of coke-chemical plants in Ukraine. Unfortunately, to date, there are no industrially developed methods for reducing the sulfur content in coal. The traditional enrichment methods (flotation, depositing, heavy-medium separation) used at the concentration plants of Ukraine do not provide an economically feasible opportunity to carry out deep demineralization (hence, desulfurization) of ordinary coal.

To this end, we have carried out a critical review of the publications recently published in the scientific literature, which are devoted to the methods of emission reduction of sulfur dioxide produced during coal combustion, incl. coal desulfurization processes. The latter can be used to prepare coal for both incineration and coking

2.1 Methods of reducing pollutions while coal combustion

Obtaining of liquefied SO_2, sulfuric acid or sulfur by well-known and technologically simple methods [3–6] would seem the most feasible methods of sulfur dioxide removal from TPS flue gas, since the liquefied SO_2, sulfuric acid or sulfur are widely used in industry. However, the content of sulfur dioxide in TPS flue gas does not exceed 0.1–0.3 vol. % (2860–8570 mg/nm^3) [7, 8]. When using coal with the content of sulfur up to 3.0 wt % at TPS or LCP [9], the concentration of sulfur (IV) oxide in flue gases will be 0.2 vol. % (6000 mg/nm^3). Therefore, in such a case the known methods to produce liquid SO_2, sulfuric acid or sulfur are sufficiently expensive (see Subsection 2.1.4) and sometimes even technically impossible.

The methods of SO_2 removal can be divided into two groups: SO_2 removal from the flue gas after and directly during raw material combustion. According to the mentioned division, the technological

processes of flue gas desulfurization (FGD) can be divided into non-regenerative (non-cyclic) (wet, semi-dry and dry) and regenerative (cyclic) technology [9, 10]. The essence of wet desulfurization process is sulfur dioxide binding in the liquid phase through its dissolution, dissociation and interaction with the sorbent. The resulting waste water with wet by-products requires treatment. Semi-dry desulfurization technology includes two phases of interaction between the sorbent and SO_2 – absorption on liquid droplets, which eventually evaporate, and adsorption on the surface of the sorbent and the product after the complete evaporation of drops. Dry desulfurization is characterized by sulfur dioxide adsorption on the sorbent surface and formation of products over it. Taking into account the above-mentioned complications arising during the use of regenerative (cyclic) technologies, the share of these processes does not exceed 5 %, while they are practically absent in the USA. Among the non-regenerative technologies, wet systems are dominated (80–85 %); the quantity of semi-dry (spray-dry) and dry (sorbent injection) processes is 10–12 % and 4 %, respectively [9–11].

2.1.1 Technologies of wet desulfurization. The most common desulfurization technology is wet desulfurization using sorbents with alkaline properties – limestone, lime, sea water, ammonia water, etc. The process using calcium compounds (limestone/lime methods) dominates among all wet desulfurization processes. Currently, more than a half of wet desulfurization processes in the world (56–88 %) use a limestone/lime method [9, 11–14]. For lime wet desulfurization the following reactions are typical:

- Dissolution and dissociation of sulfur dioxide in water:

$$SO_2 + H_2O = H_2SO_3 \quad (2.1)$$

$$H_2SO_3 = H^+ + HSO_3^- \quad (2.2)$$

- Limestone dissolution in the acid medium:

$$CaCO_3 + H^+ = Ca^{2+} + HCO_3^- \quad (2.3)$$

- the formation of calcium sulfate and removal of carbon dioxide:

$$Ca^{2+} + HSO_3^- = CaHSO_3^+ \quad (2.4)$$

$$CaHSO_3^+ = CaSO_3 + H^+ \quad (2.5)$$

$$HCO_3^- + H^+ = H_2O + CO_2 \quad (2.6)$$

- The formation of acid salts of calcium bisulfite in the zone of low pH:

$$CaSO_3 + H^+ = CaHSO_3^+ \quad (2.7)$$

$$CaHSO_3^+ + HSO_3^- = Ca(HSO_3)_2 \quad (2.8)$$

If forced oxidation takes place, the reaction (2.9) occurs:

$$CaHSO_3^+ + ½\ O_2 = CaSO_4 + H^+ \quad (2.9)$$

If the saturated solution is formed, the crystals of gypsum are formed:

$$CaSO_4 + 2H_2O = CaSO_4 \cdot 2H_2O \qquad (2.10)$$

During natural oxidation, the calcium sulfite is partially oxidised by oxygen of the flue gas. With an excess of lime, sulfite quickly saturates the solution, adds water and precipitates in the form of small crystals of calcium sulfite hemihydrate:

$$CaSO_3 + H_2O = CaSO_3 \cdot \tfrac{1}{2}H_2O + \tfrac{1}{2}H_2O \qquad (2.11)$$

Thus, gypsum or a mixture of calcium sulfate and sulfite can be formed depending on the oxygen concentration in the reaction zone. After the process ends, the products are dehydrated. FGD by-products obtained during natural oxidation poorly give back water (small size of the crystals) and have no markets. During forced oxidation, the dehydration is easy due to the large size of the gypsum crystals. In Table 2.1, both modes are compared.

Limestone (mainly $CaCO_3$) is most often used as a sorbent due to the prevalence of its world's deposits and low price (3–10 times cheaper than other sorbents) [9, 13]. Lime (CaO or $Ca(OH)_2$) was used earlier because it has higher reactivity in comparison with that of limestone. Sometimes lime is used to obtain a high-quality by-product (e.g. gypsum) because natural limestone and chalk contain calcite ($CaCO_3$) and other components.

When using limestone the lime calcination by carbon dioxide of the flue gas and harmful release of energy in the absorber are eliminated. The modern design of limestone scrubbers allows efficient sulfur removal. Generally SO_2 reduction rate according to limestone/lime method is 92–99 %.

Table 2.1 Comparison of forced and natural oxidation [15]

Mode	By-product	Size of by-product	Use of by-product	Dewatering
Forced oxidation	Gypsum (90 %) Water (10 %)	0–100 μm	Wallboard, cement	Easy (hydrocyclone and filter)
Natural oxidation	Calcium sulfite/sulfate (50–60 %) Water (40–50 %)	1–5 μm	No use (landfill)	Complicated (thickener and filter)

Seawater scrubbing process can be considered as the second most popular process [9, 16, 17]. The technology is based on the absorption of sulfur dioxide by alkaline components of sea water (primarily, carbonates) with the formation of sulfites and sulfates:

$$SO_2 + 2HCO_3^- = SO_3^{2-} + 2CO_2 + H_2O \quad (2.12)$$

$$SO_2 + 2HCO_3^- + ½O_2 = SO_4^{2-} + 2CO_2 + H_2O \quad (2.13)$$

The resulting sulfates/sulfites return with water into the sea. It is clear that seawater scrubbing process can be installed only near the springs of seawater. The effectiveness of SO_2 removal in such processes is slightly lower and comes to 85–98 %.

The next method is an ammonia (ammonium-sulfate) wet method [9, 18, 19] based on the reactions of SO_2 and SO_3 with aqueous ammonia, followed by oxidation of formed by-products to obtain stable ammonium sulfate $(NH_4)_2SO_4$. The main chemical reactions are:

- absorption of dissolved SO_2 by NH_4OH:

$$2NH_4OH + H_2SO_3 = (NH_4)_2SO_3 + 2H_2O \quad (2.14)$$

$$(NH_4)_2SO_3 + H_2SO_3 = 2NH_4HSO_3 \quad (2.15)$$

- oxidation of ammonium sulfite and ammonium bisulfite to ammonium sulfate:

$$(NH_4)_2SO_3 + ½\ O_2 = (NH_4)_2SO_4 \quad (2.16)$$

$$NH_4HSO_3 + ½\ O_2 = NH_4HSO_4 \quad (2.17)$$

$$NH_4HSO_4 + NH_4OH = (NH_4)_2SO_4 + H_2O \quad (2.19)$$

If ammonia is constantly added to the solution while maintaining the ratio of neutral and acid salts within acceptable limits, it is possible to obtain crystalline ammonium sulfate, which is used as a fertiliser.

The efficiencies of ammonia wet method, as a rule, are by 2–4 % higher than that of limestone/lime process. General SO_2 reduction rate according to this method is 95–99 %; it is possible to reduce the SO_2 content in the flue gases down to 200 mg/nm^3 (0.007 vol.%).

To remove sulfur dioxide the solutions of sodium and magnesium hydroxides (carbonates), as well as hydrogen peroxide are also used [9, 20]. The efficiency of these processes is generally higher than 90 %.

2.1.2 Technologies of semi-dry desulfurization. Semi-dry (spray-dry) methods occupy the intermediate position between the wet and dry methods. According to these methods sulfur dioxide is binding both in the

liquid phase, on the droplets of moisture introduced into the stream of flue gas (whereby the amount of introduced fluid is much smaller than that of washing liquid for wet scrubbers) and on the surface of solid sorbents [9, 21].

Slaked lime ($Ca(OH)_2$) which is in the form of powder or slurry introduced to the reaction zone is the main sorbent used in semi-dry desulfurization technology. In the reaction volume (single reactor or part of flue), a series of parallel-sequential processes takes place: SO_2 dissolution in droplets of moisture, heat and evaporation of the droplets of moisture, the chemical reaction of sulfur dioxide and the sorbent. When using the suspension of slaked lime, the mixture of dry mixture of calcium sulfite, sulfate, fly ash, and unreacted lime calcium is formed, but calcium sulfite hemihydrate ($CaSO_3 \cdot ½H_2O$) is the main product:

$$Ca(OH)_2 + SO_2 = CaSO_3 \cdot ½H_2O + ½H_2O \quad (2.20)$$

$$CaSO_3 \cdot ½H_2O + ½O_2 = CaSO_4 \cdot ½H_2O \quad (2.21)$$

The average degree of sulfur dioxide removal in semi-dry (spray-dry) processes is 85–95 %.

2.1.3 Technologies of dry desulfurization. As noted above, dry methods of the flue gas desulfurization are based on adsorption processes of sulfur dioxide on the solid surfaces [9, 13, 22]. Substances with a porous structure and relatively large specific surface are usually used as sorbents. For example, the specific surface area of CaO is 90 m^2/g. To absorb sulfur dioxide, the oxides and carbonates of alkaline earth and alkali metals are used.

Depending on the sorbent feed zone, the dry processes can be conventionally divided into furnace sorbent injection (the sorbent is fed directly into the combustion zone, the temperature is about 1000 ^{o}C), economizer sorbent injection (before/after air heater, about 540 ^{o}C), duct sorbent injection (in the flue gas flow, about 150 ^{o}C). There are also hybrid sorbent injection and circulating fluid bed (CFB) dry scrubber (the temperatures from 800 to 900 ^{o}C).

The main sorbent for a dry high-temperature desulfurization is the limestone [9, 22]. While introducing limestone particles together with coal into a fluidised bed boiler chamber, they are burned (calcinated) to form particles of quicklime (CaO) and carbon dioxide:

$$CaCO_3 = CaO + CO_2 \qquad (2.22)$$

The rate of reaction (2.22) is high at temperatures over 750 ^{o}C. Quicklime CaO particles are covered with a layer of calcium sulfate, which is formed as a result of the reaction between calcium oxide and molecules of sulfur dioxide and oxygen:

$$CaO + SO_2 + ½\ O_2 = CaSO_4 \qquad (2.23)$$

If the amount of oxygen in the flue gases is insufficient, then a significant amount of calcium sulfate may be formed. Purification products are mixed with fly ash and directed to the dump or used as a low-grade building material. Slacked lime, quicklime and sodium hydrocarbonate (carbonate) are used for other types of dry desulfurization. The efficiency of the high-temperature dry desulfurization method depends, first of all, on specific area of the adsorbent surface and residence time of sorbent

particles in the reaction zone. Therefore, to achieve high-efficiency values the sorbent is used with an excess: Ca/S molar ratio is 2–3. Further growth of limestone consumption results in the increased content of nitrogen oxides in flue gases because calcium oxide catalyzes nitric oxide formation at the temperatures below 900 ^{o}C [9, 23].

Using furnace sorbent injection, the efficiency of sulfur dioxide removal is 30–50 % (in the case of recirculation gases 70–80 % can be achieved), economizer and duct sorbent injection – 50–80 %, hybrid sorbent injection – 50–90 % and CFB processes – 90–99 %.

In [24], the combustion of two Chinese coals with and without impregnation with calcium acetate was studied. In the first case, SO_2 emissions were significantly lower. So, more than half of the sulfur substances were absorbed by calcium acetate, and the effectiveness desulfurization varied depending on reaction temperature and type of coal. In work it was found that increasing the temperature from 1000 to 1200 ^{o}C reduces the efficiency of sulfur absorption.

The potential of calcium-magnesium acetate as an SO_2 sorbent was studied in [25]. Blowing calcium-magnesium acetate into the effluent coal combustion gases at a temperature of 1100–1200 ^{o}C an 80 % decrease in the concentration of SO_2 was achieved at its initial level of 1000–1500 ppm (Ca/S ratio >2.5). According to the scientists who conducted this study, a complete absorption of SO_2 is possible with a high level of Ca/S ratio.

It is possible to use not only coal treated with limestone as a sorbent, but also limestone itself. Chinese scientists investigated the desulfurization process of coal mixed with limestone during its combustion in a cylindrical laboratory ovens. In parallel with it, the effect was also studied another sorbent – calcium acetate synthesized from natural limestone. As a result, it was found that the latter absorbs sulfur more than a natural sorbent, due to

closer contact with particles of coal sulfur. It was noted that an increase in temperature (from 1100 to 1400 ^{0}C) reduces the ability of sorbents to remove sulfur-containing compounds, because sorbents are themselves absorbed by related aluminosilicates. The result was an unexpected conclusion that coals rich in calcium can themselves adsorb SO_2 at 900 ^{o}C, while sulfur removal efficiency is not lower than natural limestone [26].

2.1.4 Regenerable processes. In regenerable processes (dry and wet), the sorbent is regenerated chemically or thermally and reused. As a result, gases with a relatively high concentration of SO_2 are obtained which are the basis for liquefied sulfur dioxide, sulfur or sulfuric acid production using known methods [4–6].

In the wet regenerable processes, sodium sulfite/bisulfite (Wellman-Lord process), ammonia water (Walther process), magnesium hydroxide/magnesium oxide and amine are used [6, 15, 27, 28]. The most popular is the Wellman-Lord process, which consists of the adsorption stage:

$$Na_2SO_3 + SO_2 + H_2O = 2NaHSO_3 \quad (2.24)$$

and the desorption stage (regeneration):

$$2NaHSO_3 = Na_2SO_3 + SO_2 + H_2O \quad (2.25)$$

During the process nonregenerable byproducts are formed (the main products are sodium sulfate and thiosulfate):

$$2Na_2SO_3 + O_2 = 2Na_2SO_4 \quad (2.26)$$

$$2Na_2SO_3 + 2NaHSO_3 = 2Na_2SO_4 + Na_2S_2O_3 + H_2O \qquad (2.27)$$

SO_2 removal efficiency of all regenerative processes is almost the same (about 90–98 %).

In the dry regenerable processes, the activated charcoal and various types of coke and semi-coke are used. ReACT technology (regenerative desulfurization technology with activated coke) is considered to be a leader [29]. According to this method, at the first stage sulfur dioxide is adsorbed on activated coke grains in the presence of ammonia in the flue gases, which forms ammonium sulfate and bounds nitrogen oxides. Activated coke grains slowly move in the absorber to ensure the uniform surface of adsorption. Activated coke efficiently captures dust particles after ash collector. At the second stage, the contaminated activated coke is regenerated by the hot air within 400–500 ^oC. Sulfuric acid, and ammonium salts are decomposed into N_2, SO_2 and water. After cooling the grains of activated coke are cleared from dust and returned to the absorber. The efficiency of ReACT technology exceeds 98 %. Most of all, the process is proposed to be used for cleaning the flue gas with an SO_2 concentration of 200–400 mg/nm^3 (160–320 ppm) to reduce its level to 5–10 ppm.

The adsorption properties of the low-metamorphosed carbon-pyrolysis residue were studied coal as a sorbent for joint removal of SO_2/NO from poor gas (linear velocity of not more than 0.12 m/s). This sorbent was obtained by carbonization and subsequent activation of coal by steam. It is used under the following conditions (stage 1): temperature 100 ^oC, space velocity 3600 h^{-1}, 6 % O_2, 10 % H_2O, 1000 ppm SO_2, 1000 ppm NO, 1000 ppm NH_3 and N_2. The conditions of the second stage, when the concentration of SO in the gas stream is low and NO is reduced to N_2 and

steam, the following: temperature 150 ^{o}C, space velocity 900 h^{-1}, 6 % O_2, 10 % H_2O, 0–500 ppm SO_2, 1000 ppm NO, 1000 ppm NH_3 and N_2.

It is shown that the presence of NO does not affect the concentration of SO_2 in the first stage, and that the low input concentration of SO_2 also does not affect the degree of NO reduction in the second stage. In addition, this adsorbent can be regenerated without decreasing the adsorption capacity, because its absorbability is increased due to the activating effect of sulfuric acid formed during the first stage of work [30].

2.2 Technologies of coal preventive desulfurization

All methods of sulfur removal from coal before its usage may be divided into four main groups: physical; biological; physical-chemical; chemical. Typically, to characterize the efficiency of FGD technologies the terms “degree of removal”, “efficiency of sulfur dioxide removal” or “process reliability” are used. These parameters characterize the reduction of environmental pollution by SO_2.

If one describes the coal preventive desulfurization, the term “degree of sulfur removal” is used. The sulfur content in the desulfurized coal depends on the ratio between the coal and sulfur conversion rates. Hence, the removal degree of sulfur (RDS) is calculated in accordance with the formula (2.28) and indicates the ratio between the rate of sulfur conversion followed by the production of gaseous products and the rate of organic matter reaction, i.e. process selectivity:

$$RDS = \frac{S_0^d - S^d}{S_0^d} \cdot 100$$

(2.28)

where s_0^d – the content of sulfur relative to the dry sample, wt %; s^d – the content of sulfur in the desulfurized coal relative to the dry sample, wt %.

Considering that during preventive desulfurization the coal yield usually decreases, the removal degree of sulfur is lower than the resulting level of environmental pollution decrease [31–33]. For correct comparison of preventive desulfurization and FGD efficiency the term "sulfur conversion (SC)" should be used. This value indicates the amount of sulfur converted into sulfur-containing products that will not be in the atmosphere while the further burning of desulfurized coal (the level of environmental pollution decrease). It is calculated in accordance with the formula (2.29), %:

$$SC = \frac{S_0^a \times 100 - S^a \times x_C}{S_0^a}$$

(2.29)

where S_0^a – the content of sulfur in the initial coal relative to the analytical sample, wt %; S^a – the content of sulfur in the desulfurized coal relative to the analytical sample, wt %; x_C – the yield of desulfurized coal, wt %.

While describing technologies of coal preventive desulfurization (Section 2.2), the authors used the RDS term, because in the majority of the analyzed works only this index is used and there are no data about coal yield. While comparing the efficiency of desulfurization technologies and

SO_2 removal from flue gases (Section 2.3), the term SC was used.

2.2.1. Physical methods. Coal enrichment can be regarded as the physical desulfurization method, the main purpose of which is mineral components removal from coal. It is based on different physical properties (electromagnetic, density, the ability to wetting) of organic and mineral matters of coal. Since inorganic sulfur (primarily pyrite sulfur) is the basis of total sulfur in high-sulfur coal [31, 34–36], then using enrichment we can obtain low-sulfur coal. The physical methods include the following enrichment technologies: flotation, gravity methods, magnetic and electrical separation [37].

By electrostatic desulfurization, only 40 % of pyrite sulfur may be removed [38], by gravity methods – 70–90 % [39, 40], by flotation process using different media – from 60 to 90 % [41, 42]. For the certain type of flotation [43, 44] or combination of gravity separation with semi coking [45] the values of RDS (pyrite) vary depending on coal type within 28–98 % [43–45].

To increase the difference between the physical properties of inorganic parts, including pyrite, and coal organic matrix, i.e. to increase the removal degree of sulfur, it is proposed to carry out agglomeration or electrolytic recovery, to treat coal by ultrasound, sonoelectrochemical or higher acids glycerides [46–48]. The method of flotation desulfurization based on coal treatment by bacteria is developed [49]. Bacterial cells with excellent hydrophilic properties are introduced into pyrite. Pyrite hydrophilicity increases and the degree of pyrite separation from coal increases as well. Application of the aforementioned additional treatments before coal enrichment allows to increase RDS (pyrite) on average by 15–30 %.

2.2.2. Biological methods. The essence of these methods is the selective oxidation of coal sulfur as a result of biologically active components introduction or creation of conditions for the intense activity of the bacteria present in coal. Thus coal sulfur turns into incombustible and / or soluble forms:

$$2FeS_2 + 7O_2 + 2H_2O \rightarrow 2FeSO_4 + 2H_2SO_4 \quad (2.30)$$

$$2FeSO_4 + ½O_2 + H_2SO_4 \rightarrow Fe_2(SO_4)_3 + H_2O \quad (2.31)$$

$$2FeS_2 + 7½O_2 + H_2O \rightarrow Fe_2(SO_4)_3 + H_2SO_4 \quad (2.32)$$

$$2S + 3O_2 + 2H_2O \rightarrow 2H_2SO_4 \quad (2.33)$$

Bacteria help to remove 40–100 % of pyrite and 20–100 % of organic sulfur [50–55]. It should be noted that using biological methods both pyrite and organic sulfur may be removed. For example, depending on the content of certain types of sulfur, RDS (pyrite) and RDS (organic) were, respectively: 55 and 38 % [56]; 29 and 45 % [57]. Coal treatment (desulfurization) by bacteria is usually proposed to be realized on the suitable enterprises. The methods of introducing bacteria directly into the coal banks have been developed [58, 59].

Authors [60] studied the biodesulfurization of semanthracites in a reactor consisting of three columns densely packed coal (5 kg each), in which an acidity of pH 1.5 was maintained. At the first stage, the coal was modified in the first column by a coal-related culture, containing mainly Thiobacillus ferrooxidaus и Leptospilillum ferrooxidaus. The filtrate from the first column was sent to the second, etc. Within 20 days, a noticeable

desulfurization effect was obtained, and the weakest effect was obtained in the third column due to the abundant precipitation of an insoluble mineral (jarosit).

An interesting study, in which biodesulfurization complements the usual physical coal cleaning. Water Coal Suspension sequentially processed in a hydrocyclone, flotation machine and biodesulfurization. Numbers presented in the table below show the degree demineralization and desulfurization when used various methods.

As can be seen from the table 2.2 below, biodesulfurization can significantly increase the degree of desulfurization of coal, in addition, the heat of combustion of coal increases sharply, and in addition, sulfur emissions, expressed in grams of sulfur per gigajoule of obtained heat of combustion, decreased to 51 % [61].

The effect of biodesulfurization on the structure bituminous coals studied using gas chromatography, mass spectroscopy and atomic adsorption.

The influence of various methods on the degree coal demineralization and desulfurization

In addition, we analyzed the content aliphatic, aromatic and polar substances in extracts using thin layer chromatography. It was found that aliphatic substances are actively destroyed during desulfurization, mainly due to the removal of n-alkanes and light acyclic isoprenoids in the extracts. A change in etirene content can also be noted. As for the content of aromatic compounds, it has not practically changed. It is concluded that the effect of desulfurization is greater, the denser the coal fraction used.

Table 2.2 Influence of various methods on the degree of demineralization and desulfurization of coal

Methods used	Degree of extraction, %	
	A^d, %	S^d_t, %
Hydrocyclone	22	21
Hydrocyclone + flotation machine	41	21
Hydrocyclone + flotation machine + biodesulfurization	59	42

A change in the content of the following elements was noted: beryllium, chromium, zinc, gallium, cadmium, cobalt, lithium, manganese, copper, molybdenum, nickel, lead and vanadium. The most important factor, according to the authors, affecting the change the concentration of inorganic elements is their affinity for the organic mass of coal [62].

2.2.3. Physical-chemical methods. The essence of this method is relatively selective dissolution (extraction) of sulfur by various chemical reagents at elevated temperatures and pressures (in most cases, extractants are in a supercritical state). These reagents are alcohols, hydrogen peroxide, perchlorethylene, carbon monoxide. “Pure” extraction allows, on average, to reach RDS (pyrite/organic) up to 20–60 % and RDS (total) – up to 20–50 % [63–65]. This group of methods includes extraction of coal sulfur when it is previously converted into soluble (primarily in water) form. Under the action of acids (nitric preferred), sulfur (primarily, pyrite sulfur) is converted into sulfuric soluble form:

$$FeS_2+5NO_3^- +4H^+ \rightarrow Fe^{3+}+2SO_4^{2-}+ 5NO+2H_2O \qquad (2.34)$$

It is possible to remove 80 % of sulfur [66]. It is proposed to "strengthen" the action of acids on coal sulfur using a microwave radiation and/or a catalyst/solvent (H_2O_2). The degree of sulfur removal was found to be about 90–100 % [67, 68]. It is possible to use alkali, which reacts with pyrite in accordance with the equation:

$$8FeS_2 + 30NaOH \rightarrow 4Fe_2O_3 + 14Na_2S + Na_2S_2O_3 + 15H_2O \quad (2.35)$$

$$2NaOH + R\text{-}SH \rightarrow Na_2S + R\text{-}OH + H_2O \quad (2.36)$$

These processes are conducted at 200–350 ^{0}C and pressures up to 17.5 MPa. Removal degree of pyrite and sulfuric sulfur exceeds 90%, and organic sulfur – 50–70 % [69]. Sodium phenoxide or butoxide react with sulfur coal similar to alkalis or KOH/CH_3OH mixture, providing the opportunity to reach RDS (pyrite) on the 50–70 % level and RDS (total) – 30–60 % [70, 71]. Under the influence of divalent copper sulfur is oxidised to sulfuric acid according to the equation:

$$FeS_2 + 14CuCl_2 + 8H_2O \rightarrow 14CuCl + FeCl_2 + 2H_2SO_4 + 12HCl \quad (2.37)$$

and organic sulfur is converted into aldehydes and sulfuric acid due to C-S bond opening. Using copper chloride, it is possible to remove total sulfur in the amount of 17–53 %, pyrite – 21–100 %, organic – 7–30 % [72]. In some cases, only 36 % of total sulfur is removed [73].

The article [74] describes the desulfurization of coal from the Moe Mou deposit (India) using supercritical ethanol and potassium hydroxide. At the result of a two-level factor analysis, it was found that only two variables, namely, temperature and KOH concentration can significantly

affect the reduction of pyrite and total sulfur (from temperature, pressure, test time and potassium hydroxide concentration).

When leaching coal samples Assam deposits (India) with a hydroxide solution potassium at a temperature of 95 and 150 ^{o}C followed by treating them with weak acid, the following results: coal demineralization effect decreased by 1–11 %, and desulfurization increased up to 26–43 % with increasing temperature up to 150 ^{o}C. Potassium hydroxide treatment leads to 2–19 % demineralization and to 16–30 % desulfurization of coal samples at a temperature of 95 ^{o}C. Decrease in value demineralization is due to rapid precipitation of potassium aluminosilicates. However, if applied later, 10 % hydrochloric acid, which decomposes potassium aluminosilicates, the degree of demineralization increases accordingly to 28–45 % and 39–68 %, and desulfurization – up to 22–35 % and 34–53 % at 95 ^{o}C and 150 ^{o}C. It should also be noted that after such processing is almost completely removed inorganic and up to 37 % organic sulfur from coal samples [75].

Data are given on the extraction of inorganic sulfur from coal using an aqueous solution of iron sulfate. It was found that >90 % finely atomized and not associated with the organic structure of coal pyrite and sulfate sulfur is removed during recovery iron sulfate. Highly dispersed pyrite is converted to iron sulfate, which later, after passing through the recovery process, returns to the cycle again. As a result, the possibility of industrial use this method for disposal high ash and sour waste enrichment [76].

Pretty interesting results were published in [77], in which pyrite from Ascalite lignite was removed with nitric acid in an aqueous suspension. As a result, when varying such factors as particle size (60, 100, 200 μm), reaction time (0–10800 s), nitric acid concentration (5–30 % wt.),

Temperature (25–103 ^{o}C) and speed mixing (0.75–20 s^{-1}) revealed that pyrite sulfur is quantitatively removed from lignite at a boiling point (-103 ^{o}C) and at 25 % concentration of HNO_3 in solution.

The effect of processing lignite under reflux conditions under pressure under the combined action of 0–30 % NaOH, 10 % HCl, and 10 % H_2SO_4 was studied in [78]. Treated and untreated samples were analyzed using infrared spectroscopy. In the sequential treatment with these solvents, it was possible to obtain a greater effect than in case of their single use, while managed to remove carboxylated structures. At as a result of processing, a 3.3 % ash level was achieved, while a large percentage of Ca and K was replaced by Na.

The data [79] concern the conversion of sulfurous substances during recovery in the system potassium-liquid ammonia (PLA). For the study was selected a method that allows you to set the temperature and pressure method (AP-TPR). It was found that recovery sulfides and disulfides in PLA leads to the formation of predominantly aromatic and aliphatic thiols. Coal recovery in the PLA system, contrary to non-thiophene sulfur transitions, also leads to rupture C-S bonds in some thiophene systems.

The authors of [80] subjected two types of high-sulfur coals “Mekvinenza” and “Illinois” No.6 to reductive and non-reductive alkylation. Recovery alkylation was carried out in a PLA system, whereas non-reducing alkylation was performed according to the method proposed by Liott. In both cases, the alkylating agent was iodomethane. Products were subjected to elemental analysis and investigated by IR spectroscopy. Besides, a pressure control technique was applied and temperature (AP-TPR). It was found that “Mekvinenza” coal contains arylthiols and almost no alkylthione, while “Illinois” No.6 contains alkylthiols and practically does not contain arylthiols.

An original method of desulfurization proposed by Turkish scientists who analyzed the effect hydrochloric acid HCI concentrations and response time to desulfurization of lignite under exposure to microwave energy. When comparing these results with the same acid treatment but in a conventional heating system, it is noted that with an increase in HCl concentration in the system degree desulfurization for all samples increases. Main the difference in these methods is extremely small the amount of time required for desulfurization when using microwave energy. Spotted decrease in the atomic ratio S_{com}/C for all samples. Fourier Transform IR Spectrometry it has been found that acid treatment is especially effective in cleavage of dithioether and thioether groups. As a result, the fundamental possibility of removing NU-functional compounds like thioethers and thiols, which usually require quite strong reducing agents, was confirmed [81].

Microwave irradiation of coal with simultaneous peroxyacetic acid has been fully studied in [82]. It was found that the degree the following factors affect desulfurization: time andradiation power, time and temperature the reaction of coal with peroxyacetic acid, and also the size of the particles of coal. As a result of such processing, the contents of pyrite, organic, and total sulfur varied, respectively, in the following intervals: from 26 to 91 %; from 2.6 to 38.4 % and from 17 to 65 %.

Infrared study spectroscopy has shown that this method can used to remove inorganic and organic sulfur without destroying organic coal structure.

The work [83] in which ultra-pure coal production was investigated sequential processing of NNO_3 and HF. For this British bituminous coal with a particle size <6.2 μm, an ash content of 5.0 % and a sulfur content of 2.4 % was sequentially treated with these acids. At the same time, ash and

sulfur content decreased to 0.2 % and 1.3 %, respectively. In addition, the calorific value decreased from 31.5 to 29.5 MJ/kg while increasing the nitrogen content from 2.0 to 2.8 %. Interestingly, an increase in nitrogen content occurs only when HNO_3 reacts with dissolved pyrite, and this suggests that the reaction products of HNO_3 with pyrite react with coal substances. The following probable mechanism is assumed: in separate sections of pyrite, sulfuric and nitric acids are converted into powerful nitrating agents NO_2^+, which then react with coal. Interestingly, after acid treatment the fluorine content in coal increases from 80 to 3240 ppm. Remaining mineral in coal presented mainly in the form of finely divided unreacted pyrite.

Developing this study, we analyzed the behavior of ultrapure coal during combustion. Ultrapure coal was carbonized in a cylindrical laboratory furnace with a subsequent study of the structure and morphology of the obtained high-carbon residues using optical and scanning electron microscopes. The reaction characteristics of these residues were studied by isothermal combustion in air at various temperatures in thermogravimetric system. The results show that leftovers, obtained by the combustion of this coal are characterized more diverse structure, morphology and reactivity rather than residues from ordinary coal. It was found that demineralization led to an increase in the thermal effect and to a decrease in the amount of harmful emissions from coal combustion [84].

During the oxidation of coal H_2O_2, it was found that the sulfur contained in the coal partially oxidizes in sulfates. Sulfur-containing substances in the liquefaction effluents were mainly in the form of sulfides, thiosulfates, sulfites, and thiosulfates were in greater quantities [85].

Some patterns are revealed when oxidation of five coals of varying degrees metamorphism and sulfur content in peroxyacetic acid (POA), 5 %

nitric acid, oxygen in an aqueous solution of 0.5 N Na_2CO_3 and in air for 7 days at a temperature of 125 ^oC. Oxidation processes tested on demineralized samples (according to Radmaker method) containing minimal amount of pyrite sulfur. The strongest oxidizing agents according to technical results, elemental and spectral analyzes revealed 5 % HNO_3 and POA. As a result of oxidation, part coal organic matter has evolved into acid soluble compounds. Depending on the oxidizing agent sulfur loss in solid oxidized products is different (the highest for coal samples oxidized at 5 % HNO_3 and POA). The formation of oxidized sulfur groups (S=0 and SO_2) is confirmed by infrared spectroscopy. ICS data provides useful information regarding development of the molecular structure of coals of various the degree of metamorphism during oxidation, especially in the carbonyl and aliphatic ranges (1800–1500 and 3500–2800 cm^{-1}) [86].

2.2.4. Chemical methods. The essence of most of these methods is the oxidation or reduction of coal sulfur to form gaseous products. The exception is the oxidation of lignite sulfur by potassium permanganate. Sulfur before coal burning is converted into non-combustible (sulfuric) form. The degree of conversion is 47 % [87]. When sulfur (organic and inorganic) reacts with hydrogen, it converts into hydrogen sulfide, for example:

$$FeS_2 + 2H_2 \rightarrow Fe + 2H_2S \quad (2.38)$$

$$R\text{-}SH + H_2 \rightarrow R\text{-}H + H_2S \quad (2.39)$$

To reduce the coal sulfur and form hydrogen sulfide it was proposed to use hydrogenation in resorcinol solution under hydrogen influence at

temperatures over 900 °C [88]; hydrogenation at low temperatures in a stream of organic compounds that can generate hydrogen (low molecular alcohols and hydrocarbons), and atomize hydrogen (O_2, NO) [89]; shallow and deep hydropyrolysis of coal at the temperatures from 450 to 900 °C in the presence of catalysts and without them [90–93]; pyrolysis with fractional selection of gases that do not contain sulfur compounds and do not require treatment (at 200–400 °C and 525–800 °C) [94]; pyrolysis with simultaneous recovery of hydrogen sulfide by calcium compounds [95]. The degree of total sulfur removal in these processes sometimes was 90 %.

Well recommended for desulfurization of coal during its pyrolysis, Ca-containing additives [96]. It was found that $Ca(OH)_2$ and CaO absorbed up to 95 % of sulfur formed in gases and tar. The sorption capacity of $Ca(OH)_2$ is higher due to its greater activity; the use of $CaCO_3$ had an insignificant effect due to its higher decomposition temperature (~900 °C) than the peak of the temperature range of emissions of sulfur-containing gases (~400–500 °C). It is noted that ultrasonic treatment increases the efficiency of desulfurization. X-ray analysis data show that sulfur absorbed by Ca-containing additives is converted to CaS.

To apply calcium to coal, you can use the method of hydrogenation by ultrasound mixtures of coal and lime. The results show that by compared to mechanical stirring ultrasonic treatment significantly increases SO_2 extraction, especially if the atomic Ca/S ratio is higher than 1.5 [97].

Three Turkish lignite was pyrolyzed at various temperatures in the range of 350–950 °C for 7 minutes. As a result, it was found that the behavior and various forms of sulfur (pyrite and organic) were significantly affected by temperature and the content of calcium oxide in coal [98].

The data of article [99] indicate that there is optimum temperature and time for maximum coal desulfurization, which vary in depending on the type of coal and thermal stability organic sulfur.

So, coal, in which there are many aliphatic sulfur, more prone to desulfurization. In addition, the work noted that during the pyrolysis of coal in O_2 (0.6 % in nitrogen), the degree of desulfurization increases.

In the next work [100], the influence of the mineral of coal on the desulfurization of Turkish lignite in various gaseous media was studied at pyrolysis.

The results show that removal pyrite and organic sulfur increases with an increase in pyrolysis temperature, while pyrolysis in a CO_2 atmosphere at elevated temperatures is more effective at removal organic sulfur. After processing in HCl extraction organic sulfur is reduced. This is because that the removal of carbonates negatively affects the removal of organic sulfur. It has been proven that pretreatment in HCl/HF increases the effect of removing pyrite and organic sulfur during pyrolysis. Increase recovery sulfurous substances after treatment with HF may be due to the removal of clay minerals from coal structure, as it is these minerals that are the cause of the fact that easily removable organic sulfur is converted into thermally stable and non-removable substances (thiophene or condensed thiophene substances).

Interesting data were obtained during hydropyrolysis coal in a hydrogen atmosphere (5 MPa) when changing temperatures from 923 to 1123 K. Results studies have shown that decomposition inorganic sulfur is affected mainly temperature whereas organic extraction sulfur from coal influenced both the temperature and pressure of hydrogen. The degree of organic sulfur removal is highly dependent on the type of coal. So, for example, a significant amount of sulfur-containing gaseous products was

retained in the structure of the carbon residue obtained by hydrolysis of Chinese coal (1023 K). Kinetic analysis shows that the order of the reaction for removing organic sulfur from coal in the presence of hydrogen is 0.2 units, energy activation of removal of total and organic sulfur is respectively 17–26 and 13–55 kJ/mol. Low activation energies prove that the transfer and removal of sulfur from coal is limited diffusion and / or thermodynamic equilibrium during hydropyrolysis [101].

Fundamentally new is the removal of sulfur compounds from coal using sodium borohydride (degree of total sulfur removal is 30–40 %) [102] and the electrochemical method in complex suspended catalytic systems in the presence of sodium metaborate or borohydride (RDS (total) reaches 50–60 %, RDS (pyrite) in some cases reaches 100 %) [103–105]. The essence of these processes is that on the anode and cathode in the presence of water and metaborate (borohydride) oxygen and hydrogen radicals, respectively, are formed. They convert sulfur compounds into gaseous (H_2S) or water-soluble (SO_4^{2-}) components, such as:

$$FeS_2 + 2H^{\cdot} \rightarrow Fe + S + H_2S \quad (2.40)$$

$$2H^{\cdot} + R–SH \rightarrow R–H + H_2S \quad (2.41)$$

$$R_1\text{-}S\text{-}R_2 + 4O + 2H_2O \rightarrow R_1\text{-}OH + R_2\text{-}OH + H_2SO_4 \quad (2.42)$$

The essence of many oxidative technologies is that sulfur (mainly pyrite sulfur) may convert into gaseous sulfur-containing components at the relatively low consumption of oxidant. In fact, the process may be the first stage of the two-stage coal combustion, when gas with high content of sulfur dioxide is obtained [106]. This gas (in contrast to TPS flue gas) may

be used to produce a concentrated sulfur dioxide, sulfuric acid or sulfur [3–6]. If the SO_2 content in gases exceeds 7 vol. % it can be concentrated by usual stepped compression [5]. Hydrogen sulfide, obtained by oxidative desulfurization of lignite can be concentrated by known chemisorption or absorption methods [5, 107]. However, if the content of hydrogen sulfide in gases is above 5 vol. %, it is advisable to process it directly into sulfur by known methods [107, 108]. Steam, air or vapor-air mixtures are suggested to be used as oxidants [105, 109, 110]. Oxidative desulfurization processes by vapor-air mixtures are discussed in more detail in Chapter 3.

Apart from other works is article [111]. It gives the results of the catalytic oxidation of coal pyrite to SO_4^{2-} and Fe^{3+}, and also gives the oxidation kinetics coal pyrite by electrolysis in dosing the reactor. The paper discusses the influence of electrolysis conditions on the pyrite conversion rate: particle size, electrolysis potential of reaction time, temperature, acidity and catalyst concentration ($MnSO_4$). The limiting stage in this case is the interaction between Mn^{3+} and pyrite. The activation energy of the oxidation of coal pyrite to SO_4^{2-} and Fe^{3+} by electrolysis is determined by the value of 29.6 kJ/mol.

2.3. Evaluation of efficiency/economy of different reduction methods of sulfur dioxide emissions

Methods of reducing pollution during coal combustion are the most effective ones among the above-mentioned (they provide removal degree of sulfur dioxide above 85–98 %), so they have found a wide range industrial applications. However, these methods have several disadvantages:

- sorption does not solve the problem of equipment corrosion, including high-temperature corrosion. For example, the use of the ammonia

method at coal block with electric power of 191 MW in Germany (Karlsruhe) showed significant problems with the absorber corrosion [112];

- if you do not take into account dividends from the environmental protection, all desulfurization methods while coal combustion or flue gases cleaning, even in the case of by-products sale (gypsum, dry ash, ammonium sulfate, etc.), are loss-making processes [113, 114] and require substantial capital contributions for the modernization of thermal power plants. The average cost of power units reconstruction with the installation of new filters and systems for sulfur (IV) oxide removal from flue gas varies from 60 to 600 dollars per 1 kW power [15, 115, 116];

- flue gas cleaning systems can reduce the efficiency of the power units by 1.5–5 % and require relatively high operating costs (3.3–6.6 $ USA per MWh; it is on average 500–1200 $ USA per 1 ton of removed SO_2), which vary from 3,3 to 9 millions $ USA per year, depending on the unit [9, 117, 118];

- degree of SO_2 removal from the flue gas via all methods depends on its concentration. Therefore, based on the necessity to obtain flue gas with SO_2 content of 200–400 mg/nm^3, the maximum content of sulfur in coal, which is used for energy production, may be 1.5–3.5 wt %., depending on the efficiency of the process. This fact is confirmed by the literature data [9, 19, 119].

However, the greatest disadvantage of the above-mentioned technologies is the problem of using flue gas cleaning products. Among the processes mentioned in Section 2.1, the wet limestone forced oxidation method with gypsum production seems to be the most promising one. However, due to easy demand for this product [114, 119], only 30–50 % of the product can be used as secondary raw materials (most often – for construction products); other 50–70 % are usually in the dump.

Another disadvantage of the wet method is that sea water is used as the absorbent. After usage, it is returned to the sea, but the biochemical oxygen content in water is reduced, resulting in depletion of marine life [120].

Among the processes mentioned in Section 2.2, only physical ones have found application in industry. Desulfurization is positioned as a side effect that accompanies the removal of the mineral part. However, the removal degree of inorganic sulfur does not only depend on the enrichment technology, but also on the form in which pyrite is present in the organic mass of coal. So, sometimes it is possible to remove almost all pyrite sulfur, sometimes (when pyrite particles in the coal organic mass are small) only small quantities of it. The level of environmental pollution by sulfur dioxide is low or high, respectively [44, 45, 121].

With a high content of sulfur in the raw material, biological desulfurization methods require extremely large residence time of carbon in the reaction zone (up to several weeks). It is a significant disadvantage of these processes [122, 123].

Physical-chemical and chemical desulfurization methods are relatively expensive and technologically complex processes. It is necessary to use the solvents/reagents, which are difficult to be separated from desulfurized coal; selectivity is relatively low – the organic part of coal is extracted/converted together with sulfur compounds. The disadvantages of physical and chemical processes using acids or alkalis are additional costs associated with subsequent neutralisation of these compounds and the formation of nitrogen oxides. But first of all, the non-implementation of physical-chemical and chemical desulfurization methods into the industry is connected with predictable high operating costs (see Table 2.3).

Oxidative desulfurization processes, which use air or vapor-air

mixture, could be the exclusion because they do not require significant costs for reagents and are relatively cheap. They could be the first stage of coal combustion. During this stage, the concentration of sulfur oxide in final flue gases is higher by order than that of TPS flue gases. Therefore, they could be concentrated by known methods. The obtained coal with relatively low sulfur content could be combusted at the second stage.

One more disadvantage of coal oxidative desulfurization is the removal of only inorganic sulfur. The content of the organic part decreases slightly. It means that it is impossible to reduce sulfur dioxide emissions in accordance with the requirements Directive EC (2001). However, application of coal oxidative desulfurization before its combustion is extremely effective in combination with the use of formed flue gases. This approach will provide an opportunity:

- to significantly reduce the amount of flue gas cleaning products that have limited use (gypsum, ammonium sulfate);

- to utilise a part of coal sulfur in the form of liquefied sulfur dioxide or sulfuric acid;

- to reduce high-temperature corrosion of TPS main equipment;

- to improve the economic performance of the flue gas cleaning units by receiving by-products of coal oxidative desulfurization, which are more expensive than coal (bitumen components or fuel oil) [126].

Capital and O&M costs for coal oxidative desulfurisation process were not calculated. We can predict a relatively low cost of the process, because one of the existing TPS boilers may be used instead of the reactor, where coal will be “burned” at 400–450 ^{o}C and air deficiency. Main advantages and disadvantages are described after methods in Table 2.3

Table 2.3 Advantages and disadvantages of different reduction methods of sulfur dioxide emissions produced while coal combustion

Method	Main advantages	Main disadvantages	Level (%) of environmental pollution decrease (SO_2 reduction rate or SC (total))	Cost[1]	
				Capital, ($/kW)	O&M ($/ton removal (decrease) of SO_2)
1	2	3	4	5	6
Methods of reducing pollutions while coal combustion					
Wet	1. High purification degree of SO_2 emissions from flue gas. 2. Technological simplicity. 3. Prevalence in industry.	1. High-temperature corrosion of the equipment (primarily, wet method). 2. High capital investments for TPS modernization. 3. High O&M costs for the flue gas desulfurization. 4. Limited usage of obtained products	85-100	65-310	750-1265
Semi-dry			85-95	40-205	660-880
Dry	1. Relatively high cost. 2. Minimization of high-temperature corrosion of the equipment.	1. Low degree of SO_2 removal (except CFB processes). 2. Limited usage of obtained products.	30-100	~ 170	~ 490

1	2	3	4	5	6
Regenerable	1. The possibility of sulfur coal recycling in the form of liquefied SO_2, sulfuric acid or sulfur. 2. The obtaining of flue gases with SO_2 content of 5-10 ppm	1. Very high capital costs. 2. The efficiency significantly depends on SO_2 concentration in flue gases.	90-100	380–650	1500-2530
Technologies of coal preventive desulfurization					
Physical	1. Prevalence in industry. 2. May be realized during coal beneficiation.	1. Dependence of sulfur removal degree on pyrite size. 2. Only inorganic sulfur removal.	10-90	–[4]	275-325[2]
Biological	1. High removal degree of sulfur. 2. Absence of reagents.	1. Great time of coal staying in the reaction zone. 2. Low efficiency.	50-100	–[4]	450-900[2]
Physico-chemical	1. Possibility of removing all types of sulfur. 2. High removal degree of sulfur.	1. Expensiveness and technological complexity. 2. To remove all types of sulfur it is necessary to use several methods.	> 30 (only extraction); up to 100 (conversion and extraction)	–[4]	960-2700[2]

1	2	3	4	5	6
Chemical (reducing)	1. Coal sulfur utilization in H_2S form. 2. High removal degree of sulfur	1. Technological complexity. 2. Low selectivity: significant destruction of coal matrix and formation of great amount of by-products.	> 60-90	–[4]	–[4]
Chemical (oxidative)	1. Coal sulfur utilization in H_2S or SO_2 form. 2. Simplicity (may be applied as the first stage of coal combustion). 3. While combining with flue gas desulfurization the amount of products with limited application (gypsum, ammonium sulfate) would be reduced. 4. Cheap reagents (air, water steam).	1. Only inorganic sulfur removal. 2. It can't be used for coal with the abnormally high content of organic sulfur.	~ 55 (lignite); 70-77 (hard coal)	–[3]	–[4]

Remarks:

[1]According to [9, 71, 119, 120, 124, 125].

[2]Calculation based on data about the value attributed to 1 ton of coal; during the calculations the average sulfur content in coal was accepted as 1.2 wt %.

[3]As the reactor one of the existing TPS boilers can be used.

[4]Data are not available.

References of chapter 2

1. Hermann, W. (2002). Coke reactivity and coke strength. Cokemaking International, 14, 18–31.

2. Ulanovsky, M., Miroshnichenko, D., Kaftan, Yu., Lichenko, A. (2003). Sulfur and reactivity of coke. Coal Chemical Journal, 3–4. 45–48.

3. Rozenknop, Z. (1952). Recovering sulfur dioxide out of gaseous substance. Moscow, USSR: State Scientific and Technical Publishing of the Chemical Literature.

4. Rameshni, M., and Santo, S. (2005). Production of elemental sulfur from SO_2. RSR (Ramenshi SO_2 reduction). Worley Parsons from http://www.worleyparsons.com/CSG/Hydrocarbons/SpecialtyCapabilities/Documents/Production_of_Elemental_Sulfur_from_SO2.pdf

5. Javorskyj, V. (2010). Operating procedure of earwax and sulfuric acid. Lviv, Ukraine: Publishing House of Lviv Polytechnic National University.

6. Dzhonova-Atanasova, D., Razkazova-Velkova, E., Ljutzkanov, L., Kolev, N., Kolev, D. (2010). Energy efficient SO_2 removal from flue gases using the method of Wellman-Lord. Journal of Chemical Technology and Metallurgy, 48, 457–464.

7. ICPS. International Centre for Policy Studies. Reducing emissions in Ukrainian cogeneration industry by meeting the requirements of European energy community. Green Book. (2011). from http://ua-energy.org/upload/files/Green%20book_TES_ICPS.pdf.

8. Syhal, I. (1988). Protection of the air basin from fuel combustion. Moscow, USSR: Bosom.

9. European Commission. Best available techniques (BAT). Reference Document for Large Combustion Plants. (2016) from http://eippcb.jrc.ec.europa.eu/reference/BREF/LCP_FinalDraft_06_2016.

10. EPA. Environmental Protection Agency. Air Pollution Control Technology. Fact Sheet. (2004). from https://www3.epa.gov/ttncatc1/dir1/ffdg.pdf.

11. Córdoba, P. (2015). Status of flue gas desulfurisation (FGD) systems from coal-fired power plants: overview of the physic-chemical control processes of wet Limestone FGDs. Fuel, 144, 274–286.

12. Schnelle, K.B, and Brown Ch., A. (2001). Air pollution control technology handbook. Boca Raton, USA: CRC PRESS

13. Zevenhoven, R., and Kilpinen, P. (2001). Control of pollutants in flue gases and fuel gases from https://www.adeq.state.ar.us/downloads/commission/p/closed%20permit%20dockets%202006-2016/08-006-p%20aep%20service%20corp.%20&%20swepco-sierra%20club%20&%20audubon(consolidated)/2009-04-24_swepco-mu-ex.11.pdf.

14. Rosemount Analytical. Lime (2014). Limestone wet scrubbing system for flue gas desulfurization. Power Industry from http://www2.emersonprocess.com/siteadmincenter/PM%20Rosemount%20Analytical%20Documents/Liq_ADS_4900-02.pdf.

15. European Commission. Integrated pollution prevention and control (IPPC). Reference Documenton Best Available Techniques for Large Combustion Plants. (2006). from http://eippcb.jrc.ec.europa.eu/reference/BREF/lcp_bref_0706.pdf.

16. Andreasen, A., and Mayer, S. (2007). Use of seawater scrubbing for SO_2 removal from marine engine exhaust gas. Energy&Fuels, 21, 3274–3279.

17. Tokumura, M., Baba, M., Znad, H., Kawase, Y., Yongsiri, Ch., and Takeda, K. (2006). Neutralization of the acidified seawater effluent

from the flue gas desulfurization process: experimental investigation, dynamic modeling, and simulation. Industrial & Engineering Chemistry Research, 45, 6339–6348.

18. Maripuu, M., Gansley, R., Olesen, R., and Crespi, M. (2006). Design of the FLOWPAC WFGD system for the Amager Power Plant from https://www.adeq.state.ar.us/downloads/commission/p/closed%20permit%20dockets%202006-2016/08-006-p%20aep%20service%20corp.%20&%20swepco-sierra%20club%20&%20audubon(consolidated)/2009-03-06_hc_sc-bp_ex_133.pdf.

19. Marsulex Environmental Technologies. Operational experience of commercial, full scale ammonia-Based wet FGD for over a decade. (2009). from http://www.met.net/Data/Sites/35/assets/Information-Library/Technical%20Papers/Operational%20Experience%20of%20Commercial,%20Full%20Scale%20Ammoniabased%20Wet%20FGD%20for%20Over%20a%20Decade%20-%20August%202009%20-%20Presented%20at%20Coal-Gen%202009.pdf.

20. Vanderschuren, J., Colle, D. (2004). Pilot-scale validation of the kinetics of SO2 absorption into sulfuric acid solutions containing hydrogen peroxide. Chemical Engineering and Processing, 43, 1397–1402.

21. Ma, X., Kaneko, T., Xu, G., Kato, K. (2001). Influence of gas components on removal of SO_2 from flue gas in the semidry FGD process with a powder–particle spouted bed. Fuel, 80, 673–680.

22. Tumanovskyy, A. (2005). Ecological problems of thermal power stations. Electric Power Plant, 1, 7–15.

23. Peltier, R. (2004). Reliant Energy's Seward project earns POWER's Plant of the Year Award. from https://online.platts.com/PPS/P=m&e=1095283125113.2309170660154904

077/?artnum=MI2004Vsn091d31L141U46_1.

24. Zhang, L., Sato, A., Ninomiya, Y., Sasaoka, E. (2004). Partitioning of sulfur and calcium during pyrolys and combustion of high sulfur coals impregnated calcium acetate as the desulfurization sorbent. Fuel, 83, 1039–1053.

25. Nimno, W., Patsias, A.A., Hampartsoumian, E. (2004). Simultaneous reduction of NO_x and SO_2 emission from coal combustion by calcium magnesium acetate (CMA). Fuel, 83, 149–155.

26. Zhang, L., Sato, A., Ninomiya, Y., Sasaoka, E. (2003). In situ desulfurization during combustion of high-sulfur coals added with capture sorbents. Fuel, 82, 255–266.

27. Department of Trade and Industry. Flue gas desulfurization (FGD) technologies. Cleaner coal technology program. Technology status report 012. (2000). from http://webarchive.nationalarchives.gov.uk/+/www.berr.gov.uk/files/file19291.pdf.

28. Mehrara, H., Shishesaz, M.R., Rouzbehani, B. (2013). A novel selective flue gas SO_2 removal with an amine absorbent. International Journal of Science & Emerging Technologies, 6, 216–221.

29. Peters, J. (2010). ReACT reduces emissions and water use. from http://www.powermag.com/react-reduces-emissions-and-water-use.

30. Izquierdo, M.T., Rubio, B., Mayoral, C., Andres, J.M. (2003). Low cost coal-based carbons for combined SO_2/NO removal from exhaust gas. Fuel, 82, 147–151.

31. Pysh'yev, S., Gunka, V., Prysiazhnyi, Y., Shevchuk, K., PattekJanczyk, A. (2012). Study of oxidative desulfurization process of coal with different metamorphism degrees. Journal of Fuel Chemistry and Technology, 40, 129–137.

32. Pysh'yev, S., Bilushchak, H., and Gunka, V. (2012). Optimization of oxidation desulfurization of power-generating coal. Chemistry & Chemical Technology, 1, 105–111.

33. Pyshyev, S. Prysiazhnyi, Iy., Miroshnichenko, D., Bilushchak, H., and Pyshyeva R. (2014). Desulfurization and usage of medium-metamorphized black coal.1. Determination of the optimal conditions for oxidative desulfurization. Chemistry & Chemical Technology, 8, 225–234.

34. Yurovskyy, A. (1960). Sulfur of coal. Moscow, USSR: Publishing House Academy of Sciences Soviet Union.

35. Pysh'yev, S., Bratychak, M., Gajvanovych, V., and Brzozowski, Z. (2004). Hard coal desulfurization and sulfur recovery from it. Ecological Chemistry and Engineering, 11, 59–62.

36. Pysh'yev, S., Gayvanovych, V., Pattek-Janczyk, A., and Stanek, J. (2004). Oxidative desulfurisation of sulfur rich coal. Fuel, 9, 1117–1122.

37. Kawatra, K., and Timothy, S. (2001). Coal desulfurization: high efficiency preparation methods. New York, USA: Taylor & Francis.

38. Gidaspow, D., Dazah, W., Snjeev, S., Shih, Y., Raghubir, G., and Aditya, M. (1986). Electrostatic desulfurization of coal in fluidized beds and conveyors. Conference "AIChE Annual Meeting", 2-7 Nouvember, 1986, Miami beach, USA.

39. Kulik, C. (1987). New dry process for precombustion coal cleaning. Turbomachinery International, 28, 14–15.

40. Uslu, T., Sahinoglu, E., Yavuz, M. (2012). Desulfurization and deashing of oxidized fine coal by Knelson concentrator. Fuel Processing Technology, 101, 94–100.

41. Bekir, O. (1984). New cleaning technologies advance coal. Part 1 - Flotation and separation processes. Coal Mining, 5, 38–41.

42. Ayhan, F. D., Abakay, H., and Saydut, A. (2005). Desulfurization and deashing of Hazro coal via a flotation method. Energy & Fuels, 19, 1003–1007.

43. Chi, S., Morsi, B., Klinzing, G., and. Chiang, S.-H. (1989). LICADO process for fine coal cleaning. Part I: Mechanism. Coal Preparation, 6, 241–263.

44. Pawlak, W., Jezry, Ja., Tyrac, A., and Ignaiak, B. (1990). Process for removing pyrite sulfur from bituminous coals. Patent Application Number: 49966608, Publication Number: 230130, IPS C 10 L 9/00, 10 Oct.1990.

45. Çelik, M.S., Yildirim, I. (2000). A new physical process for desulfurization of low-rank coals. Fuel, 79, 1665–1669.

46. Pawlak, W. (1989). High–sulfur coal upgrading by improved oil agglomeration. In Processing and Utilization of High-sulfur Coals: 3rd: International Conference Proceedings, 14-16 Nov., 1989, Amsterdam. Netherlands.

47. Zhua, H., Zhua, J., Yang, Y.-F., Zhao, W., and Ou, Ze.-Sh. (2003). Research on mechanism of enhanced desulfurizing flotation of high sulfur coal with electrolytic reduction. Coal Preparation, 5–6, 239–250.

48. Zhang, H.-X., Ma, X.-Y., and Dong, X.-Sh. (2012). Enhanced desulfurizing flotation of high sulfur coal by sonoelectrochemical method. Fuel Processing Technology, 1, 13–17.

49. Amini, E., Oliazadeh, M., Kolahdoozan, M. (2009). Kinetic comparison of biological and conventional flotation of coal. Minerals Engineering. 22, 344–347.

50. Aytar, P., Aksoy, D. O., Toptas, Y., Cabuk, A., Koca, S., Koca, H. (2014). Isolation and characterization of native microorganism from Turkish lignite and usability at fungal desulfurization. Fuel, 116, 634–641.

51. Cara, J., Moran, A., Teresa, C. Razada, F., and Aller, A. (2003). The biodesulfuration of a semiantracite in a pakedbed system. Fuel. 2003, 14–15, 2065–2068.

52. Fabianska, M., Lewinska-Preis, L., and Galimska-Stypa, R. (2012). Changes in organic matter of selected Miocene lignites and embedded sediments caused by microbial desulfurisation. Fuel, 94, 586–595.

53. Ju, L.-K. (1992). Microbial desulfurization of coal. Fuel Science and Technology International, 8, 1251–1290.

54. Marinov, S., Stefanova, M., Gonsalvesh, L., Groudevab, V., Gadjanovc, P., Carleerd, R., and Ypermand, J. (2011). Biodesulfurized low rank coals appraisal: initial, treated, their bitumens and solid residues. Fuel Processing Technology, 12, 2328–2334.

55. Roffman, H. (1994). Japanese Research Organization employs bacteria to desulfurise coal. Coal International, 51, 154.

56. Aytar, P., Gedikli, S., Şam, M., Ünal, A., Çabuk, Ah., Kolankaya, N., and Yürüm, A. (2011). Desulfurization of some low-rank Turkish lignites with crude laccase produced from Trametes versicolor ATCC 200801. Fuel Processing Technology, 1, 71–76.

57. Mishra, S., Panda, P., Pradhan, N., Satapathy, D., Subudhi, U., Biswal, S., Mishra, B. (2014). Effect of native bacteria Sinomonas flava 1C and Acidithiobacillus ferrooxidans on desulfurization of Meghalaya coal and its combustion properties. Fuel, 117, 415–421.

58. Kulkarni, S. (2016). Research and studies on coal desulfurization. International Journal of Research and Review, 3, 56–58.

59. Ramana, V., Pandey, R., and Bal, A. (1995). Reactor systems for microbial desulfurization of coal: An overview. Critical Reviews in Environmental Science and Technology, 25, 291–312.

60. Cara J., Moran A., Teresa C. et al. (2003). The biodesulfuration of a semiantracite in a packedbed sys-tem. Fuel, 82, 15–17, 2065–2068.

61. Martinez O., Diez C., Miles N. et al. (2003). Biodesulfuration as a complement to the physical cleaning of coal. Fuel, 82, 9, 1085–1090.

62. Fabianska M.J., Lewinska-Preis L., Galimska-Stypa R. (2003). Microbial alteration of organic matter of humic coal during biological desulfurization. Fuel, 82, 2, 165–179.

63. Ali, A., Srivastava, S. K., and Haque, R. (1992). Chemical desulfurization of high-sulfur coals. Fuel, 7, 835–839.

64. Lee, S., and Fullerton, K. (1992). Characterization of desulfurization extract from Midwestern U.S. coal. Fuel Science and Technology International, 7, 1137–1159.

65. Ehsani, M. R. (2006). Desulfurization of Tabas coals using chemical reagents. Iranian Journal of Chemistry and Chemical Engineering, 25, 59–66.

66. Riley, J., and Ruba, G. (1989). Comparison of sulfur in HNO_3-extracted and physically cleaned coals. Fuel, 68, 1594–1597.

67. Ambedkar, B., Nagarajan, R., and Jayanti, S. (2011). Ultrasonic coal-wash for desulfurization. Ultrasonics Sonochemistry, 18, 718–726.

68. Nomvano, M., Nomngongo, Ph., and Ngila, C. (2016). Evaluation of different microwave-assisted dilute acid extracting reagents on simultaneous coal desulfurization and demineralization. Fuel, 163, 189–195.

69. Franco, D. V., Gelan, J. M., Martens, H. J., Vanderzande, D. J.-M., Majchrowicz, B. B. (1992). ^{13}C CP/MAS n.m.r. study of changes in molecular mobility of a bituminous coal during desulfurization. Fuel, 71, 751–754.

70. Prasassarakich, P., and Thaweesri, T. (1996). Kinetics of coal

desulfurization with sodium benzoxide. Fuel, 75, 816–820.

71. Ratanakandilok, S., Ngamprasertsith, S., Prasassarakich, P. (2001). Coal desulfurization with methanol/water and methanol/KOH. Fuel, 80, 1937–1940.

72. Oguz, M., and Oleay, A. (1992). Desulfurization of Bolu-Goynuk liqnite using chloride. Fuel, 2, 199–202.

73. Meyers, R., Hart, W., Van Nice J., Van Nice L. Process for upgrading coal. Patent Application Number: 5059307, Publication Number: 419659, IPS C 10 G 1/00, 22 Oct.1991.

74. Charutawai K., Ngamprasertsith S., Prasas-sarakich P. (2003). Supercritical desulfuruzation of low rank coal with ethanol/KOH. Fuel Processing Technology, 84, 1–3, 207–216.

75. Mukherjee S., Borthakur P.C. (2003). Effect of leaching high-sulfur subbituminous coal by potassium hydroxide acid on removal of mineral matter and sulfur. Fuel, 82, 7, 783–788.

76. Srivastava S.K. (2003). Recovery of sulfur from very high ash fuel and fine distributed pyritic sulfur containing coal using ferric sulfate. Fuel Processing Technology, 84, 1–3, 37–46.

77. Karaca S., Akyvrec M., Bayracs S. (2003). The removal of pyritic sulfur Askale lignite in aqueous suspension of nitric acid. Fuel Processing Technology, 80, 1, 1–8.

78. Karaca H., Onal Y. (2003). Demineralization of lignites by single and succesive pretreatment. Fuel, 82, 12, 1517–1522.

79. Kozlowski M., Wachowska H., Yperman J. (2003). Transformations of sulfur compounds in high-sulfur coals during reducing in the potassium/liquid ammonia system. Fuel, 82, 9. 1149–1153.

80. Kozlowski M., Wachowska H., Yperman J. (2003). Reductive and non-reductive methylation of high-sulfur coals studied by atmospheric

pressure-temperature programmed reduction technique. Fuel, 82, 9, 1041–1047.

81. Elsamak G., Altuntas N., Yurum Y. (2003). Chemical desulfurization of Turkish Cayirhan lignite with HJ using microwave and thermal energy. Fuel, 82, 5, 531–537.

82. Jorjani E., Rezai B., Vossoughi M., Osanloo M. (2004). Desulfurization of Tabas coal with microwave irradiation/peroxyacetic acid washing at 25,55 and 85 ^{o}C. Fuel, 83, 7–8, 943–949.

83. Steel M.K., Patrick J.W. (2003). The production of ultra clean coal by sequential leaching with HF followed by HNO_3. Fuel, 82, 15–17, 1917–1920.

84. Rubiera F., Arenillas A., Arias B. et al. (2003). Combustion behaviour of ultra clean coal obtained by chemical demineralization. Fuel, 82, 15–17, 2145–2151.

85. Wang T., Xiaofeng Z. (2003). Sulfur transformations during supercritical water oxidation of a Chinese coal. Fuel, 82, 18, 2267–2272.

86. Pietrzak R., Wachowska H. (2003). Low temperature oxidation of coals of different rank and different sulfur content. Fuel, 82, 6, 705–713.

87. Jürü, M.G., Tüzün, F.N.T., and Murathan, A.S. (2008). Oxidative desulfurization of ayirhan lignites by permanganate solution. Energy Sources A., 16, 1508–1515.

88. Kumaz, A., and Srivastava, S. (1992). Distribution of organic sulfur in Tipong coal using temperature programmed reduction. Fuel, 6, 718–719.

89. Garcia, A., and Schobert, H. (1991). Hydrodesulfurization of a high organic sulfur Spanish lignite with impregnated nickel sulfate. Coal Preparation, 3–4, 185–197.

90. Garcia, A., and Schobert, H. (1990). Catalytic

hydrodesulfurization of a high organic sulfur Turkish lignite: amount, form, and mechanism of sulfur removal. Fuel Processing Technology, 2, 99–109.

91. Ali, A., Srivastava, N., Srivastava, S. K., Goswami, R., Yadav, R., and Hazra, S. (2009). Upgradation of high sulfur NE region Indian coals by pyrolysis in presence of hydrogen. The Open Fuels & Energy Science Journal, 2, 40–46.

92. Klimpel, R., and Hansen, R. Pyrite depressants useful in the separation of pyrite from Coal. Patent Application Number: US 4830740, Publication Number: 5840710, 19 May 1989.

93. Zhang, G., Zhang, Y., and Xie, K. (2006). Study on desulfurization of high sulfur coal in hydropyrolysis. Chemical Engineering, 4, 55–58.

94. Shiley, R., Hughes, R., Webster, Jo., Hinckley, C., Smith, G., and Wiltowski, T. Desulfurization of carbonaceous materials. Patent Application Number: US4888029 A, Publication Number: 203222, IPS C 10 L 5/00, 22 December 1989.

95. Sutcu, H. (2004). Coal desulfurization using natural Ca-based sorbents. Coal Preparation, 5–6, 249–259.

96. Guan R., Li W., Li B. (2003). Effects of Ca-based additives on desilphurization during coal pyrolysis. Fuel, 82, 15–17, 1961–1966.

97. Fan H., Matsuoka K., Wang J., Tomita A. (2003). Ultrasonic loading of calcium on coal for enhanced SO_2 captured. Fuel, 82, 5, 481–486.

98. Renedo M.J., Fernandez J. (2004). Kinetic modeling of the hydrothermal reaction of ash, $Ca(OH)_2$ and CaSO4 on the preparation of desulfurant sorbents. Fuel, 83, 4–5, 525–532.

99. Yongqin Qi, Wen Li, Haokan Chen, Baoqing Li. (2004). Desulfurization of coal through pyrolysis in a fluidized bed reactor under nitrogen and 0.6 % O_2 atmosphere. Fuel, 83, 6, 705–712.

100. Karaca S. (2003). Desulfurization of a Turkish lignite at various gas atmospheres by pyrolysis. Effect of mineral matter. Fuel, 82, 12, 1509–1516.

101. Xu W.C., Kumagai M. (2003). Sulfur transformation during rapid hydropyrolysis of coal under high pressure using a continuous free fall pyrolyzer. Fuel, 82, 3, 245–254.

102. Li, Z., Sun, T., and Jia, J. (2011). An extremely rapid, convenient and mild coal desulfurization new process: sodium borohydride reduction. Fuel Processing Technology, 9, 1162–1167.

103. Shen, Y., Sun, T., and Jia, J. (2011). Novel desulfurization method of sodium borohydride reduction for coal water slurry. Energy&Fuels, 7, 2963–2967.

104. Shen, Y., Yang, X., Sun, T., and Jia, J. (2011). Innovative desulfurization process of coal water slurry under atmospheric condition via sodium metaborate electroreduction in the isolated slot. Energy&Fuels, 11, 5007–5014.

105. Shen, Y., Sun, T., and Jia, J. (2012). A novel desulfurization process of coal water slurry via sodium metaborate electroreduction in the alkaline system. Fuel, 96, 250–256.

106. Hayvanovych, V., and Pysh'yev, S. (2003). Desulfurization of low-rank coal with high sulfur content is the first stage of coal burning at heat electric stations. Energy&Fuels, 17, 1186–1190.

107. Grebeniuk, A., Korobchansky, V., Vlasov, H., Kaufman, S. (2002). Capturing chemical goods of carbonization. Donets'k, Ukraine: East Publishing House.

108. Grunvald, V. (1992). Sulfur gas technology. Moscow, RF: Chemistry.

109. Sinha, R.K., and Walker Jr, P.L. (1972). Removal of sulfur from coal by air oxidation at 350–450 °C. Fuel, 2, 125–129.

110. Joshi, J., Shah, Y., Ruether, J., and Ritz, H. (1983). Particle size effects on oxidation of pyrite in air/water chemical coal cleaning. Fuel Processing Technology, 2, 173–190.

111. Denghin L., Jinsheng G., Guangxi Y. (2003). Catalytic oxidation and kinetics of oxidation of coal-derived pyrite by electrolysis. Fuel Processing Technology, 82, 1, 75–85.

112. Pyshyev, S., and Bratychak, M. (2015). Modern technologies of clean coal. Lviv, Ukraine: Publishing House of Lviv Polytechnic National University.

113. Bazayants, H. (1999). Forecast of technical-and-economic index desulfurization equipments of coal-fired boilers of Ukraine. Power and Electrification, 2, 48–50.

114. Pasini, R., and Walker, H. (2012). Estimating constituent release from FGD gypsum under different management scenarios. Fuel, 95, 190–196.

115. Hussar, M. (2010). Development measures and technical and economic assessments of reducing emissions of hyposulfurous oxide on thermal electric power station in Ukraine. Power and Electrification, 7, 39–42.

116. Nechayeva, T. (2011). Investigation of possible strategies of structure Ukrainian electrical energy complex taking into account the impact of environmental constraints and requirements. Problems of General Power Industry, 25, 25–31.

117. Johansson, L.-E. (2009). FGD: Choosing NID® DFGD or Open

Spray Tower WFGD. In European Users Conference, 15–17 Sept., 2009, Lisbon. Portugal.

118. Podda, E. (2009). Megalopolis WFGD: Project experience and design initiatives. In European Users Conference, 15–17 Sept., 2009, Lisbon. Portugal.

119. EPA. Environmental Protection Agency. Control of mercury emissions from coal-fired electric utility boilers. (2001). from https://www3.epa.gov/airtoxics/utility/hgwhitepaperfinal.pdf.

120. Poullikkas, A. (2015). Review of design, operating, and financial considerations in flue gas desulfurization systems. Energy Technology & Policy, 2, 92–103.

121. Pysh'yev, S., Prysiazhnyi, Yu., Gunka, V., Astakhova, O., and Bratychak, M. (2013). Effect of coal quality on its desulfurization. 2. Influence of the inorganic matter. Chemistry & Chemical Technology, 3, 327–334.

122. Acharya, C., Sukla, L., and Misra, V. (2005). Biological elimination of sulfur from high sulfur coal by Aspergillus-like fungi. Fuel, 12–13, 1597–1600.

123. Cara, J., Vargas, M., Moran, A., Gomez, E., Martinez, A., and Garcıa, F. (2006). Biodesulfurization of a coal by packed-column leaching. Simultaneous thermogravimetric and mass spectrometric analyse the biodesulfurization of a semiantracite in a pakedbed system. Fuel, 85, 1756–1762.

124. Ozbayoglu, G. (1998). Desulfurization of coal to protect the environment. In G.Gallios and K. Matis (Eds.), Mineral processing and the environment (Chapter 3, pp. 199–222). Dordrecht, Netherlands: Springer Science+Business Media.

125. Nolan, P. (2000). Flue gas desulfurization technologies for coal-

fired power plants. from https://www.babcock.com/library/Documents/br-1709.pdf

126. Shved, M., Pyshyev, S., Prysiazhnyi, Yu., and Timchuk, M. (2016). The use of pitch oxidativ purification of brown coal as a fuel oil component. In Conference “Advance in Petroleum and Gas Industry and Petrochemistry”, 16-21 May 2016 Lviv. Ukraine: Publishing House of Lviv Polytechnic National University.

CHAPTER 3
COAL OXIDATIVE DESULFURIZATION

Serhiy Pyshyev
Department of Chemical Technology of Oil and Gas Processing, Institute of Chemistry and Chemical Technology, Lviv Polytechnic National University, Lviv, Ukraine

The content of total sulfur in coal is often not higher than 1-1.5 wt %. However, there are a lot of coals belonging to sulfur-rich ones. In particular, some coals contain 7-8 wt % of sulfur (see Chapter 1, Table 3.1). The pyrite form of sulfur is the main component in the sulfur-rich coal (40-90 % of total sulfur; see Table 3.1). Therefore we can obtain low-sulfur hard fuel removing the pyrite sulfur from the coal.

The essence of technologies is the coal desulfurization by an oxidative method that is based on the coal treatment, using a mixture of air and steam at 400-500 ^{0}C. Sulfur (mainly pyrite sulfur) may convert into gaseous sulfur-containing components at the relatively low consumption of oxidant. In fact, the process may be the first stage of the two-stage coal combustion, when gas with high content of sulfur dioxide or hydrogen sulfide is obtained [1, 2]. As noted in Chapter 2, this gas may be used to produce a concentrated sulfur dioxide, sulfuric acid or sulfur. Hydrogen sulfide, obtained by oxidative desulfurization of lignite can be concentrated or converted to sulfur by known methods.

Also the process products are: solid low-sulfuric fuel (coal); decomposition resin produced during thermal cracking of the organic matter.

The author of this chapter led and participated in detailed research of the oxidative desulfurization (OD) process of different types of coal: lignite (brown coal) [3-6], low-metamorphosed black (sub-bituminous and bituminous low coking coal) coal [1, 8, 9], medium-metamorphosed black (bituminous coking) coal [10-12], and high-metamorphosed black (bituminous non-coking coal) coal, including anthracite [8, 13, 14].

We also compared the desulfurization efficiency of various types of coal, which differed in the degree of coalification, and studied the impact of coal organic and mineral parts on the process proceeding [13, 15-17].

During coal oxidative desulfurization the content of thermally unstable compounds (volatiles yield) and its ability to sintering decrease, so this process can be used to produce pulverized coal from low- and medium-metamorphosed coal with high sulfur content [18-22].

The following samples of Ukrainian coal were selected for investigations: lignite (brown coal) (LG) from Morozivskyy deposit of Dnieper brown-coal basin; candle coal (C) from Buzanska mine of Lviv-Volyn coal basin; candle-gaz coal (CG) from Belorechenskaya mine of Donetsk coal basin; gas coal (G1) from Chervonograd mine of Lviv-Volyn coal basin; gas coal (G2) from Zarichna mine of Lviv-Volyn coal basin; gas coal (G1) from Donetsk coal basin; fat coal (F1 and F3) from Samsonovska concentrating mill of Donetsk coal basin; fat coal (F2 snd F4) from Lisova mine of Lviv-Volyn coal basin; coking coal (CK) from Shchegkovka Glubokaya mine of Donetsk coal basin; lean-hot coal (LH) from Kalinina mine of Donetsk coal basin; lean coal (L) from Shidna mine of Donetsk coal basin, anthracite (A1) from Rovenska concentrating mill of Donetsk coal basin, anthracite (A2) from Luganska N 2 mine of Donetsk coal basin, and run-of-mine coal (RM) from Dobrotvirska Thermal power stations (TPS).

Unless otherwise stated, the fraction of 0.1-0.25 mm was used for researches, because it is the optimal size for coal burning at TPS.

A model mixture of pyrite (mixed with inert material in such a way that the content of pyritic sulfur in the mixture was comparable with that in the original coal) was prepared.

The results of initial coal and model mixture analyses are shown in Table 3.1.

Table 3.1 shows that all samples are high-sulfur coal ones with the pyritic sulfur amount of 40-90 %. Anomalous high content of sulfate sulfur in some coal samples can be explained by the fact that in some places there was an access for air.

To study the oxidative desulfurization process the laboratory plants were used. Their flowcharts are represented in Fig. 3.1.

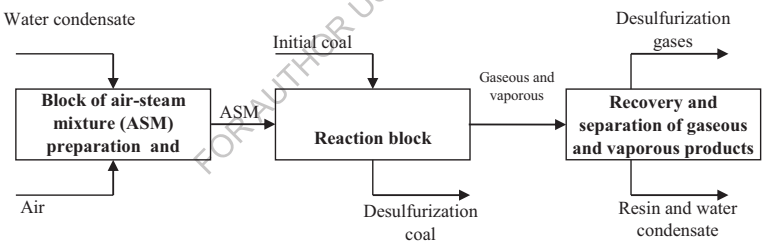

Fig. 3.1. Flowchart of the laboratory plant for coal oxidative desulfurization

The detailed scheme of the laboratory plants is given in Fig. 3.2. The desulfurization process was performed in a fluidized-bed reactor (7) under isothermal conditions. The reactor type was closed to the ideal mixing reactor. The reactor consisted of a quartz tube with a porous partition (inner diameter – 11.0 mm, height of the reaction zone – 60.0 mm). The reactor was heated by an electrical furnace (9). The temperature was controlled

using thermocouple (10) located inside the reactor. The oxidant (steam-air mixture) was fed to the bottom of the reactor. The air was supplied into the reactor through the water vaporizer (4). The rate of air flow was controlled by a manual flowmeter (3). The rate of water flow were regulated automatically by a pump (2). Obtained gaseous products were withdrawn from the top of the reactor and cooled in (11). Condensed water and resin were collected in the trap for decomposition resin (11) and desulfurization gases were collected in the gas collector (13). After the experiment, the trap with the resin was drained and the amount of formed resin and desulfurizated coal was weighted. The volume of gases was determined by an amount of NaCI displaced from the gas collector.

Table 3.1 Characteristics of the initial samples and model mixture

Size fraction, mm	Moisture content, W^a, wt %	Ash, A^d, wt %	Volatiles yield, V^{daf}, wt %	Sulfur content for dry mass, wt %				Relative content of sulfur different types, %		
				Total, S_t^d	Pyritic, S_p^d	Organic, S_o^d	Sulfate, $S_{SO_4}^d$	S_p^d/S_t^d	S_o^d/S_t^d	$S_{SO_4}^d/S_t^d$
1	2	3	4	5	6	7	8	9	10	11
Lignite (LG) or brown (B)										
0-0.1	12.64[1]	9.89	63.02	4.34	1.88	2.36	0.10	43.32	54.38	2.30
0.1-0.25	13.96[1]	9.42	63.78	4.28	2.10	2.07	0.11	49.07	48.36	2.57
0.25-0.315	14.03[1]	9.16	64.34	4.31	1.97	2.21	0.13	45.71	51.28	3.02
0.315-0.5	14.02[1]	9.25	64.83	4.25	1.80	2.23	0.22	42.35	52.47	5.18
0.5-0.75	13.49[1]	9.16	66.77	4.25	1.71	2.37	0.17	40.24	55.76	4.00
0.75-1.00	13.51[1]	9.44	66.9	4.36	1.81	2.38	0.17	41.51	54.59	3.90
1.00-1.60	13.44[1]	9.25	67.34	4.38	1.92	2.27	0.19	43.84	51.83	4.34

1	2	3	4	5	6	7	8	9	10	11
1.60-2.00	13.43[1]	8.62	66.6	4.53	1.64	2.64	0.25	36.20	58.28	5.52
Candle (C)										
0-0.1	4.82	15.77	33.70	5.00	3.09	0.17	1.64	61.76	3.36	32.77
0.1-0.25	4.85	11.36	37.67	3.98	2.34	0.54	1.10	58.84	13.46	27.70
0.25-0.315	5.00	10.42	38.68	3.72	2.08	0.71	0.93	56.09	18.98	24.93
0.315-0.40	4.71	11.02	39.39	3.75	2.30	0.70	0.75	61.34	18.77	19.89
0.40-0.63	4.65	9.90	39.42	3.72	2.35	0.74	0.63	63.10	20.00	16.90
0.63-1.00	4.59	8.91	40.20	3.30	1.78	1.00	0.52	53.97	30.16	15.87
Candle-gas (CG)										
0.1-0.25	3.91	8.15	38.08	3.16	1.60	1.20	0.36	50.76	37.99	11.25
1	2	3	4	5	6	7	8	9	10	11
0.25-0.315	4.01	8.22	38.48	2.98	1.53	1.04	0.41	51.34	34.90	13.76
0.315-0.5	4.12	8.00	38.16	2.81	1.54	0.91	0.36	54.80	32.38	12.81
Gas (G1)										
0-0.1	1.35	16.37	38.01	6.52	4.88	1.08	0.56	74.81	16.64	8.55
0.1-0.25	1.21	16.80	40.91	7.95	7.20	0.52	0.23	90.57	6.50	2.93
0.25-0.315	1.36	17.94	39.98	7.27	6.23	0.53	0.51	85.77	7.25	6.97
0.315-0.63	1.20	18.72	39.05	6.90	6.06	0.31	0.53	87.83	4.55	7.62
0.63-1.6	1.54	20.39	39.90	8.14	7.69	0.11	0.34	94.51	1.37	4.12
Gas (G2)										
0.1-0.25	1.17	20.82	41.11	7.18	6.05	0.54	0.60	84.23	7.46	8.31

1	2	3	4	5	6	7	8	9	10	11
0.25-0.315	1.22	16.73	40.33	5.53	4.84	0.32	0.36	87.55	5.86	6.59
Gas (G3)										
0-0.1	5.41	9.83	45.40	2.29	1.61	0.62	0.06	70.05	27.19	2.76
0.1-0.20	5.04	9.69	46.65	2.99	2.45	0.44	0.09	82.04	14.79	3.17
0.20-0.40	5.32	9.54	46.68	2.74	2.20	0.45	0.08	80.31	16.60	3.09
0.40-0.63	4.97	9.22	46.13	2.54	2.10	0.35	0.08	82.99	13.69	3.32
0.63-1.00	5.06	9.29	45.32	2.20	1.79	0.34	0.07	81.34	15.31	3.35
Fat (F1)										
0.1-0.25	2.33	10.14	34.32	3.68	2.35	1.31	0.02	63.86	35.60	0.54
Fat (F2)										
до 0.1	2.33	20.59	36.94	6.59	3.68	1.15	1.76	55.84	17.45	26.71
0.1-0.25	1.87	21.97	36.71	6.97	4.50	1.17	1.30	64.56	16.79	18.65
1	2	3	4	5	6	7	8	9	10	11
0.25-0.315	1.97	20.98	35.39	7.73	4.93	1.61	1.19	63.78	20.83	15.39
0.315-0.5	1.90	20.72	37.08	8.11	5.02	1.51	1.58	61.90	18.62	19.48
0.5-0.75	1.91	22.09	36.89	7.61	4.85	1.20	1.56	63.73	15.77	20.50
0.75-1.00	1.85	22.46	37.30	7.37	4.90	1.03	1.44	66.49	13.98	19.54
Fat (F3)										
0.1-0.25	3.82	9.32	33.94	2.98	1.29	0.34	1.35	43.29	11.41	45.30
Fat (F4)										
0.1-0.25	1.61	21.42	35.71	7.09	4.09	0.51	2.49	57.69	7.19	35.12
Coking (CK)										
0.1-0.25	1.35	27.71	31.86	2.74	1.13	0.75	0.86	41.24	27.37	31.39

1	2	3	4	5	6	7	8	9	10	11
Lean-hot (LH)										
0.1-0.25	1.72	27.23	21.20	3.41	1.37	0.96	1.08	40.18	28.15	31.67
Lean (L)										
<0.1	0.89	37.84	15.01	4.04	3.07	0.86	0.11	76.00	21.25	2.75
0.1-0.25	1.00	43.10	16.53	4.48	3.81	0.55	0.13	84.91	12.16	2.93
0.25-0.315	1.25	38.28	14.91	3.10	2.66	0.31	0.12	85.95	10.13	3.92
0.315-0.5	1.40	42.70	17.08	3.71	2.95	0.66	0.10	79.51	17.76	2.73
>0.5	1.46	41.81	16.52	3.64	2.88	0.65	0.11	79.11	17.83	3.06
Anthracite (A1)										
0.1-0.25	3.5	6.22	2.00	2.85	1.41	1.21	0.23	49.47	42.46	8.07
Anthracite (A2)										
0.1-0.2	6.40	19.44	5.70	3.07	1.94	0.92	0.20	63.19	30.29	6.51
0.2-0.4	6.80	18.24	6.69	2.52	1.86	0.46	0.20	73.81	18.25	7.94
Run-of-mine (RM)										
<0.5	2.83	24.42	35.80	1.92	1.52	0.3	0.10	79.17	15.63	5.21
1	2	3	4	5	6	7	8	9	10	11
Pyrite (mixture of FeS_2 and SiO_2)										
–	1.54	–	–	3.86	3.72	0.13[2]	0.01	96.37	3.37	0.26

Remarks:

[1]W^{af}.

[2]Unidentified form of sulfur.

The gas products of the desulfurization process were analyzed by chromatographic method using an Cvet-500 instrument equipped with a TCD detector and two columns, Polisorb-1 (separation of carbon dioxide, ethylene, ethane, hydrogen sulfide, propane/propylene and sulfur dioxide) and zeolite CaX (separation of nitrogen, oxygen, methane, carbon monoxide).

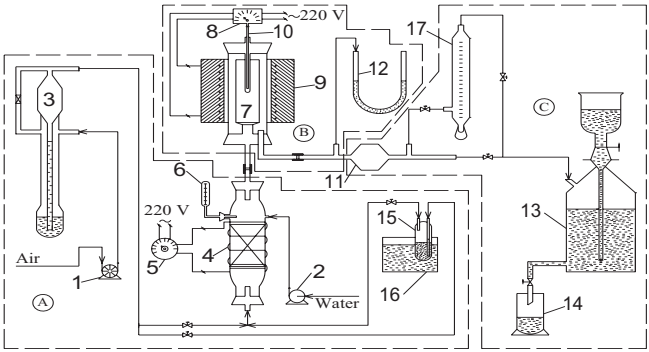

Fig. 3.2. Scheme of the laboratory plant for coal oxidative desulfurization: block of air-steam treatment and feed (A); reactor block (B) and block of volatile products elimination (C). The plant consists of: compressor (1); pump (2); rheometer (3); water vaporizer (heater) (4); electric transformer (5); thermometer (6); reactor (7); potentiometer (8); furnace (9); thermocouple (10); trap for decomposition resin (11); manometer (12); gas collector (13); beaker (14); vessel (15); thermostat (16) and flowmeter (17).

3.1. Theoretical foundations of the process

3.1.1. Effect of coal organic matter. The temperature and water steam are factors affecting the chemism of oxidative desulfurization [9, 10]:

- at 425 ^{0}C and higher temperatures the process is intensified due to the pyrite decomposition for pyrrhotite (FeS_x) and sulfur followed by their oxidation;
- if water steam is added to air, the rate and degree of pyrite oxidation increase; the reason is steam-pyrite complex formation that increases reactivity.

Table 3.2 presents possible reactions of pyrite conversion during oxidative desulfurization which are divided into pyrite reactions with

oxygen (including previous thermal decomposition), water steam, coal organic matter (COM) and possible products of the process. The thermodynamic analysis was carried out for the mentioned reaction (Table 3.2). Since the reactions proceed under the pressure close to the atmospheric one, and with small change of moles number, it was assumed that at negative value of Gibbs energy (≤ -50 kJ/mol) the reaction is not limited by achievement of thermodynamic equilibrium, *i.e.* equilibrium conversion degrees of the initial components are ≥ 99 %. At the positive value of Gibbs energy (≥ +50 kJ/mol) the reaction is thermodynamically impossible, *i.e.* equilibrium conversion degrees of the initial components are < 1 %. Within the range of values from -50 to +50 kJ/mol the reaction proceeds with thermodynamic limits.

Data from Table 3.2 allow to assert that pyrite oxidation is thermodynamically the most possible reaction within the temperature range of 350-450 ^{0}C. The great positive values of Gibbs energy for the reactions of pyrite thermal decomposition may be caused by non-stoichiometric compound with high reactivity – pyrrhotite – which is formed during the decomposition. The formation of pyrrhotite, not the iron sulfide, which characteristics were taken to consideration during calculations, is the most probable explanation of such great values.

The hydrogen sulfide formation is improbable because of the reactions of pyrite or pyrrhotite with water steam, but it is possible due to their interaction with hydrogen or coal organic matter. The analysis of the reactions between pyrite and hydrocarbons shows that the increase of hydrocarbon molecular mass increases the probability of the mentioned conversions proceeding.

Table 3.2 Calculated values of Gibbs energies of the possible reactions at 350 and 450^{0}C

No.	Equation	ΔG^0_c, kJ/mol		Temperature interval of the reaction proceeding, ^{0}C; Ref.
		350 ^{0}C	450 ^{0}C	
1	2	3	4	5
Thermal decomposition and reactions of pyrite and its decomposition products with oxygen				
		-3298.45	-3354.50	> 350–400; [24, 25]
2	$4FeS_{(s)}+5O_{2(g)}\rightarrow 2Fe_2O_{3(s.)}+2SO_{2(g)}$	-2167.97	-2154.70	[26, 27]
3	$FeS_{2(s)} + 3O_{2(g)} \rightarrow FeSO_{4(s)} + SO_{2(g)}$	-876.85	-848.26	[28]
4	$S_{(s)}+ O_{2(g)}\rightarrow SO_{2(g)}$	-317.76	-328.60	[26, 27]
5	$FeS_{2(s)}\rightarrow FeS\ (Fe_{1-x}S)_{(s)}+S_{(s)}$	35.14	–	–
6	$FeS_{2(s)}\rightarrow FeS\ (Fe_{1-x}S)_{(s)}+S_{(g)}$	–	204.28	> 500–600; [25, 26]
Reactions of pyrrhotite with water steam				
7	$FeS(Fe_{1-x}S)_{(s)}+H_2O_{(g)}\rightarrow FeO_{(s)}+H_2S_{(g)}$	54.09	55.00	[28]
8	$2FeS(Fe_{1-x}S)_{(s)}+3H_2O_{(g)}\rightarrow Fe_2O_{3(s.)}+2H_2S_{(g)}+H_{2(g)}$	115.94	126.04	[28]
Reactions of pyrite, pyrrhotite and iron sulfide with COM and its conversion products				
9	$3FeS_{2(s)}+c\text{-}C_6H_{12(g)}\rightarrow 3FeS_{(s)}+3H_2S_{(g)}+C_6H_{6(g)}$	-32.35	-94.55	–
10	$FeS_{2(s)}+H_{2(g)}\rightarrow FeS_{(s)}+H_2S_{(g)}$	-2.19	-9.98	> 500; [25, 28]
11	$FeS_{2(s)}+CO_{(g)}\rightarrow FeS_{(s)}+COS_{(g)}$	4.01	-1.72	> 800; [25, 28]
12	$FeS_{2(s)}+C_6H_{14(g)}\rightarrow FeS_{(s)}+H_2S_{(g)}+c\text{-}C_6H_{12(g)}$	16.92	4.66	–

1	2	3	4	5
13	$FeS_{2(s)}+1\text{-}C_4H_{8(g)}\rightarrow FeS_{(s)}+H_2S_{(g)}+1,3\text{-}C_4H_{6(g)}$	41.33	22.02	–
14	$FeS_{2(s)}+C_4H_{10(g)}\rightarrow FeS_{(s)}+H_2S_{(g)}+1\text{-}C_4H_{8(g)}$	43.14	21.59	–
15	$FeS_{2(s)}+C_2H_{6(g)}\rightarrow FeS_{(s)}+H_2S_{(g)}+C_2H_{4(g)}$	57.81	36.78	–
16	$FeS(Fe_{1-x}S)_{(s)}+H_{2(g)}\rightarrow Fe_{(s)}+H_2S_{(g)}$	65.48	65.49	> 800; [25, 28]
17	$FeS_{2(s)}+C_2H_{4(g)}\rightarrow FeS_{(s)}+H_2S_{(g)}+C_2H_{2(g)}$	98.25	77.47	–
18	$FeS_{2(s)}+C_{(s)}\rightarrow Fe_{(s)}+CS_{2(g)}$	165.82	145.22	> 1000; [25, 28]
19	$2FeS\ (Fe_{1-x}S)_{(s)}+C_{(s)}\rightarrow 2Fe_{(s)}+CS_{2(g)}$	233.48	220.68	> 1000; [25]
Reactions of pyrite and iron sulfide with COM and water steam				
20	$C_{(s)}+FeS_{2(s)}+H_2O_{(g)}\rightarrow H_2S_{(g)}+FeS_{(s)}+CO_{(g)}$	58.76	36.46	[28]
Reactions of COM with pyrite conversion products				
21	$C_{(s)}+2S_{(g)}\rightarrow CS_{2(g)}$	–	-338.82	[25]
22	$H_{2(g)}+S_{(g)}\rightarrow H_2S_{(g)}$	–	-214.26	[29]
23	$C_{(s)}+SO_{2(g)}\rightarrow S_{(s)}+CO_{2(g)}$	-63.21	–	[23]
24	$S_{(s)}+H_{2(g)}\rightarrow H_2S_{(g)}$	-37.33	–	[29]
25	$C_{(s)}+2S_{(s)}\rightarrow CS_{2(g)}$	27.88	–	[25]
26	$SO_{2(g)}+C_{(s)}\rightarrow S_{(g)}+CO_{2(g)}$	–	122.78	[23]
Reactions of gaseous products				
27	$2SO_{2(g)}+CH_{4(g)}\rightarrow 2S_{(s)}+CO_{2(g)}+2H_2O_{(g)}$	-165.20	–	[23]
28	$2CO_{(g)}+SO_{2(g)}\rightarrow S_{(s)}+2CO_{2(g)}$	-140.02	–	[23, 29]
29	$CS_{2(g)}+H_2O_{(g)}\rightarrow H_2S_{(g)}+COS_{(g)}$	-35.38	-35.01	[30-32]

1	2	3	4	5
30	$SO_{2(g)} + 2H_2S_{(g)} \rightarrow 3S_{(s)} + 2H_2O_{(g)}$	-33.64	–	[23, 29]
31	$COS_{(g)} + H_2O_{(g)} \rightarrow H_2S_{(g)} + CO_{2(g)}$	-22.06	-20.53	[30-32]
32	$2CO_{(g)} + SO_{2(g)} \rightarrow S_{(g)} + 2CO_{2(g)}$	–	64.07	[23, 29]
33	$2SO_{2(g)} + CH_{4(g)} \rightarrow 2S_{(g)} + CO_{2(g)} + 2H_2O_{(g)}$	–	207.76	[23]
34	$SO_{2(g)} + 2H_2S_{(g)} \rightarrow 3S_{(g)} + 2H_2O_{(g)}$	–	517.12	[23, 29]

The reactions leading to the formation of cyclic unsaturated compounds are more probable than aliphatic unsaturated compounds formation.

Hydrogen sulfide may be formed owing to the reactions of coal with sulfur and its dioxide. At 350 ^{0}C the sulfur formation due to the pyrite decomposition is impossible [9, 10], but it is possible due to the proceeding of the reactions 27 and 28 (Table 3.2).

Hydrogen sulfide formation is also possible due to the interactions between gaseous products (reactions 29 and 31).

The reactivity of COM differs depending upon the degree of chemical maturity (metamorphism, coalification) of coal. Black high-metamorphosed coal (*e.g.* L and A grade) has the inert organic matter and brown coal, on the contrary, has high reactivity.

From the literature data it is impossible to understand if the reactions between COM and FeS_2 will proceed under the conditions of oxidative desulfurization and if the reaction intensity will depend on the COM coalification degree. Therefore, the purpose of the following studies was to

establish the effect of coal organic matter on the proceeding of oxidative desulfurization process.

For describes the coal preventive desulfurization, the term “degree of sulfur removal” is used. The sulfur content in the desulfurized coal depends on the ratio between the coal and sulfur conversion rates. Hence, the removal degree of total or pyritic sulfur (RDS(T) or RDS(P)) is calculated in accordance with the formula (3.1) and indicates the ratio between the rate of sulfur conversion followed by the production of gaseous products and the rate of organic matter reaction, i.e. process selectivity:

$$RDS = \frac{S_0^d - S^d}{S_0^d} \cdot 100 \quad (3.1)$$

where S_0^d – the content of sulfur (total or pyritic) relative to the dry sample, wt %; S^d – the content of sulfur (total or pyritic) in the desulfurized coal relative to the dry sample, wt %.

Considering that during preventive desulfurization the coal yield usually decreases, the removal degree of sulfur is lower than the resulting level of environmental pollution decrease. For correct comparison of preventive desulfurization the term “total or pyritic sulfur conversion” (SC(T) or SC(P)) should be used. This value indicates the amount of sulfur converted into sulfur-containing products that will not be in the atmosphere while the further burning of desulfurized coal (the level of environmental pollution decrease). It is calculated in accordance with the formula (3.2), %:

$$SC = \frac{S_0^a \times 100 - S^a \times x_C}{S_0^a} \quad (3.2)$$

where S_0^a – the content of sulfur (total or pyritic) in the initial coal relative to the analytical sample, wt %; S^a – the content of sulfur (total or pyritic) in the desulfurized coal relative to the analytical sample, wt %; x_C – the yield of desulfurized coal, wt %.

To determine the effect of COM presence and its quality on the process, we compared the desulfurization processes of pyrite and different types of coal. We compared the effect of factors upon which the chemism of pyrite conversion depends (temperature and water steam content in the air-steam mixture), on the desulfurization process of coal with different metamorphism degree. The degree increases in the row LG → C → G → F → L →A (Table 3.2). The experimental results are represented in Tables 3.3-3.5.

The analysis of data from Table 3.4 shows that temperature effect is the same for all types of coal. The sulfur content in coal decreases and removal degree of pyritic sulfur increases with the temperature growth to 425 ^{0}C. The greatest increase is observed within the temperature range of 400–425 ^{0}C. At the temperatures higher than 425 ^{0}C the decrease of pyritic sulfur removal degree for F1 and F2 coals is observed.

Table 3.3 Characteristics of pyrite and desulfurized coal samples

Desulfurized samples of pyrite and different types of coal	Content of pyritic sulfur for analytical sample (S_p^a), mas %	Coal yield, mas %	Conversion of pyritic sulfur, %	Difference between conversion degrees of coal pyritic sulfur and model mixture $FeS_2 + SiO_2$, %
1	2	3	4	5
LG	0.61	50.37	83.21	11.97
C	0.23	82.27	91.51	20.27

1	2	3	4	5
G1	2.19	75.33	76.80	5.56
F2	1.46	83.11	72.61	1.37
L	0.88	94.05	80.01	8.77
Model mixture (FeS_2 + SiO_2)	1.07	–	71.24	–

Table 3.4 Dependence of pyritic sulfur removal degree upon the temperature

Temperature, ^{0}C	Removal degree of pyrite sulfur, %						
	LG	C	G1	G2	F1	F2	L
350	44.96	13.28	18.42	25.32	2.89	28.76	12.85
400	55.04	52.12	46.97	63.57	24.04	47.97	41.95
425	70.31	89.84	68.93	86.47	81.70	67.12	76.70
450	75.73	96.04	74.04	92.99	73.48	58.20	79.35

The reason is the above-mentioned ability of such type of coal for the conversion into plastic state and for the baking at 450-550 ^{0}C.

With the increase of water steam content in the oxidant the sulfur content in coal passes through the minimum and removal degree – through the maximum for all types of coal.

It should be noted that there is not clear dependence between pyritic sulfur removal degree and metamorphism degree that changes in the row LG → C → G → F → L → A.

Regularities occurred during the desulfurization of lignite (brown coal) differ from those observed during black coal desulfurization. For example, the temperature increase is the least influential factor for all investigated samples (Table 3.4); sulfur converts into hydrogen sulfide (Table 3.6), not in SO_2, as for black coal (Table 3.7). During

desulfurization of black coal hydrogen sulfide is observed in negligible amounts. All these facts indicate the change of desulfurization chemism while using lignite compared with black one.

Table 3.5 Dependence of pyritic sulfur removal degree upon the oxidant composition

Content in the oxidant, vol %		Removal degree of pyrite sulfur, %						
oxygen	water steam	LG	C	G1	F1	F2	L	A
20.95	0	-	90.22	75.70	-	56.00	-	-
20.06	4	70.30	93.71	87.06	80.01	57.99	70.62	53.05
17.85	15	-	94.53	91.00	81.00	61.55	72.07	57.97
14.71	30	73.60	92.41	69.18	81.70	67.12	76.64	65.00
10.5	50	79.31	84.29	54.59	86.81	58.81	67.98	80.49
6.31	70	81.65	65.32	32.12	84.83	32.65	66.93	76.43

Lignite essentially differs from black coal by the reactivity of organic matter and moisture content. In order to establish the factor (high moisture or COM reactivity) having the decisive influence on chemism during lignite desulfurization we compared dry lignite and wet anthracite. The anthracite was investigated as coal with the most inert COM. One can see from Table 3.8 that water adsorbed in coal may affect H2S formation only in the presence of organic matter with high reactivity: the content of hydrogen sulfide in the gases is less for dry lignite. At the desulfurization of dry and wet anthracite samples the hydrogen sulfide is absent in the gases. This fact indicates the dominant role of organic matter, as well as its gasification and cracking products, for the reactions of hydrogen sulfide obtaining.

Thus, it is possible to desulfurize any type of black coal at 425-450 ^{0}C due to the treatment in fluidized bed formed by air-steam mixture. Such coal may be used in power engineering because the quality of organic matter does not have an essential influence on the efficiency of sulfur removing.

Table 3.6 Gases average composition at lignite desulfurization under optimal conditions

Content in desulfurization gases, vol %								
H_2S	CH_4	C_2-C_3	CO	CO_2	O_2	N_2	Ar	H_2
8.0–12.5	2.6–3.3	2.8–4.6	5.5–6.5	23.5–25.0	0.6–1.2	45.7–54.8	0.5–0.7	0.7–1.4

Table 3.7 Gases average composition at desulfurization of C, F2, L and R coal types under optimal conditions

Content in desulfurization gases, vol %									
SO_2	H_2S	CH_4	C_2-C_3	CO	CO_2	O_2	N_2	Ar	H_2
2.5–7.0	till 0.4	0.5–3.9	0.4–2.6	1.1–3.8	5.0–9.9	1.6–11.1	71.6–78.7	0.8–0.9	till 0.4

Under the same conditions the sulfur removal degree is less for medium-metamorphosed black coal compared with other types of black coal. The reason is coal ability for conversion into plastic state and baking.

The effect of temperature (to 425 ^{0}C) and water steam content on the pyritic sulfur conversion is the same for all types of coal.

At oxidative desulfurization of lignite (compared with black one) the main amount of sulfur converts into H_2S. It is obtained due to the reactions of pyrite with coal organic matter or its conversion products.

Table 3.8 The characteristics of gases obtaining at desulfurization of wet and dry samples of coal

Content in desulfurization gases, vol %									
SO_2	H_2S	CH_4	C_2-C_3	CO	CO_2	O_2	N_2	Ar	H_2
The analytical sample of lignite (W^{af} = 13.96 mas %)									
-	7.01	1.68	1.42	3.77	23.21	1.18	60.57	0.71	0.45
The sample of dry lignite (W^{af} = 0.44 mas %)									
-	5.89	1.37	0.98	3.24	19.85	6.31	61.26	0.71	0.39
The analytical sample of anthracite (W^a = 3.55 mas %)									
0.88	-	0.78	0.35	traces	2.98	14.92	79.17	0.92	-
The sample of wet anthracite (W^a = 14.54 mas %)									
1.28	-	0.87	0.60	traces	3.59	14.43	78.32	0.91	traces

3.1.2. Effect of coal inorganic matter. These studies were performed to establish the effect of coal inorganic part on the process.

To change the amount of inorganic part the coal beneficiation was carried out *via* flotation. For this purpose the laboratory model of FL-1.5 impeller flotator was used. The one flotation cycle was as follows: pulp preparation from coal and water (ratio 1:25); addition of flotation reagent to the pulp (montanol – 30 vol % and kerosene – 70 vol %) in amount of 0.1 % regarding the raw material; pulp pouring into the flotator; air supply for 10 min, flow rate of which was 4 m^3/h for 1 kg of coal. Electron-microscopic investigations were carried out using scanning electronic microscope (SEM) ZEISS EVO 40XVP with the system of X-ray microanalysis INCA Energy. Silicon-lithium energodispersive detector was

used for microanalysis [33]. The analysis of the results of different types of coal oxidation desulfurization and flotation (Table 3.9) allows to assert that coal of C, G1, G2 and L types is well desulfurized during flotation (removal degree of the total sulfur is 43.54, 61.27, 56.20 and 50.23 %, respectively) and coal of F3 type is badly desulfurized (removal degree of the total sulfur is 25.07 %). It is assumed that coal of F3 type has pyrite fine-grained agglomeration and coal of other types – coarse-grained one.

This assumption was confirmed by photomicrographs and elemental analysis of the initial and concentrated F3 and G2 samples using SEM with the system of X-ray emission analysis (XEA). Photomicrographs and elements content in the certain points are given in Figs. 3.3-3.14 and Tables 3.10-3.21.

Table 3.9 The flotation results of coal different types

Black coal type	C	G1	G2	F3	L
Flotation reagent, mas %	65.23	77.33	72.00	64.03	61.97
Sulfur content, mas %					
total, S_t^a	2.14	3.04	3.11	5.23	2.21
pyritic, S_p^a	0.88	1.65	1.77	3.36	1.24
sulfate, $S_{SO_4}^a$	0.38	0.45	0.38	0.85	0.10
organic, S_o^a	0.88	0.94	0.96	1.02	0.87
Ash content, A^a, mas %	6.88	9.86	9.41	13.43	16.14

The point of sample composition determination is situated in the left upper corner of the marker indicating the spectrum number.

On the photomicrographs of G-2 initial coal (Figs. 3.3-3.6) one can see that inorganic matter (including the considerable part of FeS_2) is in a form of relatively large plates and agglomerations. XEA results show that:

- spectra 1 and 2 are made in the points related to the organic matter (dark parts);
- spectra 3 and 4 – mineral matter mainly, – pyrite (light parts).

In the samples depicted in Fig. 1 the main part of inorganic matter is in the form of plates; Figs. 3.4-3.6 – large agglomerates.

The character of the photos where G2 flotoconcentrate is depicted (Figs. 3.7 and 3.8) allows to assert that the form, location and sizes of FeS_2 are changed after flotation compared with the initial coal. After flotation pyrite is in the form of extremely small impregnations in the organic matter (Fig. 3.7) and in the structure of fine mineral particles (Fig. 3.8).

The appearance of F3 coal inorganic matter confirms the previous assumption concerning its fine-grained character (Figs. 3.9-3.11). XEA results show that:

- spectrum 7 is made in the points related to coal organic matter;
- spectrum 8 – in the points which are organic matter with relatively high content of pyrite;
- spectrum 9 – mixture of organic-inorganic matter, including pyrite.

In F3 coal inorganic matter is in the form of relatively small particles and associates with organic matter.

The distribution character of inorganic matter, including pyrite, is slightly changed in the case of concentrated F3 coal (Figs. 3.12-3.14). The photos show finer inorganic particles (compared with the initial coal).

For F3 coal XEA results show that dark surface (except spectrum 10) is organic matter with relatively high content of inorganic matter, including pyrite.

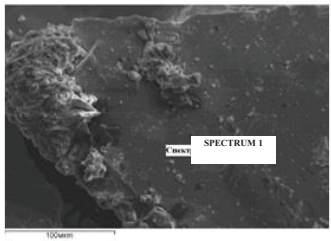

Fig. 3.3. Photomicrograph of G2

Table 3.10 XEA results for the spectrum 1

Element	Relative content	
	Wt %	Atomic %
C	84.98	93.81
S	15.02	6.19
Total	100.00	100.00

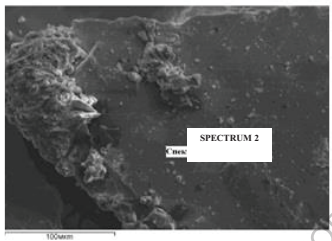

Fig. 3.4. Photomicrograph of G2 initial

Table 3.11 XEA results for the spectrum 2

Element	Relative content	
	Wt %	Atomic %
C	78.59	92.00
S	13.85	6.09
Fe	7.55	1.91
Total	100.00	100.00

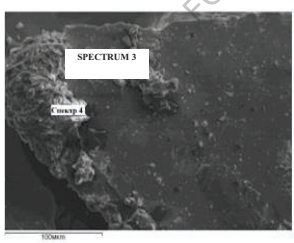

Fig. 3.5. Photomicrograph of G2 initial coal

Table 3.12 XEA results for the spectrum 3

Element	Relative content	
	Wt %	Atomic %
C	16.84	41.74
Al	1.24	1.37
Si	1.50	1.60
S	31.42	29.17
Fe	48.39	25.81
Co	0.60	0.31
Total	100.00	100.00

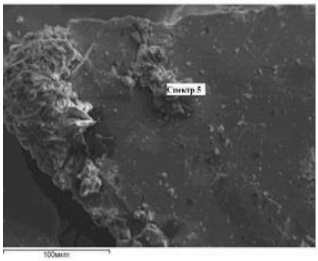

Fig. 3.6. Photomicrograph of G2 initial coal

Table 3.13 XEA results for the spectrum 4

Element	Relative content	
	Wt %	Atomic %
C	16.62	41.25
Al	1.34	1.48
Si	1.29	1.38
S	33.88	31.53
Fe	38.26	20.44
Co	0.18	0.07
Zn	8.42	3.84
Total	100.00	100.00

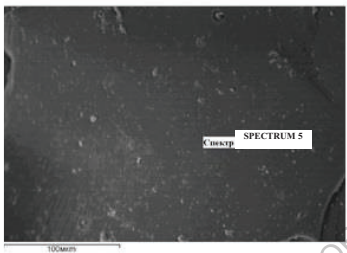

Fig. 3.7. Photomicrograph of G2 coal flotoconcentrate

Table 3.14 XEA results for the spectrum 5

Element	Relative content	
	Wt %	Atomic %
C	73.97	92.43
S	2.88	1.36
Fe	23.15	6.21
Total	100.00	100.00

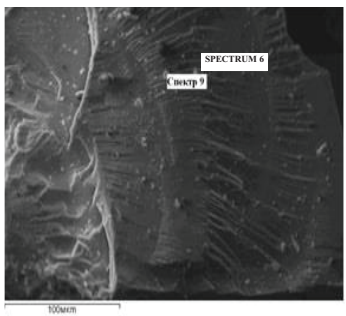

Fig. 3.8. Photomicrograph of G2 coal flotoconcentrate

Table 3.15 XEA results for the spectrum 6

Element	Relative content	
	Wt %	Atomic %
C	13.74	27.99
Al	36.33	32.95
Si	34.00	29.60
S	7.55	5.79
Fe	8.39	3.67
Total	100.00	100.00

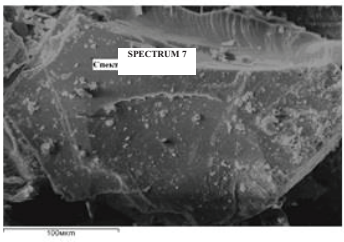

Fig. 3.9. Photomicrograph of F3 initial coal

Table 3.16 XEA results for the spectrum 7

Element	Relative content	
	Wt %	Atomic %
C	84.25	93.77
Si	1.18	0.55
S	12.24	5.11
Fe	2.33	0.58
Total	100.00	100.00

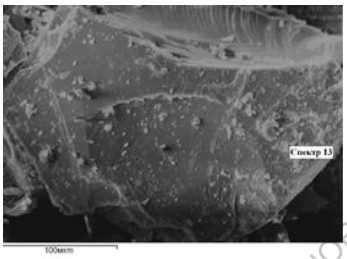

Fig. 3.10. Photomicrograph of F3 initial coal

Table 3.17 XEA results for the spectrum 8

Element	Relative content	
	Wt %	Atomic %
C	62.63	82.60
Al	5.71	3.36
Si	8.65	4.88
P	0.06	0.03
S	12.49	6.17
Fe	10.46	2.97
Total	100.00	100.00

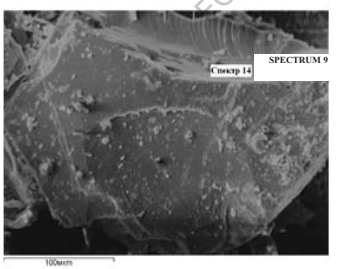

Fig. 3.11. Photomicrograph of F3 initial coal

Table 3.18 XEA results for the spectrum 9

Element	Relative content	
	Wt %	Atomic %
C	32.11	65.20
Al	1.29	1.16
Si	3.27	2.84
P	0.21	0.17
S	9.46	7.19
Fe	53.66	23.44
Total	100.00	100.00

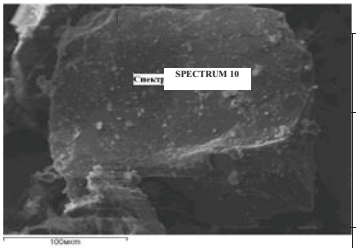

Fig. 3.12. Photomicrograph of F3 coal flotoconcentrate

Table 3.19 XEA results for the spectrum 10

Element	Relative content	
	Wt %	Atomic %
C	62.21	82.88
S	29.52	14.77
Fe	8.28	2.36
Total	100.00	100.00

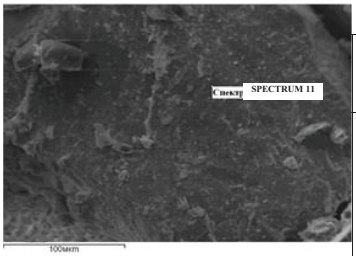

Fig. 3.13. Photomicrograph of F3 coal flotoconcentrate

Table 3.20 XEA results for the spectrum 11

Element	Relative content	
	Wt %	Atomic %
C	60.34	80.86
Al	6.53	3.89
Si	9.86	5.66
S	13.48	6.76
Fe	9.80	2.83
Total	100.00	100.00

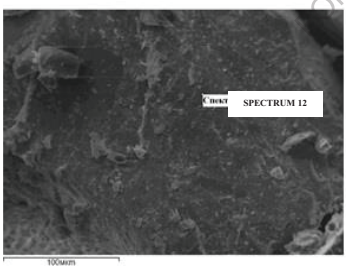

Fig. 3.14. Photomicrograph of F3 coal flotoconcentrate

Table 3.21 XEA results for the spectrum 12

Element	Relative content	
	Wt %	Atomic %
C	61.96	81.24
Al	8.45	4.93
Si	10.79	6.04
S	11.88	5.84
Fe	6.91	1.95
Total	100.00	100.00

Thus, photomicrographs and XEA results confirm the assumption that in the initial G2coal inorganic matter, including pyrite, is in the form of large plates which are removed during flotation. The result is sulfur essential removal from coal.

In the case of F3 coal inorganic part, including pyrite is in the form of fine particles associated with organic matter. Therefore sulfur content slightly decreases during flotation.

To study the effect of inorganic matter amount on the process the initial coal and flotoconcentrate were desulfurized (Table 3.22). The results show that the concentrated coal is desulfurized with the same efficiency as the initial coal. It means that the amount of inorganic matter does not affect the desulfurization process, *i.e.* the coal may be desulfurized before and after its beneficiation.

The comparison of the data from Tables 3.9 and 3.22 show that desulfurization using oxidative method is more effective than sulfur removal using beneficiation, because higher values of sulfur removal degree are achieved. Moreover, using the investigated method we may remove pyrite of both (fine-grained and coarse-grained) forms. It means that inorganic matter sizes (pyrite first of all) do not influence the character of coal desulfurization *via* oxidative method.

Thus, the desulfurization efficiency *via* oxidation method does not depend on sizes and amount of inorganic impregnations in the coal matrix. Therefore the desulfurization process may be realized before and after coal beneficiation.

Table 3.22 Comparison of sulfur removal degree during oxidative desulfurization of the initial and concentrated samples of black coal

Black coal type	C	G1	G2	F3	L
Initial coal					
Sulfur removal degree, %					
pyritic	88.79	69.20	46.66	67.41	76.66
total	49.08	60.51	36.62	51.58	65.54
Concentrated coal (flotoconcentrate)					
Sulfur removal degree, %					
pyritic	84.09	87.27	55.37	67.86	85.48
total	55.61	35.20	32.48	39.20	59.28

3.1.3. Effect of temperature and water steam. Temperature and oxidant composition effect on the chemistry of pyrite conversion. The desulfurization procedure was performed in in the temperature range of 350-450 ^{0}C, increasing the temperature in steps of 25 ^{0}C, in the air/steam atmosphere. The steam content in the gas mixture was 30 vol %. In addition, one sample (F) was studied in more wet atmosphere (70 vol % of steam) at 425 ^{0}C.

Mössbauer spectroscopy was used to study the products of pyrite transformation. The ^{57}Fe Mössbauer absorption spectra were recorded in the transmission geometry at room temperature. The data were numerically analysed by means of a least–squares procedure assuming Lorentzian shape of the absorption lines. The fits supplied the main parameters of the

hyperfine interactions of the ^{57}Fe nuclei: isomer shift, proportional to the electron density at the iron nuclei, quadrupole splitting related to the electric field gradient and Zeeman splitting proportional to the internal magnetic fields. These parameters compared to the parameters known from the literature data, were the basis for the identification of iron compounds in the samples. Moreover, the spectral area of every component was used for the determination of the relative amount of each iron compound (assuming equal recoil free fractions f for all phases).

The Mössbauer spectra of the G1 coal before treatment (sample A) and after desulfurization in different conditions (samples B, C, D, E and F) are shown in Figure 3.15. In the case of samples A and B the spectra were recorded in the low velocity scale (± 4.0 mm/s) in order to determine precisely the parameters of doublets and to perform the identification of sulfur bounded in inorganic compounds present in the coal. Such a procedure was possible because no magnetic iron phases were observed.

Samples C to F contained magnetic phases and their spectra had to be recorded in a high velocity scale (± 10.0 mm/s). From the visual inspection of the spectra it is obvious, that the specimens contain a variety of iron compounds. Thus, the numerical deconvolution of the spectra was complicated. In the first attempt all spectra were fitted within the following scheme. We assumed one doublet for low spin iron (II), assigned to pyrite, FeS_2, one or two doublets for high spin iron (II) in $FeSO_4 \cdot nH_2O$ with different n, one doublet for high spin iron (III) paramagnetic species related to $Fe_2(SO_4)_3$ and/or to small particles of Fe_2O_3 . In addition, one or two sextets for magnetically ordered Fe_2O_3 with different grain sizes were also taken into account. However, this model of fitting was not satisfactory for sample E, where additional magnetic phase was clearly observed with internal magnetic field ranging between 22 T to 30 T (see Fig. 3.15E). This

fraction was assigned to pyrrhotite, deficient in iron monosulfide FeS, with the general formula $Fe_{1-x}S$ (typically $0.06 < x < 0.12$)

Small amount of pyrrhotite and its complicated spectrum (composed of three sextets) forced us to use in numerical analysis the known from the literature [34-36] Mössbauer pyrrhotite parameters as constrained ones. Such procedure, which results in the improvement of calculations, was applied first to the spectrum of sample E and next also to samples C and F.

The final Mössbauer parameters of the phases identified in the spectra are given in Table 3.23.

In the studied coal the main part of sulfur occurs as a pyritic sulfur (see Table 3.1, coal G1). In principle, iron disulfide may appear in cubic structure of pyrite and rhombic structure of marcasite, depending on the geological origin of the coal. However these two forms have similar chemical reactivity and the name of more frequent pyrite is often used for iron disulfide FeS_2. The Mössbauer parameters of both forms are similar as well (for pyrite isomer shift IS = 0.28-0.33 mm/s and quadrupole splitting QS = 0.58-0.63 mm/s and for marcasite IS = 0.26-0.29 mm/s and QS = 0.50-0.53 mm/s [34, 36]). Thus, we did not attempt to distinquish them from Mössbauer spectra. Within this simplification the Mössbauer data (Table 3.23) confirm that in studied coal about 86 % of iron exists in pyrite and the rest in form of ferrous sulfates.

The certain amount of iron sulfates is usually present in the coal as a result of pyrite oxidising probably in the period between collection of the sample and its final studies and may be described by the reaction (analogous to reaction 3 (see Table 3.2) in the presence of steam):

$$FeS_2 + 3O_2 + nH_2O \rightarrow FeSO_4 \cdot nH_2O + SO_2 \qquad (3.3)$$

The detailed numerical analysis of the sample A showed that in the subspectrum assigned to iron sulfates at least two slightly different forms of

sulfates which differ in the number of hydrous water molecules might be distinguished: $FeSO_4 \cdot 7H_2O$ and $FeSO_4 \cdot H_2O$. Indeed, melanterite $FeSO_4 \cdot 7H_2O$, szomolnokite $FeSO_4 \cdot H_2O$ and coquimbite $Fe_2(SO_4)_3 \cdot 9H_2O$ are the most commonly observed iron sulfate minerals occurring in various kinds of coals [37].

In the studied desulfurization process after the first heating at 350 ^{0}C only tiny changes in the spectrum were observed (see Table 3.23). The amount of pyrite (precisely the amount of iron bounded in pyrite) decreases slightly from 86 to 82 % and the content of ferrous sulfates diminishes to the half of starting amount, from 14 to 8 %. Additional doublet with parameters indicating oxidation to the Fe^{3+} was attributed to the new appearing phase. This new paramagnetic doublet is probably a superposition of two doublets. One of them may be assigned to the iron(III) sulfate formed on the surface of FeS_2 and $FeSO_4$ grains. Anhydrous iron(III) sulfate gives at room temperature the paramagnetic spectrum with an isomer shift of 0.39 mm/s and a quadrupole splitting of 0.60 mm/s [38], which is significantly less than the values reported in present studies. Larger value of quadrupole splitting which indicates a deviation from the symmetrical structure of regular Fe^{3+} species may be understood if the hydrated or surface forms are taken into account [39]. The second doublet could be attributed to small particles of hematite and/or related compounds such as oxyhydroxides like FeOOH.

At higher temperature during thermal treatment (400 ^{0}C) the amount of α-Fe_2O_3 in form of big grain increases; the last is to be seen by magnetic interactions. For bulk hematite the accepted value of the hyperfine magnetic field is 51.5–51.8 T at room temperature. This value is reduced for small grains; for example for the particles of 158 nm in diameter the field is 49.6 T and for particles with 180 nm of grain size the field is 50.3

T, as it was found in the literature for supported Fe_2O_3/SiO_2 [40]. We also observe such reduction in the magnitude of magnetic field, that is an evidence of the distribution of hematite grain sizes in the studied samples.

In excess of oxygen the reaction predominantly proceeds according to the equations 1, 3 (see Table 3.2) and

$$2FeS_2 + 7O_2 \rightarrow Fe_2(SO_4)_3 + SO_2 \quad (3.4)$$

Sulfate formation is more favourable at the temperature below 400 ^{0}C [41].

Indeed, at that temperature we observed that FeS_2 decomposed to Fe^{3+} species and to Fe_2O_3. Thus, it may be concluded that this reaction takes place predominantly at surface layers of the coal grains.

At temperatures of 425 ^{0}C and 450 ^{0}C the scenario of desulfurization changes qualitatively. After such treatment the spectrum consists mainly of magnetic components (see Fig. 3.15D and Fig. 3.15E). Moreover, at 450 ^{0}C, besides hematite, a new magnetic phase with definitely lower hyperfine field in the range of 22–30 T may be clearly observed.

At room temperature the stable phases of iron monosulfide are stoichiometric FeS (troilit), hexagonal pyrrhotite $Fe_{0.90-0.94}S$ and monoclinic pyrrhotite Fe_7S_8 which composition Fe_7S_8 (or $Fe_{0.875}S$) may be derived from FeS by subtraction of one iron atom per 8 FeS units. Stoichiometric troilit is antiferromagnetic with the magnetic field of H=31 T [34, 38] and isomer shift of IS = 0.66-0.76 mm/s. Both pyrrhotite forms represent the defect structures with different vacancies distributions [34-36]. The phase Fe_7S_8 is ferromagnetic and the room temperature Mössbauer spectrum shows three well resolved sextets with hyperfine fields in the range of 29.7-30.0, 25.2-25.5 and 22.1-22.8 T corresponding to vacancies distribution. All sextets have the isomer shift values of between 0.65 and 0.70 mm/s [34].

Hexagonal pyrrhotites are analysed in the literature [34] within the model of three inequivalent iron sites with different hyperfine fields in the range of 30.0-30.3, 27.8-28.0 and 25.6-26.0 T. Thus a mixture of monoclinic and hexagonal pyrrhotites exhibits a spectrum that is a superposition of the spectra characteristic for both components and effectively consists of four Zeeman sextets (30, 28, 25 and 22 T).

Pyrite decomposition into iron sulfide and sulfur going through the nonstoichiometric phases takes place in an inert atmosphere according to the reaction 5, 6 in Table 3.2 [25, 26, 42].

In Table 3.2 (equations 5, 6) it has been foreseen that the pyrite oxidation is partly proceeded by the decomposition of FeS_2 to S and FeS (or $Fe_{1-x}S$). To elucidate the process of pyrrhotite formation sample F was desulfurized in the more wet atmosphere. It is worth to note that in case of the sample F the amount of pyrrhotite found from the Mössbauer spectrum analysis was similar to the amount determined for sample D desulfurized at the same temperature. In the sample E (reaction temperature 450 ^{0}C) the higher content of pyrrhotite was found (see Table 3.23). These observations confirmed that the process of pyrrhotite formation depends only on the temperature whereas the partial pressure of oxygen is irrelevant. Because FeS_2 decomposes to FeS in innert atmosphere, it may be concluded that in the studied samples this process appeared in bulk of the coal grains.

We did not observe the formation of FeS, but it is interesting to note that Mössbauer data confirm the presence of small amount of $Fe_{1-x}S$ (2-5%) found earlier by chemical analysis as being equal to 0.03-0.05 wt %. It may suggest that the process of coal desulfurization takes place in the kinetic regime because the pyrrhotite oxidation is far faster than the troilite (FeS) formation.

Thus, we could distinguish between the surface oxidation of pyrite which involves the following species: $FeSO_4 \cdot nH_2O$ (in virgin sample), next $Fe_2(SO_4)_3$, small grains of Fe_2O_3, bulk Fe_2O_3 and finally the solid state conversion of FeS_2 to $Fe_{1-x}S$ followed by the oxidation to Fe_2O_3. by diffusing oxygen.

In particular, at temperatures lower than 450 ^{0}C pyrite is oxidised to sulfates. Above this temperature the desulfurization is intensified due to two parallel processes: pyrite decomposition into pyrrhotite and sulfur, and pyrite oxidation to iron (III) oxide and sulfur dioxide.

For study of effect of water vapor content the desulfurization process was performed at four different temperatures (350, 400, 425 and 450°C) under dry atmosphere (air containing 4 vol % of H_2O) or wet atmosphere (mixture of air/water vapor) for 20 minutes. The volume ratios of air/water vapor were 30/70, 50/50 and 70/30. Ukrainian coal that is marked as F1 (see Table 3.1), was studied. The particle size fraction of 0.10-0.25 mm was selected for the study.

After the desulfurization runs carried out at dry and wet (70 vol % of H_2O vapor) atmosphere the behaviour of iron-containing compounds was studied by Mössbauer spectroscopy as described above.

The content of C^{daf} and H^{daf} were additionally measured using an elemental analyzer EuroVector EuroEA 3000. In order to minimize the experimental error, three analyses were performed for each sample and the averages from the obtained results were calculated.

The raw material contained sulfur in the form of pyrite, sulfates as well as organic compounds (see coal F1, Table 3.1). It should, however, be stressed that a majority of sulfur was found as FeS_2. The presence of pyrite was additionally confirmed by Mössbauer spectroscopy.

Table 3.23 Mössbauer data of the coal G1 samples

	Species	FeS_2			$FeSO_4 \cdot 7H_2O$			$FeSO_4 \cdot H_2O$		
Sample	Temp. [^{0}C]	IS[1] [mm/s]	QS[2] [mm/s]	A[3] [%]	IS [mm/s]	QS [mm/s]	A [%]	IS [mm/s]	QS [mm/s]	A [%]
A	RT	0.30(2)	0.60(2)	85.9(3)	1.27(2)	3.08(4)	7(1)	1.32(2)	2.62(2)	7(1)
B	350	0.30(2)	0.60(2)	82.5(7)	1.27(2)	3.18(4)	3.4(9)	1.33(2)	2.60(2)	5.2(9)
C	400	0.31(2)	0.62(2)	54.9(5)				1.3(1)	2.7(2)	2.0(3)
D	425	0.31(2)	0.61(2)	44.6(4)						
E	450	0.31(2)	0.64(2)	13.3(3)						
F	425	0.30(2)	0.61(2)	61.1(6)				1.32(2)	2.56(2)	6.3(3)

.

Table 3.23 Mössbauer data of the coal G1 samples (continuation)

	Species	Fe^{3+} species			α-Fe_2O_3				$Fe_{1-x}S$		
Sample	Temp. [^{0}C]	IS [mm/s]	QS [mm/s]	A [%]	IS [mm/s]	QS [mm/s]	H [T]	A [%]	IS [mm/s]	H [T]	A [%]
A	RT										
B	350	0.39(2)	1.08(2)	8.9(7)							
C	400	0.38(2)	1.11(2)	14.8(5)	0.38(2) 0.39(2)	0.20(2) 0.12(6)	52.17(2) 49.4(2)	26(1) 2.1(3)			
D	425	0.39(2)	1.09(2)	9.7(4)	0.38(2) 0.30(2)	0.20(2) 0.12(4)	51.70(2) 49.3(2)	40(1) 3.2(8)	0.66	22.6-29.8	2.5(5)
E	450	0.39(2)	1.19(2)	2.1(3)	0.38(2) 0.35(2)	0.20(2) 0.14(2)	51.80(2) 49.2(1)	63(1) 15.9(1)	0.66	22.6-29.8	5.3(4)
F	425	0.38(2)	1.08(2)	18.8(6)	0.38(2) 0.41(4)	0.22(2) 0.22(8)	50.76(7) 48.0(3)	8.4 (7) 3.4(6)	0.66	22.6-29.8	2.1(6)

Remarks:

[1]IS – isomer shift versus room temperature α–Fe.

[2]QS – quadrupole splitting.

[3]A – relative contribution to the total spectrum

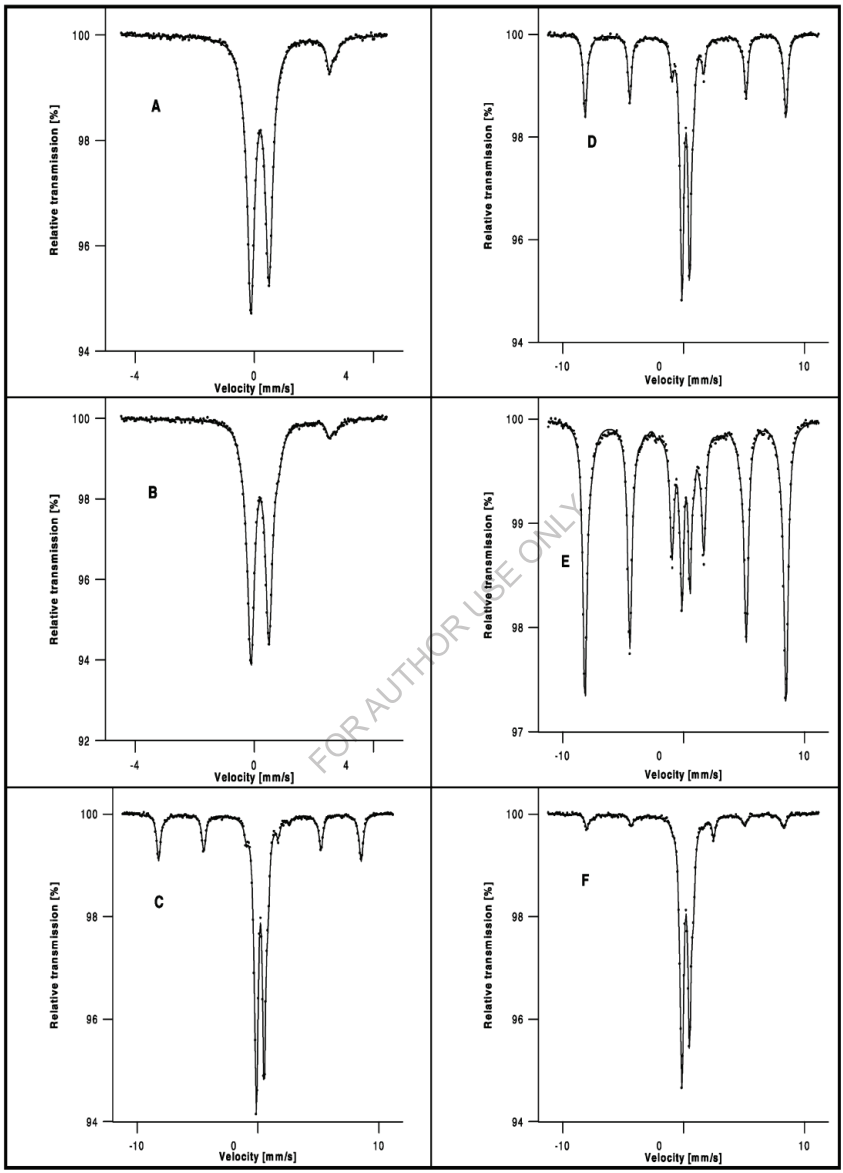

Fig. 3.15 Room temperature Mössbauer spectra of G1 coal. (A) Before treatment; (B–E) after desulfurization at 350, 400, 425, 450 ^{0}C, respectively, with 30 vol.% of steam; (F) after desulfurization at 425 ^{0}C with 70 vol.% of steam.

In the Mössbauer spectrum of the raw material (Figure 3.16) the dominant doubl with parameters of isomer shift IS = 0.30(1) mm/s and quadrupole splitting QS 0.60(1) mm/s characteristic for pyrite was found. The spectrum indicated also tl presence of small amount of iron-bearing phase with parameters IS = 1.25(2) mm and QS = 1.52(2) mm/s, which could be assigned to mineral ankerite [(Ca,Fe)(CO_3) [43]. This phase remained unchanged during the different treatment of the raw coal.

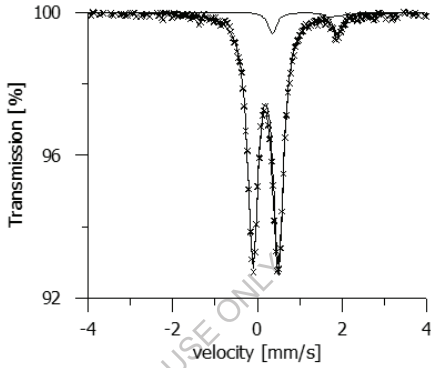

Fig. 3.16 Mössbauer spectrum of the raw coal F1

The results of technical analysis of coal samples desulfurized at differe temperatures and atmospheres are presented in Table 3.24.

It can be found that an increase in the reaction temperature resulted in significant reduction of volatile compounds content. The presence of water vapor d not play such important role in this effect. Furthermore, the content of steam in tl reaction mixture influenced the moisture of coal, especially in the process performe at low temperatures. When the volume ratio of air/water vapor was decreased at 3: and 400°C, an increase in the content of moisture in the treated coal was detecte Moreover, an increase in C^{daf} and H^{daf} amounts observed with raising the H_2O conte in the feed was favoured by low temperature of desulfurization. It should be notic that the conditions used for the desulfurization process enabled to remove sulfur fro the G-type coa

Table 3.24 Characteristics of the coal F1 after desulfurization

Content of steam in the oxidative agent (vol %)	Technical analysis		
	Volatiles,V^{daf}, (wt %)	Ash, A^{d}, (wt %)	Moisture,W^{a}, (wt %)
350°C			
4	28.18	15.04	2.38
30	29.78	13.93	3.16
50	30.66	14.11	4.78
70	30.08	15.09	5.78
400°C			
4	27.42	15.63	2.77
30	27.59	15.47	3.09
50	28.35	14.96	3.49
70	30.08	16.20	4.94
425°C			
4	20.41	15.63	2.1
30	22.39	15.60	2.33
50	22.78	16.16	3.18
450°C			
4	17.45	16.10	2.21
30	19.85	16.78	2.13
50	20.67	17.07	2.24
70	19.78	16.08	3

Table 3.24 Characteristics of the coal F1 after desulfurization (continuation)

Content of steam in the oxidative agent (vol %)	Content of sulfur (wt %)				C^{daf} (wt %)	H^{daf} (wt %)
	Total, S_t^d	Pyritic, S_p^d	Sulfate, $S_{SO_4}^d$	Organic, S_o^d		
350°C						
4	3.81	2.53	0.05	1.23	78.62	3.76
30	3.54	2.28	0.04	1.22	82.24	4.03
50	3.31	2.16	0.02	1.12	86.79	4.29
70	3.06	1.62	0.04	1.39	92.04	4.65
400°C						
4	3.16	2.00	0.10	1.06	82.1	3.67
30	3.03	1.79	0.08	1.17	86.56	4.22
50	2.46	1.03	0.06	1.37	86.77	4.46
70	1.99	0.80	0.07	1.12	91.07	4.78
425°C						
4	1.86	0.47	0.03	1.36	86.45	3.42
30	1.71	0.43	0.02	1.26	90.8	4.08
50	1.69	0.31	0.00	1.38	86.21	4.08
450°C						
4	2.23	0.66	0.02	1.54	91.24	3.57
30	1.93	0.62	0.04	1.27	88.54	3.55
50	1.89	0.59	0.02	1.28	86.9	3.68
70	1.98	0.52	0.00	1.46	87.84	3.69

However, an effectiveness of desulfurization depended on both temperature and content of steam in the reaction mixture.

It should be stressed that the process temperature was the main factor influencing the changes of coal mass. The composition of reaction mixture also affected a decrease in the mass of coal, however, this effect was less significant compared to the role of reaction temperature. Generally, an introduction of water vapor to the reactants inhibited the mass loss.

Pyrite phase was recognized as the main sulfur-containing component of raw coal. Therefore, Mössbauer spectroscopy was used for studies of FeS_2 transformation during the desulfurization process. The Mössbauer spectra recorded for the samples after desulfurization in dry and wet atmospheres at 350, 400 and 450°C are shown in Figure 3.17. After the numerical deconvolution of the spectra, the parameters of each subspectrum (doublet(s) and/or sextet(s)) attributed to different components were determined. The values of these parameters were used to identify the inorganic iron compounds present in the coal samples. The results of spectra deconvolution are shown in Table 3.25. All spectra were fitted within the following model: first doublet was assumed for low spin iron(II) in FeS_2, second doublet – for high spin iron(II) in $FeSO_4 \cdot nH_2O$ and the third doublet for high spin iron(III), that may be assigned to paramagnetic state of hematite or some oxyhydroxides like goethite FeOOH. Additionally, magnetically ordered phases like magnetite, hematite and pyrrhotite ($Fe_{1-x}S$) were fitted by 2-6 sextets depending on the spectra complication. Because of pyrrhotite was present in small amounts in the samples suitable parameters characteristic for this non-stoichiometric sulfide $Fe_{1-x}S$ (usually $0.06 < x < 0.12$) were taken from the literature [35, 44] and constrained. Such procedure significantly improved the quality of fitting.

In Figure 3.18 a correlation between the level of total sulfur removal, expressed as the ratio of the total amount of sulfur to the content of carbon in the dry ash free coal (S_t^a/C^{daf}), and the concentration of water vapor in the reaction mixture is presented. It should be noticed that an effectiveness of the desulfurization process increases with raising temperature. Nevertheless, at the highest temperature (450°C) the level of total sulfur removal is slightly lower than at 425°C. This effect should be attributed to a significant increase in the rate of coal gasification, which becomes faster than desulfurization. The promoting influence of water vapor content is observed at low temperatures (350 and 400°C). At these temperatures an increase in the H_2O content results in a gradual increase in the effectiveness of desulfurization. However, at high temperatures this effect is not so important.

Depending on the process conditions the chemical and structural transformation of pyrite undergoes with a different rate resulting in a formation of various products. The Mössbauer measurements show that FeS_2 is partially converted to $FeSO_4$ in dry atmosphere at low temperatures. An increase in the reaction temperature to 400°C leads to a subsequent oxidation of ferrous sulfate and a small amount of Fe^{3+} species, attributed to Fe in oxyhydroxide or superparamagnetic Fe_2O_3, is formed. At higher temperatures α-Fe_2O_3 is a dominant Fe-containing phase. However, the presence of Fe_3O_4 is also detected. Additionally, $Fe_{1-x}S$ appears in the samples after the desulfurization process performed at 425 and 450°C. Probably, apart from pyrite oxidation to iron oxides a thermal decomposition of FeS_2 simultaneously occurs as described above.

It should be assumed that oxygen reacts with the surface of FeS_2 grains forming the product coating [45]. The oxidation of bulk pyrite proceeds according to the classical shrinking core model, in which the rate

of reaction is controlled by oxygen diffusion through the product shell. The deficit of oxidizing agent in the grain core results in the formation of magnetite (Fe_3O_4) and pyrrhotite ($Fe_{1-x}S$) that are products of incomplete FeS_2 oxidation and its decomposition, respectively.

The Mössbauer data reveal that an increase in the H_2O content in the reaction mixture influences a rate of FeS_2 oxidation and a distribution of the products. In wet atmosphere a part of pyrite is deeply oxidized to hematite even at 350°C. For the samples desulfurized at temperatures above 400°C α-Fe_2O_3 is the only recognized product of FeS_2 transformation. Usher et al [46] observed the promoting effect of water vapor on the pyrite oxidation earlier. The quantum chemical calculations [47] and spectroscopic study [48] showed that water could adsorb on the pyrite surface. Water adsorption changes the HOMO-LUMO characteristics of the surface by electron donation from H_2O to Fe ions. The resulting LUMO states, attributed to σ^* orbitals of the S_2 dimers occurring in the bulk, can promote the surface reactions. In consequence, an acceleration of deep FeS_2 oxidation is observed when oxygen is present in the reaction mixture.

In the works described above desulfurization of low- (Table 3.23) and medium-metamorphosed coals (Tables 3.23, 3.24) with relatively high reactivity of organic matrix was investigated. It is known that COM reactivity depends on the degree of coal metamorphism. High-metamorphosed coal (for example, lean coal and anthracite) has inert organic matrix. Brown coal has higher reactivity of organic matrix than low- and medium-metamorphosed coals and high analytical moisture (usually more than 10 wt %). The possibility of (9)-(20) reactions (see Table 3.2) proceeding depends, first of all, upon COM reactivity. Therefore, the following questions emerge:

Are black high-metamorphosed and brown coals desulfurized in the same manner as the samples used in previous experiments?

Is pyrite chemism the same for all types of black and brown coals?

Thus, the purpose of the following studies was to establish the effect of COM on the oxidative desulfurization process and the dependence of the reaction rate and direction of pyrite conversion on COM characteristics.

Table 3.25 Mössbauer data of the coal F1 samples

Temp. (°C)	FeS_2			$FeSO_4 \cdot nH_2O$			Fe^{3+} species		
	IS[1] (mm/s)	QS[2] (mm/s)	A[3] (%)	IS (mm/s)	QS (mm/s)	A (%)	IS (mm/s)	QS (mm/s)	A (%)
Dry atmosphere									
RT[4]	0.30(1)	0.60(1)	93.0(6)						
350	0.30(1)	0.60(1)	91.1(5)	1.32(4)	2.74(4)	3.8(6)			
400	0.30(1)	0.62(2)	73(5)	1.25(39)	2.70(39)	6.7±1.1	0.36(23)	0.96(55)	12.5±5.5
425	0.31(1)	0.60(1)	15.5(3)						
450	0.30(1)	0.61(1)	19.0(3)						
Wet atmosphere									
350	0.30(1)	0.60(2)	76.4(6)	1.29(2)	2.86(5)	3.6(6)			
400	0.30(1)	0.61(2)	39.0(4)	1.30(4)	2.70(8)	5.2(8)			
450	0.29(1)	0.60(1)	22.4(3)						

Table 3.25 Mössbauer data of the coal F1 samples (continuation)

Temp. (°C)	Fe_3O_4			α-Fe_2O_3				$Fe_{1-x}S$[5]		
	IS (mm/s)	H (kG)	A (%)	IS (mm/s)	QS (mm/s)	H (kG)	A (%)	IS (mm/s)	H (kG)	A (%)
Dry atmosphere										
RT[4]										
350										
400										
425	0.32(1)	499(1)	10.3±1.4	0.37(1)	0.16(1)	522.3(2)	53.1±1.1	0.66	224-305	8.0±1.4
	0.64(1)	462(1)	7.7(8)							
450	0.28(4)	489(3)	2.3(5)	0.37(1)	0.18(1)	519.1(2)	56.7(6)	0.66	228-301	11.3±1.1
	0.59(5)	453(4)	5.4±1.3							
Wet atmosphere										
350				0.38(1)	0.23(2)	515(1)	9.3±2.1			
				0.38(1)	0.24(12)	489(6)	5.2±2.9			
400				0.37(1)	0.20(2)	514.2(2)	36.4±1.7			
				0.36(2)	0.22(4)	491(3)	13.8±2.5			
450				0.37(1)	0.20(1)	517.6(8)	66.3±1.0			
				0.37(2)	0.17(4)	497(2)	4.6±1.1			

Remarks:

[1]IS – isomer shift versus room temperature α–Fe.

[2]QS – quadrupole splitting.

[3]A – relative contribution to the total spectrum.

[4]The sample of studied coal contains additionaly 5-7% of component with parameters IS = 1.25(2) mm/s and QS = 1.52(2) mm/s that remains unchanged in all experiments and may be ascribed to mineral ankeryt.

[5]Isomer shift and line width were constrained in all fits.

To determine the effect of COM presence and its quality on the process proceeding the comparative investigations of pyrite desulfurization and different types of coal were carried out. The effect of water steam and temperature on desulfurization of different coals was compared. The coal rank increases in the row: LG(B)→C→G→F→L→A (Table 3.1). The obtained results also allow to determine if the temperature and water steam effect on the process chemism is similar for different types of coal.

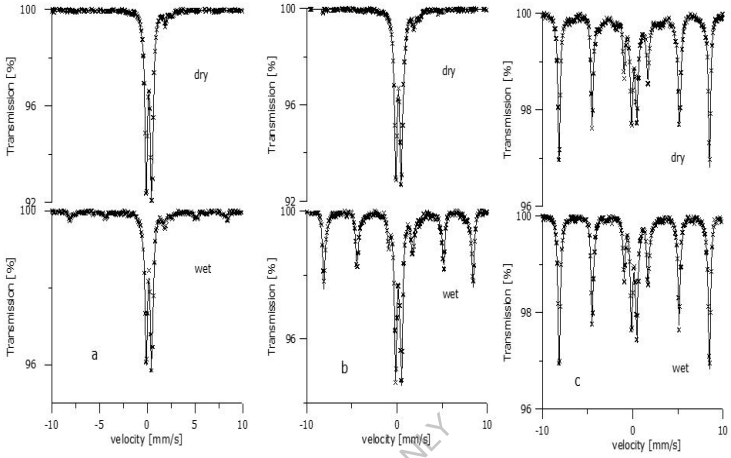

Fig. 3.17 Mössbauer spectra of the coal F1 reated at 350 (a), 400 (b) and 450°C (c) in the dry and wet atmosphere

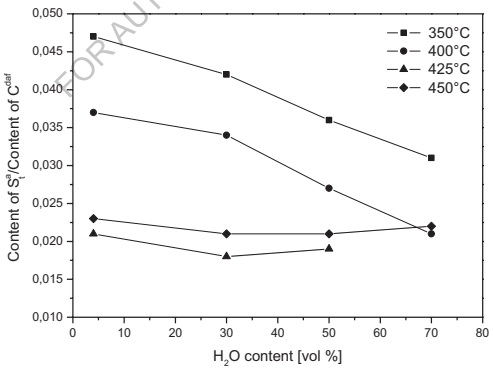

Fig. 3.18. Influence of H_2O content in the reaction mixture on the content of sulfur in the treated coal F1

The process time and oxidant flow rate were constant. The experimental results are represented in Table 3.26 and Figs. 3.19 and 3.20.

The presence of organic matrix in the reaction zone has different influence on the process proceeding. It increases conversion of pyritic sulfur by 10-20 % – for the black coal with the lowest and high metamorphism degree (C and L), approximately by 9 % – for G-type coal and only by 1.5 % – for F2. The reason of pyrite less conversion for G- and F-types is the formation of non-volatile components of thermal decomposition (the coal turns into plastic state and cake) resulting in the complication of oxidant access to the pyrite particles.

The data of Fig. 3 show the similarity of temperature effect for different types of coal. Removal degree of pyritic sulfur essentially increases with the increase of temperature to 425 °C; the greatest increase is in the range of 400-425 °C.

At high temperatures (425 and especially 450 °C) the least removal degree is observed at desulfurization of medium-metamorphosed coal of F-type (Fig. 3.19). The reason is above-mentioned difficulty for oxygen access during the process which occurs due to the ability of F-type coal to turn into plastic state and cake.

With the increase of water steam content in the oxidant the sulfur removal degrees has the maxima (Fig. 3.20).

Moreover, these maxima shift to the oxidant with greater content of water steam at increasing of total and pyritic sulfur content in the initial coal. It should be noted that there is not clear dependence between metamorphism degree and removal degree of pyritic sulfur. Obviously, the quality of COM (except for the medium-metamorphosed coal) does not practically affect the desulfurization process.

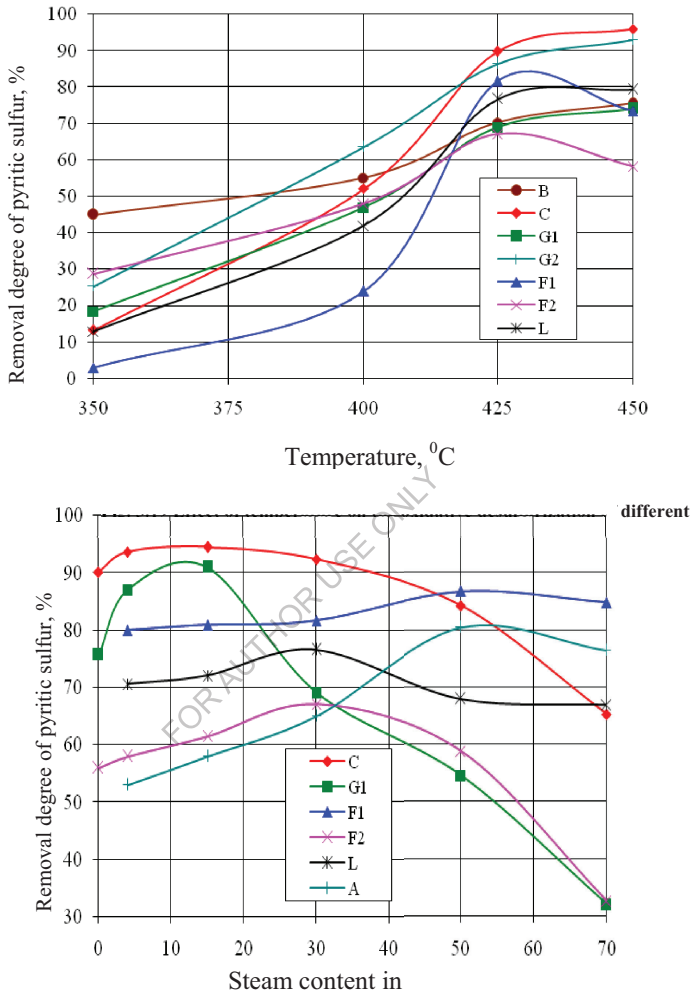

Fig. 3.20 Effect of oxidant composition on the oxidative desulfurization of different types of coal

Solid products of high-metamorphosed coal desulfurization (L-type) with the low reactivity of coal organic matrix (COM) were analyzed using the Mössbauer spectroscopy (Table 3.27, Fig. 3.21). The results show that

at 425-450 °C pyrite decomposes to pyrrhotite and sulfur followed by their oxidation. The increase of water steam amount in the oxidant decreases the amount of non-converted pyrite and increases the amount of oxidation end-products (iron oxides). The greatest effect of water steam is observed at relatively low temperatures (350-400 °C) because at higher temperatures (above 425 °C) pyrrhotite is formed independently of water steam presence or absence. Pyrrhotite interacts with the oxidant (air) with a reaction rate higher than that of water + pyrite complex. The results obtained for desulfurized coal of L-type are in good agreement with the data obtained during desulfurization of low- and medium-metamorphosed coal, which are described above. It means that chemism and mechanism of conversion of pyrite contained in black coal does not practically depend upon coalification degree.

The calculations of effective activation energies of pyrite oxidation (Table 3.28; the initial data for calculations of effective activation energies are given in Figs. 3.22-3.24) confirm the uniformity of the process chemism for black coals with different metamorphism degree at the temperatures near 425 °C. These activation energies of all three types of coal (C, G1 and L) decrease with the increase of temperature indicating the changes in the process chemism (pyrite decomposes to pyrrhotite and sulfur followed by their oxidation). The decrease of activation energy (Table 3.28) cannot be explained by the change of the process area (kinetic for diffusion) because as it was mentioned above, oxidant linear rate and grain sizes ensure pyrite oxidation reaction in the kinetic area within investigated range of temperatures.

One can see from Fig. 3.20 that removal degree of pyritic sulfur exceeds 75% for any type of coal. It should be noted that oxidant

composition effect was investigated under similar conditions for all types of coal. Therefore, the process time and oxidant amount, for example, were non-optimum at the desulfurization of L-type coal. It means that the method of sulfur removal is effective for all types of high-sulfuric black coal.

The desulfurization of brown coal has other regularities: the increase of temperature has the least effect on the process (the most flat dependence between a removal degree of pyritic sulfur and temperature, Fig. 3.19); the sufficiently high concentrations of hydrogen sulfide occur in the gases (4.6-7.1 vol %, Table 3.29). At desulfurization of black coal of different types and anthracite practically the amount of all removed sulfur turned into dioxide (Table 3.30). All these facts indicate the changes in desulfurization process chemism using brown coal (compared with black coal). Therefore we may only assume that formation of hydrogen sulfide takes place due to high reactivity of COM. It is described by the equations (10, 16, 20); see Table 3.2. The further formation of hydrogen sulfide during the process may be also caused by the moisture adsorbed in the brown coal and described by the equations (7, 8); see Table 3.2.

Analysis of literature data shows that the majority of above-mentioned reactions proceeds intensively only at temperatures higher than process temperatures (350-450 °C). On the other hand, the coal is not a pure carbon and hydrogen, therefore the proceeding of the reactions between hydrocarbon part of the coal and its sulfuric compounds is possible at lower temperatures. For instance, the authors of [49] show hydrogen sulfide formation as a result of the reaction between sulfur formed during pyrite dissociation and COM at the temperatures below 200 °C. They also predict the possible participation of pyrite in the reactions with coal organic fragments.

Table 3.31 represents the comparative composition of desulfurization gases obtained while using dry and wet samples of the brown coal with the highest reactivity of its organic mass and anthracite (the most inert COM).

The analysis of gases composition shows that water steam still takes an insignificant part in the reactions of pyrite conversion: at its high content in the oxidant (30-70 vol %) traces of hydrogen sulfide and hydrogen (see Table 3.29) appear in desulfurization gases. The results of Table 7 show the main role of COM in the reactions of hydrogen sulfide formation because H_2S and H_2 are not formed using anthracite. During desulfurization of both dry and wet brown coal the amount of all removed sulfur converts into H_2S. It should be noted that during the brown coal desulfurization hydrogen sulfide is formed even at 350 °C. This fact allows to assert the direct participation of pyrite in the reactions with COM because at such temperatures it cannot thermally decompose to pyrrhotite and sulfur as described above.

Thus, while using black coal the presence of organic matter in the reaction zone affects the pyrite oxidation (increases pyritic sulfur conversion by 1.5-20.0 %). The quality of this organic matter (its reactivity) does not practically affect the pyrite oxidation (except for medium-metamorphosed coal).

At high temperatures (425 and especially 450 °C) the least removal degrees of pyritic sulfur are observed at desulfurization of medium-metamorphosed coal. It is explained by the difficulty for oxygen access during the process of desulfurization in which F-type coal is used because it is capable to turn into plastic state and cake.

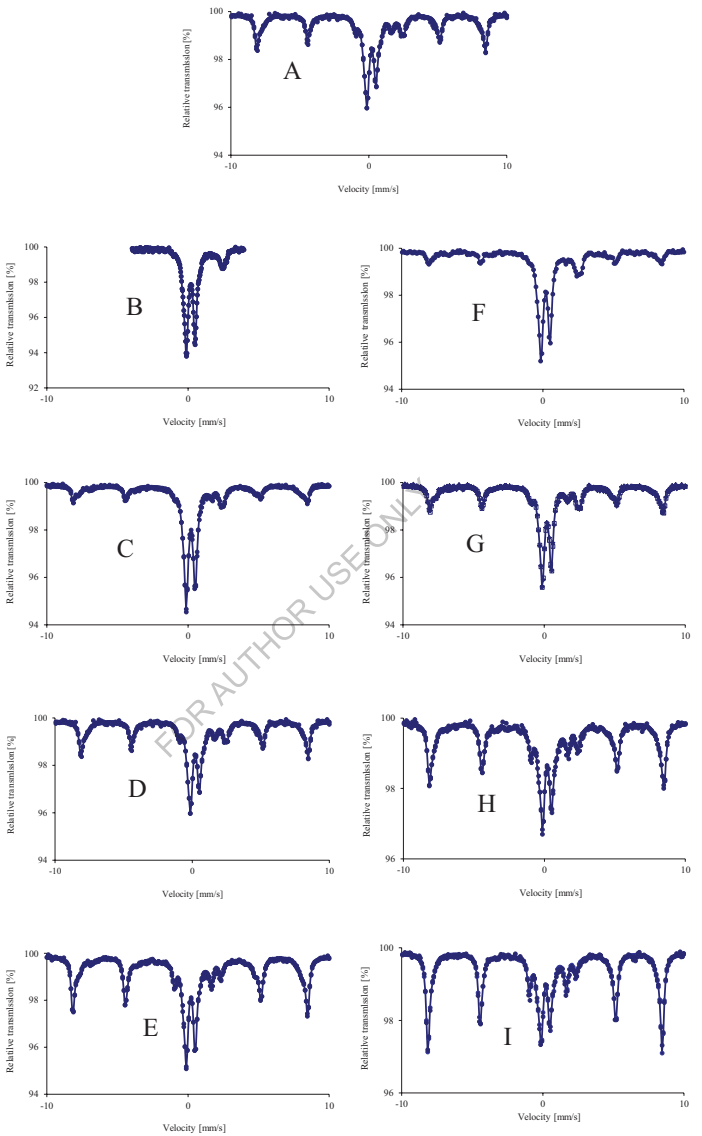

Fig. 3.21 Mössbauer spectra of initial and desulfurized L-type black coal (the symbols A-I see in Table 3.27)

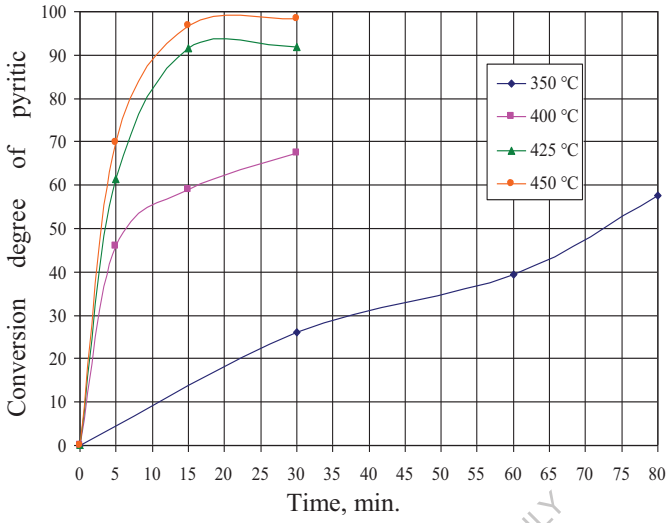

Fig. 3.22 Effect of process time on the oxidative desulfurization of C- type black coal at different temperatures

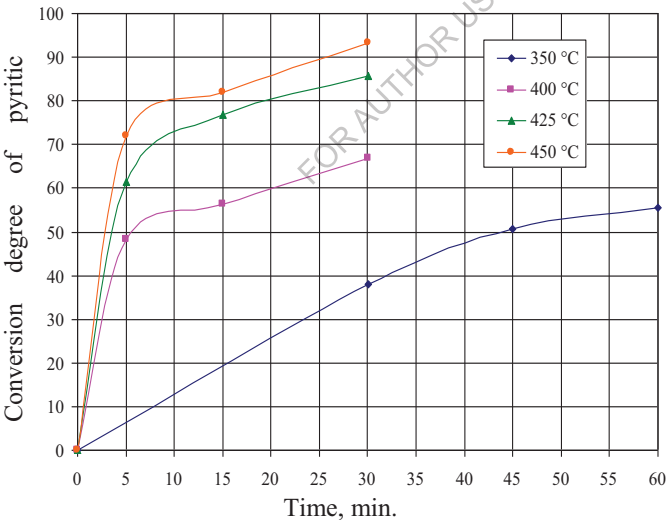

Fig. 3.22 Effect of process time on the oxidative desulfurization of G1 black coal at different temperatures

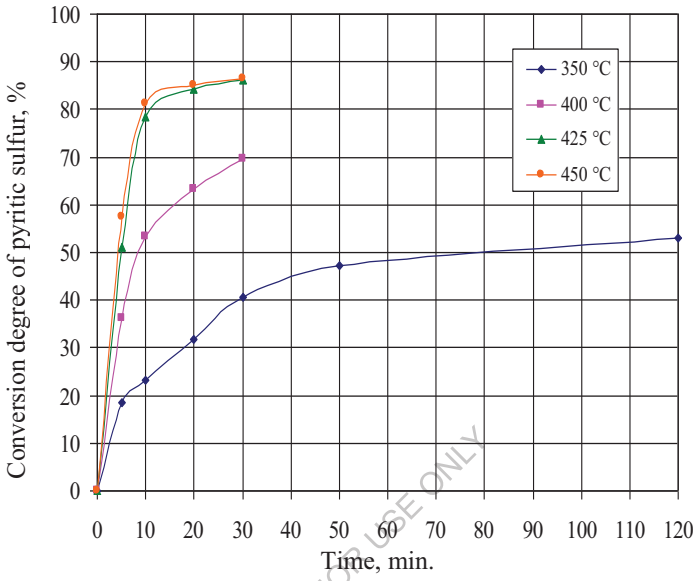

Fig. 3.23 Effect of process time on the oxidative desulfurization of L-type black coal at different temperatures

For all types of black coal at 425 °C and higher temperatures the process intensification takes place owing to the pyrite decomposition to pyrrhotite and sulfur followed by their oxidation. It is confirmed by the results of desulfurized coal with different metamorphism degree investigations using the Mössbauer spectroscopy as well as by the changes of effective activation energy from 132.8-169.0 kJ/mol at the temperatures of 350-400 °C to 25.4-29.2 kJ/mol at 425-450 °C.

Water steam may play an insignificant role in the conversion of pyritic sulfur of black coal. We may assume that water steam forms pyrite complexes increasing pyrite reactivity. Water steam has the greatest effect at low temperatures (350-400 °C) because at higher temperatures (above 425 °C) pyrrhotite is obtained independently of water steam presence or

absence. This highly reactive component reacts with the oxidant (air). Its reaction rate is higher than that of water + pyrite complex.

Using the brown coal its organic mass participates in the reactions of pyrite conversion with hydrogen sulfide formation in the end.

Schemes of sulfur conversion in lignite and black coals are shown in Figs. 3.24 and 3.25, respectively, depending on the process temperature.

Table 3.26 Characteristics of pyrite and coal desulfurized samples

Desulfurized samples of pyrite and different types of coal	Content of pyritic sulfur for analytical, wt %, S_p^a	Coal yield, wt %	Conversion of pyritic sulfur, %
C	0.23	82.27	91.51
G1	2.19	75.33	76.80
L	0.88	94.05	80.01
F2	1.46	83.11	72.61
Pyrite	1.07	–	71.24

Table 3.27 The Mössbauer spectroscopy data for black coal of L-types

Sample	Content of water steam, %	FeS_2			$FeSO_4 \cdot nH_2O$			Fe^{3+} species		
		IS[1] [mm/s]	QS2 [mm/s]	A3 [%]	IS [mm/s]	QS [mm/s]	A [%]	IS [mm/s]	QS [mm/s]	A [%]
1	2	3	4	5	6	7	8	9	10	11
Initial coal[4]										
A	–	0.30(1)	0.60(1)	79.1 (3)	1.26(1)	2.70(1)	15.5±1.4			
Coal was desulfurized at 350°C										
B	4	0.30(1)	0.60(1)	71.4(4)	1.25(1) 1.24(1)	2.70(1) 3.14(2)	10.8(5) 4.1(4)	0.38(1)	1.14(1)	7.5(3)
F	50	0.30(1)	0.62(1)	50.4(3)	1.32(1)	2.88 (1)	15.7(9)			
Coal was desulfurized at 400°C										
C	4	0.31(1)	0.63(2)	54.3(0)	1.32(4)	2.66(8)	7.0(3)			

1	2	3	4	5	6	7	8	9	10	11
G	50	0.30(1)	0.62(2)	40.6(3)	1.28(1)	2.77 (1)	8.3(4)			
Coal was desulfurized at 425°C										
D	4	0.31(1)	0.62(1)	32.6	1.31(1)	2.70(2)	7.4(4)	0.39 fix	1.16(3)	5.9(5)
H	30	0.30(1)	0.60(1)	22.7(6)				0.39 fix	1.10(2)	7.7(6)
Coal was desulfurized at 450°C										
E	4	0.31(1)	0.61(1)	27.8.(3)				0.39 fix	1.09(2)	3.8(3)
I	30	031(1)	0.60(1)	18.6(3)				0.39 fix	1.02 (2)	5.2(3)

Table 3.27 The Mössbauer spectroscopy data for black coal of L-types (continuation)

Sample	Content of water steam, %	Fe_3O_4			α-Fe_2O_3				$Fe_{1-x}S$[5]		
		IS [mm/s]	H [kG]	A [%]	IS [mm/s]	QS [mm/s]	H [kG]	A [%]	IS [mm/s]	H [kG]	A [%]
A	–										
B	4										
F	50	0.27(3)	490(3)	4.3(8)	0.37(1)	0.20(1)	515.2(6)	12.5±1.2			
		0.56(3)	446(3)	5.5(6)	0.39(2)	0.22(3)	501(2)	3.4(8)			
C	4	0.30(1)	492(1)	6.7(7)	0.38(1)	0.19(1)	517.2(3)	12.3(9)			
		0.57(2)	457)(2)	7.8(5)	0.41(2)	0.18(4)	503(2)	3.5(8)			
G	50	0.33(1)	491(1)	11.2(8)	0.37(1)	0.20(1)	514.7(3)	26.8±1.2			
		0.56 fix	447(3)	6.1(7)							
D	4				0.37(1)	0.17(1)	516.0(2)	29.6±1.8	0.66	196-297	traces
					0.38(1)	0.20	493(2)	19.4±2.6			
H	30	0.32(1)	491(2)	6.0±2.3	0.37(1)	0.19(1)	518.2(3)	32.5±2.7	0.66	196-297	8.4(4)
		0.56 fix	458(3)	5.4(7)	0.40(2)	0.18(2)	505(1)	10.3±4.1			
E	4	0.32(1)	488(1)	7.8±2.0	0.37(1)	0.20(1)	518.0(2)	31.2±1.2	0.66	217-302	9.6(3)
		0.57(2)	454(1)	7.5(5)	0.38(1)	0.16(2)	502(1)	6.7±2.7			
I	30				0.37(1)	0.20(1)	516.5(7)	52.8(8)	0.66	234-294	5.5 (5)
					0.34(1)	0.14(2)	494(1)	11.8±1.1			

Remarks:

[1]IS – isomer shift versus room temperature α–Fe.

[2]QS – quadrupole splitting.

[3]A – relative contribution to the total spectrum.

[4]The The sample of studied coal contains additionaly 5.5-8.5% of component with parameters IS = 1.08(2) – 1.10(2) mm/s and QS = 2.65(2) – 2.76(2) mm/s that remains unchanged in all experiments and may be ascribed to mineral illite Fe^{2+}.

[5]Isomer shift and line width were constrained in all fits.

Table 3.28 Calculation results of the effective activation energies within different temperature ranges

Coal type	Time, at which pyritic sulfur conversion is X %, τ_x, s				Reaction rate constant, k_i, s^{-1} $k_i = \frac{X}{\tau_x}$				Activation energy, E, kJ/mole $E = \frac{R \cdot \ln(k_{i+1}/k_i) \cdot 10^{-3}}{1/T_i - 1/T_{i+1}}$		
	At 350 ^{0}C (623 K)	At 400 ^{0}C (673 K)	At 425 ^{0}C (698 K)	At 450 ^{0}C (723 K)	At 350 ^{0}C (623 K)	At 400 ^{0}C (673 K)	At 425 ^{0}C (698 K)	At 450 ^{0}C (723 K)	At 623-673 K	At 673-698 K	At 698-723 K
1	2	3	4	5	6	7	8	9	10	11	12
At X = 30 %											
C	2322	198	144	126	0.01292	0.15152	0.20833	0.23810	171.1	49.6	22.3
G1	1416	186	144	126	0.02119	0.16129	0.20833	0.23810	141.1	39.9	22.3
L	1080	246	174	156	0.02778	0.12195	0.17241	0.19231	102.8	53.9	18.3
At X = 50 %											
C	4296	390	246	216	0.01164	0.12821	0.20325	0.23148	166.8	71.8	21.8
G1	2640	330	246	210	0.01894	0.15152	0.20325	0.23810	144.6	45.8	26.5

1	2	3	4	5	6	7	8	9	10	11	12
L	4992	480	294	258	0.01002	0.10417	0.17007	0.19380	162.8	76.4	21.9
At X = 60 %											
C	–	1014	294	252	–	0.05917	0.20408	0.23810	–	192.9	25.8
G1	–	1218	294	246	–	0.04926	0.20408	0.24390	–	221.4	29.8
L	–	966	396	330	–	0.06211	0.15152	0.18182	–	138.9	30.5
At X = 80 %											
C	–	–	540	408	–	–	0.14815	0.19608	–	–	46.9
G1	–	–	1152	678	–	–	0.06944	0.11799	–	–	88.7
L	–	–	642	534	–	–	0.12461	0.14981	–	–	30.8
The average value for C-type coal									169.0	104.7	29.2
The average value for G-type coal									142.8	102.3	41.8
The average value for L-type coal									132.8	89.7	25.4
The average value for all black coal									148.2	98.9	32.1

Table 3.29 Average characteristics of desulfurization gases composition for different types of black coal and anthracite[1]

Content in desulfurization gases, vol %							
SO_2	CH_4	C_2-C_3	CO	CO_2	O_2	N_2	Ar
2.2-4.9	0.3-1.3	0.2-1.2	0.9-3.4	5.8-13.6	0.9-7.8	78.2-80.1	0.9-0.92

Remarks:

[1]The samples obtained during desulfurization of low- and medium-metamorphosed coals contain below 0.1 vol % of hydrogen sulfide and 0.1 vol % of hydrogen. Oxidant contains 30-70 vol % of water steam.

Table 3.30 Average characteristic of desulfurization gases composition for coal LG

Content in desulfurization gases, vol %									
SO_2	H_2S	CH_4	C_2-C_3	CO	CO_2	O_2	N_2	Ar	H_2
-	3.2-7.4	0.8-1.9	1.0-1.9	2.6-5.8	18.1-28.7	1.6-3.6	56.6-71.4	0.6-0.8	0.6-1.5

Table 3.31 The characteristics of gases obtaining at desulfurization of wet and dry samples of coal

Content in desulfurization gases, vol %									
SO_2	H_2S	CH_4	C_2-C_3	CO	CO_2	O_2	N_2	Ar	H_2
The analytical sample of brown coal (W^{af} = 13.96 wt %)									
-	7.01	1.68	1.42	3.77	23.21	1.18	60.57	0.71	0.45
The sample of dry brown coal (W^{af} = 0.44 wt %)									
-	5.89	1.37	0.98	3.24	19.85	6.31	61.26	0.71	0.39
The analytical sample of anthracite (W^{a} = 3.55 wt %)									
0.88	-	0.78	0.35	traces	2.98	14.92	79.17	0.92	-
The sample of wet anthracite (W^{a} = 14.54 wt %)									
1.28	-	0.87	0.60	traces	3.59	14.43	78.32	0.91	traces

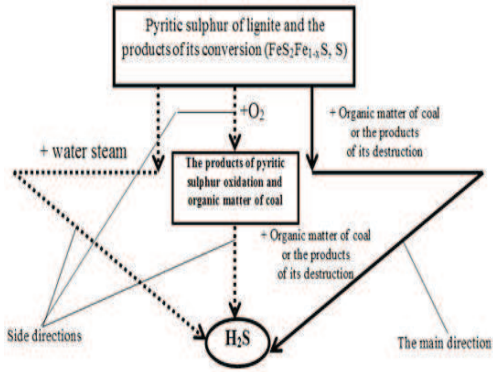

Fig. 3.24 The scheme of chemism of the conversation of black coal pyrite during the process of its oxidative desulfurization

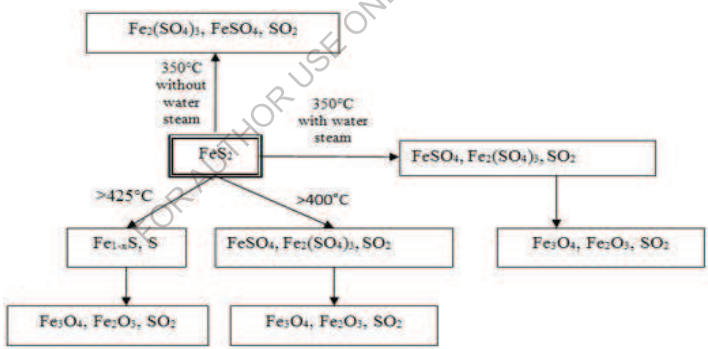

Fig. 3.25 The scheme of chemism of the conversation of black coal pyrite during the process of its oxidative desulfurization

3.2. Selection of conditions and influence of factors

3.2.1. Effect of hydrodynamic parameters. The rate of reactions between gaseous (the air-steam mixture) and solid porous bodies (coal, for which the most of the reaction centers (pyrite) is located in the bulk of grains) in the external diffusion area is defined by linear rate of the oxidant (LRO) and size of coal grain. The rate of the above-mentioned reactions, which occur in the internal diffusion area, is determined by the size of the crude particles only [50-52]. To achieve the highest possible conversion rates of sulfur (primarily pyrite) during OD process, it is necessary to find such factors of the process that will support the pyrite oxidation reactions in the kinetic area at the maximum possible temperature. In other words, if we achieve the conditions under which LRO and coal grain size will not affect the degree of sulfur conversion we may assert that the sulfur conversion occurs in the kinetic area.

LRO was calculated as the ratio between volumetric flow rate of oxidant (m^3/s) and the cross-sectional area of the reactor (m^2). To simplify the model description LRO was determined under normal conditions. The average size of coal particles was calculated as the geometric mean of two adjacent sieves.

The mass transfer coefficient per unit of the contact phase external surface (β, m/s), was calculated according to [50]:

$$\beta = Sh \cdot D / d, \tag{3.5}$$

where Sh is Sherwood number (diffusion Nusselt number); D is the diffusion coefficient of the gas phase, m^2/s; d is the average size of coal grain, m.

$$Sh = 0.01 \cdot Sc^{1/3} \cdot \mathrm{Re}/\varepsilon \tag{3.6}$$

where Sc is Schmidt number (diffusion Prandtl number); Re is Reynolds number, ε is the porosity of fluidized bed.

$$\mathrm{Re} = u^r \cdot d/v \tag{3.7}$$

$$Sc = v/D \tag{3.8}$$

where u^r is the real LRO, m/s; v is the kinematic viscosity of the gaseous reactant, m^2/s.

The porosity of fluidized bed was calculated by the following formula:

$$\varepsilon = \left(\frac{18\mathrm{Re} + 0.36\mathrm{Re}^2}{Ar} \right)^{0.21} \tag{3.9}$$

where Ar is Archimedes number.

$$Ar = \frac{d^3 \cdot g \cdot (\rho_{app} - \rho)}{\rho \cdot v^2} \tag{3.10}$$

where ρ is the density of air-steam mixture, kg/m^3; g is the acceleration of gravity, m/s^2; $\rho_{app.}$ is the apparent density of coal, kg/m^3.

All parameters of gaseous reactant in formulas (3.-3.10) were assumed and calculated under the operating conditions [50, 53-55]. Taking into account that the pressure in the reaction system was close to the atmospheric one, the calculation of the real LRO per empty cross section of reactor was carried out according to the formula:

$$u^r = u \cdot (273 + t)/273 \tag{3.11}$$

where u is the LRO under normal conditions, m/s; t is the process temperature, ^oC.

The analysis of dependencies (3.5-3.10) suggests that (in the case of a sufficient amount of gaseous reagents and a constant concentration in the

reaction medium), the oxidant linear velocity (linear rate of the oxidant, LRO) and size of coal grains are the factors that increase the total rate of the process, taking place in the external diffusion region. Therefore, we can assume the transition from the external diffusion region to kinetic or pore diffusion regions, when LRO ceases to affect the degree of sulfur removal/conversion at a fixed size of the coal grain.

The parameters of the fluidized bed (porosity), dimensionless criteria and mass transfer coefficient per unit of the outer contact surface of the phases (β, m / s), which characterize the intensity of mass transfer of gaseous reagent (oxygen) to the grain raw materials (coal, pyrite), were calculated on the basis of experimental data. Calculations are given in table. 3.32.

To ensure the course of sulfur conversion reactions in which the gaseous reagent is involved, in the kinetic region, when using coal, the Sherwood criterion must be not less than 0.002-0.003, the mass transfer coefficient - greater than 0.0015-0.0021 m/s. For brown coal, the reactions of sulfur compounds conversion with the participation of steam-air mixture begin to occur in the kinetic region at values of these parameters in 2-3 times smaller. In this case, the grain size and LRO must ensure the porosity of the fluidized bed above 0.6.

If it is needed to increase the intensity of COM conversion (in order to increase the temperature in the reactor, increase the yield of resin, etc.), it is advisable to change the process parameters to a level when Sh = 0,005-0,0056; $\beta \approx 0.004$ m/s. The porosity is close to the maximum possible values (0.8-0.95).

The intensity of the gaseous reactant external transfer increases due to the increase of grain size. The result is the transition into the internal

diffusion area. This transition occurs if values of porosity correspond to the beginning of the fluidized bed formation (about 0.4–0.5).

3.2.2. Effect of factors on black coal desulfurization. To describe the main characteristics of the process the following response functions are used: Y_1 –conversion of pyrite sulfur (SC(P)), %; Y_2 – content of sulfur dioxide in the desulfurization gases (CSD), vol %. The process parameters which are taken into consideration while the model development: X_1 – temperature, °C; X_2 – process time, min; X_3 – content of water steam in the oxidant, vol %; X_4 – repetition factor of oxidant flow rate (OFR), $m^3/h/kg$ of coal. The analysis of previous results shows that in the range of investigated coals the main characteristics of the process (response functions) do not practically depend upon the quality of coal organic mass (if coal with good coking ability is not taken into account). On the other hand, sulfur content (first of all, pyrite sulfur) affects SO_2 amount in the desulfurization gases and mostly the character of parameters influencing the fractional conversion of pyrite sulfur. Therefore, the content of pyrite sulfur in the initial coal is chosen as one more parameter of the process that indicates the influence of the raw material quality (X_5, S_p^d, mas %).

Table 3.32 The dependence of the process stages on the fluidized bed parameters and mass transfer criteria

Stage	Coal	LRO, u, m/s	Average diameter of grain, d, m	Real LRO, u^r, m/s	Porosity, ε	Reynolds number, Re	Sherwood number, Sh	β, m/s
Transition area of sulfur conversion reactions[1] (external diffusion-kinetic)	LG	0.0125	0.000158	0.0320	0.6141	0.0756	0.00098	0.00082
	F2	0.0400	0.000158	0.1023	0.7068	0.2324	0.00273	0.00210
	L	0.0250	0.000158	0.0639	0.6182	0.1453	0.00195	0.00150
Transition area of COM conversion reactions[1] (external diffusion-kinetic)	LG	0.1000	0.000158	0.2557	0.9525	0.6049	0.00507	0.00422
	F2	0.0900	0.000158	0.2301	0.8391	0.5230	0.00517	0.00398
	L	0.0950	0.000158	0.2429	0.8197	0.5520	0.00559	0.00430
Transition area of sulfur conversion reactions[1] (kinetic - internal diffusion)	LG	0.0250	0.000612	0.0639	0.3980	0.5856	0.01174	0.00252
	F2	0.0520	0.000397	0.1330	0.5081	0.7584	0.01239	0.00380
	L	0.0250	0.000397	0.0639	0.4218	0.3646	0.00717	0.00220

[1]Reactions with gaseous reactant

$$Y_1 = -1126{,}46 - 0{,}003406 \cdot X_1^2 - 0{,}004479 \cdot X_2^2 - 0{,}003291 \cdot X_3^2 - 0{,}771913 \cdot X_4^2 + 0{,}551132 \cdot X_5^2 - 0{,}005835 \cdot X_1 \cdot X_2 - 0{,}688584 \cdot X_3 \cdot X_4 - 0{,}177708 \cdot X_3 \cdot X_5 - 0{,}011040 \cdot X_1 \cdot X_3 + 0{,}017956 \cdot X_1 \cdot X_4 - 0{,}059971 \cdot X_1 \cdot X_5 - 0{,}005145 \cdot X_2 \cdot X_3 + 0{,}079830 \cdot X_2 \cdot X_4 - 0{,}002756 \cdot X_2 \cdot X_5 - 0.188538 \cdot X_4 \cdot X_5 + 4{,}080821 \cdot X_1 + 3{,}103388 \cdot X_2 + 7{,}188298 \cdot X_3 + 20{,}00892 \cdot X_4 + 25{,}94932 \cdot X_5 \quad (3.12)$$

$$Y_2 = -15{,}9544 - 0{,}000019 \cdot X_1^2 + 0{,}002910 \cdot X_2^2 + 0{,}000600 \cdot X_3^2 + 0{,}223833 \cdot X_4^2 - 0{,}000631 \cdot X_1 \cdot X_2 - 0{,}054981 \cdot X_3 \cdot X_4 + 0{,}000763 \cdot X_3 \cdot X_5 - 0{,}000299 \cdot X_1 \cdot X_3 - 0{,}000514 \cdot X_1 \cdot X_4 + 0{,}001466 \cdot X_1 \cdot X_5 - 0{,}000941 \cdot X_2 \cdot X_3 + 0{,}019109 \cdot X_2 \cdot X_4 - 0{,}019989 \cdot X_2 \cdot X_5 - 0{,}292095 \cdot X_4 \cdot X_5 + 0{,}029878 \cdot X_1 + 0{,}043360 \cdot X_2 + 0{,}278156 \cdot X_3 + 0{,}367353 \cdot X_4 + 1{,}408508 \cdot X_5 \quad (3.13)$$

To estimate the adequacy of obtained regression equation (2, 3), we substitute the given experimental parameters (X_1–X_5) and find the expected (regressive) values of response functions. In accordance with obtained values we calculate remainders:

$$\Delta Y_{ij} = Y_{ij}^{reg} - Y_{ij}, \quad (3.14)$$

where Y_{ij} – values observed during the experiments;

Y_{ij}^{reg} – values of response functions calculated using the regression equations;

i – number of response function (criterion, parameter; $(i = \overline{1,2})$);

j – number of experiment.

The estimation of model adequacy is conducted using four parameters: mean relative errors of approximation (ε_i); coefficient of determination (R_1^2); Fisher criterion (F_i) and criterion of statistics (F_{ri}).

The value of mean relative error of approximation is calculated by the formula:

$$\varepsilon_i = \frac{1}{n}\sum_{j=1}^{n}\left|\frac{Y_{ij} - Y_{ij}^{reg}}{Y_{ij}}\right|, \quad (3.15)$$

where n – sample collection (number of experiments).

To check the adequacy of multiple-factor regressive model Fisher criterion is used. It is calculated by the formula:

$$F_i = \frac{S^2_{reg_i}}{S^2_{resit_i}}, \quad (3.16)$$

where $S^2_{reg_i}$ – dispersion of experimental response functions relative to their mean values;

$S^2_{resit_i}$ – residual dispersion of response functions.

$$S^2_{reg_i} = \frac{1}{n-1}\sum_{j=1}^{n}(Y_{ij} - \overline{Y_i})^2, \quad (3.17)$$

where $\overline{Y_i}$ – average experimental value of response function.

$$S^2_{resit_i} = \frac{1}{n-m_i}\sum_{j=1}^{n}(Y_{ij}^{reg} - Y_{ij})^2, \quad (3.18)$$

where m_i –number of coefficients in the regression equation.

In accordance with mentioned calculations Fisher criterion should be greater than table value at significance level α and numbers of freeness (n-1) and ($n-m_i$). In such a case it shows how many times results scattering changes relative to the line of obtained regression equation compared with scattering relative to mean value [56].

Coefficient of determination characterizing the significance of response functions dependence on process parameters has values from 0 to 1. It was determined using the standard procedures [57].

It is proved that F_{ri} may be expressed by means of coefficient of determination [58]. The criterion of statistics which is a measure of regressive model adequacy is also a measure of statistic significance R_i^2. Therefore, to check the significance of the coefficient of determination F_{ri} is used. For this purpose zero ($R_i^2 = 0$) and alternative ($R_i^2 \neq 0$) hypotheses were stated. To check the zero hypothesis the criterion of statistics was calculated. It is connected with the coefficient of determination by the following ratio:

$$F_{r_i} = \frac{n - k_i - 1}{k_i} \cdot \frac{R_i^2}{1 - R_i^2}, \tag{3.19}$$

and has Fisher distribution with freenesses K_i and $(n-k_i-1)$

where k_i – number of regression equation coefficients without free term.

The calculated value F_{ri} was compared with the critical value F_{rcri} determined by means of tables at the level of significance α and numbers of freeness k_i and $(n-k_i-1)$. If $F_{ri} \leq F_{rcri}$, then the zero hypothesis is accepted, i.e. regression equation is statistically insignificant. If $F_{ri} > F_{rcri}$, the zero hypothesis is rejected, i.e. the alternative hypothesis about statistical significance of regression equation is accepted.

The initial results of experiments which were basis for the development of experimental-statistic model are represented in Table 3.33. For both response functions (Y_1 and Y_2) the non-linear multiple regressions were formed using STATISTICA software. The calculated values of response functions (Y_1^{reg} i Y_2^{reg}) and relative errors (ε_1 i ε_2) also are given in Table 3.33.

Table 3.33 Experimental data, calculated values of response functions and relative errors

X_1	X_2	X_3	X_4	X_5	Y_1	Y_1^{reg}	Y_2	Y_2^{reg}	Coal type	Relative errors	
										ε_1	ε_2
1	2	3	4	5	6	7	8	9	10	11	12
400	60	30	2.400	2.34	69.60	78.23	0.57	1.35	C	0.1240	1.3737
425	60	30	2.400	2.34	99.25	90.53	0.97	1.38	C	0.0879	0.4239
450	60	30	2.400	2.34	99.34	98.57	1.16	1.43	C	0.0078	0.2357
400	15	30	2.400	2.34	58.90	57.35	2.06	2.25	C	0.0264	0.0939
400	30	30	2.400	2.34	67.44	66.32	1.12	0.64	C	0.0165	0.4250
425	15	30	2.400	2.34	91.51	76.21	3.25	2.99	C	0.1672	0.0795
425	30	30	2.400	2.34	91.73	83.00	1.62	1.15	C	0.0952	0.2929
450	10	30	2.400	2.34	84.32	88.83	4.54	4.74	C	0.0535	0.0439
450	15	30	2.400	2.34	96.65	90.82	3.70	3.75	C	0.0604	0.0146
450	30	30	2.400	2.34	98.42	95.42	1.99	1.67	C	0.0305	0.1602
450	45	30	2.400	2.34	99.20	98.00	1.34	0.90	C	0.0121	0.3302
450	30	30	1.575	2.34	83.59	90.20	2.46	2.28	C	0.0791	0.0745
450	30	30	1.950	2.34	95.96	92.70	2.09	1.96	C	0.0339	0.0605
450	30	30	2.775	2.34	99.00	97.44	1.66	1.50	C	0.0158	0.0984
425	20	4	2.400	2.34	95.41	73.15	2.04	1.65	C	0.2333	0.1907
425	20	15	2.400	2.34	95.80	76.04	2.27	1.80	C	0.2062	0.2083
425	20	30	2.400	2.34	93.99	78.70	2.74	2.23	C	0.1627	0.1858
425	20	50	2.400	2.34	87.47	79.93	3.59	3.23	C	0.0862	0.1006
425	20	70	2.400	2.34	72.37	78.54	5.72	4.71	C	0.0852	0.1770
450	30	4.5	2.400	2.34	99.09	98.37	1.44	1.53	C	0.0073	0.0594
450	30	50	2.400	2.34	96.13	90.10	2.57	2.33	C	0.0627	0.0928
450	30	70	2.400	2.34	85.06	82.16	3.68	3.47	C	0.0341	0.0566
450	30	30	2.400	2.08	99.32	96.58	1.93	1.47	C	0.0276	0.2406
400	10	4.5	1.600	7.20	52.92	52.67	9.72	8.29	G1	0.0047	0.1471
400	15	4.5	1.600	7.20	62.91	56.38	6.62	7.02	G1	0.1038	0.0605
400	30	4.5	1.600	7.20	69.77	66.17	3.83	4.08	G1	0.0517	0.0664
400	60	4.5	1.600	7.20	76.43	79.69	2.11	2.14	G1	0.0427	0.0142
400	15	30	2.400	7.20	56.28	64.12	6.32	7.20	G1	0.1393	0.1387
400	30	30	2.400	7.20	66.88	72.90	3.71	4.13	G1	0.0900	0.1132
425	15	30	2.400	7.20	76.80	75.70	8.60	8.11	G1	0.0144	0.0566
425	30	30	2.400	7.20	85.62	82.29	4.69	4.81	G1	0.0389	0.0255
450	15	30	2.400	7.20	81.88	83.02	9.17	9.05	G1	0.0139	0.0127

1	2	3	4	5	6	7	8	9	10	11	12
450	30	30	2.400	7.20	93.13	87.42	5.17	5.51	G1	0.0614	0.0664
400	30	4.5	2.000	7.20	75.40	75.11	3.41	3.76	G1	0.0039	0.1027
400	30	4.5	2.800	7.20	79.42	92.25	2.57	3.33	G1	0.1615	0.2947
425	15	4	2.400	7.20	92.25	91.94	7.60	7.31	G1	0.0034	0.0376
425	15	15	2.400	7.20	94.02	85.61	8.92	7.55	G1	0.0894	0.1532
425	15	50	2.400	7.20	65.35	60.17	10.74	9.28	G1	0.0792	0.1360
425	15	70	2.400	7.20	47.41	42.02	12.49	10.93	G1	0.1137	0.1252
400	60	4.5	2.400	7.20	96.18	99.24	1.88	2.02	G1	0.0318	0.0757
400	60	15	2.400	7.20	99.07	93.65	2.25	1.89	G1	0.0547	0.1611
400	60	30	2.400	7.20	94.67	84.40	2.67	1.92	G1	0.1085	0.2793
400	60	40	2.400	7.20	83.07	77.41	2.60	2.10	G1	0.0681	0.1927
400	60	50	2.400	7.20	73.71	69.77	2.54	2.39	G1	0.0535	0.0576
400	60	70	2.400	7.20	42.32	52.50	2.35	3.34	G1	0.2406	0.4226
400	60	30	2.400	6.23	93.94	81.09	2.35	1.81	G1	0.1368	0.2296
430	30	50	1.600	7.20	73.82	72.48	8.10	8.39	G1	0.0181	0.0361
400	30	20	2.400	7.20	83.93	77.68	4.01	3.79	G1	0.0744	0.0541
430	60	20	1.600	7.20	87.70	88.10	3.06	3.02	G1	0.0046	0.0125
400	60	30	2.400	6.05	76.42	80.59	1.83	1.79	G2	0.0546	0.0223
425	60	30	2.400	6.05	90.23	87.33	2.11	1.95	G2	0.0322	0.0742
450	60	30	2.400	6.05	95.20	89.80	2.29	2.14	G2	0.0567	0.0648
425	15	30	2.400	6.05	54.53	73.47	5.02	6.90	G2	0.3473	0.3747
425	30	30	2.400	6.05	58.90	80.10	2.77	3.94	G2	0.3600	0.4233
425	45	30	2.400	6.05	82.36	84.72	2.55	2.29	G2	0.0287	0.1007
425	60	30	2.000	6.05	64.84	84.43	1.87	2.41	G2	0.3022	0.2876
425	60	30	2.800	6.05	95.98	89.97	1.97	1.57	G2	0.0626	0.2028
425	60	30	3.200	6.05	93.89	92.37	1.71	1.26	G2	0.0162	0.2637
425	60	30	2.400	4.84	76.94	86.70	1.25	1.77	G2	0.1269	0.4134
425	15	30	2.400	3.81	78.05	73.31	4.81	4.54	L	0.0607	0.0560
425	15	30	2.400	3.81	79.33	73.31	4.82	4.54	L	0.0759	0.0579
425	15	30	2.400	3.81	80.01	73.31	4.49	4.54	L	0.0838	0.0113
400	15	30	2.400	3.81	44.52	56.65	2.90	3.75	L	0.2724	0.2926
450	15	30	2.400	3.81	80.66	85.71	4.78	5.36	L	0.0626	0.1207
425	15	30	1.800	3.81	54.13	70.78	4.23	5.37	L	0.3075	0.2702
425	15	30	2.057	3.81	66.41	71.93	4.44	5.00	L	0.0831	0.1254
425	15	30	2.880	3.81	78.86	74.93	4.16	3.99	L	0.0498	0.0406
425	15	30	3.600	3.81	82.16	76.71	3.82	3.36	L	0.0664	0.1204

1	2	3	4	5	6	7	8	9	10	11	12
425	15	30	4.800	3.81	83.10	77.88	2.72	2.82	L	0.0628	0.0382
425	15	4	2.400	3.81	74.18	73.89	3.19	3.81	L	0.0039	0.1941
425	15	15	2.400	3.81	74.65	74.19	3.92	4.02	L	0.0062	0.0254
425	15	50	2.400	3.81	69.45	69.83	5.01	5.66	L	0.0055	0.1288
425	15	70	2.400	3.81	68.29	63.73	4.59	7.25	L	0.0668	0.5796
400	10	30	3.600	3.81	53.42	55.61	3.24	3.44	L	0.0410	0.0627
400	20	30	3.600	3.81	63.14	63.18	1.88	1.87	L	0.0007	0.0058
400	30	30	3.600	3.81	69.50	69.86	1.39	0.88	L	0.0052	0.3690
425	10	30	3.600	3.81	78.50	73.54	4.77	4.30	L	0.0632	0.0988
425	20	30	3.600	3.81	84.26	79.65	2.80	2.57	L	0.0547	0.0833
425	25	30	3.600	3.81	84.91	82.37	1.15	1.92	L	0.0299	0.6689
425	30	30	3.600	3.81	86.23	84.87	0.86	1.42	L	0.0158	0.6477
425	40	30	3.600	3.81	86.64	89.19	0.80	0.85	L	0.0295	0.0614
425	50	30	3.600	3.81	86.12	92.62	0.61	0.86	L	0.0755	0.4150
450	10	30	3.600	3.81	81.29	87.21	5.15	5.18	L	0.0728	0.0055
450	20	30	3.600	3.81	85.05	91.86	2.65	3.29	L	0.0801	0.2410
450	30	30	3.600	3.81	86.42	95.62	1.80	1.98	L	0.1065	0.1006
425	15	30	3.600	2.66	74.68	79.03	3.55	2.55	L	0.0583	0.2813
425	20	4	2.400	1.41	54.02	71.94	0.72	0.78	A1	0.3317	0.0866
425	20	15	2.400	1.41	58.97	76.64	1.01	0.92	A1	0.2997	0.0882
425	20	30	2.400	1.41	65.29	81.78	1.35	1.34	A1	0.2525	0.0046
425	20	50	2.400	1.41	80.39	86.32	2.27	2.33	A1	0.0737	0.0255
425	20	70	2.400	1.41	76.71	88.22	3.42	3.79	A1	0.1501	0.1087
400	30	62.5	1.800	1.94	99.01	87.46	4.82	3.55	A2	0.1167	0.2640
400	30	62.5	1.800	1.86	89.55	88.05	3.45	3.47	A2	0.0167	0.0069
Mean relative error of approximation (ε)										0.0859	0.1721

The mean relative errors of approximation calculated by (3.15), ε_1 = 0.0859 (8.59 %), ε_2 = 0.1721 (17.21 %) indicate the agreement between developed model and experimental data because it is admitted in [60] that at ε=0-10 the prognosis accuracy is high, at ε=10-20 % it is good and at ε=20-50 % – satisfactory.

The calculated values of Fisher criterion (accordingly to (3.16)) are: F_1=2.348; F_2=10.143. In accordance with the table of critical values of

Fisher criterion [61] at the level of significance α=0.05 the critical values are: $F_{1kr} = F(0.05; 92; 72) = 1.452$ та $F_{2kr} = F(0.05; 92; 73) = 1.450$. They are lower than calculated values. And this fact also confirms the adequacy of model.

Coefficients of determination R_1^2=0.6667 і R_2^2=0.9218 point that 66.67% and 92.18% of the changes in response functions Y_1 and Y_2 respectively are defined by the change of process parameters X_1–X_5. The fact that $R_1 = 0.82$ and $R_2 = 0.96$ are close to 1, reveals about the presence of "strong" bond between Y_1 and Y_2 and process parameters X_1–X_5.

The calculated values of the criterion of statistics (accordingly to (3.19)) are: $F_{r1} = 7.20$; $F_{r2} = 45.16$. In accordance with the table of critical values of Fisher criterion at the level of significance α=0.05 the critical values are: $F_{rkr1} = F(0.05; 20; 72) = 1.718$ та $F_{rkr2} = F(0.05; 19; 73) = 1{,}731$. They indicate the statistic significance of coefficients of determination.

On the basis of regression equations optimal conditions were determined using method of uniform search (minimum or maximum) of response functions [59] for three types of coal: low-metamorphosed (type C) high-metamorphosed (type L) and run-of-mine (type R).

Agreement between results obtained under optimal conditions and predicted results based on experimental-statistic model was checked using value of mean relative error of approximation. It is calculated by the following formula:

$$\varepsilon_i' = \frac{1}{n'} \sum_{j=1}^{n'} \left| \frac{Y_{ij}' - Y_{ij}^{predict}}{Y_{ij}^{predict}} \right|, \qquad (3.20)$$

where Y_{ij}' – observed values of response functions obtained during the experiments under optimal conditions;

$Y_{ij}^{predict}$ – predicted values of response functions under optimal conditions determined by regression equations;

n' – numbers of experiments under optima; conditions.

Taking into account that CSD maximum values of 3-8 vol % were obtained at SC(P) 80-90 % (see Table 3.33), the optimization task was to find such process parameters which ensure SC(P) maximum under the following limitations: $Y_1 \leq 90$, $3 \leq Y_2 \leq 8$. Predicted and results obtained under optimal conditions are represented in Table 3.34.

Mean relative errors of predicted data approximation were calculated by formula (3.20): $\varepsilon'_1 = 0.0413$ (4.13 %), $\varepsilon'_2 = 0.1324$ (13.24 %). They indicate the agreement between predicted and practical data.

The desulfurization of three coal samples we obtain a fuel with sulfur content of 1.0–1.5 mas %. It may be considered as low-sulfuric one. At the same time conversion of total sulfur (SC(T)) is 69.63-77.27 %. If we assume that all sulfur dioxide containing in the desulfurization gases is recovered or converted using known methods, then SC(T) will be equal to the degree of environmental pollution reduction by sulfuric anhydride. Hence, we may affirm that proposed method gives the possibility to burn sulfuric and high-sulfuric coal, reduce sulfuric emissions by 70-80 % and utilize free sulfur.

As mentioned above, coking coal behaves differently in the desulfurization process. The degree of pyrite sulfur conversion and SO_2 content in the desulfurization gases were the key factors of the process efficiency (response functions) during the development of experimental and statistical mathematical model (ESM) of the medium-metamorphosed coal desulfurization. Moreover, we used the response function which partially describes the coal ability to cake (the degree of volatile matter reduction).

While describing ESM the following notation of response functions and the process factors were used: Y_1 – SC(P), %; Y_2 – the content of sulfur dioxide in the desulfurization gases, vol %; Y_3 – the degree of volatile matter reduction, %.; X_1 – temperature, °C; X_2 – the process time, min; X_3 – the content of water steam in the oxidant, vol %; and X_4 – the repetition factor of the oxidant flow rate (OFR), $m^3/h/kg$ of coal. It was shown above that the impact of certain factors on the coal desulfurization partly depends on sulfur content in coal. The sulfur content in the crude, primarily pyrite sulfur, also affects the concentration of sulfur dioxide in gases. Therefore the pyrite sulfur content in the original coal (X_5, S_p^d, mas %) is another factor which describes the impact of the raw material quality on the process. The factor values and results of studies according to which a mathematical model was created are represented in Table 3.35.

For the response functions we developed the following types of dependencies that showed the best conformity to the experimental data: for Y_1 – quadratic model (Eq. (3.21)), for Y_2 – quadratic model without considering X_5^2 (Eq. (3.22)), and for Y_3 – quadratic model without X_5 (Eq. (3.23)).

$$Y_1 = -39689.50 - 0.004578 \cdot X_1^2 - 0.007040 \cdot X_2^2 - 0.003987 \cdot X_3^2 - 0.819929 \cdot X_4^2 + 5.236872 \cdot X_5^2 - 0.008412 \cdot X_1 \cdot X_2 + 0.005048 \cdot X_1 \cdot X_3 - 0.045962 \cdot X_1 \cdot X_4 - 21.7667 \cdot X_1 \cdot X_5 + 0.009846 \cdot X_2 \cdot X_3 - 0.093123 \cdot X_2 \cdot X_4 + 2.172856 \cdot X_2 \cdot X_5 + 0.005444 \cdot X_3 \cdot X_4 + 20.03125 \cdot X_3 \cdot X_5 - 2.72014 \cdot X_4 \cdot X_5 + 102.2889 \cdot X_1 - 5.19801 \cdot X_2 - 92.4872 \cdot X_3 + 45.59695 \cdot X_4 + 8578.043 \cdot X_5 \quad (3.21)$$

$$Y_2 = 5270.985 + 0.000397 \cdot X_1^2 - 0.000055 \cdot X_2^2 - 0.000482 \cdot X_3^2 + \quad (3.22)$$

$$0.197470 \cdot X_4^2 - 0.001507 \cdot X_1 \cdot X_2 + 0.001033 \cdot X_1 \cdot X_3 + 0.002877 \cdot X_1 \cdot X_4 + 2.921787 \cdot X_1 \cdot X_5 - 0.000688 \cdot X_2 \cdot X_3 + 0.006095 \cdot X_2 \cdot X_4 - 0.034453 \cdot X_2 \cdot X_5 - 0.000256 \cdot X_3 \cdot X_4 - 2.73384 \cdot X_3 \cdot X_5 - 0.595158 \cdot X_4 \cdot X_5 - 13.4622 \cdot X_1 + 0.712237 \cdot X_2 + 11.97826 \cdot X_3 - 1.20949 \cdot X_4 - 1155.34 \cdot X_5$$

$$Y_3 = -1.95206 + 0.000000 \cdot X_1^2 + 0.000060 \cdot X_2^2 + 0.000031 \cdot X_3^2 - 0.008077 \cdot X_4^2 + 0.000091 \cdot X_1 \cdot X_2 + 0.000071 \cdot X_1 \cdot X_3 - 0.001936 \cdot X_1 \cdot X_4 + 0.000009 \cdot X_2 \cdot X_3 - 0.000270 \cdot X_2 \cdot X_4 - 0.000049 \cdot X_3 \cdot X_4 + 0.005190 \cdot X_1 - 0.048557 \cdot X_2 - 0.032802 \cdot X_3 + 0.921093 \cdot X_4 \quad (3.23)$$

To estimate the adequacy of the obtained regression equations, we substituted the given experimental parameters (X_1–X_5) and found the expected (regressive) values of response functions (Y_{ij}^{reg}), which are represented in Table 3.35.

The mean relative approximation error is lower than 10 % (ε_1 = 0.0275 (2.75 %), ε_2 = 0.0971 (9.71 %), ε_3 = 0.0805 (8.05 %)). Therefore, according to [60] we may certify the high compliance with the experimental data.

The calculated values of Fisher criterion are: F_1 = 12.46; F_2 =16.91; and F_3=6.80. In accordance with the table of Fisher criterion values [61] at the level of significance α = 0.05 the critical values are: $F_{1cr} = F(0.05; 30; 10) = 2.70$; $F_{2cr} = F(0.05; 30; 11) = 2.51$ and $F_{3cr} = F(0.05; 28; 14) = 2.13$. They are lower then the calculated values and this fact also confirms the adequacy of the model. The values of the coefficient of determination are: R_1^2 = 0.9742, R_2^2 = 0.9781, and R_3^2 = 0.7396.

Table 3.34 Optimal conditions for desulfurization and obtained results

Coal type	Parameter values				Sulfur content for analytical mass, wt %				Values of response functions			
	Temperature °C	Time min	OFR, $m^3/(h \cdot kg)$	Content of water steam in the oxidant vol %	total S_t^a	pyritic S_p^a	sulfate $S_{SO_4}^a$	organic S_o^a	Fractional conversion of pyrite sulfur, %		SO_2 content, vol %	
									Y_1'	$Y_1^{predict}$	Y_1'	$Y_1^{predict}$
Calculated values												
C	418	19.5	1.72	64.5	–	–	–	–	–	90.00	–	6.08
L	446	15.0	3.06	25.5	–	–	–	–	–	90.00	–	4.45
R	433	10.5	2.24	69.0	–	–	–	–	–	90.00	–	6.16
Experimental values												
C	420	19.5	1.72	65.0	1.36	0.40	0.48	0.48	84.82	–	6.96	–
L	445	15.0	3.06	25.0	1.11	0.38	0.15	0.58	90.84	–	3.80	–
R	435	10.5	2.24	70.0	0.59	0.26	0.12	0.21	85.42	–	5.60	–

Therefore, 97.42 %, 97.81 %, and 73.96 % changes in response functions (Y_1, Y_2, and Y_3, respectively) are determined by the selected factors of the process control (X_1–X_5). The fact that $R_1 = 0.9870$, $R_2 = 0.9890$, and $R_3 = 0.860$ are close to 1, indicates the presence of "strong" bond between Y_1, Y_2, and Y_3 and process parameters (X_1–X_5).

The calculated values of the criterion of statistics are: $F_{r_1} = 18.86$, $F_{r2} = 25.88$, and $F_{r3} = 2.84$.

Table 3.35 Experimental data, calculated values of response functions, and relative errors

No.	X_1*, °C	X_2, min	X_3, vol %	X_4, m³/h·kg	X_5, mas %	Y_1, %	Y_1^{reg}, %	Y_2, vol %	Y_2^{reg}, vol %	Y_3, %	Y_3^{reg}, %	Coal type	Relative errors		
													ε_1	ε_2	ε_3
1	400	15	30	2.40	4.50	54.89	57.06	5.09	5.54	0.20	0.21	F2	0.0396	0.0877	0.0607
2	425	15	30	2.40	4.50	72.61	68.57	7.14	6.35	0.31	0.31	F2	0.0556	0.1104	0.0156
3	450	15	30	2.40	4.50	68.44	74.05	7.05	7.84	0.43	0.42	F2	0.0820	0.1118	0.0246
4	425	15	30	7.21	4.50	89.94	91.30	3.38	3.71	0.41	0.38	F2	0.0151	0.0983	0.0639
5	425	30	30	7.21	4.50	94.75	96.38	1.51	1.76	0.26	0.26	F2	0.0172	0.1638	0.0178
6	425	45	30	7.21	4.50	95.86	97.93	0.89	0.82	0.14	0.16	F2	0.0216	0.0817	0.1261
7	425	60	30	7.21	4.50	96.45	95.95	0.72	0.89	0.07	0.06	F2	0.0052	0.2387	0.1013
8	425	30	30	2.40	4.50	83.38	80.49	3.78	3.40	0.19	0.21	F2	0.0346	0.0570	0.1240
9	425	45	30	2.40	4.50	85.29	88.88	2.50	2.65	0.13	0.12	F2	0.0421	0.0615	0.0423
10	425	60	30	2.40	4.50	93.10	93.74	2.23	2.33	0.05	0.05	F2	0.0069	0.0434	0.0466
11	425	15	4	2.40	4.50	69.24	72.48	3.61	4.39	0.34	0.36	F2	0.0468	0.2168	0.0537
12	425	15	15	2.40	4.50	71.22	71.48	5.71	5.28	0.27	0.33	F2	0.0037	0.0754	0.2394
13	425	15	50	2.40	4.50	69.20	61.91	7.98	7.53	0.36	0.31	F2	0.1054	0.0559	0.1370
14	425	15	70	2.40	4.50	46.78	52.06	7.75	8.43	0.37	0.33	F2	0.1129	0.0882	0.1027
15	425	15	30	4.81	4.50	83.86	84.82	3.71	3.83	0.39	0.44	F2	0.0114	0.0326	0.1301
16	425	15	30	3.61	4.50	79.20	77.95	4.94	4.79	0.37	0.40	F2	0.0158	0.0313	0.0838
17	425	15	30	2.40	4.50	72.15	68.57	7.32	6.35	-	-	F2	0.0496	0.1323	-
18	425	15	30	7.21	4.93	84.86	87.17	2.95	3.17	0.36	0.38	F2	0.0272	0.0811	0.0661
19	425	15	30	7.21	5.02	88.74	86.83	3.17	3.05	0.40	0.38	F2	0.0215	0.0604	0.0405
20	425	15	30	2.40	4.93	59.80	60.54	7.42	7.54	0.31	0.31	F2	0.0124	0.0163	0.0156
21	425	15	30	2.40	5.02	60.00	59.39	7.89	7.79	0.34	0.31	F2	0.0102	0.0127	0.0740
22	425	25	30	4.81	1.29	91.75	92.21	0.63	0.80	0.44	0.37	F3	0.0050	0.2768	0.1684
23	425	25	30	4.81	1.37	89.82	89.35	1.02	0.84	-	-	LH	0.0052	0.1753	-
24	400	10	4	2.40	1.13	73.23	73.23	2.14	2.14	0.40	0.35	CK	0.0000	2.1818	0.1255
25	450	10	4	7.21	4.50	94.08	92.47	2.54	2.33	0.32	0.31	F2	0.0171	0.0834	0.0265
26	400	45	4	7.21	4.50	98.58	97.09	0.67	0.43	0.28	0.29	F2	0.0151	0.3525	0.0461
27	450	45	4	2.40	4.50	83.27	81.31	1.68	1.45	0.30	0.28	F2	0.0235	0.1379	0.0502
28	400	10	70	2.40	4.50	27.48	27.87	7.59	7.51	0.17	0.20	F2	0.0140	0.0101	0.2023
29	450	10	70	7.21	4.50	78.49	77.54	8.87	8.71	0.37	0.38	F2	0.0121	0.0178	0.0328
30	400	45	70	7.21	4.50	88.55	87.48	1.91	1.78	0.16	0.15	F2	0.0121	0.0698	0.0578
31	450	45	70	2.40	4.50	88.85	87.76	6.53	6.34	0.37	0.39	F2	0.0123	0.0286	0.0594
Mean relative error of approximation (ε)													0.0275	0.0971	0.0805

In accordance with the table of Fisher criterion values at the level of significance α = 0.05 the critical values are: $F_{rcr_1} = F(0.05; 20; 10) = 2.77$; $F_{rcr2} = F(0.05; 19; 11) = 2.69$, and $F_{rcr3} = F(0.05; 14; 14) = 2.50$. This indicates the statistical significance of the determination coefficients R_i^2 ($F_{rcr_i} < F_{r_i}$).

All above-mentioned data indicate the ESM adequacy for medium-coalificated coal desulfurization process, the statistical significance of the results and the presence of link between response functions and selected factors of process control.

The process optimal conditions supporting the maximum degree of sulfur conversion, the maximum SO_2 content in the desulfurization gases, and the minimal volatile reduction were found on the basis of regression equations by the method of uniform search of the values of response functions.

Under determined optimal conditions, which are presented in Table 3.36, oxidative desulfurization of F2 and F3 coal was carried out. In the researches with F2 coal the fractions 0.1–0.25 mm (denoted $F2_1$) and 0.25–0.315 mm (denoted $F2_2$) were used. In case of F3 coal the fraction 0.25–0.50 mm was used.

The technical analysis of desulfurized coal is given in Table 3.37. The sulfur content in the resulting coal and its degree of conversion and removal are represented in Table 3.38. The compositions of desulfurization gases are given in Table 3.39.

The obtained data show that due to the realization of the process the total sulfur content in the coal was reduced noticeably. The degree of total sulfur conversion is 76–79 % for F2 coal and 67 % for F3 coal. In case of the process realization at the coke plant after removal of sulfur dioxide by

known method the gases (that have heating value about 1.4 MJ/m^3) can be used as fuel in coking furnaces.

The desulfurized coal F3 has relatively low ash content because the original coal was taken from the beneficiation plant. Desulfurized coal F2 contains a rather large number of inorganic matters, therefore one of the samples of desulfurizated coal ($F2_2$) undergoes the flotation concentration. The characteristics of desulfurized and enriched coal are presented in Table 3.40.

The desulfurized coal samples $F2_2$ and F3 were used as the components of the charge for the production of special types of coke, which will be discussed below.

Table 3.36 Optimal conditions for the medium-metamorphosed coal desulfurization

Parameter	Fat ($F2_1$)	Fat ($F2_2$)	Fat (F3)
Temperature, ^{0}C (K)	445 (718)	425 (698)	425 (698)
Time, min.	21.5	60	25
OFR, m^3/h/kg	7.10	2.40	4.81
Content of water steam in the oxidant, vol %	51.0	30.0	30.0

Table 3.37 Technical analysis of the coal after desulfurization

Moisture content, W^a, mas %	Ash, A^d, mas %	Volatiles yield, V^{daf}, mas %
$F2_1$		
1.37	28.66	25.53
$F2_2$		
1.11	24.92	24.19
F3		
2.07	12.60	19.14

3.2.2. Effect of factors on lignite (brown coal) desulfurization. In contrast to hard coal, the coal organic matter (COM) lignite undergoes significant transformation during the described process. While describing conversions occurred with the COM, we assumed that conversions proceed in three directions, i. e. thermal destruction (decomposition tar is formed); gasification with the formation of combustible gases (hydrogen, hydrocarbons, CO); burning (CO_2 is obtained).

Table 3.38 Content of sulfur in the coal after desulfurization. Removal and conversion degree of sulfur

Sulfur content relative to the dry mass, mas %				RDS(T), %	RDS(P), %	SC(P), %	SC(P), %
total, S_t^d	pyritic, S_p^d	organic, S_o^d	sulfate, $S_{SO_4}^d$				
F2$_1$							
2.04	0.81	0.76	0.47	70.77	81.99	76.44	85.48
F2$_2$							
2.23	0.50	0.78	0.95	71.10	89.94	79.49	92.86
F3							
1.49	0.26	0.44	0.79	51.91	80.83	67.19	86.92

The amount of COM necessary for the production of all aforementioned products is characterized by the term “coal organic matter conversion, degree of coal organic matter conversion” (COMC). To characterize the ratio between amount of COM from which combustible products are formed (tar, hydrocarbon gases, carbon (II) oxide) and amount of burned COM (for CO_2 formation), we used the term “efficiency factor of

coal organic matter conversion" (EFCOMC or K_{ef}).

$$COMC = \frac{V_{dg}}{22{,}4 \cdot m_C} \cdot (x_{CH_4} \cdot M_{CH_4} + x_{C_2-C_3} \cdot M_{C_2-C_3} + x_{CO} \cdot M_{CO} + x_{CO_2} \cdot M_{CO_2}) + x_t \quad (3.24)$$

$$EFCOMC = \frac{\frac{V_{dg}}{22{,}4 \cdot m_C} \cdot (x_{CH_4} \cdot M_{CH_4} + x_{C_2-C_3} \cdot M_{C_2-C_3} + x_{CO} \cdot M_{CO}) + x_t}{\frac{V_{dg}}{22{,}4 \cdot m_C} \cdot x_{CO_2} \cdot M_{CO_2}} \quad (3.25)$$

where $x_{CH_4}, x_{C_2-C_3}, x_{CO}, x_{CO_2}$ – the concentrations of corresponding components in the desulfurization gases, vol %; $M_{CH_4}, M_{C_2-C_3}, M_{CO}, M_{CO_2}$ – the molecular masses of methane, C_2-C_3 the mixture and carbon, respectively; V_{dg} – the volume of desulfurization gases, m^3; m_C – the initial coal mass, kg; x_t – the tar yield, wt %.

Table 3.39 Average characteristics of desulfurization gases composition

Content in desulfurization gases, vol %										
CH_4	C_2H_4	C_2H_6	C_3	SO_2	H_2S	CO_2	CO	N_2	O_2	Ar
$F2_1$										
1.45	0.21	0.43	0.18	2.58	0.05	9.84	1.81	78.64	3.89	0.92
$F2_2$										
0.67	0.05	0.15	0.10	2.16	0.00	14.08	2.93	75.78	3.20	0.88
F3										
0.26	0.05	0.03	0.03	0.72	0.00	4.73	0.98	81.36	10.89	0.95

The modular degree of oxygen conversion was calculated by the following formula:

$$K = 1 - \frac{x'_{O_2} \cdot 78.08}{x'_{N_2} \cdot 20.95} \quad (3.26)$$

where x'_{O_2} i x'_{N_2} – the content of appropriate components in the desulfurization gases, vol %; 78.08 i 20.95 – the concentration of nitrogen and oxygen, vol %, in the resulted air.

Table 3.40 Technical analysis of the coal ($F2_2$) after desulfurization and benefication

Moisture content, W^a, mas %	Ash, A^d, mas %	Volatiles yield, V^{daf}, mas %	Sulfur content relative to the dry mass, mas %			
			total, S_t^d	pyritic, S_p^d	organic, S_o^d	sulfate, $S_{SO_4}^d$
1.17	19.86	26.59	2.10	0.47	0.84	0.79

While desulfurization of the hard coal, it was established that water steam added to the oxidant (air) stimulates the pyrite conversion and retards COM burning (see Fig. 3.25). On the other hand, the analytic sample of the lignite already contains 12-14 wt % of moisture in it. Therefore, it was necessary to check an expediency of water steam use while the lignite desulfurization.

The results concerning the oxidant composition effect (water steam content in it) on the sulfuric compounds and COM conversion are represented in Table 3.41 and Fig. 3.26-3.27.

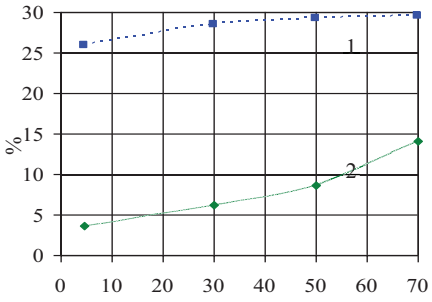

Fig. 3.26 Dependence of CCOM (1) and EFCCOM (2) of lignite on oxidant content

Table 3.41 The dependence of desulfurization gas of lignite on oxidant

Content in the oxidant, % vol.		Content, % vol.								
water steam	oxygen	H_2	CH_4	C_2-C_3	H_2S	CO_2	CO	N_2	O_2	Ar
4.5	20.1	0.29	0.62	0.77	1.89	16.45	2.41	74.92	1.78	0.87
30.0	14.7	0.33	0.94	0.69	2.41	16.22	2.84	72.15	3.58	0.84
50.0	10.5	0.37	0.98	0.72	2.99	17.27	2.50	71.30	3.04	0.83
70.0	6.3	0.43	1.18	1.04	4.64	17.75	2.76	68.04	3.37	0.79

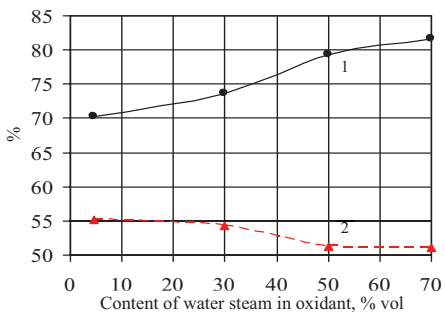

Fig. 3.27 Dependence of RDS(P) (1) and SC(T) (2) of lignite on oxidant content

The increase of water steam amount in the oxidant slightly increases CCOM and considerably increases EFCCOM (Fig. 3.26). It means that water steam retards the burning of lignite organic matter and insignificantly increases the intensity of its thermal decomposition with organic compounds formation. Hence, the content of unused oxygen in the desulfurization gases is increased (Table 3.41).

With the increase of water steam content in the oxidant, the sulfur conversion degree is constant and removal degree of total sulfur increases (Fig. 3.27). Since the amount of converted sulfur is almost the same and volume of desulfurization gases decreases (due to the vapors condensation), the concentration of H_2S in the desulfurization gases rises.

Thus, it is advisable to use water steam to increase H_2S content in the desulfurization gases, destruction products yield, the yield of organic matter gasification products and combustion heat of desulfurization gases, which will be burned after hydrogen sulfide conversion into sulfur by known methods.

Taking into account the fact that the lignite organic matter is thermally unstable, has high reaction capability, contains many functional, primarily oxygen containing groups, and is not baked. That is why the temperature impact was studied at relatively low and high temperature ranges (200-500 ^{o}C). Experimental results at different temperatures exemplified in the Table 3.42 and in the Fig. 3.28-3.29.

Temperature rise results in the increase of COMC (Fig. 3.28). These all correlate with the content rise of CO_2 and CO the desulfurization gases (Table 3.42). Temperature influences insignificantly upon the directions of COM conversion, i. e. while it is changing, EFCOMC is almost permanent (Fig. 3.28).

Table 3.42 Dependence of desulfurization gas content on temperature

T, ºC	Content, vol %								K
	CH_4	C_2-C_3	H_2S	CO_2	CO	N_2	O_2	Ar	
1	2	3	4	5	6	7	8	9	10
200	0.13	0.13	0.18	7.24	1.06	83.88	6.40	0.98	0.72
250	0.16	0.31	0.65	10.88	1.38	82.29	3.37	0.96	0.85
280	0.18	0.40	0.86	12.89	1.72	79.93	3.09	0.93	0.86
1	2	3	4	5	6	7	8	9	10
300	0.23	0.56	1.19	14.48	1.84	77.94	2.85	0.91	0.86
350	0.52	0.66	1.48	16.02	1.94	76.15	2.34	0.89	0.89
400	0.59	0.71	1.59	16.33	2.17	75.61	2.12	0.88	0.90
425	0.65	0.82	1.89	16.45	2.53	74.92	1.87	0.87	0.91
450	0.93	0.95	2.06	17.74	2.98	73.09	1.40	0.85	0.93
500	1.51	1.29	2.06	19.17	3.38	70.61	1.16	0.82	0.94

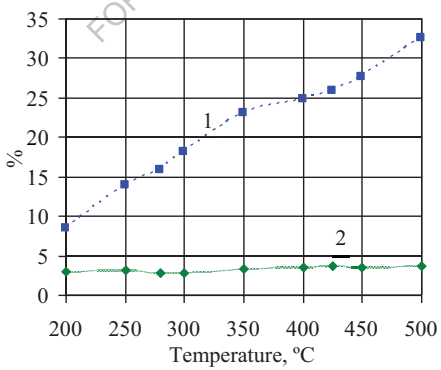

Fig. 3.28 Dependence of COMC (1) and EFCOMC (2) on temperature

If temperature reaches 425ºC, RDS(P) and SC(T) (Fig. 3.28) as well as H_2S in desulfurization gases rise (Table 3.42). Removal degrees of sulfur are characterized with ratio between reaction rates of sulfur conversion and COM. The greater is the ratio, the less is the sulfur content in coal obtained and appropriately the bigger is sulfur removal degree. That is why we can state that if temperature exceeds 425-450ºC, conversion rates of sulfur compounds and COM become equal.

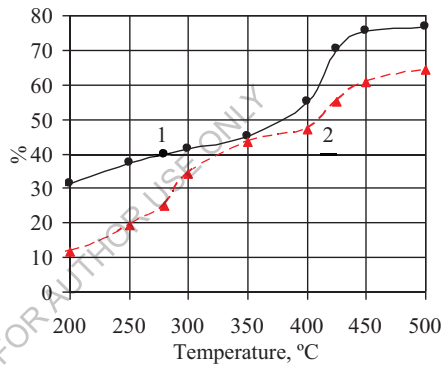

Fig. 3.29 Dependence of RDS(P) (1) and SC(T) (2) on temperature

It is understood that in case of temperature rise, the increase of sulfur conversion intensity and COM will facilitate the decrease of quantities of non-converted oxygen in desulfurization gases and «K» rise (Table 3.42).

Taking into consideration the aforementioned, optimum temperatures should be considered close to 425-450ºC.

Reaction rate of gaseous-phase reagents with solid bodies and conversion degrees of final substances are substantially influenced by the ratio between the number of reagents. To characterize this ratio, we use the

notion of OFR.

On the process under research, we can state that it should be conducted with the least oxidant losses, which would provide sufficiently high sulfur removal and conversion degrees, as far as the ratio rise of oxidant consumption (m^3/h) to coal mass (kg) will result in increasing volume of desulfurization gases and appropriately decreasing the content of substances of sulfur conversion in them.

The results obtained are presented in the Table 3.43 and Fig. 3.30-3.31.

In case of the increase of oxidant that is being given per a unit of raw material, insignificant rise of COMC (Fig. 3.30) occurs, and the content of oxygen-containing gaseous products (CO_2 and CO) decreases in twice if OFR rises, and appropriately, the volume of desulfurization gases – in 8 times (from 0.6 to 4.8 $m^3/(h \cdot kg)$, Table 3.43). During the process course, COMC can decrease as a result of gasification reactions, thermal decomposition and burning, and can increase resulting from adhesion of oxygen and water steam by organic part (synthesis reaction). Taking into consideration insignificant rise of COMC and absolute quantity of CO and CO_2, it can be stated that mainly OFR rise contribute to destruction reactions than to the synthesis of COM. It should be noticed that to a considerable extent the OFR rise intensifies the reactions of COM burning than the reactions of its destruction and gasification, as far as EFCOMC decreases (Fig. 3.30).

The process implementation without oxidant feed (OFR =0) causes sufficiently high degree of sulfur conversion. It is confirmed by the proposal that the conversion reactions of sulfurous compounds of lignite take place mainly due to the participation of reaction capable part of COM in them. If little quantity of oxidant (OFR =0.6 $m^3/(h \cdot kg)$) is fed in the

reaction zone, the process intensification of sulfurous compound conversion occurs (Fig. 3.31). It indicates that air oxygen takes insignificant part in the reactions of pyritic sulfur conversion. The increase of OFR from 0.6 to 4.8 $m^3/(h \cdot kg)$ leads to insignificant decrease of sulfur removal and conversion degrees, as far as the OFR rise intensifies gasification and thermal destruction of organic matrix, what causes the reduction of number of reaction capable parts of COM.

Table 3.43 Dependence of the content of desulfurization gases on OFR

OFR, $m^3/(h \cdot kg)$	Content, vol %								K
	CH_4	C_2-C_3	H_2S	CO_2	CO	N_2	O_2	Ar	
0[1]	5.07	4.66	15.68	62.07	9.86	0[2]	2.66	0	–
0.6	1.69	1.42	7.05	23.31	3.79	60.84	1.19	0.71	0.93
1.2	0.88	0.80	3.62	18.13	2.62	71.43	1.69	0.83	0.91
2.4	0.79	0.41	1.72	12.97	2.08	76.06	5.08	0.89	0.75
4.8	0.49	0.27	0.78	12.70	1.38	76.03	7.46	0.89	0.63

Remarks:

[1]The cold system of coal was blown through by nitrogen and heated rapidly up to the temperature of the process.

[2]The quantity of nitrogen was not taken into consideration in calculating the gas composition.

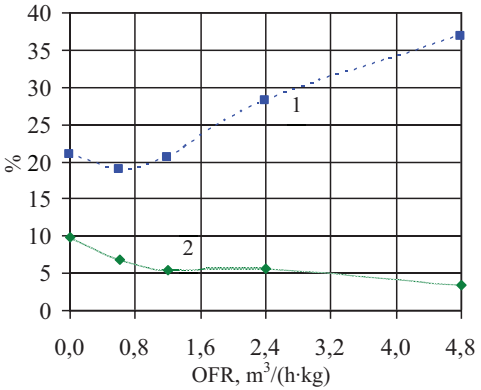

Fig. 3.30 Dependence of COMC (1) and EFCOMC (2) on OFR

All aforementioned allow to recommend conducting the process of lignite desulfurization with minimum admissible values of OFR (close to 0.6 $m^3/(h \cdot kg)$), which provide maximally possible RDS(P), SC(T) and the content of H_2S in desulfurization gases and are sufficient for keeping up the process temperature due to burning out the part of COM.

The reaction intensity in the desulfurization system, that consists of solid body and gas, substantially depends upon the ratio of reagents and the period of their contact. That is why it so important to define which should be the optimum duration of the process with the minimum oxygen consumption (close to 0.6 $m^3/(h \cdot kg)$). The results obtained are presented in Table 3.44 and Fig. 3.32-3.33.

The obtained data makes possible stating that the process duration prolongation causes deepening the processes of burning, gasification and decomposition of COM, what results in COMC (Fig. 3.32).

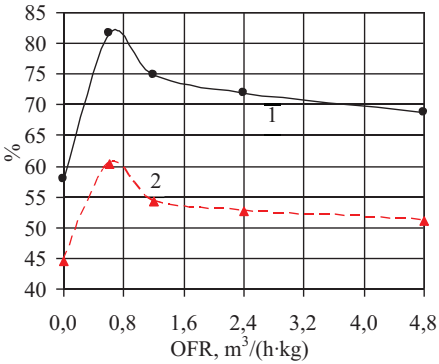

Fig. 3.31 Dependence of RDS(P) (1) and SC(T) (2) on OFR

Moreover, the duration rise intensifies primarily the reactions of burning the organic part (EFCOMC decreases).

Intensity rise of coal matrix burning with time increase of raw material stay in the reactor is confirmed by insignificant decrease of the content of CO_2 in desulfurization gases, though the volume of gases increases direct proportionally to the process duration rise (Table. 3.44).

Table 3.44 Dependence of the content of desulfurization gases on the process duration

Duration, minute	Content, vol %,								K
	CH_4	C_2-C_3	H_2S	CO_2	CO	N_2	O_2	Ar	
5	1.16	1.78	7.38	23.40	3.84	58.19	3.57	0.68	0.77
10	0.92	1.28	4.70	20.93	3.72	64.53	3.17	0.75	0.82
15	1.00	0.99	3.53	20.23	3.69	68.10	1.67	0.79	0.91
20	0.76	0.91	2.85	19.93	2.09	70.11	2.53	0.82	0.87
30	0.42	0.68	2.06	18.50	1.02	73.22	3.25	0.85	0.83

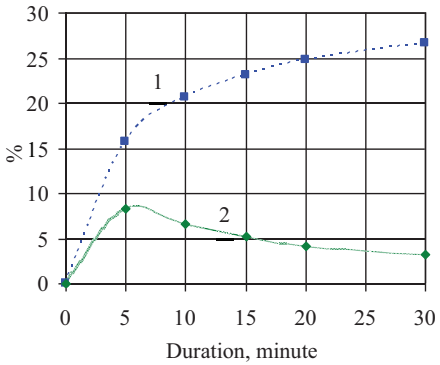

Fig. 3.32 Dependence of COMC (1) and EFCOMC (2) on duration

If the process duration is equal to over 10-15 minutes, the COM conversion reactions take place less intensively, what is confirmed by the decrease of «K» (Table 3.44).

In according to the data of Fig. 3.33 the sulfur conversion takes place at the beginning of the process, i. e. the maximum degrees of sulfur removal and conversion are within 5-10 minutes. The further process duration prolongation does not lead to significant increase of RDS(P) and SC(T) (Fig. 3.33).

Thus, the optimum process duration should be considered 5-10 minutes, as far as its further increase does not lead to significant rise of RDS(P) and SC(T), but causes the reduction of H_2S quantity in desulfurization gases.

So, in case of lignite desulfurization, RDS(P) and SC(T) depend substantially on temperature, which optimum values should be considered

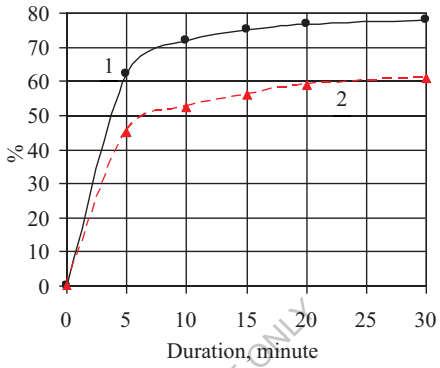

Fig. 3.33 Dependence of RDS(P) (1) and SC(T) (2) on duration

425-450 °C. The process can be carried out with minimum quantities of oxidant (0,6 m^3/h air per 1 kg of coal) during 5-10 minutes. Relatively high degrees of lignite sulfur desulfrization are reached while heating raw material in vacuum. The data confirms the assumption suggested that in the course of lignite desulfurization, the main sulfur conversions take place as a result of pyritic sulfur reaction with high reaction organic mass and/or the products of is destruction and gasification; only insignificant number of reactions of sulfurous compound conversion is carried out with oxidant part.

The use of water steam in oxidant (in the mixture with air) practically does not influence upon the intensity of sulfurous compound conversion, but makes possible increasing the content of sulfur desulfurization products in desulfurization gases. In the researches

presented in the paper, only air was used as oxidant. Even in the case, it is possible to obtain desulfurization gases with the content of hydrogen sulfide equal to vol 7-8 %., what will make it possible to reprocess them for obtaining element sulfur by known methods.

The general sulfur conversion degrees are equal to sulfur quantity that passes to the gas phase, and in case of further coal burning, it does not get into the atmosphere. That is why the results obtained allow stating that with the use of the process in TPS, we can decrease environment pollution with sulfur dioxide at least to 55-65 %.

3.3. Using of oxidative desulfurization process

The application of the process of coal oxidative desulfurization can occur in several directions:

- In energy;
- For obtaining the components of the charge for the production of special types of coke;
- For the production of pulverized coal;
- For energy-technological processing of coal (primary lignite).

3.3.1. Using of oxidative desulfurization in energy. The fraction less than 0.1 mm of the G3 coal and 0.1-0.25 mm of the G1 and C coal were used to carry the experiments under optimal conditions. Such size of grains caused by the fact of process realisation in the power industry and it has to be no more than 0.1-0.2 mm during the burning at TPS.

Experiments show that process optimal conditions different for different coals and depend mainly on the content of total and pyrite sulfur: greater sulfur amount, greater reaction time and rate of air-steam mixture.

The characteristic of desulfurizated coal and material balances are given in the Tables 3.45, 3.46.

Table 3.45 Characteristics of desulfurized coal

Coal	Moisture content, W^a, wt %	Ash, A^d, wt %	Volatiles yield, V^{daf}, wt %	Sulfur content for dry mass, wt %			
				Total, S_t^d	Pyritic, S_p^d	Organic, S_o^d	Sulfate, $S_{SO_4}^d$
G1	2.09	26.00	25.42	1.92	0.69	0.80	0.43
G3	1.21	11.68	26.60	1.09	0.12	0.59	0.38
C	3.22	15.93	26.34	1.45	0.06	0.21	1.18

Table 3.46 Material balance of the process

Balance items	Coal G1	Coal G3	Coal C
1	2	3	4
Directed mass percentage (wt %) for the raw material			
1. Coal	100.00	100.00	100.00
including sulfur	7.85	2.17	3.79
2. Air-steam mixture	215.33	30.66	176.00
Total	315.33	130.66	276.00
Obtained mass percentage (wt %) for the raw material			
1	2	3	4
1. Resin of decomposition	11.00	14.47	13.65
including sulfur	0.36	0.31	0.11
2. Desulfurization gases	140.33	24.39	113.65
including C_1-C_3 hydrocarbons	1.56	0.32	2.17
including CO	3.09	0.75	1.70
including CO_2	23.21	2.81	21.22
3. Condensate and losses	94.33	17.13	76.00
Total	315.33	130.66	276.00

We can see from the results that it is possible to obtain solid fuel with the content of total sulfur <2 wt % from the G1 coal containing almost 8 wt % of sulfur and low-sulfur fuel (sulfur content < 1.5 wt %) from the G3 and C coal.

The results from the Table 3.45 show that the sharp reduction of the pyrite sulfur in the desulfurizated coal is accompanied by the change of the organic and sulfate sulfur. However, if there is an increase of pyrite sulfur content after the desulfurization, what is the consequence of bum out of an organic part and pyrite oxidation with sulfate formation, the amount of the organic sulfur is different in different coals.

The organic sulfur content is changed in the raw C>G3>G1 as follows: it decreases (C), doesn't change (G3) and increases (G12. The reason is that mercaptanes or sulfides are the majority of sulfur in the coal with low metamorphism. The increase of metamorphism degree increases the fraction of sulfur, which is the part of stable thiophane structures. The content of the organic sulfur can reduce due to its conversion during a process (mainly to SO_2) but can increase due to the burning and thermal decomposition of the hydrocarbon part of the coal. At the desulfurization of the coal with the lowest metamorphism (the C coal) the decomposition and oxidation of the organic sulfur are more intensive than those of the hydrocarbon part; at the desulfurization of the G3 coal both these processes are in equilibrium.

The desulfurization gases contain also C_1-C_3, CO and CO_2, what reveals the proceeding of partial destruction and burning of the coal matrix. This fact is confirmed also by partial increase of ash content, decrease of the yield of volatile substances and obtaining of 11-14.5 wt % of the resin (see Table 3.46).

Conducted researches show, that during treatment of coal by air-steam mixture at 400 – 450 ^{0}C, because of selective oxidation of pyrite, we can exclude from coal practically all pyrite-sulfur and provide possibilities of it's utilization.

Approximate heat balances of the reactor block were calculated on the basis of material balance for the estimation of energy consumption. The results are given in the Table 3.47.

It was adopted that the heat is directed to the reactor, consists of the heat of coal, air and water, and the heat as a consequence of the different reactions proceeding. The withdrawn heat is within the desulfurizated coal, resin of the decomposition, desulfurization gases (including steam formed as a result of the burning of coal organic matrix) and steam formed during the water vaporisation. For the convenience the values of heat amount measured by MJ related to 1 ton of the initial coal. It was adopted also that the heat directed to the reactor block is calculated as the heat of the pyrite and coal burning minus the heat of hydrocarbons decomposition reactions.

From provided results we can see, that the amount of heat evolved during the process of desulfurization, is 1.43 - 1.59 times bigger then amount of heat needed for conducting of the process (heating up coal till reaction temperature and preparing of air-steam mixture), in other words, process ensures itself energy-wise.

Because the process of desulfurization of coal lets us exclude practically all pyrite sulfur along with minimum destruction of organic matrix of coal and suffices itself with energy, then process can be realized on separate unit to improve quality of market coal or as first stage of two-step coal burning at TPS.

Realization of process of coal desulfurization on TPS is more profitable, because coal heat evolved from reactor of desulfurization is

effectively used. Besides this, there is no need decide problems of cooling and transporting of grinned coal.

During using the process on TPS, it should be equipped with low temperature coal burning (desulfurization) unit, which consist of two blocks: block of coal desulfurization (first stage of burning) and block of processing of desulfurization gases (see Fig.3.34).

The desulfurization block is meant to burn out pyrite sulfur from coal at comparatively low temperatures and small volumes of air. Desulfurized coal, at the temperature a bit lower than the desulfurization temperature, is supplied to the usual TPS boiler for burning at high temperatures (second stage of burning). Block of processing of desulfurization gases is meant for cooling of gases and condensation of reaction water, removing of $S0_2$ and burning up the hydrocarbons C_1 – C_3 and CO, which is present in desulfurization gases.

Table 3.47 Heat balance of the reactor block of the desulfurization unit

Balance items	T, ^{0}C	Phase stage	Enthalpy[1], $q_i^t\ (kJ/kg)$	Coal G1		Coal G3		Coal C	
				$G_i\ (kg)$	$Q_i = G_i \times q_i^t \times 10^{-3}$ (MJ)	$G_i\ (kg)$	$Q_i = G_i \times q_i^t \times 10^{-3}$ (MJ)	$G_i\ (kg)$	$Q_i = G_i \times q_i^t \times 10^{-3}$ (MJ)
1	2	3	4	5	6	7	8	9	10
Directed									
1.Coal	20	Solid	26.00	1000.0	26.000	1000.0	26.000	1000.0	26.000
2. Air	120	Gas	100.00	1328.6	132.860	189.2	18.920	1085.9	108.590
3. Water	50	Liquid	209.00	824.7	172.362	117.4	24.537	674.1	140.887
4. Reaction[2]					4683.016		1133.616		3519.422
Total					5014.236		1203.073		3794.899
Expended									
1. Desulfurizated coal	648	Solid	487.50	696.7	339.641	746.7	364.016	727.0	354.413

1	2	3	4	5	6	7	8	9	10
2. Decomposition resins	423	Liquid	291.25	110.0	32.038	144.7	42.144	136.5	39.756
3. Steam	423	Gas	2778.35	824.7	2291.305	117.4	326.178	674.1	1872.886
4. Desulfurization gases	423	Gas	162.68-179.48	1522.1	247.610	297.8	53.449	1222.4	202.346
5. Losses[3]					234.151		56.681		175.971
Total					3144.745		842.468		2645.372

Remarks:

[1]The enthalpy of the desulfurization gases differed between themselves, depending on their content, and were calculated using the additive rule $q^t_{d.g.} = \sum q^t_i x^i$, where q^t_i is the enthalpy of gas component i (in units of kJ/kg) and x^i is the mass fraction of component i in the gas.

[2]The heat of reaction is calculated by following equation: $Q_r = G_S q_r^{SO2} + G_{CO} q_r^{CO} + G_{CO_2} q_r^{CO2} + G_{H_2O} q_r^{H_2O} - G_{Res.} q_r^{Res.}$, where G_S, G_{CO}, G_{CO_2}, and G_{H_2O}, respectively, are the amounts of sulfur that changed to dioxide, burned to CO, burned to CO_2, and burned to H_2O (all given in kilograms). $G_{Res.}$ is the amount of created resin (given in kilograms); q_r^{SO2}, q_r^{CO}, q_r^{CO2}, $q_r^{H_2O}$, and $q_r^{Res.}$ are the amounts of heat from the respective reactions (given in units of MJ/kg). Following amounts G_S, G_{co}, G_{CO_2}, G_{H_2O}, and $G_{Res.}$ were calculated on the basis of the matter balance and the content of desulfurization gases.

[3]Heat losses were 5%, relative to the heat of the reaction

Resin, which is created during coal desulfurization, can be used as raw material for coal-and-chemical production or can be burned in TPS boilers. Heat evolved from resin burning, burning up of desulfurization gases and excess of heat in reactor of desulfurization are used for producing of medium preasure steam.

At the determination of the optimal conditions, the aim of the experiments was not to achieve the maximal recovery degree of the sulfur only but also to obtain small volumes of the desulfurization gases with high SO_2 content. Oxidative desulfurization at 420-445 °C and process time of 10-21.5 min. allows converting 77-90 % of pyrite sulfur (30-75 % of total sulfur) into gaseous compounds. The average content of SO_2 in desulfurization gases of black coal is 2.6-7.0 vol. % (see Table 3.48).

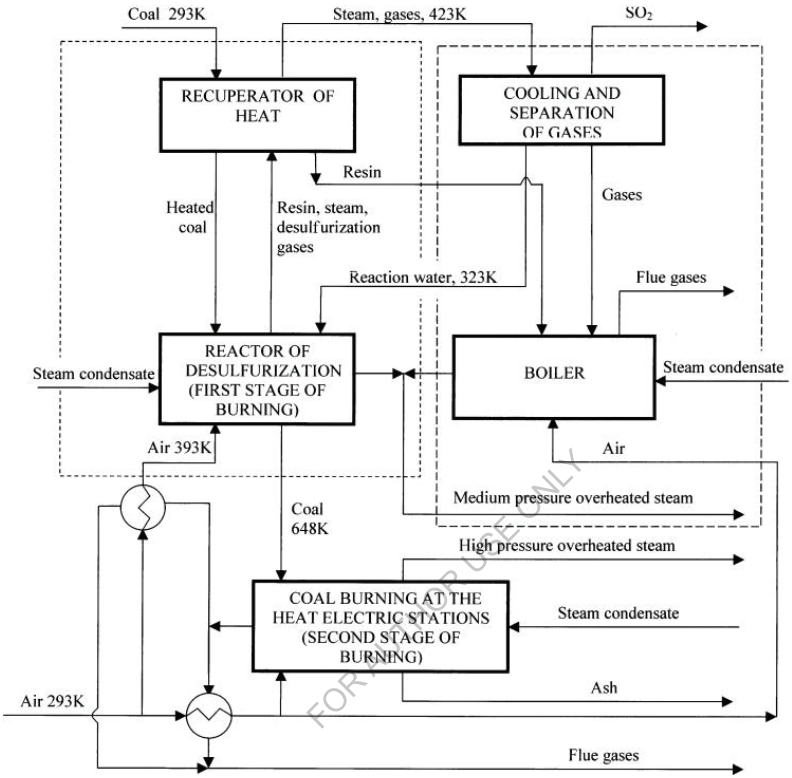

Fig. 3.34. Schematic diagram of the two-staged burning of coal in the plant. The area enclosed by the short dashed line represents the coal desuphurization block, whereas the region bordered by the long dashed line represents the block of processing of desulfurization gases.

Table 3.48 Composition of desulfurization gases of different types of coal

Gases	Content, vol.%					
	Coal C	Coal G1	Coal G3	Coal F2	Coal L	Coal RM
SO_2	6.96	4.24	4.03	2.58	3.80	5.60
H_2S	0.32	–[1]	–[1]	0.05	0.00	0.34
H_2	0.21	–[1]	–[1]	0.00	0.00	0.29
CH_4	2.70	1.07	1.05	1.48	0.51	3.83
C_2H_4	0.36	0.45	0.73	0.21	0.12	0.40
C_2H_6	1.05			0.43	0.14	1.56
C_3	0.60			0.18	0.16	0.56
CO	3.25	2.47	3.36	1.81	1.09	3.77
CO_2	8.13	11.81	8.07	9.84	5.07	9.44
O_2	3.09	1.77	2.64	3.89	11.02	1.69
N_2	72.49	78.19	80.12	78.64	77.18	71.69
Ar	0.85			0.89	0.91	0.84

Remark:
[1]Not determined

So the fulfilled investigations show the possibility of high-pyrite coal desulfurization by air-steam treatment. The process products are: solid fuel with the small content of sulfur, the resin of decomposition and the desulfurization gases with the high content of sulfur dioxide (2.6-7.0 vol. %). The desulfurization process is ensured by power by itself.

The proposed process can be realised in the power industry as a first stage of the coal burning at TPS, where the main part of sulfur would be

burned at relatively low temperatures. In such a case the high-temperature corrosion of the equipment would reduce considerably. After the first stage the desulfurizated coal would supply to the usual boiler at the temperature some less than the reaction temperature (the second stage of the burning). The resin produced during the process can be used as a raw material for coal-and-chemical production or can be burned directly at TPS.

The desulfurization gases can be used by three ways at least. It depends on TPS location, market etc.:

- The oxidation of SO_2 to $S0_3$ and sulfuric acid production [88];
- $S0_2$ concentrating by well known cyclic methods [86-89];
- Sulfur production (when gas containing H_2S is present) [90].

3.3.2. Using of oxidative desulfurization for obtaining the components of the charge for the production of special types of coke. To determine the possibility of desulfurized coal using as an additive to the raw material while producing special types of coke we carried out the plastometry of basic charge (BC) and BC with additives of the initial and desulfurized coal.

The composition and characteristics of BC are represented in Tables 3.49 and 3.50.

The investigated charge was prepared using the basic charge with the additives of 2–10 mas % of the desulfurized coal F3, as well as desulfurized and cleaned coal $F2_2$ (see Table 3.37, 3.38). One of the samples was prepared with the addition of F2 coal and decomposition resin formed during the desulfurization due to the destruction of coal organic part. The characteristics of obtained charges are represented in Table 3.51 One can see that prepared samples do not practically differ from the initial charge. The samples obtained using desulfurized coal (No. 2-4, 6 and 7) are

characterized by lower sulfur content and volatile matter yield compared with the charge with addition of the initial coal (No. 1 and 5) that is logically explained by the characteristics of the initial components.

Table 3.49 Quantitative and qualitative composition of the basic charge

Coal origin	Coal type	Content in charge, mas %
Ukraine, concentration plant "Samsonovskaya"	G	30
Ukraine, concentration plant "Belorechenskaya"	F	20
Ukraine, concentration plant "Mykhailovskaya"	F	30
Ukraine, concentration plant "Uzlovskaya"	LH	20

Table 3.50 Technical analysis of the basic charge

Moisture content, W^a, mas %	Ash content, A^d, mas %	Volatile matter yield, V^{daf}, mas %	Sulfur content, mas %			
			total	pyrite	organic	sulfate
			S_t^d	S_p^d	S_o^d	$S_{SO_4}^d$
1.76	9.63	33.38	2.37	1.02	0.24	1.11

Thermolysis of the basic charge, BC with addition of desulfurized coal, non-volatile residues (NVR) and coke was carried out using Q-1500 D derivatograph of Paulik-Paulik-Erdey system recording the analytical signals of mass loss and heat effects. The samples were analyzed under dynamic mode with the heat rate of 10 K/min in the argon medium (for BC and BC with desulfurized coal) and in the CO_2 medium (for NVR and coke). The sample mass was 50 mg.

Table 3.51 Characteristic of the initial charges

Sample	Charge composition	Moisture content, W^a, mas %	Ash content, A^d, mas %	Volatile matter yield, V^{daf}, mas %	Sulfur content, mas %			
					total	pyrite	sulfate	organic
					S_t^d	S_p^d	$S_{SO_4}^d$	S_o^d
1	95 % BC + 5 % initial F3	1.92	9.01	33.41	2.42	1.05	1.16	0.21
2	98 % BC + 2 % desulf. F3	1.82	9.63	33.09	2.38	1.01	1.13	0.24
3	95 % BC + 5 % desulf. F3	1.88	9.58	32.67	2.29	0.98	1.07	0.24
4	90 % BC + 10 % desulf. F3	1.88	9.86	31.95	2.25	0.95	1.03	0.27
5	95 % BC + 5 % initial $F2_2$	1.74	10.41	33.49	2.66	1.17	1.23	0.26
6	95 % BC + 5 % desulf. $F2_2$	1.71	9.77	32.83	2.30	0.98	1.12	0.20
7	95 % BC + 4.5 % desulf. F3 + 0.5 % resin	1.82	9.72	32.10	2.35	1.00	1.11	0.24

As a result of pyrite sulfur oxidation ferrum converts into the oxides, Fe_2O_3, first of all, the content of which in the desulfurized coal is calculated according to the formula:

$$X_{Fe_2O_3} = \left(\frac{\left(S^a_{p(in)} - \frac{S^a_{p(des.coal)} \cdot x_{des.coal}}{100} \right) \cdot M_{Fe_2O_3}}{2 \cdot M_S \cdot x_{des.coal}} \right) \cdot 100 \qquad (3.27)$$

where $S^a_{p(in)}$ – pyrite sulfur content for analytical sample in the initial coal, mas %; $S^a_{p(des.coal)}$ – pyrite sulfur content for analytical sample in the desulfurized coal, mas %; $x_{des.coal}$ – desulfurized coal yield, mas %; $M_{Fe_2O_3}$ – Fe_2O_3 molecular mass, g/mol; M_S – sulfur molecular mass, g/mol.

We analyzed the capability of samples 1–8 to turn into plastic state and to be caked. The results of these plastometric investigations are represented in Table 3.52. One can see that addition of desulfurized and initial coal, as well as desulfurized coal together with decomposition resin

(2–5 mas %) does not actually affect the thickness of plastic layer and plastometric subsidence. The content of 10 mas % of desulfurized coal F3 negatively affects the capability of the raw materials to turn into plastic state – the plastic layer thickness decreases by 25 % (compared with BC), though the plastometric subsidence of NVR increases. The latter fact allows to predict the improvement of coke column unloading from coking boxes while using desulfurized coal as an additive to the charge.

The investigation results concerning the effect of additives type and amount on the technical analysis values, content of total sulfur and its variations, abrasive hardness, reactivity and mechanical strength of NVR are represented in Table 3.53.

One can see from Table 3.53 that NVR yields of the samples 1–7 and BC are the same. The ash and sulfur contents are also unchanging. It should be noted that the latter values of the samples 1 and 5 (with addition of the initial coal) are slightly higher than those of the samples 2–4, 7 and 6 (with addition of desulfurized coal). The volatile matter yield of the samples with addition of desulfurized coal F3 increase: the slight increase we observe while adding 2–5 mas % of the coal and considerable increase – adding 10 mas %.

Apparently, during oxidative desulfurization the coal organic matrix is converted and forms more thermostable compounds. Part of them turns into volatile matter at the temperatures higher than maximum temperature of the plastometric investigations.

The addition of the initial and desulfurized coal to BC does not practically affect its caking ability (Table 3.52), hence its mechanical strength and abrasive hardness of non-volatile residue (Table 3.53). Some improvement in NVR mechanical properties is observed while adding the initial and desulfurized coal F3 in amount of 5 mas % to BC.

Table 3.52 Plastometric indexes of the initial charges

Raw materials	Plastometric subsidence X, mm	Thickness of plastic layer Y, mm
Basic charge	33	12
Sample 1	36	13
Sample 2	33	13
Sample 3	35	12
Sample 4	40	9
Sample 5	35	13
Sample 6	35	12
Sample 7	33	13

Table 3.53 Characteristics of the non-volatile residues

Non-volatile residue	Yield, mas %	Ash content A^d, mas %	Volatile matter content V^{daf}, mas %	Total sulfur content S_t^d, mas %	Abrasive hardness AH, mg	Reactivity K_m, $cm^3/g \cdot s$	Mechanical strength according to Rog method RI, units
Basic charge	79.91	10.94	9.27	1.95	20	1.54	93.63
Sample 1	81.36	10.81	8.94	2.19	22	1.62	95.44
Sample 2	80.77	10.73	9.63	1.99	19	1.62	95.62
Sample 3	79.90	11.08	9.84	2.09	21	1.70	95.94
Sample 4	80.92	10.92	12.11	2.05	19	1.81	94.62
Sample 5	80.79	10.91	8.22	2.02	19	1.47	94.95
Sample 6	81.08	10.50	9.65	1.94	19	1.78	95.07
Sample 7	79.02	9.85	7.61	1.86	17	1.46	92.03

The addition of desulfurized coal (comparing with BC and BC+initial coal) inconsiderably increases the reactivity of the residue that is in good agreement with the changes of volatile matter yield (Table 3.53).

While using even small amount of thermal decomposition resin as additive, we observe the worsening of coke properties: mechanical characteristics of the sample 7 are worse and reactivity is less compared with other samples.

To examine the indentity of coke obtained from the same raw material and NVR quality indexes, reactivity first of all, we carried out following investigations:

1) according to the procedure described in [62] we obtained coke with BC and BC+5 mas % of desulfurized coal $F1_2$ (sample 6, Table 3.51)

2) we analyzed the following samples using derivatographic analysis (DTA):

- BC and sample 6 in the argon medium;
- NVR+BC and NVR of the sample 6 in CO_2 medium;
- coke with BC and coke of the sample 6 in CO_2 medium.

DTA results are represent ed in Table 3.54 and Figs. 3.35-3.40.

The values of mass loss and thermal effects of thermodestructive processes for BC and sample 6 are almost the same (Figs. 3.35 and 3.36). The difference in the final mass loss is 3 mas % (Table 3.54). Taking into account that the amount of organic mass introduced into BC+coal F2 is approximately 4 mas % during the sample 6 preparation, the above-mentioned difference in mass loss may be explained by the change in BC reactivity while adding desulfurized coal with 12 mas % of Fe_2O_3 (Eq. (3.27)). It is known [63] that while heating ferrum (III) oxide is an active component and intensifies destruction during coking. The mass losses of both samples are accompanied by exoeffects which are actually equal. However, destruction processes are more intensive for the sample 6, therefore its total thermal effect is lower (Fig. 3.35).

Table 3.54 Derivatographic analysis results

Stage	Temperature range, K	Mass loss at the stage, mas %	Total mass loss, mas %
1	2	3	4
BC[1]			
I	273–399	1	1
II	399–601	–	1
III	601–776	9	10
IV	776–1029	16	26
V	1029–1223	12	38
VI	1223–1273	7	45
Sample No.6[1]			
I	273–393	1	1
II	393–607	–	1
III	607–776	9	10
IV	776–1028	16	26
V	1028–1163	9	35
VI	1163–1273	13	48
NVR of BC[2]			
I	273–408	3	
II	408–593	1	4
III	593–948	16	20
IV	948–1078	7	27
V	1078–1158	5	32
VI	1158–1273	23	55
NVR of the sample No.6[2]			
I	273–443	3	3
II	443–603	–	3

1	2	3	4
III	603–893	21	24
IV	893–1063	13	37
V	1063–1173	9	46
VI	1173–1273	26	72
Coke from BC[2]			
I	273–708	0,4	0.4
II	708–883	11	12
III	883–943	6	18
IV	943–1013	6	24
V	1013–1093	6	30
VI	1093–1143	3	33
VII	1143–1273	15	48
Coke from the sample No.6[2]			
I	273–713	1	1
II	713–868	11	12
III	868–973	10	22
1	2	3	4
IV	973–1033	6	28
V	1033–1118	8	36
VI	1118–1188	9	45
VII	1188–1273	17	62

Remarks:

[1]Derivatographic analysis was carried out in argon medium

[2]Derivatographic analysis was carried out in CO_2 medium

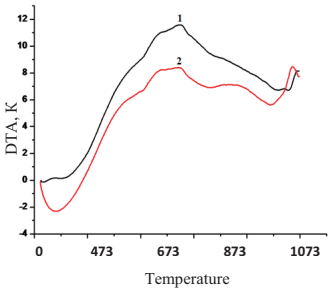

Fig. 3.35. DTA in argon medium: BC (1) and the mixture of 95 mas % BC + 5 mas % desulfurized coal Fl_2 (2)

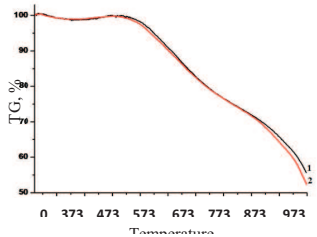

Fig. 3.36. Dependence of mass loss on the temperature in argon medium: BC (1) and the mixture of 95 mas % BC + 5 mas % desulfurized coal Fl_2 (2)

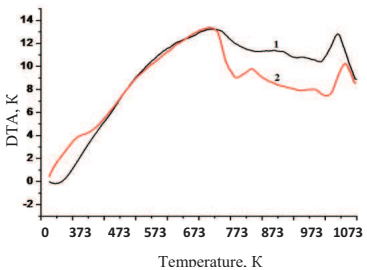

Fig. 3.37. DTA in CO_2 medium: NVR of BC after plastometry (1) and NVR of the mixture 95 mas % BC + 5 mas % desulfurized coal $F1_2$ after plastometry (2)

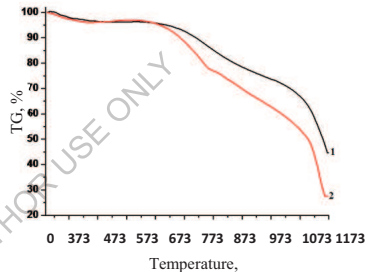

Fig. 3.38. Dependence of mass loss on the temperature in CO_2 medium: NVR of BC after plastometry (1) and NVR of the mixture 95 mas % BC + 5 mas % desulfurized coal $F1_2$ after plastometry (2)

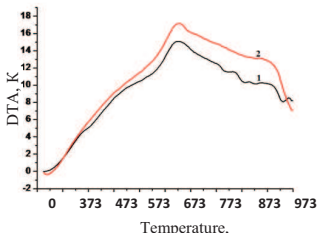

Fig. 3.39. DTA in CO_2 medium: coke of BC (1) and coke of the mixture 95 mas % BC + 5 mas % desulfurized coal $F1_2$

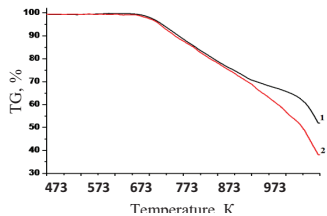

Fig. 3.40. Dependence of mass loss on the temperature in CO_2 medium: coke of BC (1) and coke of the mixture 95 mas % BC + 5 mas % desulfurized coal $F1_2$

The analysis of TG and DTA thermolysis curves in CO_2 medium of NVR and coke obtained from BC and sample 6 allows to assert that NVR and coke reactivity is higher for the sample 6 than that for BC (Figs. 3.37-3.40). According to TG curves the difference between total mass losses of BC and sample 6 after plastometry is 17 mas % for NVR and 14 mas % for coke (Table 6). The NVR and coke masses decrease due to the reaction between the coal organic matrix and carbon (IV) oxide followed by thermal destruction. The above-mentioned difference between the yields of thermolysis residues may be explained by the increase in residues reactivity obtained during coking and/or plastometry because the difference between total mass losses (due to the destruction of BC organic matrix and the sample 6) is only 3 mas %.

The character of thermal conversions in CO_2 medium is confirmed by DTA curves. They show the total exothermal effect of the reactions proceeding during residues thermal conversion in CO_2 medium. The reason is predominance of the synthesis reactions with heat release over cracking reactions with heat absorption. At the temperatures about 823 K and higher the increase of DTA curve becomes slower, i.e. intensity ratio between SR (synthesis reactions) and CR (coking reactions) equalizes.

It is known that the reactions between carbon and CO_2 characterize the coke reactivity and proceed with appreciable endoeffect (ΔH = 189.1 kJ/mol). CO_2 conversion above 50 % is achieved at the temperatures higher than 1073 K [64-68]. That is why we observe the decrease of DTA curve at the temperatures higher than 1213–1233 K (Fig. 3.37). While using coke within the range of 1143 (1188)–1273 K we observe clear endothermic effects caused by stimulation of the reaction between coal organic matrix and CO_2. Moreover, while using the residues of the sample 6 the

stimulation of endothermic reactions proceeds more intensively compared with the thermolysis reactions of residues with BC.

All above-mentioned allows to assert that addition of desulfurized coal to BC enhances its capability of thermal destruction during coal carbonization. Due to these deep conversions and first of all, due to the presence of Fe_2O_3 great amount in the desulfurized coal, the reactivity of coke produced from BC and desulfurized coal increases.

The similar character of DTA and TG curves obtained in CO_2 medium during thermolysis of plastometry NVR and coke indicates that we can predict the reactivity of coke as itself based on the reactivity of non-volatile residues.

So pyrite sulfur, which is the main part of total sulfur in high-sulfuric coal, converts first of all into Fe_2O_3 oxide as a result of oxidative desulfurization of medium-metamorphosed black coal. The Fe_2O_3 content in the desulfurized coal is 10–15 mas %. Such content worsens the capability of medium-metamorphosed coal to turn into plastic state and be caked but allows to use the desulfurized coal as an additive (under 5 mas % relative to the finished mixture) to the raw material for the production of special types of coke. Moreover, the quality indexes of obtained coke are constant or improved compared with those of BC or BC + additives of the initial sulfuric or high-sulfuric coal.

We do not recommend to use the resin obtained as a result of thermal decomposition of coal organic matrix during oxidative desulfurization as additives to the raw material.

3.3.3. Using of oxidative desulfurization for the production of pulverized coal. For the production of cast iron the world and Ukrainian

metallurgical enterprises use expensive fuel and energy resources (coke and gas) which, in turn, increase the price of finished steel [69].

Also despite significant global coal reserves, metallurgical coal is a relatively scarce raw material. The volume of coal production and consumption is constantly increasing, and all mined coking coal is used exhaustively. The situation is complicated by the fact that majority of similar untapped coal deposits are poor in quality due to high ash, and high sulfur content.

Alternatively, the direct utilization of high-quality thermal coal for blast-furnace production otherwise called “pulverized coal injection” technology (PCI) [70, 71].

The crux of PCI technology is a partial replacement of coke and natural gas by steam coal through its direct injection into the blast furnace. The method was developed in the 70s and 80s of the last century [72]. In 2004, nearly a half of the cast iron volume in the world (300 mln. tons) was produced through PCI. The share of coke replaced by coal ranged from 20% to 50% [73, 74].

In practice, low ash and sulfur content coal are best suited for utilization as thermal coal in blast furnaces due to its impact on product quality and process efficiency. As a result, the level of quality indicators should not exceed ash and sulfur content of coke used in the enterprise. Similarly, the content of volatile substances in coal can vary widely with potential influence on the price of raw materials and specific technological conditions (Table 3.55). Therefore, it is important to analyze the characteristics of coals selected for PCI method. The basic requirements are; low ash content and sulfur content. Typically lower the ash content improves the effectiveness of the higher the PCI process. Additionally, sulfur is one of the most harmful chemical elements in a blast furnace.

Therefore, sulfur composition in coal should be minimal and not exceed the sulfur content of coke used in blast furnace smelting. According to studies by Diez et al., ACCCI, Chauhan and Vijayavergia [75-77] the sulfur content should not exceed the range 0.5-1.5 wt % and moisture content (12 wt %) which is the threshold for the materials' looseness.

Furthermore, the particle size of the coal needs to meet the quality requirements of pulverization for PCI technology. Since grinding is typically carried out at one-stage plants, the initial particle size must not exceed 50-80 mm.

As observed in data, coal reserves with a sulfur content <1.5 wt % or ash content of 10 wt % are limited. Also, a considerable part of hard coals (with a low degree of coalification) cannot be used in this process due to the high yield of volatiles. Taking into account the world practice of PCI application [76, 78], there are strict requirements for the raw material used in PCI (Table 3.56), sulfur content in particular. This chemical element is detrimental for blust-furnace production, thus it is desirable the quantity of sulfur in coal would be minimum and does not exceed the quantity of sulfur in coke used for blust-furnace smelting.

Table 3.55 Yield of ash content and volatiles of coal used for pulverized coal injection by key steel manufacturers [78]

Company	Ash content, wt %	Volatiles' yield, wt %
Kobe Steel	7.4-10.1	32.5-33.3
Shoudu	13.8-15.1	8.0-8.5
Thysscn	6.9-10.0	9.1-29.3
Kawasaki	9.8-11.8	22.8-34.3
British Steel	2.2-9.5	6.5-34.1
Hoogovens	3.6-7.5	32.0-36.2
Tata steel	10.5-17.5	24.5-25.0

Table 3.56 Quality requirements for coal effective use in PCI technology [79]

Coal type	Size of coal, mm	Ash content, A^d, %	Moisture content, W^r_t, %	Content of total sulfur, S^d_t, %	Volatiles yield, V^{daf}, %
1	2	3	4	5	6
Raw material to produce pulverized coal No.1					
Candle coal	0–50	≤ 8.0	≤ 10.0	≤ 1.0	≤ 38.0
Candle-gas coal	0–50	≤ 8.0	≤ 10.0	≤ 1.0	≤ 38.0
Gas coal	0–50	≤ 8.0	≤ 10.0	≤ 1.0	≤ 38.0
Raw material to produce pulverized coal No.2					
Candle coal	0–50	≤ 10.0	≤ 11.0	≤ 1.2	≤ 38.0
Candle-gas coal	0–50	≤ 10.0	≤ 11.0	≤ 1.2	≤ 38.0
Gas coal	0–50	≤ 10.0	≤ 11.0	≤ 1.2	≤ 38.0
1	2	3	4	5	6
Raw material to produce pulverized coal No.3					
Candle coal	0–70	≤ 10.0	≤ 12.0	≤ 1.5	≤ 38.0
Candle-gas coal	0–70	≤ 10.0	≤ 12.0	≤ 1.5	≤ 38.0
Gas coal	0–70	≤ 10.0	≤ 12.0	≤ 1.5	≤ 38.0
Raw material to produce pulverized coal No.4					
Candle coal	0–100	≤ 10.0	≤ 12.0	≤ 1.5	≤ 40.0
Candle-gas coal	0–100	≤ 10.0	≤ 12.0	≤ 1.5	≤ 40.0
Gas coal	0–100	≤ 10.0	≤ 12.0	≤ 1.5	≤ 40.0

The reserves of Ukrainian coal is sufficiently great (approximately 33,873 mln. tons; 3.8 % of world reserves) [80]. However, the source of raw materials which may be used for PCI technology is limited. The reason is restricted quantity of coal with sulfur content to 1 % (100,000 tons) [81].

Research demonstrates that the required level of sulfur in coal can be achieved through oxidative desulfurization method. Low-rank candle-gas coal used for the experiments.

Based on the weight of the initial coal, yields of COM decomposition resin and desulfurized coal, the sulfur content in the initial and desulfurized coal, volume and composition of desulfurization gases we calculated a number of indices characterizing the process efficiency.

The removal degree of pyritic sulfur and the total sulfur conversion are calculated in accordance with the formulas (3.1) and (3.2). The degree of coal organic matter conversion (COMC) and efficiency factor of COM conversion (K_{ef}) are calculated in accordance with the formulas (3.24) and (3.25).

The degree of ash increase (DAI), %:

$$DAI = \frac{A^d - A_0^d}{A_0^d} \cdot 100, \qquad (3.28)$$

where A^d – ash content of desulfurized coal relative to the dry mass, wt %; A_0^d – ash content of the initial coal relative to the dry mass, wt %

Change of volatiles yield (CVY), %:

$$CVY = \frac{V_0^{daf} - V^{daf}}{V_0^{daf}} \cdot 100, \qquad (3.29)$$

where V_0^{daf} – yield of volatiles of the initial coal relative to the dry ash-free sample, wt %

To characterize the depth of COM conversion we calculated the third index (COMC), which describes the relative quantity of coal spent for the formation of resin and desulfurization gases.

K_{ef} determines the direction of COM conversion, *i.e.* the ratio between quantity of COM, from which combustible products are formed, and quantity which is burnt (spent for CO_2 formation).

DAI and CVY characterize the effect of oxidative desulfurization parameters (in this case oxidant linear velocity and coal particles size) on ash content and volatiles yield of desulfurized coal.

Calculation of hydrodynamic and kinetic parameters was carried out according to formulas (3.5-3.11).

To determine the LRO range, in which it is expedient to study its impact on the oxidative desulfurization process. According to the most common method [26, 82], we calculated actual critical rates of quasi-liquefaction (the beginning of the fluidised bed formation, $u^a_{cr.}$) and particles' removal (destruction of the fluidised bed, $u^a_{p.rm.}$).

The calculated values for the different coal fractions investigated are presented in Table 3.57. The calculations show that the fluidised bed will be formed at the oxidant velocity of 0.0148 m/s or higher. The raw materials should not be ground because the smallest particles are already carried off at u = 0.1620 m/s. Therefore, the LRO range of 0.022–0.099 m/s was chosen for these investigations.

The temperature, oxidant flow rate, composition (content of water vapour in the air-steam mixture), and the process time are the main factors that affect the nature of sulfur conversion, primarily pyrite, and the organic matter of coal. To characterise the oxidant flow ratio, the term "oxidant flow rate ratio" (OFR) was used.

Table 3.57 Calculated values of oxidant linear velocity for different fractions of the investigated coal

Fraction, mm	Actual linear velocity, m/s		LRO, m/s	
	$u^{a}_{cr.}$	$u^{a}_{p.rm.}$	$u_{cr.}$	$u_{p.rm.}$
0.10-0.25	0.0060	0.4142	0.0024	0.1620
0.25-0.315	0.0192	1.1437	0.0075	0.4473
0.315-0.50	0.0379	1.9527	0.0148	0.7637

The values of the factors were kept constant during the entire processes described in this subsection. Additionally the factors were selected based on the optimal conditions for oxidative desulfurization of various grades of coal in 3.2.2.

As a result of experimental studies, we obtained the samples of desulfurized coal and by-products of the process, namely:

- pasty mass – resin, formed with thermal decomposition/gasification of organic matter;

- gaseous products (desulfurization gases).

Yields of solid and liquid products and experimental results are in Tables 3.58-3.61 and Figs. 3.41-3.47.

One can see from Figs. 3.41 to 3.44 that LRO's impact on the yield of solid and liquid products is the same for all three fractions of the studied coal, namely, the increase in LRO decreases the yield of desulfurized coal (Fig. 3.41), increases the decomposition resin yield (Fig. 3.42) and decreases the total yield (Fig. 3.43). It is logical that the degree of coal

organic matter conversion increases as well (Fig. 3.44). The increase in LRO accelerates oxidation (combustion), and the thermal decomposition and gasification of organic matter. This is confirmed by the increase in amounts of (C2-C3+), CO, and CO2 in desulfurization gases (Table 3.59).

Table 3.58 Technical analysis of the desulfurized coal

LRO, m/s	Moisture content (W^a), wt %	Ash content (A^d) wt %	DAI, %	Volatiles' yield (V^{daf}), wt %	CVY, %
1	2	3	4	5	6
Fraction 0.1-0.25 mm					
0.000	1.10	8.35	2.48	34.44	9.55
0.022	1.05	8.74	7.26	35.58	6.56
0.033	1.32	9.48	16.26	36.93	3.02
0.044	1.17	10.13	24.28	37.66	1.10
0.055	1.20	10.18	24.93	38.05	0.07
0.066	1.23	10.28	26.09	38.37	-0.75
0.077	1.27	10.59	29.99	40.53	-6.45
0.088	1.20	10.91	33.88	41.91	-10.06

1	2	3	4	5	6
Fraction 0.25-0.315 mm					
0.000	1.06	9.31	13.24	37.52	2.49
0.022	1.10	9.61	16.86	38.17	0.82
0.033	1.20	10.07	22.52	39.25	-1.99
0.044	1.18	10.99	33.69	40.50	-5.24
0.055	1.19	11.08	34.82	40.87	-6.22
0.066	1.22	11.16	35.72	41.02	-6.60
0.077	1.24	11.61	41.29	43.09	-11.97
0.088	1.27	11.78	43.30	42.88	-11.44
Fraction 0.315-0.5 mm					
0.000	1.04	8.55	6.86	34.00	10.90
0.022	1.07	9.01	12.58	35.86	6.03
0.033	1.24	9.14	14.29	38.13	0.09
0.044	1.19	10.08	26.00	37.75	1.08
0.055	1.16	10.22	27.73	37.96	0.51
0.066	1.25	11.04	37.97	39.78	-4.26
0.077	1.26	11.31	41.41	39.45	-3.39
0.088	1.20	11.53	44.10	40.18	-5.29
0.099	1.22	11.64	45.53	40.46	-6.02

The increase in particles' size increases the desulfurization coal yield (Fig. 3.41), decreases the resin decomposition yield (Fig. 3.42), and increases the total yield (Fig. 3.43). This trend can be explained by the fact that the increase in the particles' size reduces the total surface region of the solid material (coal), and rates of the reactions mentioned above partly depend on the pore diffusion processes.

Table 3.59 Desulfurization gases composition

LRO, m/s	Content in desulfurization gases, vol.%										
	CH_4	C_2H_4	C_2H_6	C_{3+}	SO_2	H_2S	CO_2	CO	N_2	O_2	Ar
Fraction 0.1-0.25 mm											
0.000[1]	–	–	–	–	–	–	–	–	–	–	–
0.022	0.48	0.04	0.11	0.09	1.29	0.03	7.34	1.02	80.92	7.74	0.93
0.033	0.50	0.07	0.31	0.12	1.48	0.05	8.83	1.13	79.99	6.63	0.92
0.044	0.71	0.17	0.35	0.19	1.46	0.09	10.01	1.28	78.90	5.90	0.91
0.055	0.85	0.19	0.39	0.20	1.68	0.09	10.99	1.36	77.87	5.49	0.90
0.066	0.90	0.27	0.52	0.20	1.65	0.11	11.99	1.42	76.65	5.40	0.89
0.077	0.98	0.31	0.54	0.22	1.66	0.11	12.49	1.59	76.06	5.17	0.88
0.088	1.05	0.32	0.56	0.23	1.68	0.11	12.55	1.61	75.92	5.09	0.88
Fraction 0.25-0.315 mm											
0.000*	–	–	–	–	–	–	–	–	–	–	–
0.022	0.45	0.03	0.09	0.07	1.08	0.04	7.01	1.12	80.47	8.71	0.93
0.033	0.48	0.06	0.25	0.11	1.22	0.05	8.57	1.20	79.74	7.41	0.92
0.044	0.66	0.15	0.31	0.15	1.22	0.08	9.98	1.32	78.67	6.56	0.91
0.055	0.77	0.19	0.42	0.19	1.39	0.10	11.08	1.47	77.72	5.78	0.90
0.066	0.85	0.24	0.45	0.22	1.54	0.12	11.80	1.64	76.72	5.54	0.88
0.077	0.89	0.29	0.47	0.23	1.55	0.09	12.05	1.77	76.32	5.46	0.88
0.088	0.94	0.31	0.51	0.23	1.55	0.12	12.47	1.79	76.19	5.02	0.88
Fraction 0.315-0.5 mm											
0.000*	–	–	–	–	–	–	–	–	–	–	–
0.022	0.42	0.02	0.08	0.06	0.96	0.06	7.06	1.22	80.05	9.15	0.92
0.033	0.48	0.05	0.19	0.10	0.97	0.07	8.64	1.35	79.48	7.76	0.92
0.044	0.65	0.11	0.27	0.14	1.07	0.09	9.80	1.47	78.33	7.17	0.90
0.055	0.72	0.17	0.33	0.16	1.11	0.10	10.57	1.55	77.53	6.87	0.89
0.066	0.84	0.23	0.39	0.19	1.19	0.11	10.96	1.59	76.81	6.81	0.88
0.077	0.87	0.26	0.43	0.22	1.24	0.12	11.51	1.69	76.27	6.51	0.88
0.088	0.89	0.29	0.45	0.24	1.29	0.13	11.88	1.77	76.07	6.12	0.88
0.099	0.90	0.31	0.49	0.24	1.30	0.13	12.03	1.87	75.85	6.01	0.87

Remark:

[1]Gases were not analyzed.

Table 3.60 Sulfur content in desulfurized coal

LRO, m/s	Total (S_t^d), wt %	Pyritic (S_p^d), wt %	Sulfate ($S_{SO_4}^d$), wt %	Organic (S_o^d), wt %
Fraction 0.1-0.25 mm				
0.000	3.07	1.54	0.36	1.17
0.022	1.62	0.42	0.35	0.84
0.033	1.46	0.36	0.25	0.84
0.044	1.34	0.29	0.22	0.82
0.055	1.02	0.22	0.20	0.60
0.066	1.01	0.21	0.19	0.61
0.077	0.99	0.19	0.16	0.64
0.088	0.97	0.19	0.14	0.64
Fraction 0.25-0.315 mm				
0.000	2.95	1.50	0.41	1.04
0.022	1.72	0.58	0.39	0.75
0.033	1.51	0.46	0.30	0.75
0.044	1.47	0.39	0.26	0.81
0.055	1.31	0.35	0.22	0.73
0.066	1.13	0.24	0.22	0.67
0.077	1.11	0.22	0.20	0.69
0.088	1.10	0.21	0.19	0.70
Fraction 0.315-0.5 mm				
0.000	2.78	1.42	0.36	0.99
0.022	1.71	0.59	0.35	0.77
0.033	1.61	0.46	0.33	0.82
0.044	1.52	0.43	0.31	0.78
0.055	1.48	0.35	0.28	0.84
0.066	1.37	0.33	0.27	0.76
0.077	1.32	0.32	0.25	0.74
0.088	1.21	0.26	0.24	0.71
0.099	1.21	0.25	0.25	0.71

Table 3.61 Dependence of the pyritic sulfur conversion stages on fluidized bed parameters and mass transfer criteria

Stage	Fraction, Mm	Average diameter of coal particle (d), m	LRO, m/s	Actual LRO (W_r), m/s
Transition region of sulfur conversion[1] (from external diffusion to kinetic or pore diffusion)	0.10-0.25	0.000158	0.055	0.14062
	0.25-0.315	0.000281	0.066	0.16875
	0.315-0.50	0.000397	0.088	0.22500
Transition region of V^{daf} increase above 38 wt %	0.10-0.25	0.000158	0.054	0.13807
	0.25-0.315	0.000281	0.016	0.04091
	0.315-0.50	0.000397	0.032	0.08182
Transition region of A^d increase above 10 wt %	0.10-0.25	0.000158	0.042	0.10738
	0.25-0.315	0.000281	0.031	0.07926
	0.315-0.50	0.000397	0.043	0.10994
Transition region of S_t^d decrease below 1.2 wt %	0.10-0.25	0.000158	0.050	0.12784
	0.25-0.315	0.000281	0.059	0.15085
Transition region of S_t^d decrease below 1.5wt %	0.10-0.25	0.000158	0.030	0.07670
	0.25-0.315	0.000281	0.040	0.10227
	0.315-0.50	0.000397	0.050	0.12784

Table 3.61 Dependence of the pyritic sulfur conversion stages on fluidized bed parameters and mass transfer criteria (continuation)

Stage	Porosity (ε)	Reynolds number (Re)	Sherwood number ($Sh \cdot 10^3$)	Mass transfer coefficient ($\beta \cdot 10^3$), m/s
Transition region of sulfur conversion[1] (from external diffusion to kinetic or pore diffusion)	0.7751	0.3196	3.422	2.635
	0.6290	0.6807	8.979	3.896
	0.5779	1.2834	18.428	5.664
Transition region of V^{daf} increase above 38 wt %	0.7721	0.3138	3.372	2.597
	0.4661	0.1650	2.938	1.275
	0.4658	0.4667	8.315	2.551
Transition region of A^d increase above 10 wt %	0.7322	0.2440	2.766	2.130
	0.5359	0.3197	4.950	2.148
	0.4959	0.6271	10.494	3.220
Transition region of S_t^d decrease below 1.2 wt %	0.7596	0.2905	3.174	2.444
	0.6142	0.6085	8.221	3.567
Transition region of S_t^d decrease below 1.5wt %	0.6820	0.1743	2.121	1.633
	0.5656	0.4125	6.052	2.626
	0.5121	0.7292	11.817	3.626

Remark:

[1]Reactions with participation of gaseous reagent.

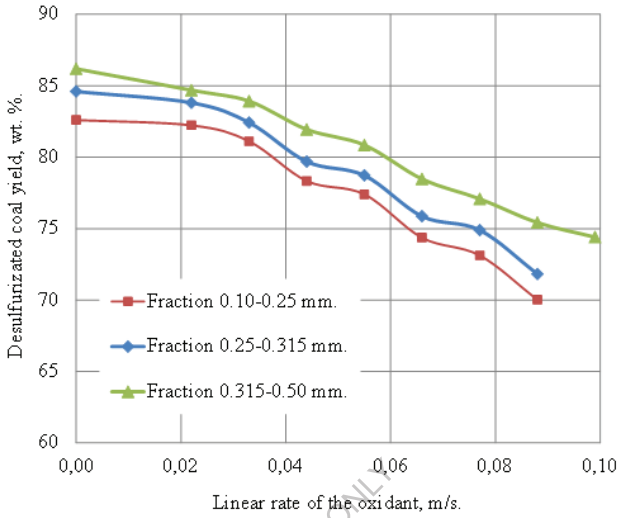

Fig. 3.41 Desulfurized coal yield vs. LRO and coal particles' size.

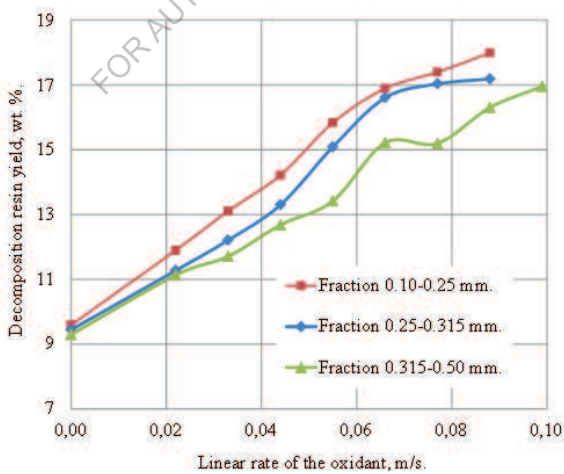

Fig. 3.42 Decomposition resin yield vs. LRO and coal particles' size.

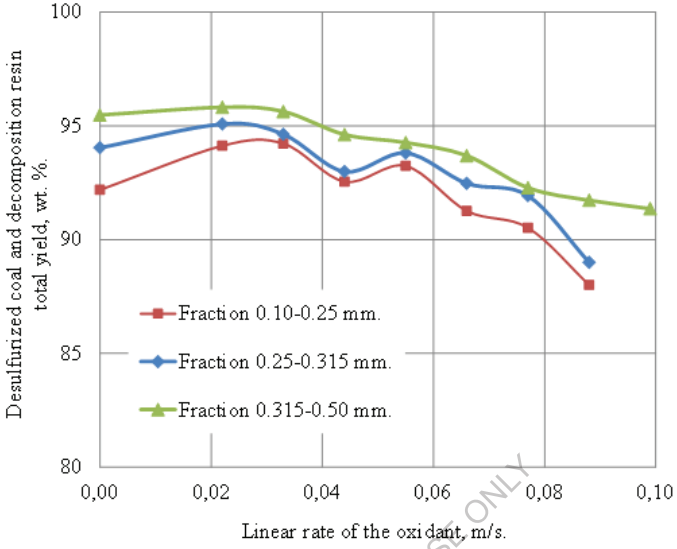

Fig. 3.43 Desulfurized coal and decomposition resin total yield vs. LRO and coal particles' size.

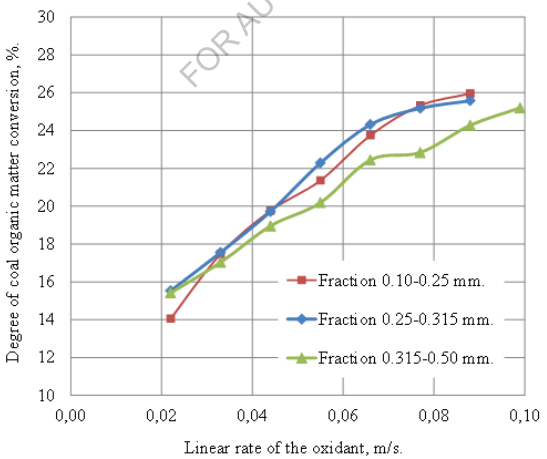

Fig. 3.44 The degree of coal organic matter conversion vs. LRO and coal particles' size.

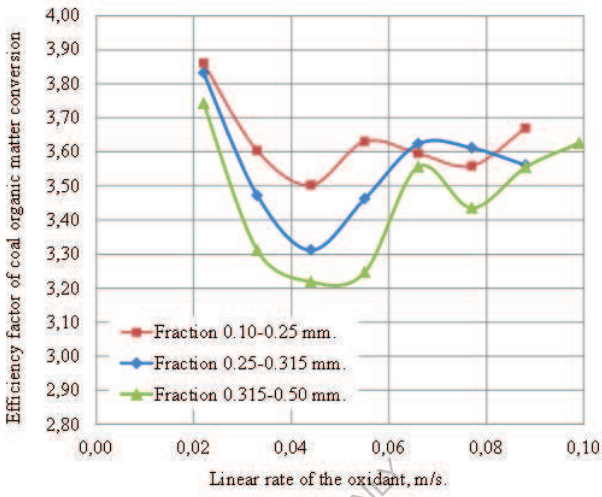

Fig. 3.45 Efficiency of coal organic matter conversion vs. LRO and coal particles' size.

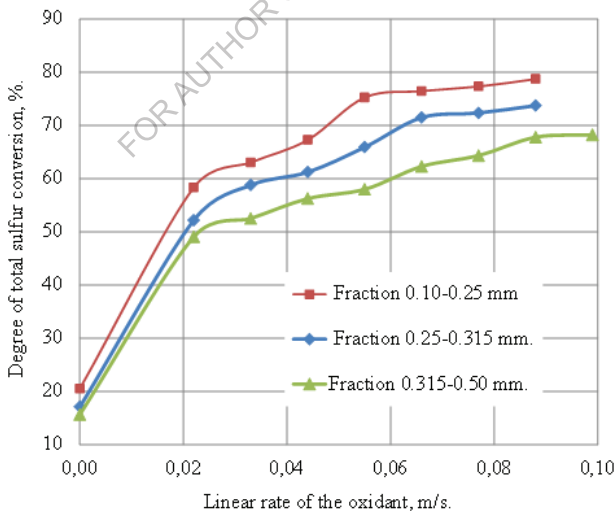

Fig. 3.46 The degree of total sulfur conversion vs. LRO and coal particles' size.

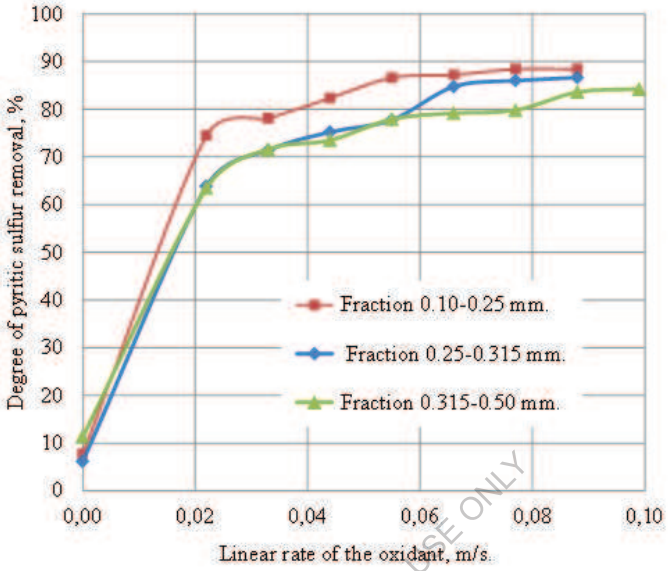

Fig. 3.47 The degree of pyritic sulfur removal vs. LRO and coal particles' size.

The minimum value of the efficiency factor of coal organic matter conversion is LRO=0.044 m/s. For LRO ≥(0.055-0.066) m/s, the efficiency factor is unchanged (Fig. 3.45). The higher the relative content of combustible components in desulfurization gases (CH_4, C_2H_4, C_2H_6, C_{3+}, and CO), the easier (after SO_2 removal) is post-combustion in waste heat boilers. This indicates that it is desirable to carry out the process at LRO ≥(0.055-0.066) m/s.

Regardless of the coal size (Table 3.58), the increase in LRO leads to an increase in ash content and, consequently, increase in DAI. Additionally, this leads to an increase in volatiles' yield and, consequently, a decrease in CVY. The first item is related to the decrease of COM during the process, the second (with the formation of low molecular and thermally

unstable compounds which remain in coal) are vaporised/decomposed during the determination of volatiles. At a DAI value of 20-22% and a CVY value of 0-5%, the ash content and volatiles' yield are within acceptable limits relative to the requirements for raw materials to produce pulverized coal (Table 3.56).

The increase in LRO above 0.022-0.055 m/s decreases CVY below 0-1% (volatiles' yield is above 38-40 wt %), which is unacceptable from the standpoint of producing more pulverized coal № 1-3 (Table 3.56) from desulfurized coal. Also, the increase in LRO above 0.022-0.034 m/s increases DAI above 22-24% (coal ash content of desulfurized coal is above 10 wt %).

Analyzing the data presented in Table 9, we can conclude that regardless of the size and LRO value, almost all sulfur (primarily pyritic sulfur), reacting with an oxidant (vapour-air mixture) is converted to sulfur(IV) oxide. A minor amount of H_2S confirms this compared to SO_2.

Concerning the sulfur content in the resulting product (Table 3.60) from PCI technology, the oxidative method can be used to obtain raw material for the production of pulverized coal. According to the requirements (see Table 3.56), total sulfur content does not exceed 1.0-1.5 wt %.

The most intensive changes for total and pyritic sulfur conversion (Figs. 3.46 and 3.47, respectively) were observed in the LRO range of 0.055–0.088 m/s. Further increase in LRO value only slightly affects the degree of sulfur removal and conversion. It can be inferred that the total rate of sulfur conversion is not limited by the oxidant external diffusion processes at those LRO values, under which the degree of sulfur removal and conversion are not significantly changed. This basically means that the transition from external diffusion to kinetic or pore diffusion regions takes

place at 0.055 m/s for the fraction 0.1-0.25 mm; 0.066 m/s – fraction 0.25–0.315 mm; 0.088 m/s – fraction 0.315-0.5 mm.

To characterize the mass transfer intensity of gaseous reagents (oxygen and water vapor) to the grain of raw materials (coal and pyrite) we calculated the fluidized bed parameters (porosity), dimensionless criteria, and mass transfer coefficients per unit of contact phase surface (β, m/s) under parameters describing key changes during the conversion of pyritic sulfur and COM. The calculations are presented in Table 3.61.

To ensure sulfur conversion with the participation of a gaseous reagent in the kinetic region the mass transfer coefficient should be higher than $2.64 \cdot 10^3$-$5.66 \cdot 10^3$ m/s. At the same time, the grain size and LRO should provide fluidised bed porosity of above 0.58-0.78.

On the other hand, to reduce COM degradation (to achieve ash content in desulfurized coal to 10 wt % and volatiles' yield to 38 wt %.) the mass transfer coefficient should not exceed $1.28 \cdot 10^3$-$3.22 \cdot 10^3$ m/s, and porosity should not exceed 0.47-0.77.

It should also be noted that if oxidant external diffusion limits the rate of sulfur conversion, desulfurized coal with sulfur content less than 1.2-1.5 wt % may be obtained (Table 3.61).

Figs. 3.48 to 3.50 show the areas of hydrodynamic parameters under which it is possible to achieve characteristics of desulfurized coal and the requirements for PCI technology. Only the fraction 0.1-0.25 mm was found to be suitable for finding desulfurized coal that fully meets the requirements of the raw materials to produce pulverized coal, Nos. 3 and 4 (see Table 3.56).

The increase in LRO increases the intensity of coal organic mass conversion, resulting in the reduction of desulfurized coal yield, an increase in ash content, and volatiles' yield. The rate of total sulfur conversion is not

limited by the oxidant external diffusion processes (transition from external diffusion to kinetic or pore diffusion regions takes place) under the following conditions:

- For fraction 0.1-0.25 mm at LRO = 0.055 m/s ($\varepsilon = 0.77$; $Sh \cdot 10^3 = 3.42$; $\beta \cdot 10^3 = 2.64$ m/s);

- For fraction 0.25-0.315 mm at LRO = 0.066 m/s ($\varepsilon = 0.63$; $Sh \cdot 10^3 = 8.698$; $\beta \cdot 10^3 = 3.90$ m/s);

- For fraction 0.315-0.5 mm at LRO = 0.088 m/s ($\varepsilon = 0.58$; $Sh \cdot 10^3 = 18.43$; $\beta \cdot 10^3 = 5.67$ m/s).

To obtain desulfurized coal meeting all requirements for raw materials pulverized coal, it is necessary to use the smallest fraction of coal (0.1-0.25 mm) and carry out the process at LRO = 0.030-0.042 m/s (ε = 0.68 -0.73; $Sh \cdot 10^3 = 2.12$-2.77; $\beta \cdot 10^3 = 1.63$-2.13 m/s).

In most cases, LRO optimal values (from the standpoint of sulfur maximum removal) differ from those providing the acceptable depth of destruction and burning of coal's organic matter (to obtain desulfurized coal with satisfactory values of ash content and volatiles'yield). Therefore, to minimize the extent of COM conversion, it is necessary to conduct researches to establish other optimal parameters of the process (temperature, time and flow ratio, and composition of the oxidant). In further research we used the fraction 0.1–0.25 mm of CG coal.

The experimental-statistical model (ESM) was developed with the aim of establishing optimal conditions of the OD process. Under the "optimal conditions" we understand the conditions under which we obtain the product which meets the requirements for raw materials for the PC production.

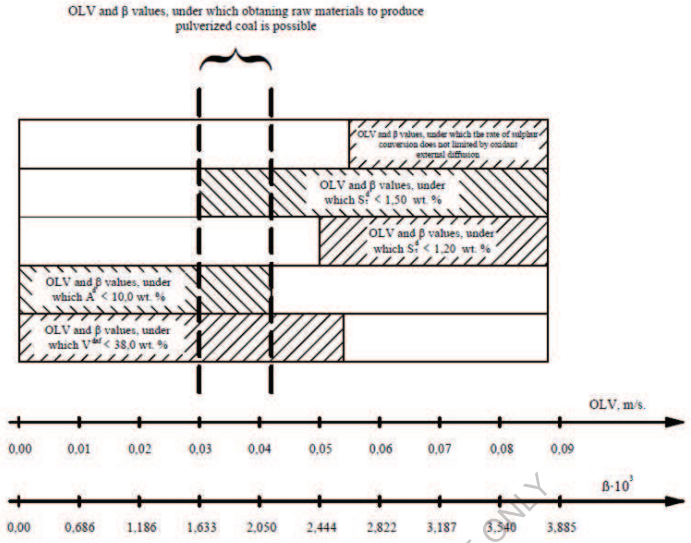

Fig. 3.48 LRO and β values, under which obtaning raw materials to produce pulverized coal is possible. Initial fraction 0.1-0.25 mm.

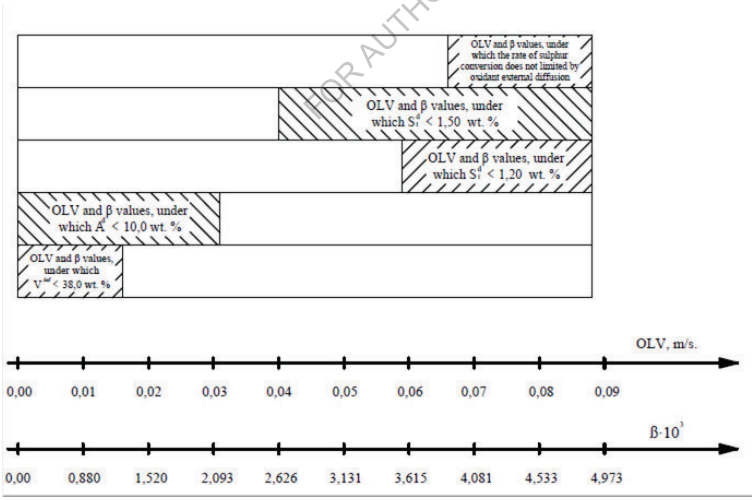

Fig. 3.49 LRO and β values, under which obtaning raw materials to produce pulverized coal is possible. Initial fraction 0.25-0.315 mm.

For the description (development) of ESM we used the following symbols (response functions and the process parameters): Y_1 – the degree of pyrite sulfur conversion, %; Y_2 – the degree of volatiles yield change, %; Y_3 – the degree of ash content increase; X_1 – temperature, °C; X_2 – process time, min; X_3 – water vapor content in the oxidant, vol %; X_4 – oxidant flow rate ratio (OFR), $m^3/(h \cdot kg)$.

To evaluate the adequacy of the developed model, the values of X_1–X_4 were substituted in the dependences $Y_i = f(X_1–X_4)$ and for each experiment the expected values of the response functions (Y_{ij}^{reg}) were found.

The model adequacy was evaluated by 4 parameters: average relative error of approximation (ε_i), determination coefficient (R_i^2), F-test (F_i) and F-statistic (F_{ri}) (see the section 3.2.2).

It was suggested above the process of oxidative desulfurization of low-metamorphosed coal in order to obtain raw materials for PVC to be carried out with a grain size of 0.1–0.25 mm and at a linear velocity of the oxidant equal to 0.03-0.04 m/s. Taking into account previous results the following conditions for ESM development were chosen: temperature of 425-500 ^{0}C; time 10–60 min; water vapor content in the oxidant 15–70 vol %; OFR 2.99–12.83 $m^3/(h \cdot kg)$.

The results are presented in Table 3.62. The purpose of ESM development was finding the optimal conditions for the investigated OD process, namely those conditions under which it would have been possible to achieve the highest values of the degree of pyrite conversion sulfur (response function) under following limitations of other response functions: CVY $\geq$ 0.25 % and DAI $\leq$ 22.69 %.

Different types of dependencies on the process parameters were developed for the response functions.

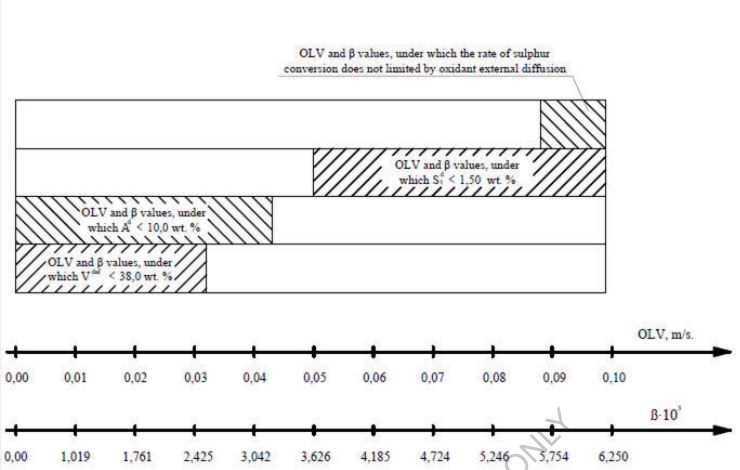

Fig. 3.50 LRO and β values, under which obtaning raw materials to produce pulverized coal is possible. Initial fraction 0.315-0.5 mm.

We chose those of them, which showed the best conformity with the experimental data (Eqs. (3.30)–(3.32)).

$$Y_1 = -2.61128 - 0.042721 \cdot X_2^2 - 0.013453 \cdot X_3^2 - 1.04597 \cdot X_4^2 + 0.171645 \cdot X_2 \cdot X_3 + 0.559559 \cdot X_2 \cdot X_4 + 0.711020 \cdot X_3 \cdot X_4 + 0.369708 \cdot X_1 - 4.23107 \cdot X_2 - 4.79155 \cdot X_3 - 11.1441 \cdot X_4 \quad (3.30)$$

$$Y_2 = 0.114128 - 0.001298 \cdot X_1^2 - 0.007936 \cdot X_2^2 + 0.004725 \cdot X_3^2 - 0.203869 \cdot X_4^2 - 0.020244 \cdot X_1 \cdot X_2 - 0.013733 \cdot X_1 \cdot X_3 - 0.002929 \cdot X_1 \cdot X_4 + 0.296141 \cdot X_2 \cdot X_3 + 0.132179 \cdot X_2 \cdot X_4 + 0.156875 \cdot X_3 \cdot X_4 - 0.202102 \cdot X_1 + 0.090766 \cdot X_2 - 0.106417 \cdot X_4 \quad (3.31)$$

$$Y_3 = 0.111027 + 0.002395 \cdot X_1^2 - 0.014426 \cdot X_2^2 + 0.006024 \cdot X_3^2 - \quad (3.32)$$

$0.307674 \cdot X_4^2 - 0.029509 \cdot X_1 \cdot X_2 - 0.021324 \cdot X_1 \cdot X_3 - 0.006784 \cdot X_1 \cdot X_4$
$+ 0.462636 \cdot X_2 \cdot X_3 + 0.163834 \cdot X_2 \cdot X_4 + 0.216878 \cdot X_3 \cdot X_4 - 0.432638 \cdot X_1$
$+ 0.090191 \cdot X_2 + 0.113302 \cdot X_4$

When checking the validity of Eqs (3.30)–(3.32), the following results were obtained.

Calculated mean relative errors of approximation are: $\varepsilon_1 = 0.1192$ (11.92 %); $\varepsilon_2 = 0.3208$ (32.08 %); $\varepsilon_3 = 0.2567$ (25.67 %). According to [60], at $\varepsilon = 0$–10 % the prediction accuracy is high, at $\varepsilon = 10$–20 % – good, and at $\varepsilon = 20$–50 % – satisfactory. So, the developed model is valid.

The values of F-test are: $F_1 = 2.88$; $F_2 = 20.81$; $F_3 = 32.11$. According to [61] at equal significance $\alpha = 0.05$ the table values of F-tests are: $F_{1cr} = F(0.05; 23.13) = 2.43$; $F_{2cr} = F(0.05; 23.10) = 2.74$; $F_{3cr} = F(0.05; 23.10) = 2.74$, i.e., they are less than the calculated ones. This also confirms the model adequacy.

The values of determination coefficients are: $R_1^2 = 0.8039$; $R_2^2 = 0.9791$; $R_3^2 = 0.986532$. It means that 80.39; 97.91 and 98.65 % change of response functions (Y_1, Y_2 and Y_3, respectively) are determined by selected factors of process control (X_1–X_4). The values $R_1 = 0.8966$; $R_2 = 0.9895$ and $R_3 = 0.9932$ are close to 1, indicating the presence of a "strong" connection between Y_1, Y_2 and Y_3 and selected factors (X_1–X_4).

The values F-statistic are: $F_{r1} = 15.27$; $F_{r2} = 9.54$; $F_{r3} = 17.26$.

According to [61] at equal significance $\alpha = 0.05$ the table values of F-statistic are: $F_{r1} = F(0.05; 10; 13) = 2.67$; $F_{r2} = F(0.05; 13; 10) = 2.89$; $F_{r3} = F(0.05; 13; 10) = 2.89$. This indicates the statistical significance of the determination coefficients R_i^2 ($F_{rcr_i} < F_{r_i}$).

The obtained data testify to the ESM adequacy for the low-metamorphosed coal desulfurization, the statistical significance of the results and the existence of a connection between the response functions and the selected factors of process control.

Optimal conditions of the process were found on the basis of regression equations by the method of uniform search of their maximum values under the following limits: $400 \le X_1 \le 450$ (with step ±5); $10 \le X_2 \le 50$ (with step ±1); $30 \le X_3 \le 50$ (with step ±1); $3.0 \le X_4 \le 5.0$ (with step ±0.1); $Y_1 \le 95$; $Y_2 \le 0.25$; $Y_3 \le 22.6$.

The optimum conditions and the predicted results are presented in Table 3.63, the technical analysis of coal under optimal conditions – in Table 3.64.

Thus, it is possible to obtain the desulfurized product, which fully meets the raw material requirements for the production of PC.

So, in order to obtain raw material for PC production, the oxidative desulfurization of high-sulfur low-metamorphosed coal must be carried out at the process temperature 430 ^{0}C; time 15 min; oxidant flow rate ratio 5.10 m3/(h·kg); water vapor content in the oxidant 47.0 vol %. The resulting product obtained under optimum conditions meets the raw materials requirements for the production of pulverized fuel and has the following characteristics: moisture content 1.16 w t %; ash content 9.24 wt %; volatiles yield 37.88 wt %; total sulfur content 1.38 wt %.

Table 3.62 Experimental data, calculated response functions and relative errors

X_1, ^0C	X_2, min	X_3, vol %	X_4, $m^3/(h \cdot kg)$	Y_1, %	Y_1^{reg}, %	Y_2, vol %	Y_2^{reg}, vol %	Y_3, %	Y_3^{reg}, vol %
350	15	30	4.80	40.99150	40.17864	-1.95323	-2.02809	0.95283	0.09707
375	15	30	4.80	51.33000	49.42133	-1.31303	-1.80073	1.34969	4.82443
400	15	30	4.80	64.44875	58.66402	-0.33495	0.0489	19.9766	12.54602
425	15	30	4.80	86.29225	67.90672	1.10179	3.52079	24.27612	23.26184
450	15	30	4.80	92.74100	77.14941	11.98731	8.61495	36.60813	36.97188
475	15	30	4.80	91.73381	86.39210	14.30366	15.33138	59.22916	53.67614
500	15	30	4.80	90.89000	95.63479	23.50315	23.67007	70.81	73.37464
425	15	30	12.83	74.16241	69.03856	19.06151	19.22872	30.23334	29.4438
425	15	30	8.98	72.27089	85.32250	15.19489	14.97863	29.02666	31.42997
425	15	30	6.74	68.96538	80.51257	10.72555	9.71046	27.93595	28.37958
425	15	30	3.85	51.93316	58.83602	-0.62601	-0.08251	18.66118	19.90053
425	15	30	2.99	32.90671	49.06623	-2.50579	-3.63651	14.52938	16.40366
425	5	30	4.80	28.75975	40.40929	-6.05943	-4.95143	3.27251	4.00412
425	10	30	4.80	59.22550	55.22603	-0.87462	-0.51692	15.80841	13.99363
425	25	30	4.80	87.86000	86.85994	7.42105	10.40578	36.56442	39.63437
425	30	30	4.80	89.45200	93.13247	12.37468	13.25306	46.95204	46.73869
425	45	30	4.80	90.02000	99.13376	21.06092	19.41405	66.01227	63.72387
425	60	30	4.80	90.84663	85.91060	21.57594	22.00376	73.34194	74.21738
425	15	0	4.80	43.43538	44.13380	17.86415	18.51612	50.18345	50.30294
425	15	4	4.80	53.11250	48.70262	15.70851	16.02533	45.74583	46.07095
425	15	15	4.80	59.56656	59.04715	12.72358	9.9553	34.77449	35.42695
425	15	50	4.80	80.83881	70.30249	-1.33685	-1.75098	10.33626	11.25859
425	15	60	4.80	75.18000	67.46453	-2.28466	-2.96933	3.80368	7.06422
425	15	70	4.80	53.41863	61.93601	-3.62001	-3.24265	6.43563	4.07467
Mean relative errors of approximation, ε									

Table 3.62 Experimental data, calculated response functions and relative errors (continuation)

X_1, ^0C	Relative errors		
	ε_1	ε_2	ε_3
350	0.01983	0.038329	0.898125
375	0.037184	0.371438	2.574473
400	0.089757	1.145981	0.371964
425	0.213061	2.195506	0.041781
450	0.16812	0.281327	0.009936
475	0.058231	0.07185	0.093755
500	0.052204	0.007102	0.036219
425	0.069089	0.008772	0.026115
425	0.180593	0.014233	0.082797
425	0.167435	0.094643	0.01588
425	0.132918	0.868203	0.066413
425	0.491071	0.451242	0.129
425	0.405064	0.182856	0.223562
425	0.06753	0.408983	0.114798
425	0.011382	0.402197	0.08396
425	0.041145	0.070982	0.004544
425	0.101242	0.078196	0.034666
425	0.054334	0.019829	0.011937
425	0.01608	0.036496	0.002381
425	0.083029	0.020168	0.007107
425	0.00872	0.217571	0.018763
425	0.130337	0.309777	0.089232
425	0.102627	0.299678	0.857204
425	0.159446	0.104242	0.366858

Table 3.63 Optimum conditions of OD process and results obtained under them

Parameters				Coal yield, wt %	Pyrite sulfur content (S_p^a), wt %	Response functions					
T, K	Time, min	OFR, $m^3/(h \cdot kg)$	Water vapor content in the oxidant, vol %			Degree of pyrite sulfur conversion, %		Degree of volatiles yield decrease, %		Degree of ash increase, %	
						Y_1'	$Y_1^{predict}$	Y_2'	$Y_2^{predict}$	Y_3'	$Y_3^{predict}$
Calculated values											
703	15	5.10	47.0	–	–	–	78.57	–	0.42	–	15.40
Experimental results											
703	15	5.10	47.0	77.54	–	85.14	–	0.52	–	13.37	–

Table 3.64 Technical analysis of desulfurized coal

Moisture content, (W^a), wt %	Ash content (A^d), wt %	Volatiles yield (V^{daf}), wt %	Total sulfur content (S_t^d), wt %
1.16	9.24	37.88	1.38

3.3.4. Using of oxidative desulfurization for energy-technological processing of coal. The task of this section of the monograph was to summarize previous studies on lignite desulfurization by the oxidation method (see section 3.2.2), and on their basis to:

- Create a flow sheet;
- Estimate material and heat balances;
- Suggest possible ways of using main and by-products in practice.

The thermal effect of the oxidative desulfurization of lignite was

estimated according to the formula, MJ:

$$Q_r = \frac{G_{H_2S} \cdot q_r^{H_2S} + G_{CO} \cdot q_r^{CO} + G_{CO_2} \cdot q_r^{CO_2} + G_{H_2O} \cdot q_r^{H_2O} + G_r \cdot q_r^r}{1000}, \qquad (3.33)$$

where $G_{H_2S}, G_{CO}, G_{CO_2}, G_{H_2O}, G_r$ are the amount of sulfur, kg, that is converted to hydrogen sulfide; carbon burned to CO; carbon burned to CO_2; hydrogen burned to H_2O; the amount of decomposition tar, respectively. These quantities (except for G_{H_2O}) were assessed on the basis of the material balances and the contents of desulfurized gases;

$q_r^{H_2S}, q_r^{CO}, q_r^{CO_2}, q_r^{H_2O}, q_r^r$ denote the thermal effects of corresponding reactions, kJ/kg.

The amount of hydrogen (H), converted to H_2O during combustion of coal organic matter (COM), was calculated assuming that the ratio of C/H is the same both in the initial and desulfurized coal by the formula:

$$G_{H_2O} = (G_{CO} + G_{CO_2}) \cdot \frac{H}{C}, \qquad (3.34)$$

where H = 6 and C = 65 wt % mean the average content of hydrogen and carbon in lignite.

The thermal effects of reactions were calculated and accepted according to [83]. It was, nevertheless, admitted that conversion of pyrite in the lignite to hydrogen sulfide occurs by the given chemical equation:

$$FeS_2 + H_2 \rightarrow H_2S + FeS \qquad (3.35)$$

In compiling the heat balance of the process of oxidative desulfurization of coal, the amount of heat, released due to the burning of desulfurized gases after extraction of H_2S from them, was considered. The useful calorific value of desulfurized gases, MJ, was calculated by the standard procedures:

$$Q_k = \frac{\eta \cdot (G_{gas} - G_{H_2S})}{\rho_{gas}} \cdot (0.358 \cdot CH_4 + 0.637 \cdot C_2H_6 + 0.912 \cdot C_3H_8 + 0.591 \cdot C_2H_4 + 0.108 \cdot H_2 + 0.126 \cdot CO), \qquad (3.36)$$

where G_{gas}; G_{H_2S} – the amount of desulfurized gases and hydrogen sulfide, respectively, kg;

ρ_{gas} – density of desulfurized gases, kg/m^3;

η =0.8 – furnace efficiency;

CH_4, C_2H_6, C_3H_8, C_2H_4, H_2, CO – the contents of corresponding constituents in fuel, vol%.

As mentioned above, detailed studies into the effect of factors and fluid dynamics parameters on the process of oxydesulfurization of lignite were undertaken to obtain low-sulfur solid fuel, the use of which would enable to reduce sulfur emissions at TPS. Upon the oxidative desulfurization of lignite, the calorific value increases by 5.0 % (from 22165 to 23284 kJ/kg per analytical sample) and by 7.6 % (from 26769 to 28817 kJ/kg per organic matter) which is due to the decreasing moisture and increasing carbon content in the organic matter. This altogether and a significant reduction in the sulfur content upon the oxydesulfurization makes it possible to anticipate the successful utilization of desulfurized coal in the power industry.

In the process of the lignite oxidative desulfurization, the decomposition tar of organic matter is also produced. The amount of this tar obtainable depends on the process conditions and can be equal up to 26 wt %, which is approximately 1/3 of the main product amount. It is assumed that the cost of this tar, if used, for example, as fuel oil, can exceed by several times the price of desulfurized coal. Taking into account the above, the study on the effect of factors on the quality of tar derived from decomposition of lignite organic matter and on establishing new cost-effective ways of tar application is rather promising. Therefore, those process conditions were determined that would provide the maximum

amount of the decomposition tar of lignite organic matter with the minimum density so that it could be used as the fuel oil or its component. That said, the effect of the oxidant composition (the content of water vapor in the air-steam mixture), temperature, oxidant flow rate (OFR) coupled with duration on the process was investigated.

The results obtainable for the effect of oxidant composition are shown in Table 3.65.

After analyzing the data in Table 3.65, it becomes apparent that the water vapor inhibits the combustion reaction (the yield of the desulfurized coal and tar of coal organic decomposition increases with an increasing amount of tar in the oxidant). As the amount of water vapor in the oxidant increases, the density and kinematic viscosity of decomposition tar of COM is observed to be decreased. The sulfur content in tar is slightly reduced, which indicates a minor effect of water vapor on the reactions where lignite pyritic sulfur is conversed. Therefore, for the purpose of maximum production of tar from the oxidative treatment of lignite, the further researches were carried out at the content of water vapor 70 vol%.

Table 3.65 Effect of the oxidant composition

Water vapor content in the oxidant, vol %	Yield of desulfurized coal, wt %	Yield of tar, wt %	Density at 20 °C, kg/m^3	Tar kinematic viscosity at 100 C, sSc	Sulfur content, wt %
0	50.68	17.85	1061	18.32	1.68
4.5	51.12	18.26	1058	18.25	1.65
30	54.48	23.16	1054	17.58	1.52
50	60.05	24.96	1050	17.02	1.41
70	63.08	26.58	1048	16.53	1.35

The experimental results showing the effect of temperature on the amount and quality of tar of lignite oxidative desulpurization are given in Table 3.66.

Table 3.66 Effect of temperature

Temperature, °C	Yield of desulfurized coal, wt %	Yield of tar, wt %	Density at 20 °C, kg/m^3	Tar kinematic viscosity at 100 C, sSc	Sulfur content, wt %
350	74.97	15.31	1020	14.96	1.72
400	69.17	21.23	1033	15.32	1.53
425	63.08	26.58	1048	16.53	1.35
450	55.91	26.66	1055	16.98	1.27
475	48.55	26.75	1061	17.32	1.22
500	43.94	26.83	1073	17.48	1.20

As the data in Table 3.66 show, the yield of tar increases dramatically as the temperature is raised to 425 °C; there is also an increase in the density and kinematic viscosity of tar due to decomposition of COM. That is, the temperature rise is conducive to decomposition reactions of highly condensing organic structures. As for the sulfur content in tar, the content of tar is decreased with the increasing temperature. Accordingly, further researches were conducted at the temperature of 425 °C.

The experimental results showing the effect of OFR on the amount and quality of tar of lignite oxidative desulfurization are illustrated in Table 3.67.

Table 3.67 OFR effect

OFR, $m^3/(h \cdot kg)$	Yield of desulfurized coal, wt %	Yield of tar, wt %	Density at 20 ˚C, kg/m^3	Tar kinematic viscosity at 100 C, sSc	Sulfur content, wt %
1.20	61.61	17.18	1036	15.87	1.18
1.80	62.13	21.12	1040	16.11	1.27
2.40	63.08	26.58	1048	16.53	1.35
3.60	63.25	26.96	1054	16.85	1.62
4.80	63.52	27.41	1066	17.02	1.88

As the data in Table 3.67 show, an increase in OFR is followed by a rise in the tar density and viscosity, that is, the increasing OFR contributes to decomposition reactions of highly condensing organic structures. As the multiplicity of oxidant consumption is increased, the sulfur content in the decomposition tar increases as well. At OFR values equal to 2.40 $m^3/(year \cdot kg)$ the yield of tar is relatively high (26.58 wt %) and continues to rise slightly. That is why, this OFR value can be considered optimal.

The experimental results in studying how the process duration influence the yield and quality of tar are given in Table 3.68.

As the data in Table 3.68 show, with the increasing process duration, a rise of the tar density and viscosity is observed, that is, an increase in the passage time of reactions intensifies the decomposition of highly condensing organic structures.

Table 3.68 Effect of duration

Duration, min.	Yield of desulfurized coal, wt %	Yield of tar, wt %	Density at 20 °C, kg/m^3	Tar kinematic viscosity at 100 C, sSc	Sulfur content, wt %
5	74.21	15.58	1032	14.12	1.82
10	69.12	20.62	1040	15.64	1.52
15	63.08	26.58	1048	16.53	1.35
20	56.12	27.12	1055	16.78	1.3
30	51.42	27.73	1061	17.18	1.28

As the process duration is increased, the sulfur content of decomposition tar of lignite organic matter declines. At the 15-minute duration a relatively high yield of tar is proved to be attained.

In sum, the optimal conditions for the oxydesulfurization of lignite in this case were chosen so that to ensure the maximum yield of decomposition tar at its relatively low viscosity, density and sulfur content of up to 1.5 wt %. For these reasons, the following conditions were chosen:

- LRO – 0.025 m/s;
- water vapor content in the oxidant – 70 vol%;
- temperature – 425 °C;
- OFR c 2.4 m^3/(h·kg);
- duration – 15 min.

The researches have formed the basis for estimations of technological process parameters (primarily, material and heat balances of the processes which are presented in Table 3.69). During calculations of heat balances the values of heat (expressed in MJ) reported and consumed in-process are relative to 100 kg of initial coal. The calculations were made

for three possible areas the process of oxidative desulfurization of lignite can take place:

1) Power generation: achievement of the maximum degree of desulfurization of coal at minimum energy costs. It was performed without adding water vapor to the air (the mean content of water vapor in the relatively dry air accounted for 4.5 vol%);

2) Power generation and technology: aiming at producing the maximally possible degree of sulfur removal and the highest content of H_2S in desulfurized gases. It was conducted by adding water vapor to the air (the content of water vapor in the oxidant was 50 vol%);

3) Technology: aiming at producing the maximum degree of decomposition tar and the satisfactory degree of sulfur removal (> 50 %). It was executed by adding water vapor to the air (the content of water vapor in the oxidant was 70 vol%).

Calculations were made for cases in which the processes were conducted under optimal conditions that are above specified for the technology direction. The optimal conditions for realization of the process by other two directions were mentioned above and are found to be:

- power generation direction:
  - LRO – 0.01875 m/s;
  - content of water vapor in the oxidant – 4.5 vol%;
  - temperature – 425 °C;
  - OFR – 0.6 $m^3/(h \cdot kg)$;
  - duration – 10 min;
- power generation and technology direction:
  - LRO – 0.01875 m/s;
  - content of water vapor in the oxidant – 50.0 vol%;

- temperature – 425 °C;
- OFR – 0.6 $m^3/(h \cdot kg)$;
- duration – 10 min.

Table 3.69 Material and heat balances of the lignite oxidative desulfurization

Articles	t, ºC	Phase condition	Enthalpy, kJ/kg	Amount, G_i, kg	Heat amount, MJ
1	2	3	4	5	6
4.5 vol% of water vapor in the oxidant (power generation direction)					
Feeding:					
1. Lignite	20	S	29.00	100.00	2.90
2. Air	20	G	20.10	12.35	0.25
3. Water	20	L	83.80	0.36	0.03
4. Heat of reaction	-	-	-	-	81.71
5. Useful heat of combustion of desulfurized gases after H_2S removal	-	-	-	-	42.06
Total:	-	-	-	-	126.95
Received:					
1. Desulfurized lignite	50	S	70.00	55.41	3.88
2. Decomposition tar	150	L	298.81	18.85	5.63
3. Water vapor	150	V	2778.35	12.06[2]	33.50
4. Desulfurized gases	150	G	158.35	19.52	3.09
5. Heat residue	-	-	-	-	76.76[3]
6. Losses	-	-	-	-	4.09[1]
Total:	-	-	-	-	126.95
50 vol% water vapor in the oxidant (power generation and technology direction)					

1	2	3	4	5	6
Feeding:					
1. Lignite	20	S	29.00	100.00	2.90
2. Air	20	G	20.10	6.47	0.13
3. Water	20	L	83.80	4.02	0.34
4. Heat of reaction	-	-	-	-	53.11
5. Useful heat of combustion of desulfurized gases after H_2S removal	-	-	-	-	37.60
Total:	-	-	-	-	94.08
Received:					
1. Desulfarized lignite	50	S	70.00	61.06	4.27
2. Decomposition tar	150	L	298.81	20.65	6.17
3. Water vapor	150	V	2778.35	14.86[2]	41.29
4. Desulfurized gases	150	G	161.37	12.38	2.00
5. Heat residue	-	-	-	-	35.64[3]
6. Losses		-	-	-	4.70[1]
Total	-	-	-	-	94.08
70 vol% water vapor in the oxidant (technology direction)					
Feeding:					
1. Lignite	20	S	29.00	100.00	2.90
2. Air	20	G	20.10	23.27	0.47
3. Water	20	L	83.80	33.75	2.83
4. Heat of reaction	-	-	-	-	92.44
5. Useful heat of combustion of desulfurized gases after H_2S removal	-	-	-	-	27.17
Total:	-	-	-	-	125.81
Received:					
1. Desulfurized lignite	50	S	70.00	63.15	4.42

1	2	3	4	5	6
2. Decomposition tar	150	L	298.81	26.58	7.94
3. Water vapor	150	V	2778.35	44.53[2]	123.71
4. Desulfurized gases	150	G	154.21	29.14	4.49
5. Heat residue	-	-	-	-	-21.05[4]
6. Losses	-	-	-	-	6.29[1]
Total:	-	-	-	-	125.81

Remarks:

[1]Losses into the environment were taken in the amount of 5 % of the reaction heat.

[2]Amount of water vapor to be fed with the oxidant and formed due to a decrease in coal moisture.

[3]Heat amount released from the set-up.

[4]Heat amount that needs to be additionally provided to the set-up, for instance, by burning the part of tar or desulfurized coal

As the given calculations show, the heat amount, emitted as the result of reactions that proceed during the process, and generated due to the afterburning of desulfurized gases, is enough to heat coal to the temperature of reaction and oxidant preparation. The heat residue (in the amount of 0.36-0.77 MJ per kg of coal) can be used to obtain water vapor.

Results of the material balance confirm that during the lignite desulfurization the following is obtained:

- 55.4-63.1 wt % relative to the feed stock of desulfurized coal;
- 18.9-26.6 wt % relative to the feed stock of decomposition tar;
- 12.4-29.1 wt % relative to the feed stock of desulfurized gases.

The characteristics of desulfurized lignite and key technological process parameters are given in Table 3.70 and Table 3.71.

Table 3.70 Characteristic of desulfurized lignite

Moisture, W^{af}, wt %	Ash, A^{d}, wt %	Volatility, V^{daf}, wt %	Sulfur content, wt %			
			total, S_t^d	pyritic, S_p^d	organic, S_o^d	sulfate, $S_{SO_4}^d$
4.5 vol % water vapor in the oxidant (power generation direction)						
2.3	14.4	44.3	3.02	0.49	0.29	2.24
50 vol % water vapor in the oxidant (power generation and technology direction)						
3.0	13.4	46.9	2.92	0.46	0.31	2.15
70 vol % water vapor in the oxidant (technology direction)						
4.1	14.0	39.5	2.99	0.38	0.32	2.29

Table 3.71 Lignite sulfur removal and conversion degrees

Water vapor in the oxidant, vol %	Removal degree of sulfur, RDS, %,		Sulfur conversion, SC, %,	
	total	pyritic	total	pyritic
4.5 (power generation direction)	29.4	76.7	56.0	85.5
50 (power generation and technology direction)	31.8	78.1	53.5	85.1
70 (technology direction)	30.1	81,90	54.2	95,09

The data obtainable show that during the desulfurization of lignite the total sulfur content can be reduced, on average, only by 3.0 wt % (Table 3.70). Accordingly, the degrees of removing total sulfur are 29.4-31.8 % (Table 3.71). This is due to the abnormally high content of organic sulfur in feed coal, the amount of which throughout the process remains virtually unchanged, and to the low yield of desulfurized coal caused by the high moisture content in the feed stock and high reactivity typical of the lignite organic matter. However, if assuming that all hydrogen sulfide contained in

desulfurized gases will be removed or converted to sulfur, the degree of conversion of total sulfur will be equal to the level of reducing environmental pollution. We can, therefore, assert that the method proposed allows emissions of sulfur compounds to the atmosphere during combustion of lignite be reduced, on average, by 53.5-56.0 %.

As noted above, the oxidative desulfurization of lignite produces volatile organic compounds that when condensed form a paste-like or semi-liquid brown substance (a decomposition tar). The tar derived from desulfurization of lignite resembles in appearance furnace fuel oil. So research into its quality was done in view of the perspective to be utilized as fuel components.

Before analysis, coal solids were filtered from the tar produced during the technologically performed process. Upon filtration, a range of analyses of quality parameters of decomposition tar of lignite organic matter were made, which are presented in Table 9. For conducting comparative analysis, the standard requirements for furnace fuel oil of "100" mark and marine high-viscosity fuel are given in Table 3.72.

After having analyzed the results obtained (Table 3.72), it can be concluded that against all characteristics tar of lignite oxidative purification complies with the standard for furnace fuel oil of "100" mark and can, therefore, be used as this type of fuel. Given the slight differences between the tar parameters and the requirements of marine high-viscosity fuel, it can be argued that tar can also be used as a component of the given type of fuel.

Table 3.72 Comparison between the quality parameters of lignite tar with the requirements for furnace fuel oil of "100" mark and marine high viscosity fuel

Name of parameter	Requirements for		Quality parameters of decomposition tar	Procedure[1]
	Furnace fuel oil of "100" mark according to DSTU 4058:2001	Marine high-viscosity fuel according to TU38.1011314-90		
Relative viscosity at 80 ˚C, nominal degrees	≤ 16.0	≤16.0	4.6	GOST 33:2000 (ISO 3104:1994)
Kinematic viscosity at 80 ˚C, cSt	≤118.0	≤118.0	33.1	
Ash content, wt %	≤0.14	≤0.15	0.09	GOST 1461:1975
Density at 20 ˚C, kg/m^3	Not rated	1015	1048	GOST 3900:1985
Sulfur content, wt %	≤ 2.0	≤ 5.0	1.3	GOST 1437:1975
Conradson carbon residue, wt %	Not rated	22.0	9.5	GOST 19932:1999 (ISO 6615:1993)
Water weight, wt %.	≤1.0	Not rated	0.8	GOST 2477:1965
Open cup flash point, ˚C	≥ 110	≥ 100	114	GOST 4333:1987
Chilling point, ˚C	≤ 42	≤ 25	42	GOST 20287:1991

Remark:

[1]DSTU, TU and GOST refer to Ukrainian national standards

Since coal is a natural macromolecular aromatic compound, it can be assumed that the tar from decomposition of lignite organic matter may also include aromatic structures and surface-active substances that can enhance the adhesive and plastic properties of bitumens. Based on the foregoing and

considering the low relative viscosity of decomposition tar, the studies were carried out on the use of this tar as a plasticizer for petroleum-based bitumens.

Coumarone-indene resin (CIR) modified bitumens were used for research. It was found in the works [84, 85] that the addition of CIR to bitumen allows the softening point of bitumens be significantly increased and the adhesive properties be substantially enhanced. It is worth noting that this tar is priced noticeably less than the most prevalent industrial polymer additives (for example, SBS type). On the contrary, adding CIR worsens markedly the plastic properties of the bitumen (penetration and ductility). So for the improvement of these properties of polymer-modified bitumens, it was suggested to utilize tar formed due to decomposition of lignite organic matter. The experimental results are shown in Table 3.73.

As the experimental data (Table 3.73) show, while modifying bitumen with CIR, the softening point increases significantly, however, the plastic properties (depth of needle penetration and extensibility) decline. The addition of plasticizer (decomposition tar) facilitates improvements of bitumen plastic properties, though this almost does not lead to a decrease in the softening point. Increasing the amount of plasticizer leads to an increase in the penetration and a decrease in the ductility of the mixture. Therefore, the optimal content of plasticizer in the mixture is 9 wt % (with the amount of 7 wt % modifier), which makes it possible to obtain PMB that by main characteristics is in compliance with the regulation documents for polymer-modified bitumen.

It should be noted that the use of tar formed due to decomposition of lignite as a plasticizer allows the adhesion of PMB not to be lessened and, correspondingly, obtain PMB with excellent adhesive properties (providing a strong bond of binder with the mineral material), regardless of the ratio of

components.

To determine possible ways of disposition of desulfurized gases, they were examined by the chromatographic analysis (Table 3.74).

Table 3.73 Research on lignite tar as a polymer-modified bitumen (PMB) plasticizer

Blend composition, wt %			Characteristics of PMB			
bitumen	CIR	plasticizer	Softening point (ball & ring method) according to GOST[1] 11506:1973, °C	Ductility at 25 °C according to GOST[1] 11505:1975, cm	Penetration at 25 °C according to GOST[1] 11501:1978, m×10^{-4}	Adhesion to glass according to DSTU[1] BV.2.7-81:1998, %
100	0	0	47	75	62	46
93	7	0	52	36	38	100
86		7	52	40	42	100
85		8	52	36	47	100
84		9	52	28	62	100
83		10	51	27	65	100
Standard for PMB 60/90-52 bitumen according to DSTU[1] BV.2.7.-135:2007			52-54	≥ 25	61-90	≥ 75

Remark:

[1]DSTU, TU and GOST refer to Ukrainian national standards

Table 3.74 Gases composition of desulfurized lignite

Component	Water vapor in the oxidant, vol %		
	4.5 (power generation direction)	50 (power generation and technology direction)	70 (technology direction)
H_2S	8.01	12.49	5.71
H_2	0.79	1.34	–[1]
CH_4	2.68	3.28	1.12
C_2H_4	0.68	0.98	0.31
C_2H_6	0.93	1.56	0.36
C_3	1.23	1.97	0.51
CO	5.51	6.45	2.81
CO_2	23.54	24.99	18.12
O_2	1.23	0.65	66.66
N_2	54.76	45.76	3.62
Ar	0.64	0.53	0.78

Remark:

[1]The content of H_2 was not determined

Hydrogen sulfide produced by oxydesulfurization of lignite, whose content in desulfurized gases is 5.7-12.5 vol% (Table 3.74), can be concentrated using the traditional chemisorption or absorption methods [88, 91]. Concentrated H_2S, most commonly, is used to produce sulfuric acid or sulfur by the traditional Claus process [90]. However, in cases where the content of hydrogen sulfide in gases is greater than 5 vol%, it is a good practice to convert it directly to sulfur by known methods [88, 91].

The researches have underpinned a block schematic diagram for the process of desulfurization of lignite by the oxidation method.

The technology of oxydesulpurization can be implemented into

production if the following stages are to be reached:

- heating the oxidant and initial coal to the temperature of the process;
- making a reliable contact between the oxidant and coal in the reaction zone;
- heat regeneration of desulfurized gases;
- separation of gases from decomposition tar;
- direct discharging of hot coal into boiler units of the second stage of combustion (in the case of the process at a steam power plant) or of cooled desulpurized coal (if necessary, coal can be transported to a consumer);
- purification (filtering) of tar from solid particles or tar application without being filtered as plasticizers for modified bitumen.

All things considered, a block schematic diagram of lignite oxidative desulfurization is suggested (Fig. 3.51).

Lignite is crushed to the size of 0.1-0.75 mm. The crushed coal is fed to the heat exchanger, where it is heated to 220-300 °C due to the cooling of volatile products from desulfurization. The heated lignite enters a fluidized-bed reactor, coming in contact with the oxidant at 425-450 °C. When the oxidant contacts with lignite, sulfur is converted to H_2S, leaving the reaction zone together with other gases and vapors.

From the reaction zone the water vapor, desulfurized gases and tar derived from decomposition comes into the heat exchanger where they undergo condensation and cooling to the temperatures of 140-180 °C. Condensed lignite tar after being filtered from mechanical impurities can be utilized as a component of furnace fuel oil or as a plasticizer in

modification of petroleum-based road bitumen. Desulpurized coal leaving the reaction zone enters directly into the boiler units of the TPS (II stage of combustion).

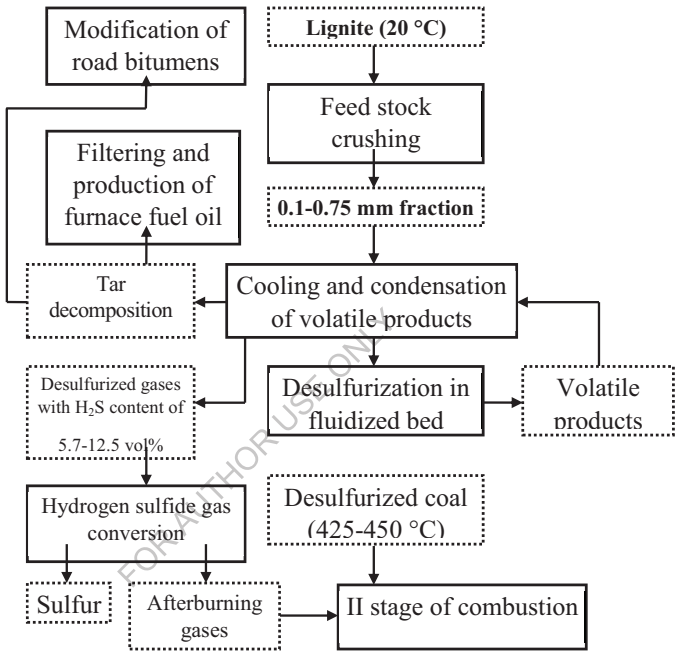

Fig. 3.51 Block schematic diagram of the oxidative desulfurization of lignite

The desulpurized gases of lignite are conversed to produce sulfur. The desulpurized gases, after H_2S has been removed from them, are subjected to the secondary combustion.

Taking into consideration all above, the technological scheme of setting the facility for oxidative desulfurization of lignite has been suggested (Fig. 3.52).

The coal from the store is transferred into the feedstock bin (1), next

with the batcher – into the mill (2), where it is comminuted to the size 0.1-0.75 mm. The comminuted coal is classified with a sieve (3) and via the screw (4) is transferred into the bin (bunker/hopper) (5). From the bunker the comminuted coal is transferred into the middle part of the upper section of the heat utilizer (6), where it is heated up to 220-300 °C through cooling desulfurization gases. Small quantities of flue gases are transferred from the waste-heat boiler/furnace (14) into the utilizer (6). The gases contact with the coal directly, preventing adhesion of coal particles and facilitating its movement down by utilizer section (6).

The heated coal poured into the reactor, that consists of two sections, i.e. the bottom reaction (7) and the top separation (8) ones. In the reaction area at 425-450 °C the coal contacts with the oxidant in the apparatus of the fluidized bed (7). The necessary-for-reaction quantity of previously heated water steam in the section (8) and in the boiler (15) is transferred under the distribution grid of the low area (7). In the area of desulfurization (7) via the contact of the oxidant with the coal, the processes of sulfur conversion into H_2S occur. H_2S is derived from the reaction area along with the other gases and steams. To remove the excess heat into the coiler, which is mounted in the reaction area of separation (8), water is sprayed.

Water steam, desulfurization gases and resin decomposed from the reaction area (7) are transferred into the separation section (8), where coal dust is separated, next is the bottom (distribution) section of heat utilizer (9) and then – its upper section (6), where all these are condensed and cooled to the temperature 140-180 °C. The cooled flue gases, water steam and resin of decomposition get into the separator (10). From the bottom distribution section of the utilizer (9) and the separator (10), the condensed resin of distribution gets into the system of filters (11) for separating mechanical impurities and is withdrawn from the facility.

Desulfurized coal from the reaction area (7) gets directly into the boilers of TPS. In case the coal desulfurization facility is independent, the desulfurized coal is precooled by the air in the remote heat-exchange unit (15) and then transported to its destination. The air entering the remote heat-exchange unit (15) is heated up to 180-220 °C and gets into the reaction area of the reactor (7). If the coal does not enter the heat-exchange unit (15), the air is heated up to the necessary temperature in the heat-exchange unit (16) via the heat of the combustion gases.

The gases of lignite desulfurization from the top separator (10), after drying up, are processed to give off sulfur. The gases of desulfurization, after extraction of H_2S, get into the postcombustion furnace (13), next – to the waste-heat boiler (14), where water steam is obtained as a result of cooling. The cooled flue gases emit into the atmosphere.

So, three technological fields of applying the oxidative desulfurization of high-sulfur lignite, i.e. power generation, power generation and technology, and technology field of application – have been suggested. The optimal conditions of each area are as follows:

- Power generation: LRO – 0.01875 m/s; the content of water vapor in the oxidant – 4.5 vol%; the temperature – 425 °C; OFR – 0.6 $m^3/(h \cdot kg)$; the duration – 10 min;
- Power generation and technology: LRO – 0.01875 m/s; the content of water vapor in the oxidant – 50.0 vol%; the temperature – 425 °C; OFR – 0.6 $m^3/(h \cdot kg)$; the duration – 10 min.

– Technology: LRO – 0.025 m/s; the content of water vapor in the oxidant – 70 vol%; the temperature – 425 °C; OFR – 2.4 $m^3/(h \cdot kg)$; the duration – 15 min.

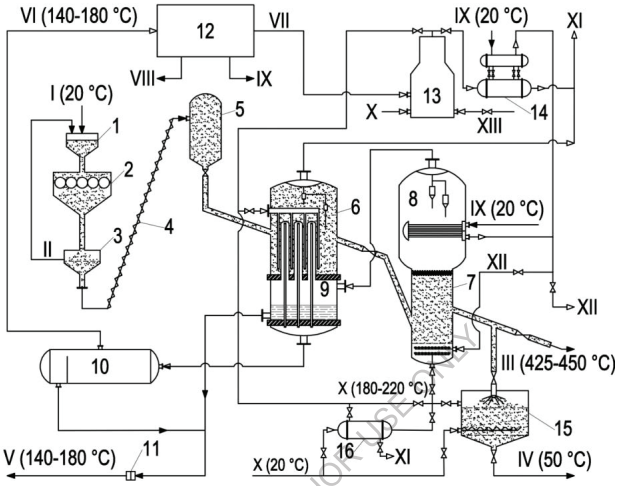

Fig. 3.52 Principal technological scheme of installation for oxidative desulfurization of lignite: 1 – feedstock bin; 2 - mill; 3 - sieves; 4 - screw; 5 – bin (bunker); 6 – upper section of heat utilizer; 7 – reaction area of desulfurization reactor; 8 – separation area of desulfurization reactor; 9 – bottom section of heat utilizer; 10 - separator; 11 - filter; 12 – processing unit of desulfurization gases; 13 – postcombustion furnace; 14 – waste-heat boiler; 15, 16 – heat-exchange unit; I – feedstock (lignite); II – fraction lignite > 0,75 mm.; III – desulfurization of uncooled coal; IV – desulfurized cooled coal; V – resin of decomposition; VI – gases of desulfurization and water steam for treatment; VII – cleaned gases of desulfurization from H_2S for burning up; VIII – sulfur; IX – combustion gas; X – air; XI – cooled combustion gases; XII – water steam; XIII – fuel gas

References of chapter 3

1. Hayvanovych, V., and Pysh'yev, S. (2003). Desulfurization of low-rank coal with high sulfur content is the first stage of coal burning at heat electric stations. Energy&Fuels, 17, 1186-1190.
2. Pyshyev, S., Prysiazhnyi, Y., Shved, M., Namiesnik, J., and Bratychak, M. (2017). State of the art in the field of emission reduction of sulphur dioxide produced during coal combustion. Critical Reviews in Environmental Science and Technology, 24, 2387-2414.
3. Gunka, V., and Pyshyev, S. (2014). Lignite oxidative desulphurization. Notice 1: process condition selection. International Journal of Coal Science & Technology, 1, 62-69.
4. Gunka, V., and Pyshyev, S. (2015). Lignite oxidative desulphurization. Notice 2: effects of process parameters. International Journal of Coal Science and Technology, 2, 196-201.
5. Gunka, V., Shved, M., Prysiazhnyi, Y., Pyshyev, S., Miroshnichenko, D. (2018). Lignite oxidative desulphurization: notice 3 – process technological aspects and application of products. International Journal of Coal Science & Technology, 6, 63-73.
6. Pysh'yev, S., Gunka, V., Bratychak, M., and Grytsenko, Yu. (2011). Kinetic regularities of high-sulphuric brown coal oxidative desulphurization. Chemistry & Chemical Technology, 1, 107-113.
7. Pyshyev, S., and Gunka, V. (2015). Technology of oxidative desulphurization of lignite. Petroleum and Coal, 6, 696-704.
8. Bratychak, M., Gajvanovych, V., Pysh'yev, S., and Brzozowski, Z. (2004). Hard coal desulphurization and sulphur recovery from it. Ecological Chemistry and Engineering, 11, 59-62.

9. Pysh'yev, S., Gayvanovych, V., Pattek-Janczyk, A., and Stanek, J. (2004). Oxidative desulphurisation of sulphur rich coal. Fuel, 9, 1117-1122.
10. Pysh'yev, S., Shevchuk, K., Chmielarz, L., Kuśtrowski P., Pattek-Janczyk A. (2007). Effect of the water-vapor content on the oxidative desulphurization of sulfur-rich coal. Energy & Fuels, 21, 216-221.
11. Pyshyev, S. Prysiazhnyi, Iy., Miroshnichenko, D., Bilushchak, H., and Pyshyeva R. (2014). Desulphurization and usage of medium-metamorphized black coal.1. Determination of the optimal conditions for oxidative desulphurization. Chemistry & Chemical Technology, 8, 225-234.
12. Pyshyev, S., Prysiazhnyi, Iy., Kochubey, V., and Miroshnichenko, D. (2014). Desulphurization and usage of medium-metamorphized black coal. 2. Desulphurized coal used as an additive for the production of special types of coke. Chemistry & Chemical Technology, 8, 467-474.
13. Pysh'yev, S., Gunka, V., Prysiazhnyi, Y., Shevchuk, K., PattekJanczyk, A. (2012). Study of oxidative desulphurization process of coal with different metamorphism degrees. Journal of Fuel Chemistry and Technology, 40, 129-137.
14. Shevchuk, Kh., Bratychak, M., Pysh'yev, S., Shyshchak, O., and Wacławek, W. (2007). Effect of the temperature and oxidant feed rate on high-metamorphic coal desulphurization process. Ecological Chemistry and Engineering, 7, 747-752.
15. Pysh'yev, S., Prysiazhnyi, Yu., Gunka, V., Astakhova, O., and Bratychak, M. (2012). Effect of coal quality on its desulphurization. 1. Influence of the organic matter. Chemistry & Chemical Technology, 4, 443-450.
16. Pysh'yev, S., Prysiazhnyi, Yu., Gunka, V., Astakhova, O., and

Bratychak, M. (2013). Effect of coal quality on its desulphurization. 2. Influence of the inorganic matter. Chemistry & Chemical Technology., 3, 327-334.

17. Pyshyev, S. Bilushchak, H., Gunka, V. (2012). Optimization of oxidation desulphurization of power-generationg coal. Chemistry & Chemical technology, 6, 105-111.
18. Pysh'yev, S., Prysiazhnyi, Yu., and Shved, M. (2015). Raw material for the production of powdered-coal fuel from high-sulphuric low- and medium-metamorphized black coal. Journal of Coal Chemistry, 6, 10-16.
19. Prysiazhnyi, Y., Shved, M., Kułażyński, M., Pyshyev, S. (2019).A new method for preparation of raw materials for production of pulverized fuel. Przemysl Chemiczny, 98, 52-55.
20. Pysh'yev, S., Prysiazhnyi, Yu., and Shved, M. (2017). Effect of oxidant relative flow rate on obtaining raw material for pulverized coal production from high-sulfuric low grade coal. Chemistry & Chemical technology, 11, 236–241.
21. Pysh'yev, S., Prysiazhnyi, Yu., Shved, M., Bilushchak, H., and Pyshyeva A. (2018). Determination of optimum conditions effect of coal oxidative desulfurization to produce pulverized coal. Chemistry & Chemical technology, 12, 355–364.
22. Pysh'yev, S., Prysiazhnyi, Yu., Shved, M., Kułażyński, M., Miroshnichenko, D. (2018). Effect of hydrodynamic parameters on the oxidative desulphurisation of low rank coal. International Journal of Coal Science & Technology, 5, 213–229.
23. Rozenknop, Z. (1952). Recovering sulphur dioxide out of gaseous substance. Moscow, USSR: State Scientific and Technical Publishing of the Chemical Literature..

24. Yurovskyy, A. (1960). Sulphur of coal. Moscow, USSR: Publishing House Academy of Sciences Soviet Union..
25. Attar, A. (1978). Chemistry, thermodynamics and kinetics of reactions of sulphur in coal-gas reactions: A review. Fuel, 57, 201-212.
26. Ternovska, A. and Korenberg, Ya. (1971). Fluidized bed pyrite burning. Moscow, Chemistry.
27. Smirnov, V.(1966). Roasting of copper ores and concentrates. Moscow, Metallurgy.
28. Jasienko, S. (1995). Chemia i fizyka wegla. Wroclaw Polytechnica, Wroclaw.
29. Nekrasov, B. (1973). Basic chemistry. Moscow, Chemistry.
30. Pelix, A., Petrov, E. and Kotomkina, R. (1986). Chemistry and Technology carbon disulfide. Moscow, Chemistry.
31. Carbon disulfide from http://ru.wikipedia.org/wiki/ Carbon disulfide.
32. Huang, H., Young, N., Williams, B., Taylor, S., Hutchings, G. (2006). High temperature COS hydrolysis catalysed by γ-Al2O3. Catal. Lett, 110, 243–246.
33. Reed, S. (2005). Electron microprobe analysis and scanning electron microscopy in geology. Cambridge University Press, Cambridge.
34. Huffman, G., Huggins, F. E. (1978). Mossbauer studies of coal and coke: quantitative phase identification and direct determination of pyritic and iron sulphide sulphur content. Fuel, 57, 592-604.
35. Gupta, V.P., Singh, A.K., Chandra, K. and Jaireth, S.K. (1984). Mössbauer investigations on pyrrhotite. Phys. Stat. Sol, 81, 281-291.
36. Jeandey, C., Oddou, J.L., Mattei, J.L., Fillion,G. (1991). Mössbauer investigation of the pyrrhotite at low temperature. Solid State Communications, 78(3), 195-198.

37. Casagrande, D. J., (1987). Sulphur in peat and coal, in: Coal and Coal-Bearing Strata: Recent Advances (A. C. Scott, ed.). Geol. Soc. Spec., 32, 87–105

38. Greenwood, N., Gibb, T. (1971). Mössbauer Spectroscopy. London, Chapman & Hall.

39. Montano, P.A. (1977). Mössbauer spectroscopy of iron compounds found in West Virginia coals. Fuel, 56, 397-400.

40. Chen, J.P., Hausladen, M.C. and Yang R.T.(1995). delaminated fe_2o_3-pillared clay: its preparation, characterization, and activities for selective catalytic reduction of No by NH_3. Journal of Catalysis, 1995, 151, 135-146.

41. Stephenson, M., Rostam-Abadi, M., Johnson, L., and Kruse, C. (1985). Processing and utilization of high sulfur coals. Coal Science and Technology, 9, 353-372.

42. Rao, V.U.S. (1994). Evaluation of particle size measurement techniques for dispersed iron catalysts. Energy & Fuels, 8, 44-47.

43. Taneja, S., Jones, C. H. W. (1984). Mössbauer studies of iron-bearing minerals in coal and coal ash. Fuel, 63, 695-701.

44. Montano, P., Granoff, B. (1980). Stoichiometry of iron sulphides in liquefaction residues and correlation with conversion. Fuel, 59, 214-216.

45. Dunn, J. G. (1997). The oxidation of sulphide minerals. Thermochim. Acta, 300, 127-139.

46. Usher, C. R., Paul, K. W., Narayansamy, J., Kubicki, J. D., Sparks, D. L., Schoonen, M. A. A., Strongin, D. R. (2005). Aspects of pyrite oxidation in an oxidizing gaseous environment: an in situ HATR-IR isotope study. Environ. Sci. Technol., 39, 7576-7584.

47. Stirling, A., Bernasconi, M., Parrinello, M. J. (2003). Ab initio simulation of water interaction with the (100) surface of pyrite [J]. Chem. Phys., 118, 8917-8926.
48. Kendelewicz, T., Doyle, C. S., Bostick, B. C., Brown, G. E. (2004). Initial oxidation of fractured surfaces of FeS_2 (100) by molecular oxygen, water vapor, and air. Surf. Sci., 558, 80-88.
49. Kalmuk, S. D., Bryk, D. V., Makitra, R. G. (2008). Alternative formation of hydrogen sulphide from coal. Coal Chemistry J., 1-2: 54.
50. Todes, O. M., Tcytovych, O. B. (1981). Fluidized and granular bed apparatus. Chemistry, L. 296.
51. Baskakov, A. P., Lukachevskyi, B. P., Muhlenov, I. P. (1986). Calculations in a fluidized bed. Chemistry, L., 352.
52. Ioffe, I., Pismen, L. (1972). Chemical engineering of heterogeneous catalysis. Chemistry, L., 463.
53. Pavlov, K. F., Romankov, P. G., Noskov, A. A. (1987). Examples and tasks on the course processes and apparatuses of chemical technology. Chemistry, L., 572.
54. Chemist's guide. (1968) Chemistry, L., T. 1-6.
55. Vagraftic, N. B. (1972). Handbook of thermophysical properties of gases and Liquids. Science, Moskva, 721.
56. Kafarov, V. (1971). Methods of cybernetics in chemistry and chemical technology. Moskva, Himija.
57. Drejper, M., Smit, G. (1986). Finance & statistics.
58. Jerina, A. (2001). Statistical modeling and forecasting. KNEU, Kyjiv, 170s.
59. Gavuryk, M., Malozemov, V. (1984). Extremal problems with linear constraints. Izd-vo Lening. un-ta, Leningrad, 176s.

60. Tcegelyk, G. G. (2011). Fundamentals of econometrics. Ivan Franko National University of Lviv, Lviv, 134.
61. Bolshev, L. N., Smirnov, N. V. (1983). Math statistics tables. Nauka, Moskva, 415.
62. Skliar, M., Tiutiunnikov, Iu. (1985). Chemistry of solid fuels. Vyshcha shkola, Kyiv.
63. Lazarenko, A., Chuishchev, V., Kaufman. S. (2004). Coke and chemistry, 1, 24.
64. Guliaev, V. (2012). D.Sc. thesis, Ukr. Derg. Vuglekhim. Inst. (UKhIN), Kharkiv.
65. Barsky, V., Vlasov, G, Rudnitsky, A. (2009). Composition and structure of coal organic mass. Analytical review. Chemistry & Chemical Technology, 3, 315.
66. Barsky, V., Vlasov, G., Rudnitsky, A. (2011). Composition and structure of coal organic mass. 2. Kinetic models of metamorphism. Chemistry & Chemical Technology, 5, 139.
67. Barsky, V., Vlasov, G., Rudnitsky, A. (2011). Composition and structure of coal organic mass. 3. Dinamics of coal chemical structure during metamorphism. Chemistry & Chemical Technology, 5, 285.
68. Barsky, V., Vlasov, G., Rudnitsky, A. (2011). Composition and structure of coal organic mass. 4. Generalized conception of the composition of solid fuel molecular structures and chemism of metamorphism process. Chemistry & Chemical Technology, 5, 439.
69. Lohutova, T., Poltoratska, O. (2015). Innovative economy, 1, 18.
70. Pohlmann, JuG., Osorio, E., Vilela, A., Borrego, A. (2010). Reactivity to CO_2 of chars prepared in O_2/N_2 and O_2/CO_2 mixtures for pulverized coal injection (PCI) in blastfurnace in relation to char petrographic characteristics. International Journal of Coal Geology, 84, 293-300.

71. Zhao, Z., Tang, H., Quan, Q., Zhang, J., Shi, S. (2015). Simulation study on performance of novel oxygen-coal lances for pulverized coal combustion in blast furnacetuyere. Procedia Engineering, 102, 1667-1676.
72. Du, Sh-W., Chen, WH., John, A. (2010). Pulverized coal burnout in blast furnace simulated by a drop tube furnace. Energy, 35, 576-581.
73. Schott, R. (2013). State-of-the-art PCI technology for blast furnace ensured by continuous technological and economic improvement. Iron & Steel Technology, 10, 63-75.
74. Savchuk, N.A., Kurunov, I.F. (2000). Blast-furnace production on the border of XXI Century. News of Ferrous Metallurgy Abroad part II, 1-42.
75. ACCCI (American coke and coal chemicals institute) (2016).
76. Diez, M.A., Alvarez, R., Barriocanal, C. (2002). Coal for metallurgical coke production: predictions of coke quality and future requirements for coke making. International Journal of Coal Geology, 50, 389 – 412.
77. Chauhan, G.I.S., Vijayavergia, R.K. (2006). Coking coals & coke making: Challenges & Opportunities. Viva Books Private Limited.
78. Hutny, W.P., Lee, G.K., Price, J.T. (1991). Fundamentals of coal combustion during injection into a blast furnace. Progress in Energy and Combustion Science, 17, 373-395.
79. Coals for pulverized coal injection into a blast furnace (2012). TS U 10.1-30962337-006:2009. Changes №1.
80. BP Statistical Review of World Energy June (2016). [Electronic resource] – Access mode: https://www.bp.com/content/dam/bp/pdf/energy-economics/statistical-review-2016/bp-statistical-review-of-world-energy-2016-full-report.pdf

81. Drozdnik, I.D., Starovoit, A.G., Gusak, V.G., Filatov, Yu.V., Emchenko A.V. (2011). Coals for coking and pulverized coal. Kharkiv, Contrast, 188 p.
82. Handbook of Chemist. (1968). Chemistry, Leningrad, vol. 5.
83. Ryabov, V.A., Ostroumov, M.A., Sweet, T.F. (1977). Thermodynamic properties of substances. Moscow, Chemistry.
84. Pyshyev, S., Gunka, V., Grytsenko, Y., Bratychak, M. (2016). Polymer modified bitumen: Review. Chemistry and Chemical Technology, 10, 631-636
85. Pyshyev, S., Gunka, V., Grytsenko, Y., Shved, M., Kochubei, V. (2017). Oil and gas processing products to obtain polymers modified bitumen. International Journal of Pavement Research and Technology, 10, 289-296.
86. Rozenknop, Z. (1952). Recovering sulfur dioxide out of gaseous substance. Moscow, USSR: State scientific and technical publishing of the chemical literature.
87. Rameshni, M., and Santo, S. (2005). Production of elemental sulfur from SO_2. RSR (Ramenshi SO_2 reduction). Worley Parsons from http://www.worleyparsons.com/CSG/Hydrocarbons/SpecialtyCapabilities/Documents/Production_of_Elemental_Sulfur_from_SO2.pdf
88. Javorskyj, V. (2010). Operating procedure of earwax and sulfuric acid. Lviv, Ukraine: Publishing House of Lviv Polytechnic National University.
89. Dzhonova-Atanasova, D., Razkazova-Velkova, E., Ljutzkanov, L., Kolev, N., Kolev, D. (2010). Energy efficient SO_2 removal from flue gases using the method of Wellman-Lord. Journal of Chemical Technology and Metallurgy, 48, 457–464.
90. Grunvald, V. (1992). Sulfur gas technology. Moscow, RF: Chemistry.

91. Grebeniuk, A., Korobchansky, V., Vlasov, H., Kaufman, S. (2002). Capturing chemical goods of carbonization. Donets'k, Ukraine: East Publishing House.